

UC Irvine

UC Irvine Electronic Theses and Dissertations

Title

Determining Absolute Configuration of Chiral Epoxides Using the Competing Enantioselective Conversion Method, Developing a Colorimetric Detection Method for the Competing Enantioselective Conversion Method A Computationally Inspired Approach to the T...

Permalink

<https://escholarship.org/uc/item/5bt7q4mq>

Author

Suryn, Gregory M.

Publication Date

2017

Peer reviewed|Thesis/dissertation

UNIVERSITY OF CALIFORNIA,
IRVINE

Determining Absolute Configuration of Chiral Epoxides Using the Competing Enantioselective
Conversion Method

Developing a Colorimetric Detection Method for the Competing Enantioselective Conversion
Method

A Computationally Inspired Approach to the Total Synthesis of (+)-Fastigiatine

And

Progress Towards the Total Synthesis of Lyconadin A–E

DISSERTATION

submitted in partial satisfaction of the requirements
for the degree of

DOCTOR OF PHILOSOPHY

in Chemistry

by

Gregory Michael Suryn

Dissertation Committee:
Professor Scott D. Rychnovsky, Chair
Professor Christopher D. Vanderwal
Professor Kenneth J. Shea

2017

DEDICATION

To my Mother, Father, Sister

&

Friends

For your everlasting love and support

TABLE OF CONTENTS

	Page
DEDICATION	ii
LIST OF TABLES	vii
LIST OF FIGURES	ix
LIST OF SCHEMES	xii
LIST OF ABBREVIATIONS	xvi
ACKNOWLEDGMENTS	xix
CURRICULUM VITAE	xxi
ABSTRACT OF THE DISSERTATION	xxv
 Chapter 1. Determining the Absolute Configuration of Chiral Epoxides Using the Competing Enantioselective Conversion Method	 1
1.1 Introduction to Chirality	1
1.2 Introduction to the Competing Enantioselective Conversion (CEC) Method	2
1.3 Developing a CEC Method for Epoxides	8
1.4 Synthesis of the Chiral Diamine Catalyst	11
1.5 Synthesis of Cyclic Epoxides and Initial CEC Reactions	14
1.6 Synthesis and CEC Testing of Terminal Epoxides	22
1.7 Conclusion	26
1.8 Experimental	27
1.9 References:	61

Chapter 2.	Developing a Colorimetric Detection Method for the Competing Enantioselective Conversion Method.....	67
2.1	Introduction to Visual Detection.....	67
2.2	Introduction to Utilizing Colorimetric Detection in the CEC Method	69
2.3	A Quantitative Approach Using UV-VIS Spectroscopy	71
2.4	Aromatic Bases	72
2.5	Aromatic Esters and Mixed Anhydrides.....	73
2.6	A Qualitative Approach Using Acetate Sensors.....	83
2.7	A Qualitative Approach Using Acid Sensitive Indicators	86
2.8	Conclusion	93
2.9	Acknowledgement	94
2.10	Experimental	94
2.11	References:.....	112
Chapter 3.	Introduction to the <i>Lycopodium</i> Alkaloids	114
3.1	Introduction.....	114
3.2	Highlights of Shair's Synthesis of (+)-Fastigiatine	115
3.3	Highlights of Shair's Synthesis of Lyconadin A and B	117
3.4	Highlights of Smith's Synthesis of Lyconadin A and B.....	118
3.5	Highlights of Waters's Synthesis of Lyconadin C	119
3.6	Highlights of Sarpong's Synthesis of Lyconadin A	120
3.7	Highlights of Fukuyama's Synthesis of Lyconadin A–C.....	121
3.8	Highlights of Dai's Synthesis of Lyconadin A and C	124
3.9	Conclusion	125

3.10	References:.....	125
Chapter 4. A Computationally Inspired Approach to the Total Synthesis of (+)-Fastigiatine		
	127	
4.1	Introduction.....	127
4.2	1st Generation Synthesis of (+)-Fastigiatine	128
4.3	2nd Generation Synthesis of (+)-Fastigiatine: A Computationally Inspired Approach	
	129	
4.4	Conclusions.....	138
4.5	Experimental Contributions	139
4.6	Experimental	139
4.7	References:.....	173
Chapter 5. Progress Towards a Unified Approach to Lyconadin A–E		
	174	
5.1	Introduction.....	174
5.2	Retrosynthetic Analysis	175
5.3	Revised Synthetic Approach.....	183
5.4	Current Progress.....	185
5.5	Future Directions	186
5.6	Conclusions.....	189
5.7	Experimental	190
5.8	References:.....	214
Appendix A. Chapter 1 Supporting Data		10
Appendix B. Chapter 2 Supporting Data		17
Appendix C. Chapter 4 Supporting Data		30

Appendix D. Chapter 5 Supporting Data 37

LIST OF TABLES

Table	Page
Table 1.1: Select reactions in the optimization of the hydrogenation and deprotection procedure to produce 1.13	13
Table 1.2: Ring opening of epoxides 1.18 , 1.20 , 1.22 , and 1.25 with LiDMID, DBU with or without (control) diamine 1 catalysts to the corresponding allylic alcohols.	16
Table 1.3: CEC reactions with epoxides 1.50 , 1.51 , and 1.52 with varying temperatures for epoxide 1.52 . % conversion corresponds to both (3S)- 1.1 and (3R)- 1.1	22
Table 2.1: Initial experiments testing different acyl sources (2.1a–2.1c , 2.6) in the CEC reaction of (1R,2S)-2-phenylcyclohexan-1-ol.....	70
Table 2.2: CEC reactions in various solvents with different acyl sources. Conversion monitored by ¹ H NMR.	79
Table 2.3: Effect of HBTM salt counter ion X on the kinetic resolution of racemic secondary alcohol. Experiments run by Dr. Shawn Miller and Dr. Alex Wagner.....	79
Table 2.4: CEC reactions with mixed anhydride 2.3 or propionic anhydride. Conversions determined by ¹ H NMR.	81
Table 2.5: a) Tested acetate sensors; Color changes for different acetate sensors in MeCN (b) or toluene (c) upon addition of base, base + acid, or TBAA.	85
Table 2.6: Solvent screen to see the effect of different solvents on the color of 2.20 when DBU was added or DBU and propionic acid.	85
Table 2.7: CEC reactions with acetate sensors 2.24 and 2.21 under various conditions for 1 hour. <i>S</i> - and <i>R</i> -HBTM catalyzed reactions run side-by-side and colors determined visually.	93

Table 4.1: Computational studies on the conformation of alcohols 4.11–4.14 . DFT basis set: B3LYP/6-31G(d).	130
Table 4.2: Comparison between the organocuprate and photochemical conjugate addition on protected alcohols 4.19, 4.27, and 4.28	134
Table 4.3: Optimization of conditions for deprotection of TBS alcohol 4.33	135
Table 4.4: Screening of various hydride sources for the reduction of decalone 4.7	137
Table 5.1: Screening of conditions and partners for the reductive amination of ketone 5.12	176
Table 5.2: Conditions for Negishi cross coupling of 5.21 with organozinc bromide 5.23 . Detection of 1,2/1,4-addition and 5.24 ¹⁰ by ESIMS.	178
Table 5.3: Screened conditions for the reductive Heck (product A) or Heck (product B) reactions of bromoenones 5.21 or 5.22 with ethyl acrylate or acrylonitrile.	179
Table 5.4: Screen of conditions for the Suzuki coupling of bromoenone 5.21 and pinacol boronic ester 5.27	180
Table 5.5: Screening of conditions for the Sonogashira coupling of 5.22 or 5.30 with various propargyl alcohols.	181
Table 5.6: Screening of conditions for the Suzuki coupling of 5.22 with allyl alcohol 5.43	185

LIST OF FIGURES

Figure	Page
Figure 1.1: Energy diagram for a kinetic resolution of substrate (S) to product (P) utilizing either enantiomer of the kinetic resolution reagent (cat_S or cat_R).	3
Figure 1.2: Energy diagram comparing the transition state energy of the side-by-side CEC reactions of substrate (S_R) with either enantiomer of the catalyst (cat_S or cat_R) to form product (P_R).	4
Figure 1.3: Possible catalysts for the enantioselective opening of chiral epoxides utilizing a HKR.	6
Figure 2.1: Bases tested in UV-VIS in neutral and protonated forms.	73
Figure 2.2: Overlap in UV-VIS absorption between cyclopropenimine base 2.2 and (<i>S</i>)-HBTM.	73
Figure 2.3: Substituent effect on the UV absorption of UV active π systems.	73
Figure 2.4: Main tested aromatic mixed anhydrides 2.3 and 2.4 , and aromatic esters 2.5 and 2.6 for use in the CEC method.	75
Figure 2.5: UV-VIS spectra of 2.1a , 2.1b , 2.5 , and 2.6 as the phenol, Et_3N salt, and propionate ester.	76
Figure 2.6: UV-VIS traces of propionate esters 2.6 and 2.5 at varying concentrations, and Beer's Law plots of Abs. vs concentration (mM).	77
Figure 2.7: Structures of acetate sensors 2.13 and 2.14	84
Figure 2.8: Change in color over 60 minutes for both <i>S</i> -HBTM (<i>S</i>) and <i>R</i> -HBTM (<i>R</i>) catalyzed reactions with (<i>S</i>)-(-)-1-(1-naphthyl)ethanol, bromocresol green, propionic anhydride, and DIPEA in toluene.	88

Figure 2.9: Equilibrium positions of Rhodamine B vs a Rhodamine B amide.....	90
Figure 2.10: Color change exhibited by Rhodamine B hydrazide 2.21	90
Figure 2.11: Structures of Rhodamine B amides 2.22 and 2.24 ; and benzimidazole 2.23	91
Figure 2.12: a) Basic (left) and acidic (right) forms of indicator 2.22 . b) Fluorescence for basic (left) and acidic (right) forms of indicator 2.22 using a long wave UV lamp (365 nm).....	91
Figure 2.13: a) Compound 2.24 color before and after addition of acid. b) Fluorescence before and after addition of acid.	92
Figure 3.1: Representative compounds from the four classes of <i>Lycopodium</i> alkaloids.	114
Figure 3.2: <i>Lycopodium</i> alkaloids of interest to the Rychnovsky laboratory.	115
Figure 5.1: Unified synthesis of <i>Lycopodium</i> alkaloids via bromoenone.....	174
Figure 5.2: Borazine 5.25 formed from reduction of acrylonitrile with $\text{BH}_3 \cdot \text{THF}$	179
Figure B1. UV-VIS spectra of 2.3 and 2.4 as the phenol, Et_3N salt, and propionate ester.....	24
Figure B2. Concentration study of various possible species in the CEC reaction.....	24
Figure B3. ^1H NMR studies of 2.5 with HBTM.	24
Figure B4. UV-VIS spectra of additional benzoic acids studied.	24
Figure B5. Concentration study of 2-methyl-6-nitro benzoate tetramethylpiperidine salt 2.4a . UV-VIS spectra run at 37 °.....	25
Figure B6. Beer's Law plot generated using the Abs vs [2.4a] (M), and the molar extinction coefficient (ϵ) determined.	25
Figure B7. Concentration study of 2-methyl-6-nitro benzoate tetramethylpiperidine salt 2.4a . UV-VIS spectra run at 37 °C.	26

Figure B8. Beer's Law plot generated using the Abs vs [2.4] (M), and the molar extinction coefficient (ϵ) determined.	26
Figure B9. Calculations relating Abs _{obs} to [salt].	27
Figure B10. Calculations relating Abs _{obs} to [OH](alcohol in reaction).	28
Figure B11. Calculations and amounts for simulating the conversion of mixed anhydride 2.4 to the benzoate salt 2.4a.	29
Figure B12. Conversion of Abs _{obs} to conversion for both enantiomers of HBTM catalyst with (S)-alcohol with anhydride 2.4 as the acyl source.	29
Figure B13. Rate plots of 1/(1-x) utilizing the normalized conversion x (initial conversion set to 0).	29
Figure C14. Conformations for ketones 4.11–4.14 DFT: B3LYP/6-31G(d).....	30
Figure C15. TLC data of the ratio for β -TBS alcohol 4.27 and β -TIPS alcohol 4.28 showing an ~1.0:2.2 ratio for the desired diastereomer.	35
Figure C16. TLC data of the ratio for β -TIPS alcohol 4.28 showing an ~1:4.9 ratio for the desired diastereomer.	36

LIST OF SCHEMES

Scheme 1.1: Representative scheme of the Mosher method for determining absolute configuration of secondary alcohols.	2
Scheme 1.2: Acylation of a secondary alcohol in side-by-side reactions utilizing both enantiomers of HBTM; example of the predictive mnemonic used to determine absolute configuration.	5
Scheme 1.3: CEC reaction of primary amine with both pseudoenantiomers of acylation catalyst; example of the predictive mnemonic used to determine absolute configuration.	6
Scheme 1.4: Enantioselective opening of chiral epoxides utilizing HKR.	7
Scheme 1.5: Epoxide opening and subsequent alcohol derivatization to determine absolute configuration.	9
Scheme 1.6: a) Desymmetrization of cyclohexene oxide using Asami's chiral diamine b) Desymmetrization of cyclohexene oxide by Andersson using a bridged diamine. ²⁴	9
Scheme 1.7: General CEC reactions for the ring opening of the chiral epoxide; predictive mnemonic for assigning absolute configuration.	10
Scheme 1.8: Proposed transition states for the reaction of the chiral epoxide with both enantiomers of deprotonated diamine catalyst Li-1.1 . Solvent or DBU left out for clarity.	11
Scheme 1.9: First generation synthesis of chiral diamine catalyst (3R)-1.1	12
Scheme 1.10: Synthesis of 1.1 via the revised route.	12
Scheme 1.11: Ring opening of epoxides 1.18 , 1.20 , 1.22 , and 1.25 with diamine catalysts. Conversion by ¹ H NMR.	15
Scheme 1.12: Formation of stoichiometric base LiDMID from 1,2-dimethylimidazole.	16

Scheme 1.13: CEC reaction with both enantiomers of limonene oxide 1.25 and 1.29 .	17
Scheme 1.14: CEC reaction of epoxide 1.33 with Asami's chiral diamine 1.32 .	18
Scheme 1.15: Synthesis of epoxides 1.37 and 1.40 .	19
Scheme 1.16: CEC and control reactions with epoxides 1.37 and 1.40 to form allylic alcohols 1.42 and 1.43 respectively. Control reactions without chiral diamine showed only starting material.	19
Scheme 1.17: Synthesis of epoxides 1.45 and 1.47 .	20
Scheme 1.18: CEC reactions with epoxides 1.45 and 1.47 to form allylic alcohols 1.48 and 1.49 .	21
Scheme 1.19: CEC reactions of 1.53 with catalysts 1.1 at different temperatures and with different stoichiometric bases.	23
Scheme 1.20: CEC reaction of epoxide 1.55 with diamines 1.1 , and formation of oxetane ring 1.56 .	24
Scheme 1.21: CEC reactions on epoxide 1.58 with both LDA and LiDMID.	25
Scheme 1.22: CEC reactions on epoxide 1.58 with both LDA and LiDMID.	25
Scheme 1.23: CEC reactions with epoxides 1.65 and 1.66 with both LDA and LiDMID.	26
Scheme 2.1: General schematic for a visual detection method.	67
Scheme 2.2: Modification of the CEC method to incorporate a chromophore in either the acyl source or the base.	71
Scheme 2.3: Catalytic cycle for HBTM catalyzed acylation of alcohols with an aromatic mixed anhydride or ester. ⁹	74
Scheme 2.4: Formation of HBTM salt 2.7 or 2.8 with ester 2.5 and 2.6 , and observation of the precipitating of 2.7 out of solution over time.	78

Scheme 2.5: General overview of using an acetate sensor or a pH sensor to detect progression of the CEC reaction by visual color change.....	82
Scheme 2.6: HBTM catalytic cycle incorporating the use of a pH sensitive indicator.....	83
Scheme 2.7: Reaction scheme for incorporating an acid sensitive indicator to detect the fast reacting catalyst/substrate pair visually.	87
Scheme 3.1: Synthesis of enamine 3.15 by Shair.....	116
Scheme 3.2: Endgame to (+)-fastigiatine 3.1 by Shair.....	117
Scheme 3.3: Final steps of Shair's synthesis of lyconadin A (3.5) and B (3.6) from 3.12	118
Scheme 3.4: Synthesis of lyconadin A or B (3.5 or 3.6) by Smith.	119
Scheme 3.5: Synthesis of lyconadin C 3.7 by Waters.....	120
Scheme 3.6: Synthesis of tetracycle 3.50 in Sarpong's synthesis of lyconadin A 3.5	121
Scheme 3.7: C–N bond formation and methyl cleavage to form lyconadin A 3.5	121
Scheme 3.8: Fukuyama's synthesis of lyconadin A 3.5	122
Scheme 3.9: Synthesis of lyconadin B 3.6 by Fukuyama.	123
Scheme 3.10: Synthesis of lyconadin C (3.7) by Fukuyama.....	123
Scheme 3.11: Dai's synthesis of lyconadin A (3.5) and C (3.7).	124
Scheme 3.12: Transformation of 3.67 to 3.70 <i>en route</i> to lyconadin C (3.7).....	125
Scheme 4.1: Retrosynthetic analysis of the a) Shair and b) Rychnovsky synthesis of (+)-fastigiatine 4.1	127
Scheme 4.2: 1 st generation synthesis of (+)-fastigiatine.....	129
Scheme 4.3: Synthesis of α - or β -protected alcohols 4.19 , 4.27 , and 4.28	131
Scheme 4.4: a) Generation and conjugate addition of organocuprate 4.18 with cyclohex-2-en-1-one. b) Effect of X group on 1,4- vs 1,2-addition to cyclohex-2-en-1-one.	132

Scheme 4.5: Formation of tricycle 4.5 under organocuprate or photochemical conditions.	133
Scheme 4.6: Transformation of silyl alcohols 4.34 , 4.36 , and 4.38 to tricycles 4.5a and 4.5b . ..	136
Scheme 4.7: Overall route for 2 nd -generation (+)-fastigiatine synthesis.	138
Scheme 5.1: Initial retrosynthetic analysis of lyconadins A, B, and C (5.3–5.5).....	175
Scheme 5.2: Competition experiment between α -haloenones and β -haloenones in a Negishi cross coupling.	181
Scheme 5.3: Suzuki coupling of 5.30 with pinacol boronate ester 5.34	182
Scheme 5.4: a) Precedent by Herzon lab. ¹⁸ b) Attempt to diiodocyclopropanate ketone 5.12 . ..	183
Scheme 5.5: Suzuki cross-coupling between <i>N</i> -Boc allylamine 5.39 and bromoenone 5.21	183
Scheme 5.6: Revised retrosynthesis of lyconadins A–C (5.3–5.5).	184
Scheme 5.7: Current progress towards the total synthesis of lyconadins A–C (5.3–5.5).	186
Scheme 5.8: Steps until the branching point, tricycle 5.50	187
Scheme 5.9: End game for lyconadins A/B and C (5.3–5.5).	188
Scheme 5.10: Endgame for the synthesis of lyconadins D or E (5.6, 5.7) from tricycle 5.50 . ..	188
Scheme 5.11: a) Key intermediates in the synthesis of lyconadins D or E utilizing the 1 st -generation or b) a 2 nd -generation (+)-fastigiatine synthesis.....	189

LIST OF ABBREVIATIONS

Å	Angstroms
Ac	Acetyl
Atm	Atmosphere
Bn	Benzyl
Boc	tert-butoxycarbonyl
Bp	Boiling point
Bu	Butyl
<i>n</i> -BuLi	Butyllithium
°C	Degree Celsius
cat.	Catalytic
CSA	Camphorsulfonic acid
CI	Chemical ionization
CMC	<i>N</i> -Cyclohexyl- <i>N'</i> -(2-morpholinoethyl)carbodiimide metho- <i>p</i> -toluenesulfonate
d	day(s)
DBU	1,8-Diazabicyclo[5.4.0]undec-7-ene
δ	Chemical shift
DIBAL-H	Diisobutylaluminum hydride
DMAP	4-Dimethylaminopyridine
DMF	<i>N,N</i> -Dimethylformamide
DMP	Dess-Martin periodinane
DMPU	1,3-dimethyl-3,4,5,6-tetrahydro-2(1H)-pyrimidinone
DMSO	dimethyl sulfoxide
dppf	1,1'-bis(diphenylphosphino)ferrocene
d.r.	Diastereomeric ratio
ee	Enantiomeric excess
EI	Electron-impact ionization
e.r.	Enantiomeric ratio
eq.	Equation

equiv.	Equivalents
ESI	Electrospray ionization
Et	Ethyl
GC	Gas chromatography
h	hour(s)
HMPA	<i>N,N,N',N',N'',N''</i> -hexamethylphosphoramide
HRMS	High resolution mass spectrometry
Hz	Hertz
<i>i</i>	iso
IR	Infrared spectrometry
<i>J</i>	Coupling constant
KHMDS	Potassium hexamethyldisilazide
LAH	Lithium aluminium hydride
LiDBB	Lithium di- <i>tert</i> -butylbiphenylide
LDA	Lithium diisopropylamide
LiHMDS	Lithium hexamethyldisilazide
μ	micro
m	milli
M	Molar
<i>m</i> -CPBA	3-Chloroperoxybenzoic acid
min	minute(s)
Me	Methyl
MHz	Megahertz
MS	Mass spectrometer
n	nano
NMR	Nuclear magnetic resonance
nOe	Nuclear Overhauser Effect
Ph	Phenyl
ppm	parts per million
rt	room temperature
sec	second(s)

<i>t</i>	tert
TBAF	tetra- <i>n</i> -butylammonium fluoride
TBS	<i>t</i> butyldimethylsilyl
TBDPS	<i>t</i> butyldiphenylsilyl
TES	triethylsilyl
Tf	trifluoromethanesulfonyl
TFA	trifluoroacetic acid
THF	Tetrahydrofuran
THP	Tetrahydropyran
TIPS	Triisopropylsilyl
TLC	Thin layer chromatography
TMS	Trimethylsilyl
Ts	4-Toluenesulfonyl
TsOH	4-Toluenesulfonic acid

ACKNOWLEDGMENTS

- I would like to thank Professor Scott D. Rychnovsky for his ever-supportive personality, and the patience with me when I probably taught more classes than I should have. I am quite certain that I am the instructor I am today because you allowed me to pursue many teaching avenues throughout graduate school. You have been an amazing PI both in the lab and outside of the lab, and I'll always remember your Jerk chicken and unicycling at your house.
- Professor Christopher Vanderwal and Professor Kenneth Shea for participating on both my doctoral committee and my advancement committee. I have truly enjoyed learning from you through classes, personal meetings, and in the hallways. May your lab ever be full, and your funding endless.
- To my amazing teaching mentor Dr. Susan King, I have learned so much from being both your TA and your peer. My students have had wonderful comments on my reviews, and I can honestly say that those find their way back to you and your teaching style and passion.
- Dr. De Gallow, you have modeled for me the type of teacher I hope to achieve someday. I learned a great deal from getting to interact with you in the Pedagogical Fellowship program, and I know that the community you built will continue to benefit my teaching style even in the future.
- Thanks to my high school chemistry teacher Lea Stage and my college organic professor Steve Sieck, you instilled a curiosity and drive for chemistry that set me on the path I'm on today.
- I have been blessed over the years to have been surrounded by lab mates that I could truly call friends. You all made coming to work every day a pleasant experience, and I can't wait to see where your lives take you.
- To all my classmates, and honorary classmates, you have made this period in my life unforgettable. Not many people can say that they had a blast during graduate school, but the memories that we formed will stick with me long after I leave the hood.
- Thanks to my late Grandpa Neal, you always provided a warm a loving home to get away from lab. You will always be the master of Mickey Mouse Waffles (MMW's).

- To my California extended family, thank you for welcoming me to all the holiday celebrations with open arms.
- To my Colorado immediate family, I know I couldn't always be near, but I always knew your love and support was just a phone call away. You have supported me through all the ups and the downs, even when it may not have been easy.

CURRICULUM VITAE

Gregory M. Suryn

Education and Training

Sep. 2011 **University of California, Irvine** (Irvine, California)

– June 2017 Ph.D., Chemistry
Thesis Advisor: Professor Scott D. Rychnovsky

Research

- Synthesized both enantiomers of a chiral diamine organocatalyst
- Synthesized and screened a variety of chiral cyclic, acyclic, and terminal epoxides for their use in our method for determining the absolute configuration
- Development towards a colorimetric and fluorimetric detection method for determining the absolute configuration of alcohols, lactams, and oxazolidinones
- Progress towards a universal synthesis of Lycopodium alkaloids and the synthesis of Lyconadin A, B, C, D, and E.
- Analysis of protecting group choice towards a diastereoselective second generation synthesis of (+)-Fastigiatine.

Aug. 2007 **Grinnell College** (Grinnell, Iowa)

– May 2011 B.A. in Chemistry from Grinnell College

June 2010 **University of Kansas** (Lawrence, Kansas)

– Aug. 2010 National Science Foundation Research Experience for Undergraduates (NSF-REU)
Research Advisor: Professor Paul Hanson

- Completed 12 steps in the synthesis of Macrolactin A, a 24-membered polyene macrolide
- Worked on a one-pot ring closing metathesis (RCM)/cross metathesis (CM)/hydrogenation procedure

Teaching Experience

June 2015 **Department of Chemistry Instructor of Record, UC Irvine (115–345 students)**

– June 2017 Lecture Class: Responsible for preparing and leading lectures, preparing course material, preparing homework assignments, writing exams, monitoring exams, grading exams, and submitting final grades.

- Chem 1B: General Chemistry Lecture (taught once, 400 students)
- Chem 51A: Organic Chemistry Lecture (taught once, 345 students)
- Chem 51B: Organic Chemistry Lecture (taught three times, 115–145 students)

Aug. 2015 **Department of Chemistry Head Teaching Assistant, UC Irvine**

– June 2016 Lab Classes: Responsible for managing Teaching Assistants (TA), managing students' online tools, leading weekly TA meetings, and handling emergency situations.

- Chem 51L: Organic chemistry lab series

- Jan. 2015 **UCI Chemistry Outreach Coordinator**
 – June 2015 Responsible for: Preparing the chemistry outreach visits, leading the chemistry outreach demonstrations, coordinating the visits with teachers and volunteers, developing new chemistry outreach demonstrations, and maintaining inventory and purchasing supplies.
- Sep. 2011 **Department of Chemistry Teaching Assistant, UC Irvine**
 – June 2017 Lecture Classes: Responsible for leading discussion sessions, monitoring exams, and grading exams
 – Chem 51B: Organic chemistry lecture (taught three times)
 – Chem 51C: Organic chemistry lecture (taught two times)
 Lab Classes: Responsible for leading lab, ensuring safety, and grading of lab reports and notebooks
 – Chem 160: Upper division organic synthesis lab (taught two times)
 – Chem H52LA/M52LA: Honors and majors organic chemistry lab (taught one time)
 – Chem 51LA: Organic chemistry lab (taught one times)
 – Chem 51LB: Organic chemistry lab (taught two times)
 – Chem 11C: General chemistry lab (taught one time)
- Sep. 2015 **Mentorship**
 – May 2016 Mentored an undergraduate in a graduate laboratory setting, developing a colorimetric and fluorimetric method for determining the absolute configuration of alcohols, lactams, and oxazolidinones.

Scholarships/Fellowships/Awards

- May 2017 Departmental Service Award
 June 2016 Most Promising Future Teacher Organic Chemistry
 June 2016 Contributions to Education by a Chemistry Department TA, Honored by the School of Physical Sciences
 June 2016 Department Safety Award
 Jan. 2015 Certificate of Teaching Excellence
 –May 2016
 March 2015 Pedagogical Fellowship–Competitive (\$2,000)
 –Dec. 2016
 June 2015 Outstanding Contribution to Chemistry Department Teaching Program by a TA
 Jan. 2015 Undergraduate Research Opportunities Program, Multidisciplinary Design Project Fellow
 Aug. 2009– Tammy Zywicki '93 Memorial Scholarship
 May 2010

Service

- Oct. 2016 Science and Engineering Night at the Santiago School
 July 2016 Advisory Board for UCI CIRTL

–Aug. 2016
April 2016 IPSF STEAM Carnival

Sep. 2015 Teaching Assistant Professional Development Program (TAPDP)
July 2015 IPSF STEAM Carnival
Jan. 2015 Orange County STEMploration Fair
Oct. 2011 Chemistry Outreach Program (UC, Irvine)
–June 2017
May 2014 Teaching Assistant Panel for TAPDP training program
May 2013 DanceChemistry Videos
– March 2014
Sep. 2012 Outside Review Member for CHM 325 at Grinnell College
– Sep. 2013
April 2011 Chemistry Demo Day at Grinnell High School
Sep. 2010 Deaf Awareness month at Marion Downs Hearing Center

Professional Development

Mar. 2015 University Studies 390A: Advanced Pedagogy and Academic Job Preparation
– June 2015 – How students learn
 – Active teaching and learning techniques
 – Instructional technologies for the classroom
 – Design of the Teaching Assistant Professional Development Program (TAPDP)
Sep. 2015 University Studies 390B: Advanced Pedagogy and Academic Job Preparation
– Dec. 2015 – Different types of higher education institutions
 – Academic job search and selection
 – Preparing for the job market
 – Observation and consultation
 – Application review

Presentations

Gregory Suryn, Determining the Absolute Configuration of Chiral Epoxides Using the

Competing Enantioselective Conversion Method, Asymmetric Reactions & Syntheses, ACS Meeting San Diego, March 2016. (poster presentation)

Gregory Suryn; et. al. DanceChemistry: An interdisciplinary intersection between the arts and sciences, University of California, Irvine, CA May 2015. (oral presentation)

Gregory Suryn, Determination of the Absolute Configuration of Chiral Epoxides, Graduate Student and Postdoc Colloquium, University of California, Irvine, CA April 2015. (oral presentation)

Gregory Suryn; et. al. Application of Phosphate Tethers in Synthesis: Macrolactin A and One-pot RCM/CM/Hydrogenation Studies, Grinnell, Iowa, September 2010. (oral presentation)

Gregory Suryn; et. al. Application of Phosphate Tethers in Synthesis: Macrolactin A and One-pot RCM/CM/Hydrogenation Studies, Lawrence, Kansas, August 2010. (poster presentation)

Gregory Suryn; et. al. Application of Phosphate Tethers in Synthesis: Macrolactin A and One-pot RCM/CM/Hydrogenation Studies, Lawrence, Kansas, July 2010. (oral presentation)

Publications

A Phosphate Tether-Mediated, One-Pot, Sequential Ring-Closing Metathesis/Cross-Metathesis/Chemoselective Hydrogenation Protocol, Venukadasula, P. K.; Chegondi, R.; Suryn, G. M.; Hanson, P. R. *Org. Lett.* **2012**, *14*, 2634–2637.

Designed the cover image: Generation, structure, and reactivity of tertiary organolithium reagents, Perry, M. A.; Rychnovsky, S. R. *Nat. Prod. Rep.* **2015**, *32*, 517–533.

Related Employment

Sep. 2011 **Research Group Jobs**

– June 2017 Safety Representative

- Ensured the safety training of new graduate and undergraduate researchers
- Lab safety training and standards kept up to date
- Standard Operating Procedures (SOP) written to ensure safe handling of hazardous chemicals

Regulated Chemicals Manager

- Kept inventory of DEA regulated chemicals
- Allowed access to locked chemicals

Ozone Generator Manager

- Ensured training of researchers on how to use the ozone generator
- Kept the ozone generator in working order

Group Website Manager

- Rychnovsky group website kept up to date
 - Managed contact information and group jobs
-

References

Scott Rychnovsky, Ph.D.

Department of Chemistry
1102 Natural Sciences II
University of California,
Irvine
Irvine, CA 92697
(949)517-8075
srychnov@uci.edu

De Gallow, Ph.D.

Center for Engaged
Instruction
Division of Teaching and
Learning
University of California,
Irvine
Irvine, CA 92697-4150
(949)824-6189
dgallow@uci.edu

Susan King, Ph.D.

Department of Chemistry
2133 Natural Sciences II
University of California,
Irvine
Irvine, CA 92697
(949) 824-5452
s3king@uci.edu

ABSTRACT OF THE DISSERTATION

Determining Absolute Configuration of Chiral Epoxides Using the Competing Enantioselective Conversion Method

Developing a Colorimetric Detection Method for the Competing Enantioselective Conversion Method

A Computationally Inspired Approach to the Total Synthesis of (+)-Fastigiatine

and

Progress Towards the Total Synthesis of Lyconadin A–E

By

Gregory Michael Suryn

Doctor of Philosophy in Chemistry

University of California, Irvine, 2017

Professor Scott Douglas Rychnovsky, Chair

The first chapter of this thesis illustrates the application of kinetic resolution reagents for determining the absolute configuration. This method utilizes each enantiomer of the kinetic resolution reagent in parallel reactions with the epoxide of interest. The competing enantioselective conversion (CEC) method was initially applied to cyclic six-membered epoxides using ^1H NMR to monitor the conversion of the reactions. The substrate scope was explored with more complex epoxides, as well terminal epoxides. The CEC method was based on a chiral lithium-diamide base. The synthesis of both enantiomers of the diamine base, the substrate scope, and the difficulties encountered will be discussed.

The second chapter discusses the attempt to develop a colorimetric method to use with the competing enantioselective conversion method. This method was meant to compliment the already existing ^1H NMR, TLC, and mass spectrometry detection methods. Aromatic bases and aromatic acyl sources were initially explored, followed by acetate anion sensors and pH sensors. The CEC method that was used to study these colorimetric options was the acylation of secondary alcohols with the chiral acyl-transfer reagent homobenzotetramisole (HBTM).

Chapters 3–5 discuss the *Lycopodium* alkaloids and the development of a unified approach to synthesizing several members of this family of natural products. The third provides an overview of the past syntheses of select molecules of interest. The fourth chapter discusses the use of computer modeling in inspiring a second-generation approach to a molecule previously synthesized by our group: (+)-fastigiatine. The fifth, and final chapter, provides the groundwork for a unified approach to synthesizing lyconadin A–E. The screening of conditions, the challenging steps, and the current progress will be discussed.

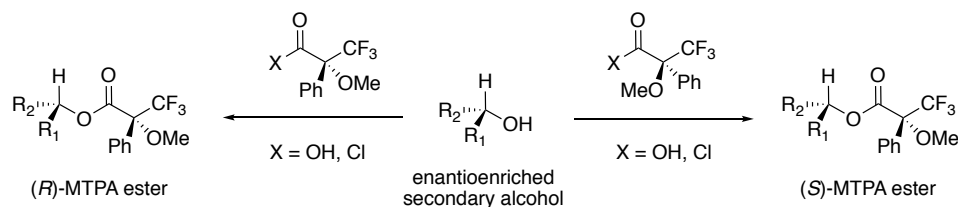
Chapter 1. Determining the Absolute Configuration of Chiral Epoxides Using the Competing Enantioselective Conversion Method

1.1 Introduction to Chirality

Even before the discovery of chiral molecules by chemist Louis Pasteur in 1848, during his experiments with the sodium ammonium salt of tartaric acid, chirality played a crucial role in many areas of biology and chemistry. Our bodies, the foods we eat, the drugs we take, and the numerous molecules we interact with daily all contain chiral molecules. Unfortunately, while chiral molecules may be abundant outside of a laboratory, the synthesis, isolation, and characterization of one enantiomer of a chiral molecule in the laboratory can be a challenging task. In particular, the characterization of the relative and absolute configuration of these organic molecules is a vital part of the synthesis of new organic compounds. Current methods for determining the absolute configuration of a chiral molecule include the Mosher analysis,^{1, 2} X-ray crystallography,³ circular dichroism,⁴ chiral lanthanide shift reagents,⁵ Kishi's NMR spectroscopy method,⁶ and Horeau's method.^{7, 8}

The most common technique used by chemists for determining the absolute configuration of secondary alcohols and primary amines is Mosher's method (Scheme 1.1). Treatment of a single enantiomer of the substrate with both the (*R*) and (*S*)-enantiomers of 2-methoxy-2-phenyl-2-trifluoromethylacetic acid or acid chloride in separate reaction vessels yields the MTPA ester or amide. These derivitized compounds are diastereomers of each other, and show chemical shift differences upon analysis of the two NMR spectra (¹H or ¹⁹F).^{2, 9} While this approach has found wide-spread use as a practical method, it also requires that the original compound be derivitized and is limited to secondary alcohols or primary amines on a secondary carbon atom.

Scheme 1.1: Representative scheme of the Mosher method for determining absolute configuration of secondary alcohols.



X-ray crystallography is another common method for determining the absolute configuration of a chiral molecule. A crystal of the compound is bombarded with X-rays generating a diffraction pattern; this pattern is used to establish an electron density map which can be correlated with the compound to identify the absolute configuration. This method is limited by the need for a crystal of suitable size and purity. In addition, even if a crystal can be grown, compounds with only light atoms may not provide a significant diffraction intensity difference to determine the absolute configuration.³

1.2 Introduction to the Competing Enantioselective Conversion (CEC) Method

Enantioselective catalysis and kinetic resolution methodology¹⁰ has seen tremendous advances in the past few decades. The increasing need for reliable and simple methods for determining the absolute configuration of chiral centers has prompted our lab to develop the Competing Enantioselective Conversion (CEC) method.

The CEC method is based upon the concepts that drive kinetic resolution reactions, namely that both enantiomers of a compound react at different rates when reacting with a single enantiomer of another compound. In a traditional kinetic resolution, a racemic substrate (S_S and S_R) is reacted with a single enantiomer of a chiral kinetic resolution reagent (cat_S). The energy difference between the two diastereomeric transition states ($\Delta\Delta G^\ddagger_A$) is responsible for the product distribution (P_S and P_R), thus leading to enantioenrichment of the original substrate

(Figure 1.1). The diastereomeric catalyst/substrate pair with the lower transition state energy (ΔG^\ddagger) will result in a higher yield of the product and is denoted the “matched” pair. The higher transition state energy and lower product yield and is denoted the “mismatched” pair. The lower energy transition state is typically a result of favorable orbital overlap, stabilizing intermolecular interactions, or minimized steric interactions. If the enantiomer of the chiral kinetic resolution reagent (cat_R) is used, the same energetic profile for the kinetic resolution is expected; however, with the opposite enantiomer of the substrate leading to the matched catalyst/substrate pair. The concept of matched and mismatched enantiomers of a catalyst/substrate was critical for the development of the CEC method.

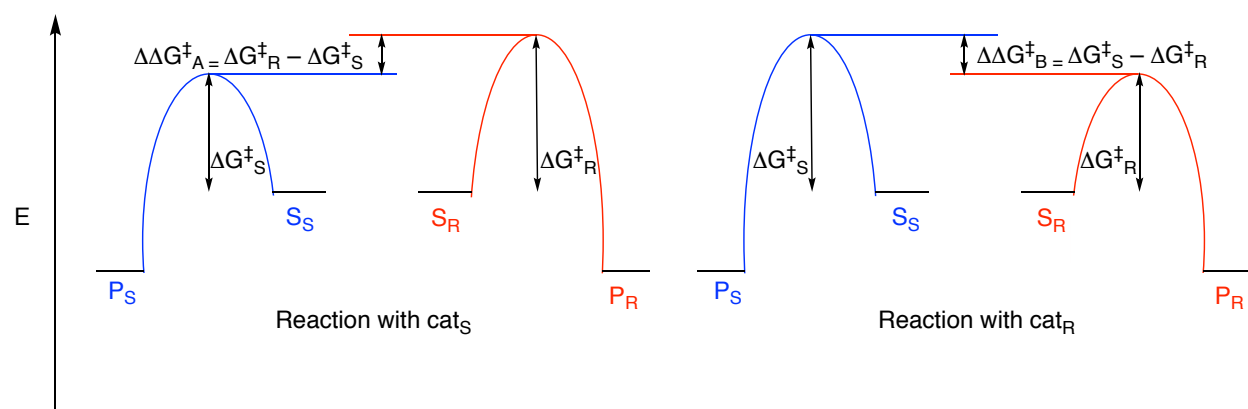


Figure 1.1: Energy diagram for a kinetic resolution of substrate (S) to product (P) utilizing either enantiomer of the kinetic resolution reagent (cat_S or cat_R).

The CEC method takes the concept of matched and mismatched enantiomers of a catalyst/substrate and switches the roles performed. Instead of using both enantiomers of a substrate (racemic) and a single enantiomer of the kinetic resolution reagent, the CEC method utilizes a single enantiomer of substrate (S_S or S_R) and both enantiomers of the chiral kinetic resolution reagent (cat_S and cat_R) (Figure 1.2). These side-by-side reactions exhibit a similar matched/mismatched catalyst/substrate energetic profile to the kinetic resolution.

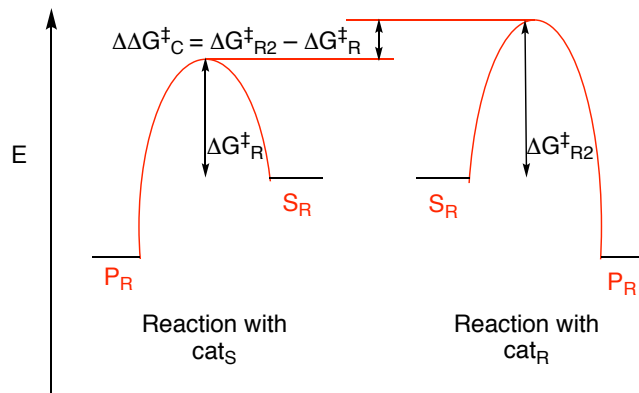


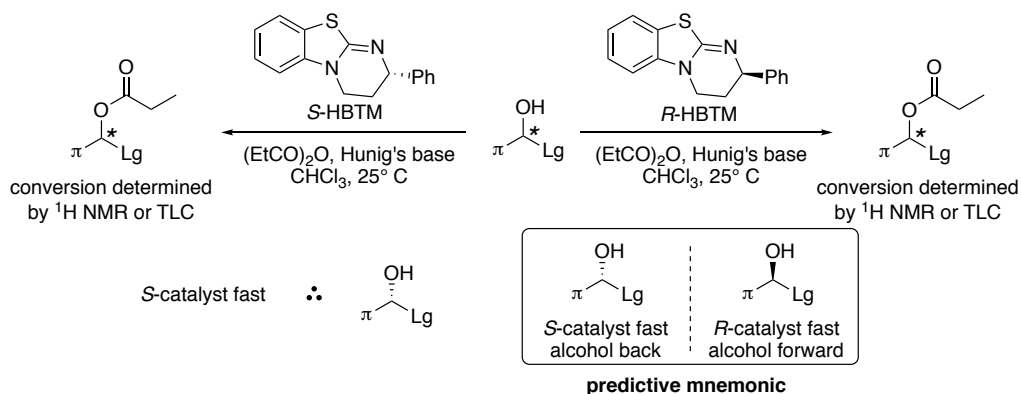
Figure 1.2: Energy diagram comparing the transition state energy of the side-by-side CEC reactions of substrate (S_R) with either enantiomer of the catalyst (cat_S or cat_R) to form product (P_R).

Examining the transition state energies (ΔG^\ddagger_R and ΔG^\ddagger_{R2}) of each reaction of substrate S_R with both enantiomers of catalyst, we see that the difference in transition state energies ($\Delta\Delta G^\ddagger_C$) will lead to a higher conversion to product P_R when substrate S_R reacts with cat_S than when substrate S_R reacts with cat_R . Using the opposite enantiomer of substrate S_R , we would expect equal and opposite reactivity, leading to a lower transition state energy and higher conversion to P_R with cat_R . This theoretical concept laid the foundation for the CEC method. In practice, determining the absolute configuration of a chiral molecule depends on identifying the “matched” or fast-reacting catalyst.

Initial experiments were pioneered by Dr. Alex Wagner in our lab¹¹ and utilized the kinetic resolution catalyst homobenzotetramisole (HBTM) developed by Birman for the acylation of secondary alcohols.¹² Side-by-side reactions of the enantioenriched alcohol are reacted with both enantiomers of the HBTM catalyst, and after a predetermined time period, the conversion of the two reactions is determined by ^1H NMR (Scheme 1.2). The configuration of the alcohol can then be determined based on a developed mnemonic. Substrates of known absolute configuration are either purchased or synthesized using known methods, and the

mnemonic is developed by screening these substrates and analyzing the trend in catalyst reactivity. In theory, once the mnemonic is developed, a researcher could run a CEC reaction on a substrate with similar structural motifs and determine the absolute configuration based on which catalyst reacted faster. The relative “fast” and “slow” reactions can be determined by reaction conversion using a variety of characterization techniques such as ^1H NMR,^{11, 13} TLC,^{14, 15} and mass spectrometry.¹⁶ In theory, the CEC method is applicable to any functional group with a developed kinetic resolution catalyst. In addition to secondary alcohols, our lab has continued to develop CEC protocols for primary alcohols, primary amines,¹⁶ secondary amines, lactams/oxazolidinones.¹⁷

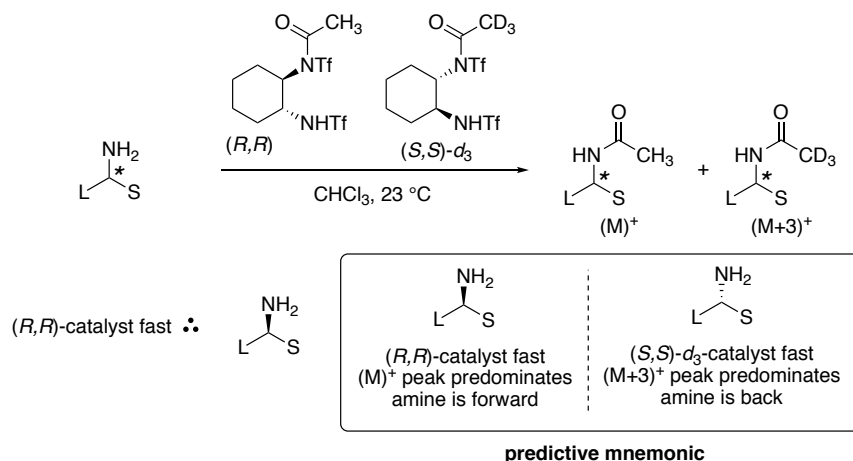
Scheme 1.2: Acylation of a secondary alcohol in side-by-side reactions utilizing both enantiomers of HBTM; example of the predictive mnemonic used to determine absolute configuration.



The next step was to apply the CEC method to amines, since they are one of the most common functional groups found in pharmaceuticals and natural products. Due to the enhanced reactivity of amines, a stoichiometric use of anhydride with the HBTM system was not a feasible approach; instead, use of a stoichiometric kinetic resolution reagent was required (Scheme 1.3). Initially, both pseudoenantiomers of Mioskowski's enantioselective acetylating reagent were used along with ^1H NMR to determine reaction conversion. It was found that by using one deuterio and one proteo pseudoenantiomer of the acetylating reagent, the resulting ratio of the

$[M]^+$ and $[M+3]^+$ peaks in mass spectrometry (MS) could provide the identity of the faster reacting pseudoenantiomer, and thus the configuration of the amine. Through the use of a more sensitive characterization technique, not only was the assignment of amines on nanomole-scale possible, but also the absolute configuration of multiple substrates within the same reaction.

Scheme 1.3: CEC reaction of primary amine with both pseudoenantiomers of acylation catalyst; example of the predictive mnemonic used to determine absolute configuration.



With developed methods for alcohols, amines, and lactams/oxazolidinones, our lab set out to develop a method for determining the absolute configuration of chiral epoxides. Previous work by Dr. Maureen Reilly in our group attempted to develop a method using Co or Cr-salen complexes (Figure 1.3) to selectively open up epoxides utilizing the Jacobsen hydrolytic kinetic resolution (HKR) (Scheme 1.4).

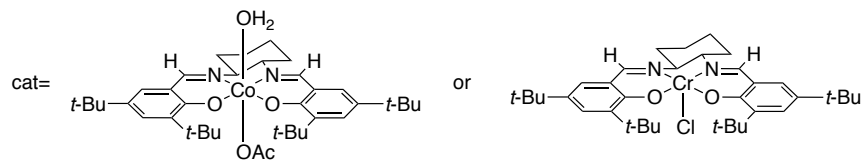
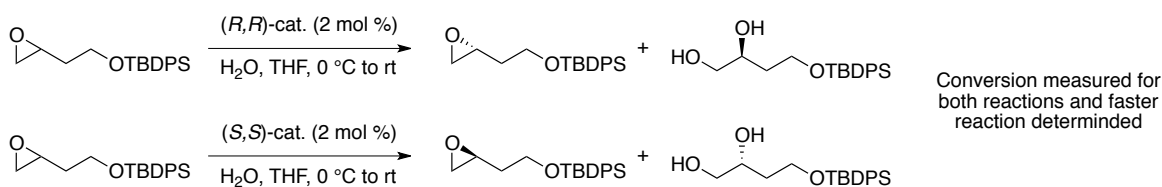


Figure 1.3: Possible catalysts for the enantioselective opening of chiral epoxides utilizing a HKR.

Scheme 1.4: Enantioselective opening of chiral epoxides utilizing HKR.



Developing a method around the HKR was advantageous due to the commercial availability or facile synthesis of terminal epoxides. In addition, both enantiomers of the chiral salen complexes are commercially available or easily synthesized, afford high enantioselectivity, and have been extensively studied. Unfortunately, the development of a suitable analytical technique hindered the use of HKR for our method. GC/MS would be ideal for analysis of the reactions; however, the results obtained by GC/MS were too inconsistent for this to be a viable technique with this system. The diol was not observable by GC/MS, and monitoring the disappearance of the starting material was not possible, because standard solutions did not provide the consistent results necessary for a useable calibration curve. ^1H NMR was explored as an analytical technique, but was abandoned due to severe line broadening from the catalyst and low selectivities (s -values) obtained under the required conditions. To monitor the reaction by NMR it was necessary to run the reaction diluted in CDCl_3 . Unfortunately, this lowered the s -value for the reaction compared to the neat kinetic resolution conditions and made ^1H NMR an ineffective analysis method. Due to the issues encountered by using HKR as a method for determining the absolute configuration of chiral epoxides, we decided to explore an alternative method utilizing a chiral diamine kinetic resolution reagent.

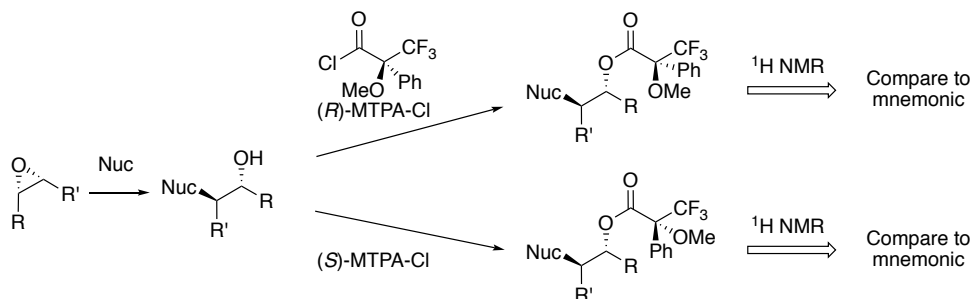
1.3 Developing a CEC Method for Epoxides

While epoxides are not as common in natural products, they have become useful synthons for the synthesis of many natural products. Numerous methods to form enantioenriched

epoxides from olefins, aldehydes, and other substrates have been developed over the past two decades, including the Jacobsen–Katsuki epoxidation,¹⁸ Sharpless Asymmetric epoxidation,¹⁹ and Shi epoxidation.²⁰ The development of asymmetric epoxidation reactions has increased the synthetic utility of enantioenriched epoxides as a powerful way to introduce adjacent chiral centers, as well as form tertiary alcohols in complex molecules.²¹ Numerous methods to form these stereocenters have been developed; however, in order to be synthetically useful the absolute configuration of the epoxide must be determined.

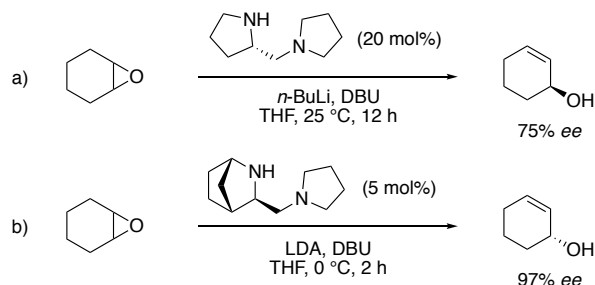
The absolute configuration of epoxides is difficult to establish, because current methods are not general. The most widely established methods for assigning the absolute configuration of epoxides involve two-step procedures in which the epoxide is first opened to give a secondary alcohol and then further modified with chiral derivatizing reagents, or chiral lanthanide shift reagents. The most common chiral derivatizing agent is Mosher's MTPA ester; however, this method is limited to secondary alcohols derived from disubstituted or terminal epoxides (Scheme 1.5).^{2,1} Similarly, chiral lanthanide shift reagents also require formation of the alcohol in order to determine the absolute configuration of epoxides. Another method that has been developed is analysis of the observed Cotton effect of an epoxide using circular dichroism; however, this method is limited to electron-rich, terminal epoxides, making it less useful as an analytical technique.⁴ These current methods are either limited in scope or require manipulation of the epoxide before the absolute configuration can be determined, warranting the need for a more general method.

Scheme 1.5: Epoxide opening and subsequent alcohol derivatization to determine absolute configuration.



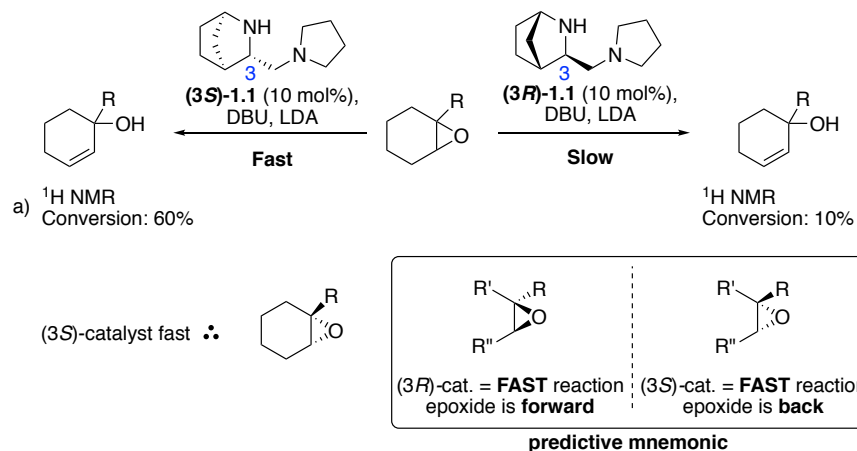
Due to these limitations in the current methodology for determining the absolute configuration of epoxides, the design of a general method that would allow for establishing the absolute configuration directly from the epoxide was desired. The epoxide resolution method established by Asami²² and further developed by Andersson²³ (Scheme 1.6) provided a useful transformation to test out our CEC method.

Scheme 1.6: a) Desymmetrization of cyclohexene oxide using Asami's chiral diamine b) Desymmetrization of cyclohexene oxide by Andersson using a bridged diamine.²⁴



To test the CEC method with this transformation both enantiomers of kinetic resolution catalyst diamine (**3R**)-1.1 and (**3S**)-1.1 would react with the epoxide in side-by-side reactions. After a predetermined period of time, the conversion of the two reactions could be analyzed quantitatively by ¹H NMR or qualitatively by TLC. The faster reacting enantiomer of the catalyst is ascertained by a higher conversion to the allylic alcohol. Based on prior work done by Asami and Andersson a tentative mnemonic was expected (Scheme 1.7).^{25,26}

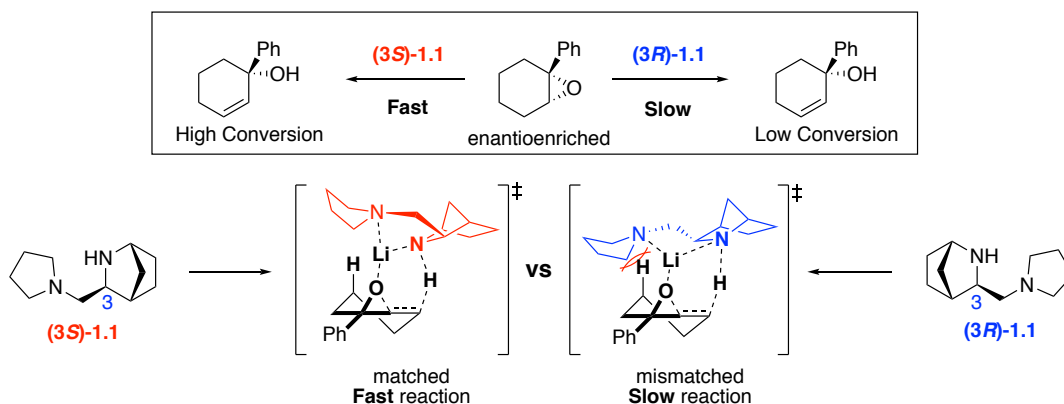
Scheme 1.7: General CEC reactions for the ring opening of the chiral epoxide; predictive mnemonic for assigning absolute configuration.



The anticipated reactivity of each enantiomer of the catalyst with the substrate is driven by steric repulsion between the γ -substituents on the cyclic epoxide interacting with the pyrrolidine ring of the catalyst in the transition state (Scheme 1.8).^{25,26} Diamine **1.1**, which contains the rigid azanorbonyl motif, was selected as the catalyst system, because it has shown >90% ee at 55% conversion for the desymmetrization of *meso*-epoxides and is available as both enantiomers.²⁴ Our method uses catalytic diamine **1.1** and lithium diisopropylamide (LDA) as a stoichiometric base to form **Li-1.1**, which then performs a β -elimination of the chiral epoxide (Scheme 1.8).

Lithium-amide bases have been shown to coordinate with epoxides and effect *syn*- β -elimination to produce allylic alcohols.^{27,25} Selectivity is achieved by minimizing steric interactions during epoxide and lithium-amide coordination that leads to β -elimination (Scheme 1.8). Extensive kinetic studies by Andersson and Dinér have shown the transition state to include one molecule of **Li-1.1**, one molecule of epoxide, and one molecule of solvent or DBU.^{25,28}

Scheme 1.8: Proposed transition states for the reaction of the chiral epoxide with both enantiomers of deprotonated diamine catalyst **Li-1.1**. Solvent or DBU left out for clarity.



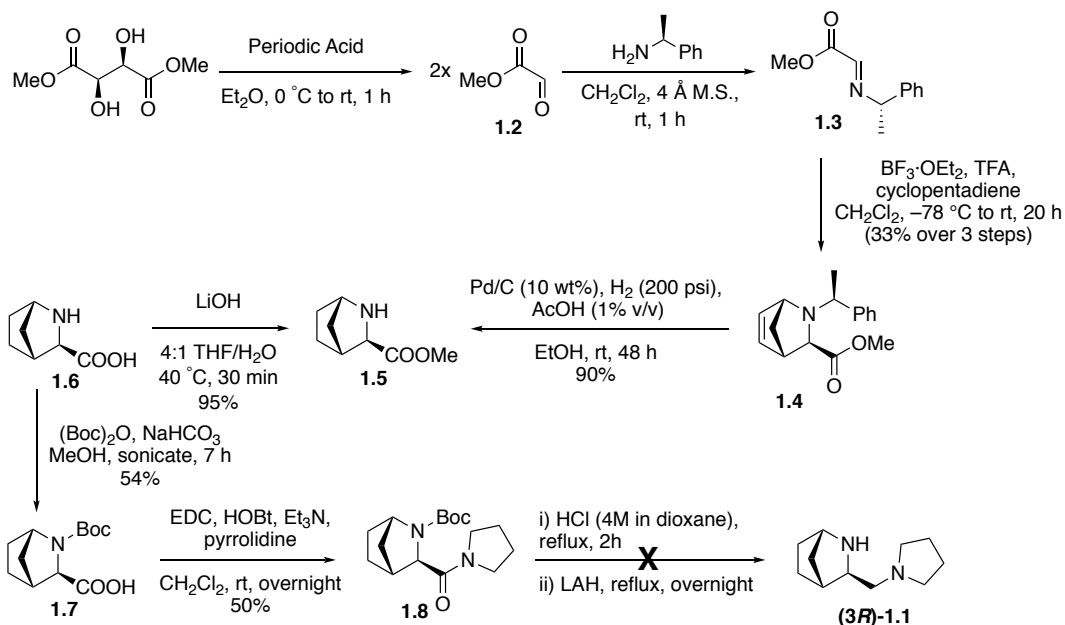
The CEC method utilizes the difference in rate caused by the steric interactions, allowing for the determination of the absolute configuration of the epoxide. Efforts towards the synthesis of both enantiomers of diamine **1.1** and the development of a new method for determination of the absolute configuration of epoxides are discussed in this report.

1.4 Synthesis of the Chiral Diamine Catalyst

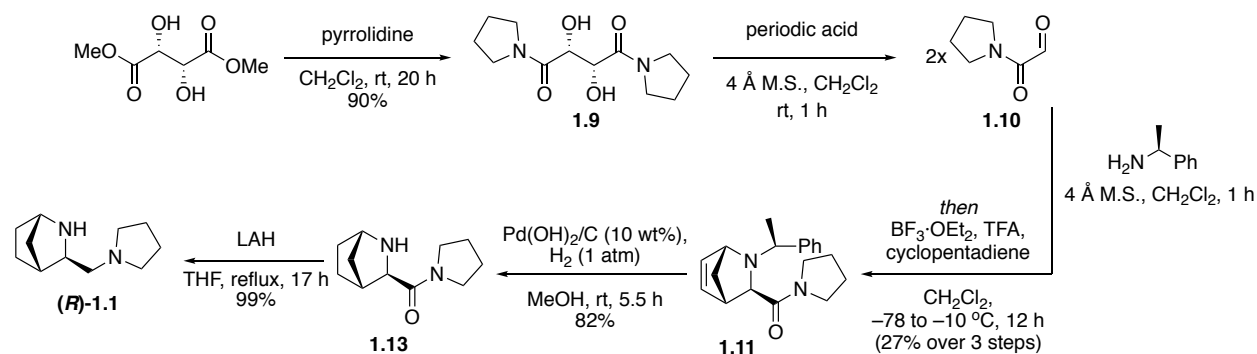
Diamine catalyst **1.1** has been previously synthesized by the Andersson group from dimethyl *L*-tartrate in seven steps (Scheme 1.9).²⁴ Oxidative cleavage of dimethyl *L*-tartrate with periodic acid yielded the methyl glyoxylate **1.2**, which was immediately condensed with α -methylbenzylamine to form imine **1.3**. The enantiomer of α -methylbenzylamine that is used dictates which enantiomer of Diels-Alder adduct **1.4** that is formed, and ultimately the enantiomer of catalyst **1.1** that is formed. Bicycle **1.4** was then hydrogenated to remove both the double bond and deprotect the amine. Methyl ester **1.5** was then hydrolyzed to the carboxylic acid **1.6**, and Boc protected to yield **1.7**. Standard amino acid coupling conditions with pyrrolidine provided amide **1.8**, however, attempts to cleanly deprotect the amine and reduce the

amide to form **(3R)**-**1.1** were not successful. The previously described route was abandoned as it was discovered that the Andersson group had published on a more concise synthesis.²⁹

Scheme 1.9: First generation synthesis of chiral diamine catalyst **(3R)**-**1.1**.



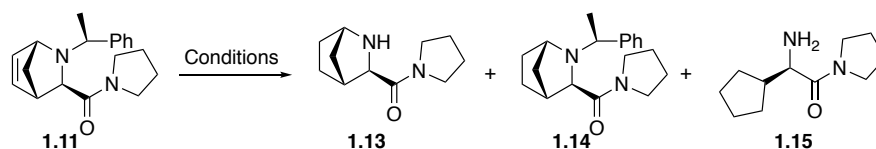
Scheme 1.10: Synthesis of **1.1** via the revised route.



The revised synthesis (Scheme 1.10) contains several attractive features, including fewer steps, no protecting groups, and an overall higher yield. Crucially, this route also maintains the diastereoselective aza-Diels–Alder reaction derived from *(R)*- or *(S)*- α -methylbenzylamine, thus providing a route to both enantiomers of the catalyst. Diamide **1.9** can be formed by addition of pyrrolidine to dimethyl *L*-tartrate according to a literature procedure.³⁰ Oxidative cleavage with

periodic acid to form **1.10**, followed by formation of imine, and the aza-Diels–Alder reaction yielded 4.80 g of **1.11** as the pure *exo*-diastereomer by NMR after recrystallization. Palladium catalyzed hydrogenation and deprotection formed amide **1.13**, followed by LAH reduction to afford diamine (**3R**)-**1.1**. The hydrogenation and deprotection proved to be troublesome, due to the formation of products **1.14** and **1.15** (Table 1.1). It was found that acidic conditions favored the formation of the ring-opened product **1.15**, while basic conditions favored formation of the hydrogenated but not debenzylated product **1.14**.³¹ The transfer hydrogenation reagents ammonium formate, hydrazine, and cyclohexene were also attempted; however a mixture of products was observed.^{32,33} A solvent screen of EtOH, THF, and MeOH showed MeOH to provide the cleanest reaction.

Table 1.1: Select reactions in the optimization of the hydrogenation and deprotection procedure to produce **1.13**.



entry	conditions	product	% yield (1.13)
1	Pd(OH) ₂ /C (20 wt%), H ₂ (1 atm), MeOH, rt, 4 h	1.13	98
2	Pd(OH) ₂ /C (20 wt%), H ₂ (1 atm), EtOH, rt, 4 h	2.8:1 1.13 : 1.15	82
3	Pd(OH) ₂ /C (20 wt%), H ₂ (1 atm), THF, rt, 21.5 h	4.7:1 1.13 : 1.15	50
4	Pd/C (10 wt%), HCO ₂ NH ₄ , MeOH, reflux, 45 min	1:3:1.4 1.13 : 1.14 : 1.15	21
5	Pd/C (10 wt%), N ₂ H ₄ , EtOH, reflux, 3 h	1:2.5:2.1 1.13 : 1.14 : 1.15	23
6	Pd/C (20 wt%), H ₂ (1 atm), AcOH (27% v/v), EtOH, rt, 21 h	1.15	76 (1.15)
7	Pd(OH) ₂ /C (20 wt%), H ₂ (1 atm), K ₂ CO ₃ , MeOH, rt, 42 h	1.14	
8	Pd(OH) ₂ /C (20 wt%), cyclohexene, EtOH, rt, 25 h	no reaction	
9	Na/NH ₃ , THF, -78 °C, 90 min	decomposition	
10	Li, (H ₂ NCH ₂) ₂ , Et ₃ N, THF, rt, 2 h	decomposition	

Unfortunately, when the hydrogenation and deprotection reactions were scaled up, mixtures of **1.13**, **1.14**, and **1.15** were again an issue. Due to their highly polar nature and their similar elution characteristics on silica, separating these substrates proved to be a challenge.

Instead, by taking advantage of the different acid/base characteristics of each of these species a series of buffered washes was developed based on studies done by Jha.³⁴ It was found that dissolving the mixture of compounds **1.13**, **1.14**, and **1.15** in CH₂Cl₂ and extracting with pH 7.0 sodium monophosphate buffer isolated **1.13** in the aqueous layer from **1.14** and **1.15**. Washing the aqueous layer with additional CH₂Cl₂ removed any last traces of **1.5**, and after free basing the aqueous layer, pure **1.13** could be extracted with CH₂Cl₂. Not only did this procedure cut down on the time and waste associated with running the column, but it also allowed the formation of **1.1** without the need for column chromatography after the LAH reduction. This removed the final chromatographic purification step from the synthesis.

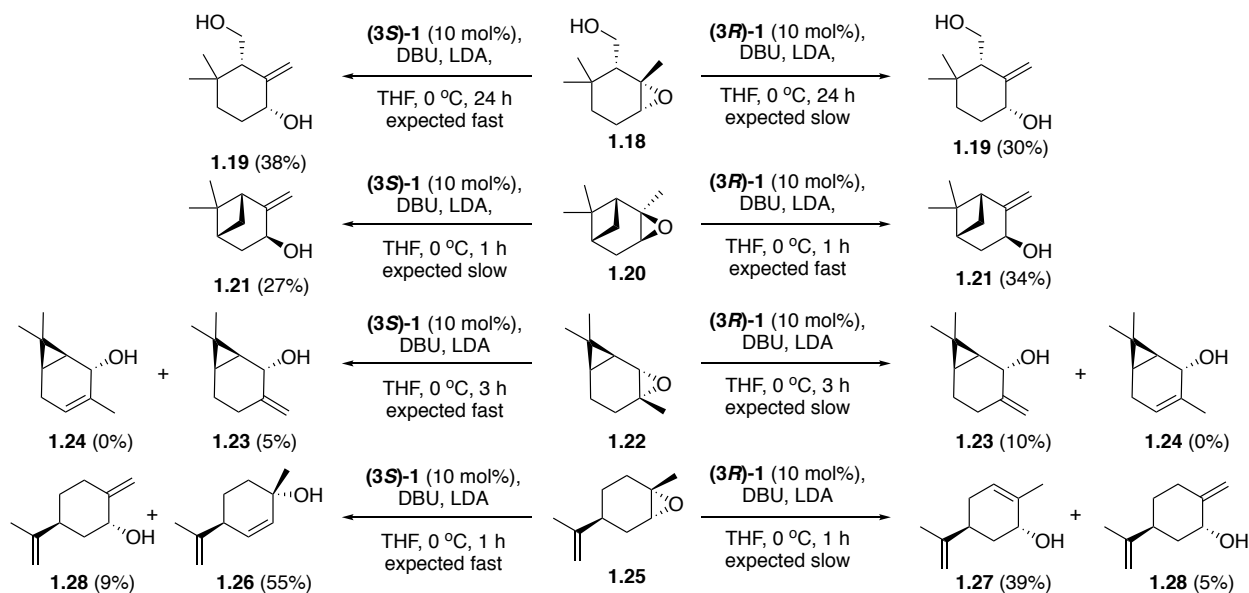
Once conditions for the synthesis and purification of **1.13** were optimized, LAH reduction of the amide gave pure **(3R)-1.1** in 20% overall yield (Scheme 1.10). The **(3S)-1.1** diamine was synthesized in 26% overall yield following the same procedure as **(3R)-1.1**; using the (*R*)-enantiomer of α -methylbenzylamine in the aza-Diels–Alder reaction (SI substrates **1.9**, **1.10**, **1.16**, and **1.17**). This route provided sufficient quantities of both **(3R)-1.1** and **(3S)-1.1** to carry out testing of our proposed method.

1.5 Synthesis of Cyclic Epoxides and Initial CEC Reactions

With the two enantiomers of catalyst **1.1** synthesized, we investigated the viability of our proposed method on chiral epoxides. Initially our efforts were focused on enantioenriched epoxides that could be made in few steps. Epoxide **1.18**, was synthesized according to the procedure by Vidari and co-workers,^{35–38} α -pinene oxide **1.20**³⁹ and (2)-carene oxide **1.22**, were synthesized diastereoselectively with *m*-CPBA, and *cis*-(*S*)-(-)-limonene oxide **1.25** was synthesized by a kinetic resolution developed by Singaram;⁴⁰ all are useful intermediates in the

synthesis of several natural products and fine chemicals.⁴¹ The ease of synthesis and their prevalence in the literature made these epoxides ideal test substrates to test out an epoxide CEC method (Scheme 1.11).

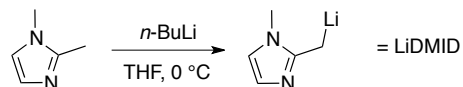
Scheme 1.11: Ring opening of epoxides **1.18**, **1.20**, **1.22**, and **1.25** with diamine catalysts. Conversion by ¹H NMR.



The expected β -elimination to form the internal alkene was only observed for epoxide **1.25**. Instead, elimination of the methyl proton was the predominant product. Elimination of the methyl proton is known for these types of substrates, so a set of control reactions were run with LDA and LDA/DBU to verify the extent of non-selective elimination by our stoichiometric base.^{35–37,39,42,43} Formation of *trans*-pinocarveol **1.21** occurred in 20% and 37% respectively over one hour when LDA or LDA/DBU was used. These control experiments show that elimination by the stoichiometric base alone was comparable to the reaction with the chiral diamine, suggesting that the small difference in reaction conversions is not due to selectivity differences between the enantiomers of the chiral catalyst. Alternative stoichiometric bases were considered to mitigate elimination by the non-chiral base.

Ahlberg studied the effect of different stoichiometric bases on the desymmetrization of cyclohexene oxide.⁴⁴ It was found that the stoichiometric base 2-(lithiomethyl)-1-methylimidazole (LiDMID) (Scheme 1.12) was effective at regenerating the chiral lithium amide, without participating in non-enantioselective elimination of the epoxide.

Scheme 1.12: Formation of stoichiometric base LiDMID from 1,2-dimethylimidazole.



The new stoichiometric base was then tested out with epoxides **1.18**, **1.20**, **1.22**, and **1.25** to see whether the selectivity of the reaction would improve (Table 1.2). Control experiments with LiDMID/DBU showed little reduction of external alkene for epoxide **1.18** or **1.25** (Table 1.2, entry 1 and 4); however, epoxide **1.20** and **1.22** showed a significant reduction in external alkene (Table 1.2, entry 2 and 3). When epoxides **1.18** and **1.20** were tested under the CEC conditions with LiDMID neither selectivity between the two catalyst, or formation of the internal alkene were observed, suggesting that the sterics of these epoxides disfavor elimination even by the matched diamine catalyst. Epoxides **1.22** and **1.25** showed significant selectivity between the two enantiomers of the catalyst. Formation of the elimination product **1.24** and *trans*-carveol **1.27** from the more hindered side of the trisubstituted epoxide was observed for both of these substrates.

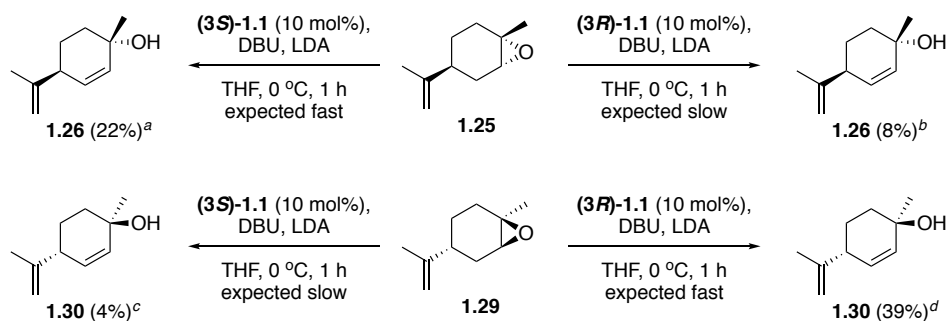
entry	epoxide	time (hour)	base	control	%conversion (3 <i>S</i>)-1.1	%conversion (3 <i>R</i>)-1.1
1	1.18	3	LiDMID	15 (1.19)	28 (1.19)	24 (1.19)
2	1.20	1	LiDMID	5 (1.21)	6 (1.21)	5 (1.21)
3	1.22	3	LiDMID	11 (1.23)	3 (1.23), 91 (1.24)	7 (1.23), 80 (1.24)
4	1.25	1	LiDMID	3 (1.27)	42 (1.26), 8 (1.28)	37 (1.27), 5 (1.28)

Table 1.2: Ring opening of epoxides **1.18**, **1.20**, **1.22**, and **1.25** with LiDMID, DBU with or without (control) diamine **1** catalysts to the corresponding allylic alcohols.

Even though unexpected allylic alcohols are formed for epoxides **1.22** and **1.25**, the allylic alcohols formed in both reactions match our model for the fast reacting enantiomer of the catalyst; allowing us to correlate our results back to the absolute configuration of the starting epoxide. Based on observations for these epoxides, when sterics of the epoxide slow the reaction with the chiral diamine, elimination of the external hydrogen by the stoichiometric base predominates. The observed result that epoxide **1.25** formed the internal alkene, even in the presence of LDA, suggests that formation of the internal alkene is favored, unless steric bulk or constrained geometry slows this elimination pathway.

Limonene oxide was chosen as an ideal substrate to test both enantiomers to establish if the diamine catalysts **1.1** are showing equal and opposite reactivity. The enantiomer of **1.25** was synthesized utilizing the kinetic resolution starting with (+)-limonene oxide to yield **1.29**. When subjected to the CEC conditions there was an obvious opposite reactivity with the catalyst, with **1.25** reacting faster with the (**3S**)-**1.1** and **1.29** reacting faster with (**3R**)-**1.1** (Scheme 1.13). This opposite reactivity matches the expected mnemonic; however, the two substrates varied in their conversion to the allylic alcohol. Further work is needed to determine the source of this discrepancy.

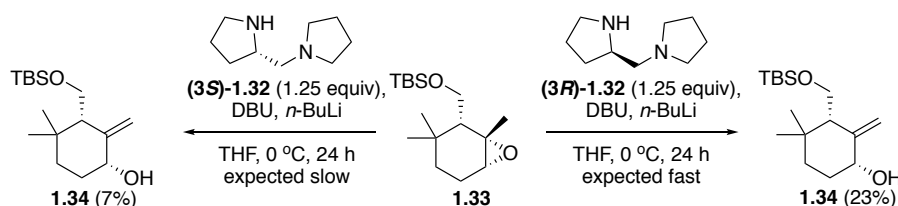
Scheme 1.13: CEC reaction with both enantiomers of limonene oxide **1.25** and **1.29**.



a: Contained 26% of triolefin **1.27** and 22% external olefin **1.28** *b*: Contained 19% of triolefin **1.27** and 8% external olefin **1.28** *c*: Contained 20% of triolefin **1.31** and 2% external olefin **1.32** *d*: Contained 14% of triolefin **1.31** and 13% external olefin **1.32**.

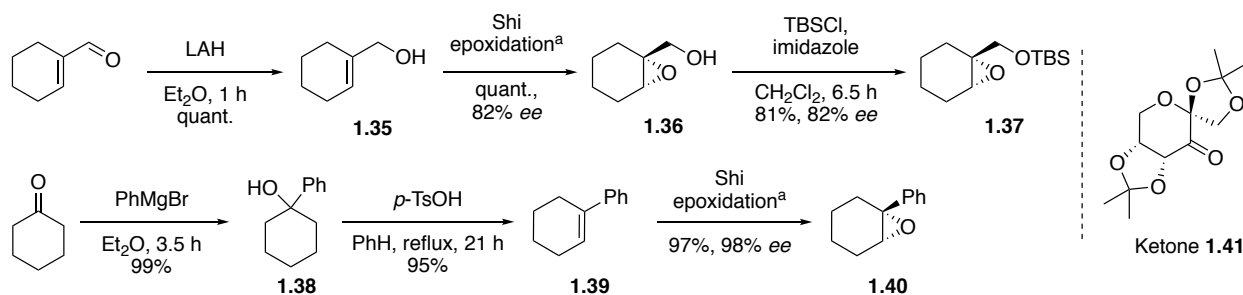
To investigate whether the free alcohol on **1.18** was an issue in the reaction, the substrate was protected (**1.34**). Epoxide **1.18** showed no internal elimination in initial reactions. It was hypothesized that either the free alcohol was participating in the elimination, or the stoichiometric base was causing the elimination instead of the chiral diamine base. To test this, chiral diamine base was used stoichiometrically instead of catalytically (Scheme 1.14). We chose to go with the chiral diamines **1.32** developed by Asami due to their commercial availability.^{22,45} After three hours under CEC conditions epoxide **1.33** went to a higher conversion to the exo-alkene with (**3R**)-**1.32**. This is the expected fast catalyst, for the chiral diamine is performing a β -elimination of proton from the external methyl group. This result was promising, as it suggested that cases where an achiral stoichiometric base participates in the elimination could be mitigated by using stoichiometric chiral base instead. Only exo-olefin **1.34** was observed, suggesting that the internal olefin is not preferred, even with the protected alcohol.

Scheme 1.14: CEC reaction of epoxide **1.33** with Asami's chiral diamine **1.32**.



Implementing the lessons learned from previous epoxide work, new epoxides were synthesized and tested (Scheme 1.15). Epoxides **1.37** and **1.40** were chosen as suitable substrates because they could be accessed in a few steps and with high enantiopurity using the Shi epoxidation.²⁰

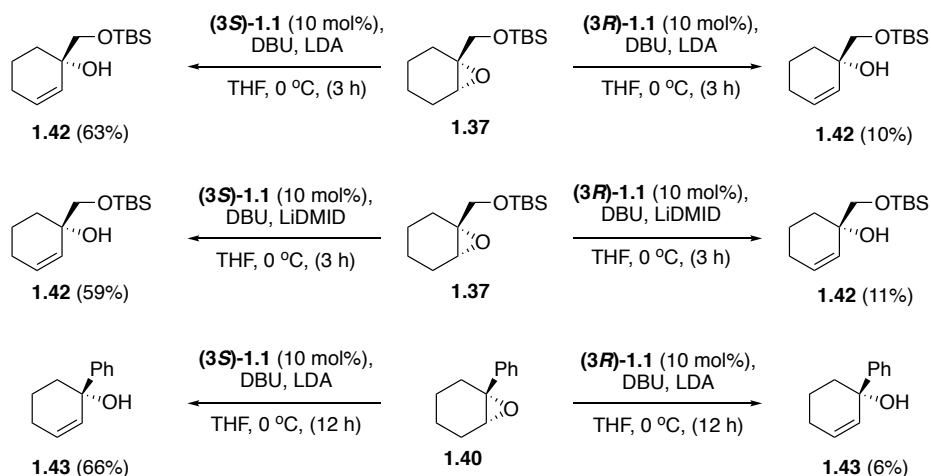
Scheme 1.15: Synthesis of epoxides **1.37** and **1.40**.



^a Shi epoxidation conditions: Ketone **1.41**, Na₂B₄O₇·10H₂O buffer, Bu₄NH₄HSO₄, Oxone, K₂CO₃, 2:1 DMM/acetonitrile, -10 °C, 3 h.

Both epoxides **1.37** and **1.40** showed significant selectivity between the two enantiomers of the diamine catalyst (Scheme 1.16). In both cases the **(3S)**-**1.1** is the predicted fast catalyst based on the epoxide going back, and experimental results match with the **(3S)**-**1.1** reacting faster for both epoxides **1.37** and **1.40**.

Scheme 1.16: CEC and control reactions with epoxides **1.37** and **1.40** to form allylic alcohols **1.42** and **1.43** respectively. Control reactions without chiral diamine showed only starting material.

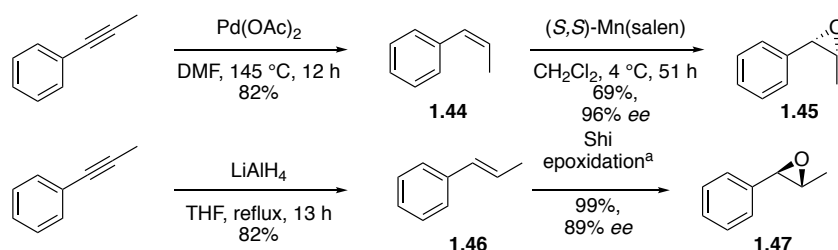


For epoxide **1.37**, no elimination to form the external olefin was observed with either LDA or LiDMID. This result suggests that compared to the methyl substituted epoxides, the bulky TBS group prevents elimination from external hydrogens. No reaction was observed for

control reactions with epoxide **1.40** and LDA or LDA/DBU, highlighting observations by Asami that elimination of the internal hydrogen is significantly faster with the diamine than the stoichiometric base.⁴⁵ Based on the results from epoxides **1.37** and **1.40**, it is evident that substitution at the epoxide plays a predominant role in which side the elimination can occur. With bulkier 1-substituted epoxides (**1.37** and **1.40**) elimination was observed from only a single side of the epoxide, whereas with smaller 1-methyl substituted epoxides (**1.22** and **1.25**) elimination could occur from either side. With these results, we decided to test two acyclic epoxides.

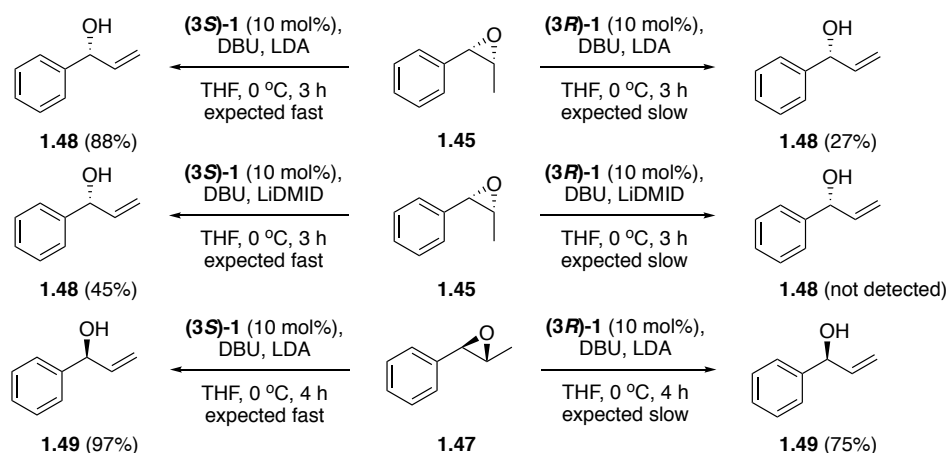
Acyclic epoxides **1.45** and **1.47** were both synthesized in two steps from 1-phenyl-1-propyne (Scheme 1.17). Pd(OAc)₂ transfer semihydrogenation to the *cis*-alkene,⁴⁶ followed by Jacobsen epoxidation afforded epoxide **1.45**.⁴⁷ Epoxide **1.47** was synthesized by LAH reduction of the alkyne to the *trans*-alkene **1.46**, followed by Shi epoxidation.²⁰

Scheme 1.17: Synthesis of epoxides **1.45** and **1.47**.



The similar orientation to previously tested cyclic epoxides led us to predict that *cis*-epoxide **1.45** would follow the previously established mnemonic. CEC reactions with both *cis* and *trans*-epoxides showed selectivity, with the (**3S**)-**1** diamine enantiomer proceeding to higher conversions for both epoxides (Scheme 18).

Scheme 1.18: CEC reactions with epoxides **1.45** and **1.47** to form allylic alcohols **1.48** and **1.49**.

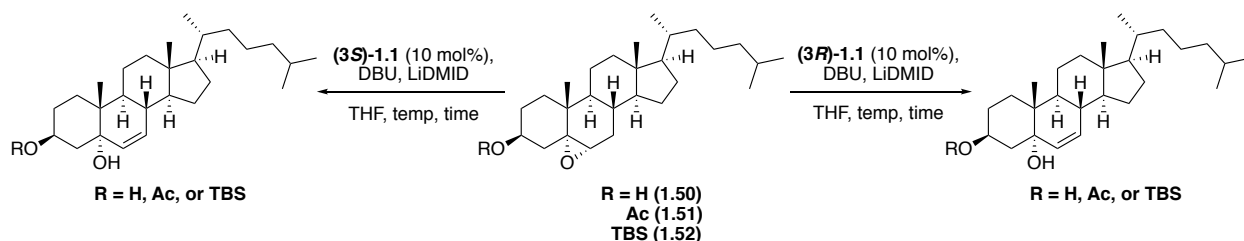


While both epoxides showed significant selectivity when the CEC reactions were run with LDA, testing *cis*-epoxide **1.45** with LiDMID showed an increased difference in percent conversion. This result suggests that while background elimination by LDA is present, it is outcompeted by the chiral diamine base.

Cholesterol was chosen as a substrate to test our method on larger, more complex, ring systems. Cholesterol and its derivatives can be epoxidized to form either the α or β -epoxide with reasonable diastereoselectivity.^{48–50} Several α -epoxides were synthesized and tested with the CEC method (Table 1.4). Epoxide **1.50**, **1.51**, and **1.52** were epoxidized with 81:19, 71:39, and 80:20 α : β selectivity, respectively, using *m*-CPBA. Under the established CEC conditions, epoxide **1.50** failed to yield any product after three hours. To rule out that the free alcohol was preventing the reaction from occurring, cholesterol acetate was epoxidized and tested. Unfortunately, under the reaction conditions, epoxide **1.51** was completely deacylated within one hour. The more robust TBS protected epoxide **1.52** was synthesized from TBS protected cholesterol **1.52a**. CEC reactions at 0 °C and 25 °C failed to yield any allylic alcohol; higher

temperatures were not attempted since lower temperatures are important for selectivity between enantiomers of the catalyst, as well as stability of the lithium amide.

Table 1.3: CEC reactions with epoxides **1.50**, **1.51**, and **1.52** with varying temperatures for epoxide **1.52**. % conversion corresponds to both **(3S)**-**1.1** and **(3R)**-**1.1**.



entry	R-group	temp. (°C)	time (hour)	% conversion
1	Ac	0	3	deacylation
2	H	0	1	0
3	TBS	0	3	0
4	TBS	25	1	0

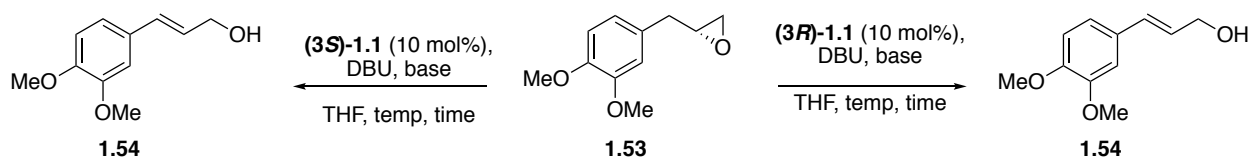
Unfortunately, the same ridged backbone and steric bulk that allowed for diastereoselectivity in epoxidation of cholesterol and the derivatives caused the CEC reactions to fail. Work by Holland and Jahangir on eliminations of epoxy-steroids found that elimination was only possible with smaller lithium amide bases, such as lithium diethylamide; bulkier bases, such as LDA, failed to yield any product.⁵¹ The rigidity of the steroid backbone also hinders the alignment needed to undergo β -elimination of the epoxide. With examples of cyclic epoxides working with our CEC method, we next looked at the possibility of using terminal epoxides with the CEC method.

1.6 Synthesis and CEC Testing of Terminal Epoxides

Due to their usefulness as chiral synthetic intermediates, terminal epoxides were also explored as possible substrates for the CEC method. Enantioenriched terminal epoxides can be easily synthesized from the racemic epoxide using the Jacobsen HKR (Scheme 1.19).⁵² Terminal

epoxide **1** was synthesized from methyl eugenol oxide utilizing the Jacobsen HKR and subjected to CEC conditions. A TLC of the reaction at five minutes showed complete consumption of the starting material. The reaction was then cooled down to $-78\text{ }^{\circ}\text{C}$ to reduce the rate of the reaction so that the selectivity between both enantiomers of catalyst could be elucidated, unfortunately the reaction had still proceeded to high conversions. Due to the small difference between the reactions with **(3S)**-**1.1** and **(3R)**-**1.1** (entry 2) control reactions without the chiral bases were run (entries 3, 4, and 5). With both stoichiometric bases the reaction had reached almost full conversion after five minutes. Due to the high reactivity of the benzylic protons, terminal epoxides without β -benzylic protons were examined.

Scheme 1.19: CEC reactions of **1.53** with catalysts **1.1** at different temperatures and with different stoichiometric bases.

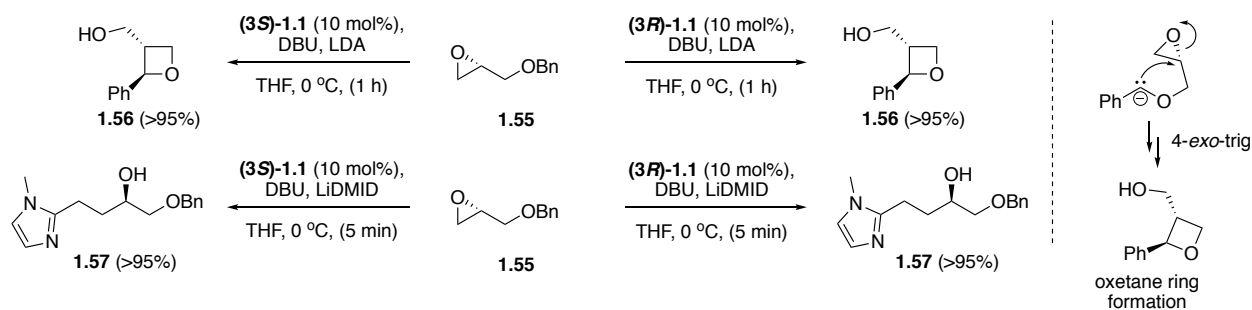


entry	base	temp. ($^{\circ}\text{C}$)	time (min)	% conversion (3S) - 1.1	% conversion (3R) - 1.1	% conversion control
1	LDA	0	5	100	100	–
2	LDA	-78	5	86	82	–
3	LDA	0	5	–	–	100
4	LDA (no DBU)	0	5	–	–	90
5	LiDMID	0	5	–	–	88

Terminal epoxide **1.55** was synthesized by benzyl protection of commercially available (*R*)-glycidol.⁵³ The short distance between the β -protons of the epoxide and the protected alcohol caused concern about the size of the protecting group and whether a large protecting group would prevent elimination due to steric bulk. Benzyl protection was chosen to provide a smaller protecting group; however, this provided issues with competing reaction pathways. The only products observed were oxetane ring **1.56** and nucleophilic epoxide opened product **1.57**

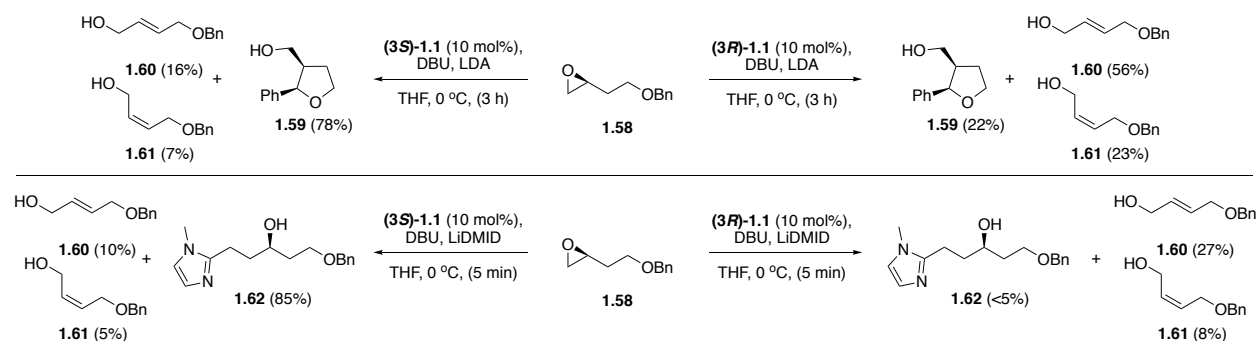
exclusively, with LDA and LiDMID, respectively. Oxetane **1.56** is a result of attack on the epoxide via a 4-*exo*-tet ring closure by the benzyl anion (Scheme 1.20).⁵⁴

Scheme 1.20: CEC reaction of epoxide **1.55** with diamines **1.1**, and formation of oxetane ring **1.56**.



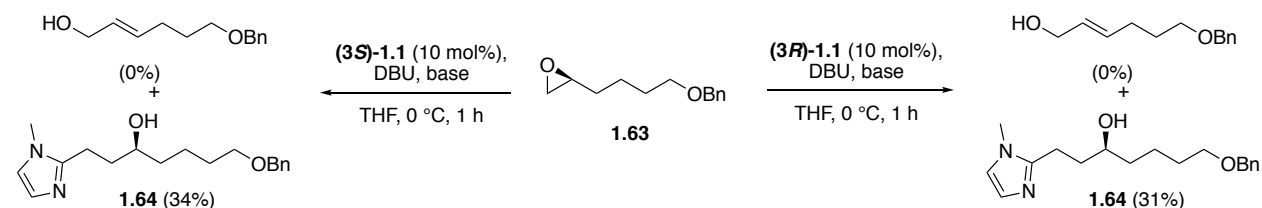
Epoxide **1.58** was synthesized by *m*-CPBA epoxidation of benzyl protected 3-buten-1-ol, followed by the Jacobsen HKR of 2-(2-(benzyloxy)ethyl)oxirane.⁵² When epoxide **1.58** was tested with LDA a mixture of *E*-isomer **1.60**, *Z*-isomer **1.61**, and tetrahydrofuran (THF) product **1.59** were observed. With the **(3R)-1.1** catalyst, more alkene products, **1.60** and **1.61**, were observed, while with **(3S)-1.1** catalyst, more THF **1.59** was observed (Scheme 1.21). When LiDMID was tested the *E* and *Z*-alkene were the major product with the **(3R)-1.1** catalyst, while nucleophilic epoxide-opened product **1.62** was the major product with the **(3S)-1.1** catalyst. It is possible that the **(3R)-1.1** catalyst is the matched catalyst, undergoing higher conversion to the elimination products, while sluggish elimination with the **(3S)-1.1** catalyst favors formation of undesired side products **1.59** and **1.62**. However, without additional testing this cannot be confirmed.

Scheme 1.21: CEC reactions on epoxide **1.58** with both LDA and LiDMID.



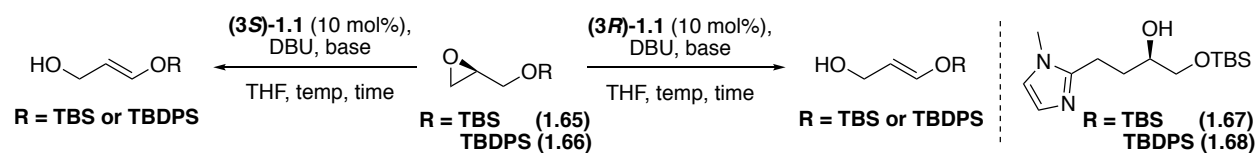
The formation of cyclic ethers **1.56** and **1.62** prompted the use of a longer alkyl chain with the hope that cyclization to produce an oxepane ring would mitigate against the undesired cyclization pathway. Racemic 2-(4-(benzyloxy)butyl)oxirane was found in the Rychnovsky group's homemade chemicals. A Jacobsen hydrolytic kinetic resolution furnished enantioenriched epoxide **1.63**. The CEC was then tested on epoxide **1.63** with both LDA and LiDMID (Scheme 1.22). Surprisingly, no reaction was observed between epoxide **1.63** and LDA, and reaction with LiDMID led solely to ring opened product **1.64**. To mitigate the issues encountered with the benzyl protecting group, silyl protecting groups were tested.

Scheme 1.22: CEC reactions on epoxide **1.58** with both LDA and LiDMID.



Terminal epoxides **1.65** and **1.66** were synthesized by TBS⁵⁵ and TBDMS protection of (*S*)-glycidol, respectively. Upon exposure to CEC conditions TBS protected substrate **1.65** formed the ring opened product **1.67** exclusively, while TBDPS protected substrate **1.66** failed to react (Scheme 1.23).

Scheme 1.23: CEC reactions with epoxides **1.65** and **1.66** with both LDA and LiDMID.



entry	epoxide	base	temp. (°C)	time (hour)	% conversion (3S)-1.1	% conversion (3R)-1.1
1	1.65	LDA	0	1	0	0
2	1.65	LiDMID	0	1	17 (1.67)	34 (1.67)
3	1.66	LDA	0	3	0	0
4	1.66	LiDMID	0	3	0	0
5	1.66	LiDMID	25	3	0	0

1.7 Conclusion

Results for the CEC method for determining the absolute configuration of chiral epoxides have been promising. Difficulties presented by current absolute configuration methods are addressed with our CEC method, since an unknown epoxide can be tested directly. Enantioenriched cyclic and acyclic epoxides show significant selectivity towards the different enantiomers of the chiral diamine catalyst **1.1**. Trisubstituted epoxides are suitable substrates; however, trisubstituted epoxides with external methyl groups tend to give a mixture of elimination products. Use of LiDMID as a stoichiometric base has been shown to reduce elimination from the stoichiometric base and increase selectivity for certain substrates. Use of stoichiometric chiral diamine also shows promise for substrates that undergo facile elimination with the achiral stoichiometric base. Terminal epoxides have shown compatibility issues with the current protecting groups and certain lengths of alkyl chains, limiting a general procedure using the current CEC method.

1.8 Experimental

General experimental and laboratory conditions

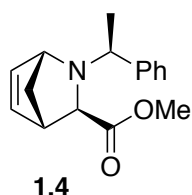
Air and moisture-sensitive reactions were run under an inert atmosphere of argon in flame or oven dried glassware with magnetic stir bars using standard syringe and septa techniques. All commercially available reagents were used as received, with the exception of tetrahydrofuran (THF), diethyl ether (Et₂O), and methylene chloride (CH₂Cl₂), which were degassed with argon and dried using vacuum filtration through activated alumina according to the procedure by Grubbs.⁵⁶ Et₃N was distilled from CaH₂. DBU was distilled from CaH₂ and stored over 3 Å molecular sieves. Pyrrolidine was distilled from BaO. Thin Layer Chromatography (TLC) was performed using Whatman 250 μm layer silica gel glass-backed plates. TLC was visualized with either Dragendorff–Munier, potassium permanganate (KMnO₄) staining solutions, or ultraviolet light. Flash column chromatography was performed according to the method by Still, Kahn, and Mitra⁵⁷ using Millipore Geduran Silica 60 (40–63 μm). Reactions were kept at 0 °C with a Neslab RTE-111 refrigerated bath and a recrystallizing dish filled with isopropyl alcohol.

Instrumentation

Optical rotations were measured on a JASCO DIP-370 digital polarimeter. Infrared spectra were recorded on a Shimadzu MIRacle 10 Single Reflection ATR Accessory. HPLC were recorded on an Agilent 1100 Series. SFC determinations of enantiopurity were performed on a Berger Analytical instrument. NMR spectra were referenced to either CDCl₃ (7.26 ppm) or tetramethylsilane (0.00 ppm); ¹H NMR spectra were recorded at 500 MHz and ¹³C NMR at 125 MHz on either a Bruker Avance 500 with a TCI cryoprobe, GN 500 with a BBO probe, or at 600 MHz and 150 MHz respectively on an Avance 600 with TBI probe. Characterization is presented

as follows: chemical shift, multiplicity (s = singlet, d = doublet, t = triplet, q = quartet, m = multiplet, br = broad, app = apparent), coupling constant(s) in Hertz (Hz), and integration. ^{13}C NMR spectra are reported in ppm relative to CDCl_3 (77.07 ppm). Mass spectra were measured using a MicroMass AutoSpec E, a MicroMass Analytical 7070E, or a MicroMass LCT Electrospray instrument.

(1*S*,3*R*,4*R*)-2-[(1*S*)-1-phenylethyl]-2-azabicyclo[2.2.1]hept-5-ene-3-carboxylic acid methyl ester (1.4):



Experimental: To a three-neck flask, equipped with a mechanical stirrer and addition funnel, was added 4 Å molecular sieves, methyl glyoxylate **1.2** (9.14 g, 104 mmol) and CH_2Cl_2 (346 mL). The vessel was cooled to 4 °C, charged with (*S*)-(-)-methyl phenylamine (26.5 mL, 208 mmol), and stirred for 90 min. The reaction mixture was then cooled to -78 °C followed by sequential addition of trifluoroacetic acid (15.9 mL, 208 mmol), $\text{BF}_3 \cdot \text{OEt}_2$ (25.6 mL, 208 mmol), and freshly cracked cyclopentadiene⁵⁸ (20.9 mL, 249 mmol, diluted in 40 mL CH_2Cl_2) in 10 min intervals, and stirred for 22 h. The resultant reaction mixture was warmed to room temperature, quenched with sat. aq. Na_2CO_3 , and stirred for 3 h. The biphasic mixture was filtered through Celite and the aqueous extracted with CH_2Cl_2 (3 x 100 mL). The combined organic layers were dried over MgSO_4 , filtered, and adsorbed on SiO_2 . The resulting solid was washed with (9:1 EtOAc:pentane) and the filtrate was concentrated *in vacuo*. The crude oil was then purified by

column chromatography (9:1 hexanes:EtOAc) to give a light yellow solid, which was recrystallized from hot pentane to afford **1.4** as a white crystalline solid (8.82 g, 33%).

Physical State: White crystalline solid.

MP: 49.5–50.5 °C.

TLC: R_f = 0.18 (10% EtOAc in hexanes, Dragendorff-Munier stain).

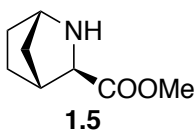
$[\alpha]_D^{22} = +120.2$ (c 1.50, CH_2Cl_2).

^1H NMR (500 MHz, CDCl_3) δ 7.28–7.26 (m, 2H), 7.23 (app. t, $J = 7.2$ Hz, 2H), 7.17 (app. tt, $J = 7.2, 1.6$ Hz, 1H), 6.43–6.41 (m, 1H), 6.27 (dd, $J = 5.6, 1.8$ Hz, 1H), 4.31 (app. d, $J = 1.4$ Hz, 1H), 3.35 (s, 3H), 3.04 (q, $J = 6.5$ Hz, 1H), 2.91 (s, 1H), 2.22 (s, 1H), 2.10 (d, $J = 8.5$ Hz, 1H), 1.44 (s, 1H), 1.41 (d, $J = 6.5$ Hz, 3 H).

^{13}C NMR (125 MHz, CDCl_3) δ 175.0, 145.1, 136.7, 133.2, 128.3, 128.1, 127.3, 122.7, 65.2, 64.2, 62.8, 51.8, 49.3, 45.7, 22.8.

HRMS (CI/MeOH) m/z calculated for $\text{C}_{16}\text{H}_{19}\text{O}_2\text{N}$ ($\text{M} + \text{Na}$)⁺ 280.1313, found 280.1308.

Methyl (1*S*,3*R*,4*R*)-2-azabicyclo[2.2.1]heptane-3-carboxylate (1.5):

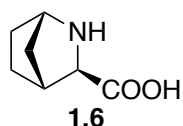


Experimental: To a solution of **1.4** (5.00 g, 19.4 mmol) in MeOH (33 mL) was added 5 wt% Pd/C (0.25g, 20 wt%). Acetic acid (0.32 mL) was added, and the atmosphere pressurized to 200 psi H_2 (g) with vigorous stirring. After 48 hours the pressure was released and the mixture filtered through Celite. The volatiles were removed *in vacuo*. Purification by column chromatography (10% MeOH in EtOAc) afforded amino ester **1.5** (2.66 g, 88%) as yellow crystals. ^1H and ^{13}C NMR spectra matched those previously reported for this compound.⁵⁹

Physical State: Yellow crystals.

TLC: $R_f = 0.14$ (10% MeOH in EtOAc, Dragendorff-Munier stain).

(1*S*,3*R*,4*R*)-2-azabicyclo[2.2.1]heptane-3-carboxylic acid (1.6):

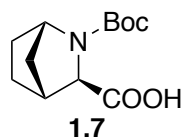


Experimental: To a mixture of amine **1.5** (2.66 g, 17.2 mmol) in THF/H₂O (24:6 mL) was added LiOH (792 mg, 18.9 mmol, 56% monohydrate). The solution was heated to 40 °C and stirred until completion by TLC. The volatiles were removed *in vacuo*, and the residual water removed with a Dean-Stark trap and toluene. The toluene was removed under reduced pressure, and the light yellow solid was taken forward without purification. ¹H and ¹³C NMR spectra matched those previously reported for this compound.⁵⁹

Physical State: Light yellow solid.

TLC: $R_f = 0.04$ (20% MeOH in EtOAc, Dragendorff-Munier stain).

(1*S*,3*R*,4*R*)-*N*-tert-butoxycarbonyl-2-azabicyclo[2.2.1]heptane-3-carboxylic acid (1.7):



Experimental: To a solution of amine **1.6** (3.00 g, 20.4 mmol) in MeOH (102 mL) was added NaHCO₃ (5.10 g, 61.2 mmol). Solid (Boc)₂O (4.45 g, 20.4 mmol) was transferred to the reaction mixture, and the round bottom flask was topped with a septum with a vent needle. The mixture was sonicated in an ultrasound bath for 2 hours. The mixture was then filtered through Celite and concentrated *in vacuo*. The residue was dissolved in H₂O and cooled to 0°C before being

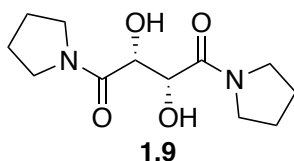
acidified to pH 2 with sat. aq. H₂SO₄. The solution was extracted three times with Et₂O, dried over Na₂SO₄, filtered, and concentrated to afford *N*-Boc amine **1.7** (3.02 g, 61%) as a viscous, orange oil.

¹H and ¹³C NMR spectra matched those previously reported for this compound.⁵⁹

Physical State: Viscous, orange oil.

TLC: *R_f* = 0.14 (EtOAc, Dragendorff-Munier stain).

(2R,3R)-2,3-Dihydroxy-1,4-dipyrrolidin-1-yl-butane-1,4-dione (1.9**):**



Experimental: To a flask containing pyrrolidine (1.3 mL, 16 mmol) was added (–)-Dimethyl *L*-tartrate (1.0 g, 5.6 mmol). The reaction mixture was allowed to stir at room temperature for 20 h and concentrated *in vacuo*. The oil was then purified via flash column chromatography (EtOAc to 9:1 EtOAc:MeOH) to give a light orange solid, which was then recrystallized (1:1 CH₂Cl₂/Et₂O) to afford **1.9** as a white crystalline solid (1.29 g, 90%).

Physical State: White crystalline solid.

MP = 131–134 °C.

TLC: *R_f* = 0.36 (20% MeOH in EtOAc, KMnO₄ stain).

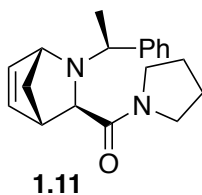
[α]_D²² = +37.6 (*c* 0.99, EtOH).

¹H NMR (500 MHz, CDCl₃) δ 4.51 (d, *J* = 6.0 Hz, 2H), 4.22 (d, *J* = 6.5 Hz, 2H), 3.66–3.50 (m, 8 H), 2.03–1.85 (m, 8H).

^{13}C NMR (150 MHz, CDCl_3) δ 169.4, 70.9, 46.6, 46.4, 26.2, 23.8 IR (thin film) 3410, 3363, 2986, 2949, 1642 cm^{-1} .

HRMS (CI/MeOH) m/z calculated for $\text{C}_{12}\text{H}_{20}\text{O}_4\text{N}_2$ ($\text{M} + \text{Na}$) $^+$ 279.1321, found 279.1326.

[(1*S*,3*R*,4*R*)-2-((*S*)-1-phenylethyl)-2-azabicyclo[2.2.1]hept-5-en-3-yl]-pyrrolidin-1-yl-methanone (1.11):



Experimental: Periodic acid (7.51 g, 32.8 mmol) was added portion wise over 1 hour to a solution of amide **1.9** (6.00 g, 23.5 mmol) in CH_2Cl_2 (47 mL). After 2 hours of stirring, 4A molecular sieves were added and the mixture stirred for an additional 10 min. The salts were filtered out, and the volatiles removed under reduced pressure. The crude aldehyde **1.10** was used immediately. In a three-neck flask, equipped with a mechanical stirrer and addition funnel, a solution of unpurified aldehyde **1.10** (7.65 g, 60.2 mmol) in CH_2Cl_2 (147 mL) was treated with 4 Å molecular sieves and (*S*)-phenylethylamine (7.29 mL, 60.2 mmol) at room temperature for 2 h. The reaction mixture was then cooled to -78 °C followed by sequential addition of trifluoroacetic acid (5.20 mL, 66.2 mmol), distilled $\text{BF}_3 \cdot \text{OEt}_2$ (8.25 mL, 66.2 mmol), and freshly cracked cyclopentadiene (6.10 mL, 72.3 mmol, diluted in 40.0 mL CH_2Cl_2) in 10 min intervals, and stirred for 12 h while warming. The resultant -10 °C reaction mixture was warmed to room temperature, quenched with sat. aq. NaHCO_3 (125 mL), and extracted with CH_2Cl_2 (3 x 125 mL). The combined organics were washed with sat. aq. NaHCO_3 (2 x 125 mL), dried over MgSO_4 , filtered, and concentrated to give a light orange solid (10.2 g), which was recrystallized from hot

tert-butylmethylether. The crystals were washed with 2,2,4-trimethyl pentane to afford **1.11** as light orange solid (4.80 g, 27%).

Physical State:

MP = 143–147 °C.

TLC: *R_f* = 0.47 (10% MeOH in CH₂Cl₂, Dragendorff-Munier stain).

[α]²¹_D = +60.2 (*c* 0.940, CHCl₃).

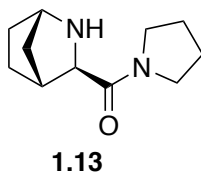
¹H NMR (500 MHz, CDCl₃) δ 7.32 (d, *J* = 7.5 Hz, 2H), 7.20 (t, *J* = 7.3 Hz, 2H), 7.15 (app. t, *J* = 7.3 Hz, 1H), 6.40 (app. s, 1H), 6.29 (d, *J* = 5.5 Hz, 1H), 4.31 (s, 1H), 3.22–3.12 (m, 2H), 3.08 (q, *J* = 6.5 Hz, 1H), 2.98–2.94 (m, 1H), 2.75 (s, 1H), 2.56 (d, *J* = 8.0 Hz, 1H), 2.19 (s, 1H), 2.11 (app. q, *J* = 6.75 Hz, 1H), 1.64–1.55 (m, 2H), 1.40 (app. d, *J* = 6.5 Hz, 6H).

¹³C NMR (125 MHz, CDCl₃) δ 172.2, 145.8, 136.7, 133.3, 128.0, 127.9, 126.9, 64.5, 63.0, 48.8, 45.8, 45.5, 45.2, 26.0, 23.9, 23.4.

IR (thin film) 3107, 2970, 1641 cm⁻¹.

HRMS (CI/MeOH) *m/z* calculated for C₁₉H₂₄N₂O (M + Na)⁺ 319.1786, found 319.1792.

(1*S*,3*R*,4*R*)-2-azabicyclo[2.2.1]heptan-3-yl(pyrrolidin-1-yl)methanone (1.13):



Experimental: A solution of amide **1.11** (10.4 mg, 34.0 μmol) in MeOH (0.380 mL) was charged with 20 wt% Pd(OH)₂/C (5.1 mg, 10 wt%) and H₂ (1 atm). After stirring at room temperature for 5.5 h, the heterogeneous mixture was filtered through a pad of Celite,

concentrated *in vacuo*, and chromatographed (10% MeOH in EtOAc to 10% MeOH in CH₂Cl₂, pH 7 SiO₂) to afford **1.13** as a light yellow oil (0.0054 g, 82%).

pH wash purification procedure: Crude mixture of compounds **1.13**, **1.14**, and **1.15** were dissolved in CH₂Cl₂ and extracted with pH 7.0 sodium monophosphate buffer. Free amine **1.13** dissolved in the aqueous layer, while **1.14** and **1.15** remained in the organic layer. Washing the aqueous layer with additional CH₂Cl₂ removed any last traces of **1.5**. Free basing the aqueous layer with 1.0 M NaOH (aq.) afforded pure **1.13** after extraction with CH₂Cl₂ (3 times).

Physical State: Light yellow oil.

TLC: *R_f* = 0.09 (1:9 MeOH in CH₂Cl₂, Dragendorff-Munier stain).

$[\alpha]_D^{22} = +25.6$ (*c* 0.915, CH₂Cl₂).

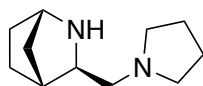
¹H NMR (500 MHz, CDCl₃) δ 3.53 (s, 1H), 3.51–3.39 (m, 4H), 3.29 (s, 1H), 3.14 (br. s, 1H), 2.42 (s, 1H), 1.95 (pentet, *J* = 7.0 Hz, 2H), 1.87–1.83 (m, 2H), 1.61–1.51(m, 3H), 1.47 (d, *J* = 10, 1H), 1.43 (m, 1H), 1.20 (d, *J* = 9.5 Hz, 1H).

¹³C NMR (125 MHz, CDCl₃) δ 171.7, 63.6, 56.2, 46.2, 45.9, 41.1, 35.7, 30.5, 29.0, 26.2, 24.1.

IR (thin film) 32.67, 2961, 2868, 1628 cm⁻¹.

HRMS (CI/MeOH) *m/z* calculated for C₁₁H₁₈N₂O (M+H)⁺ 195.1497, found 195.1488.

(1*S*, 3*R*, 4*R*)-3-(*N*-pyrrolidinyl)methyl-2-azabicyclo[2.2.1]-heptane ((*R*)-1**):**



(*R*)-1.1

Experimental: A solution of amide **1.12** (0.032 g, 0.16 mmol) in THF (0.96 mL) at 0 °C was charged with LiAlH₄ (0.058 g, 1.5 mmol) and heated at reflux for 17 h. The resulting reaction was cooled to 0 °C, diluted with Et₂O (0.63 mL) and quenched with H₂O (0.058 mL), aqueous

2M NaOH (0.058 mL), and H₂O (0.17 mL). The resulting slurry was washed with Et₂O, dried with MgSO₄, and concentrated *in vacuo* to afford (**R**)-**1.1** as a clear oil (0.021 g, 72%).

Physical State: Clear oil.

TLC: *R_f* = 0.11 (10% MeOH in CH₂Cl₂, Dragendorff-Munier stain).

$[\alpha]_{\text{D}}^{22} = -1.46$ (*c* 0.985, CH₂Cl₂).

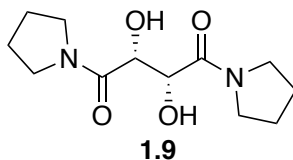
¹H NMR (600 MHz, CDCl₃) δ 3.41 (s, 1H), 2.82 (t, *J* = 7.2 Hz, 1H), 2.52–2.46 (m, 4H), 2.33 (dd, *J* = 12, 7.2 Hz, 1H), 2.26 (dd, *J* = 12, 7.2 Hz, 1H), 2.23 (br s, 1H), 1.75 (br s, 4 H), 1.60 (m, 2 H), 1.48 (d, *J* = 9.6 Hz, 1 H), 1.36 (m, 2 H), 1.12 (d, *J* = 9.6 Hz, 1H).

¹³C NMR (150 MHz, CDCl₃) δ 62.7, 60.6, 55.8, 54.5, 40.0, 34.9, 32.30, 32.28, 28.9, 23.4.

IR (thin film) 3287, 2958, 2868 cm⁻¹.

HRMS (CI/MeOH) *m/z* calculated for C₁₁H₂₀N₂ (M + Na)⁺ 203.1524, found 203.1514.

(2R,3R)-2,3-Dihydroxy-1,4-dipyrrolidin-1-yl-butane-1,4-dione (1.9):



Experimental: To a flask containing pyrrolidine (29.0 mL, 347 mmol) was added (+)-diethyl *L*-tartrate (20.8 mL, 121 mmol). The reaction mixture was allowed to stir at room temperature for 20 h and concentrated *in vacuo*. The crude oil was then purified via flash column chromatography (EtOAc to 10% MeOH in EtOAc) to give a light orange solid, which was then recrystallized (1:1 CH₂Cl₂/Et₂O) to afford **1.9** as a white crystalline solid (11.9 g, 38%).

Physical State: White, crystalline solid.

MP = 131–134 °C.

TLC: *R_f* = 0.36 (20% MeOH in EtOAc, KMnO₄).

$[\alpha]_D^{22} = +31.6$ (c 0.980, EtOH).

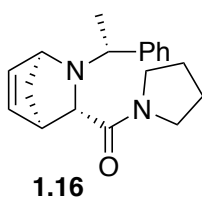
$^1\text{H NMR}$ (500 MHz, CDCl_3) δ 4.51 (s, 2H), 4.26 (br s, 2H), 3.66–3.49 (m, 8 H), 2.02–1.85 (m, 8H).

$^{13}\text{C NMR}$ (125 MHz, CDCl_3) δ 169.4, 70.9, 46.6, 46.4, 26.2, 23.8.

IR (thin film) 3412, 3368, 2935, 2878, 1643, 1628 cm^{-1} .

HRMS (CI/MeOH) m/z calculated for $\text{C}_{12}\text{H}_{20}\text{O}_4\text{N}_2$ ($\text{M} + \text{Na}$) $^+$ 279.1321, found 279.1319.

[(1*R*,3*S*,4*S*)-2-((*S*)-1-phenylethyl)-2-azabicyclo[2.2.1]hept-5-en-3-yl]-pyrrolidin-1-yl-methanone (1.16):



Experimental: Periodic acid (7.51 g, 32.8 mmol) was added portion wise over 1 hour to a solution of amide **1.9** (6.00 g, 23.5 mmol) in CH_2Cl_2 (47 mL). After 2 hours of stirring, 4A molecular sieves were added and the mixture stirred for an additional 10 min. The salts were filtered out, and the volatiles removed under reduced pressure. The crude aldehyde **1.10** (6.06 g) was used immediately. In a three-neck flask, equipped with a mechanical stirrer and addition funnel, a solution of crude aldehyde **10** (5.85 g, 46.0 mmol) in CH_2Cl_2 (115 mL) was treated with 4 Å molecular sieves and (*S*)-phenylethylamine (5.90 mL, 46.0 mmol) at room temperature for 2 h. The reaction mixture was then cooled to -78 °C followed by sequential addition of trifluoroacetic acid (3.9 mL, 0.051 mol), $\text{BF}_3 \cdot \text{OEt}_2$ (6.3 mL, 0.051 mol), and freshly cracked cyclopentadiene (4.7 mL, 0.055 mol, diluted in 40 mL CH_2Cl_2) in 10 min intervals, and stirred for 24.5 h. The resultant reaction mixture was warmed to room temperature, quenched with sat.

aq. NaHCO₃ (100 mL), and extracted with CH₂Cl₂ (3 x 85 mL). The combined organics were dried over MgSO₄, filtered, concentrated, and purified by column chromatography (CH₂Cl₂ – 9:1 CH₂Cl₂/MeOH, column and eluent deactivated with 0.5% NH₄OH) to give a light orange solid, which was recrystallized from hot *tert*-butylmethylether. The crystals were washed with 2,2,4-trimethyl pentane to afford **1.16** as an off-white crystalline solid (5.17 g, 38%).

mp = 132–135 °C.

Physical State: Off-white crystalline solid.

TLC: *R_f* = 0.44 (10% MeOH in CH₂Cl₂, Dragendorff-Munier stain).

$[\alpha]_D^{21} = -59.1$ (*c* 0.950, CHCl₃).

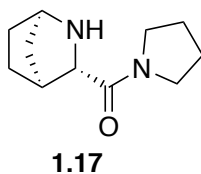
¹H NMR (600 MHz, CDCl₃) δ 7.33 (d, *J* = 8.4 Hz, 2H), 7.20 (t, *J* = 7.2 Hz, 2H), 7.15 (tt, *J* = 7.2, 1.3 Hz, 1H), 6.41–6.40 (m, 1H), 6.30 (dd, *J* = 5.6, 1.6 Hz, 1H), 4.30 (app. d, *J* = 1.3 Hz, 1H), 3.23–3.12 (m, 2H), 3.08 (q, *J* = 6.6 Hz, 1H), 2.98–2.94 (m, 1H), 2.75 (bs, 1H), 2.57 (app. d, *J* = 8.2 Hz, 1H), 2.20 (s, 1H), 2.14–2.10 (m, 1H), 1.63–1.57 (m, 2H), 1.40 (d, *J* = 6.5 Hz, 3H and m, 3H).

¹³C NMR (150 MHz, CDCl₃) δ 172.1, 145.7, 136.7, 133.2, 128.0, 127.9, 126.8, 64.5, 63.0, 62.1, 48.8, 45.7, 45.5, 45.2, 26.0, 23.8, 23.4.

IR (thin film) 3051, 2980, 1641, 1429 cm⁻¹.

HRMS (CI/MeOH) *m/z* calculated for C₁₉H₂₄N₂O (M + Na)⁺ 319.1786, found 319.1794.

(1*R*,3*S*,4*S*)-2-azabicyclo[2.2.1]heptan-3-yl(pyrrolidin-1-yl)methanone (1.17):



Experimental: A solution of amide **1.16** (2.00 g, 6.75 mmol) in MeOH (75 mL) was charged with 5% Pd/C (2.66 g, 7 wt %) and H₂ (1 atm). After stirring at room temperature for 5.5 h, the heterogeneous mixture was filtered through a pad of Celite, concentrated *in vacuo*, and chromatographed (Et₂O to 10% MeOH in CH₂Cl₂, column and eluent deactivated with 0.1–0.5% NH₄OH) to afford **1.17** as a light yellow oil (1.01 g, 77%).

Physical State: Light yellow oil.

TLC: *R_f* = 0.11 (10% MeOH in CH₂Cl₂, Dragendorff-Munier stain).

$[\alpha]_D^{22} = -30.1$ (*c* 1.00, CH₂Cl₂).

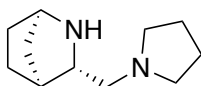
¹H NMR (500 MHz, CDCl₃) δ 3.58(s, 1H), 3.57–3.40 (m, 5H), 3.34 (s, 1H), 2.88 (bs, 1H), 2.46 (s, 1H), 1.98 (app. sextet, *J* = 6.7 Hz, 2H), 1.91–1.84 (m, 2H), 1.60 (s, 3H), 1.53–1.42 (m, 2H), 1.23 (d, *J* = 9.5 Hz, 1H).

¹³C NMR (125 MHz, CDCl₃) δ 169.8, 62.7, 56.6, 46.2, 45.9, 40.6, 35.3, 28.8, 28.3, 25.9, 23.9.

IR (thin film) 3267, 2962, 286, 1628 cm⁻¹.

HRMS (CI/MeOH) *m/z* calculated for C₁₁H₁₈N₂O (M+H)⁺ 195.1497, found 195.1489.

(1*R*, 3*S*, 4*S*)-3-(*N*-pyrrolidinyl)methyl-2-azabicyclo[2.2.1]-heptane ((*S*)-1.1):



(*S*)-1.1

Experimental: A solution of amide **1.17** (0.601 g, 3.09 mmol) in THF (38.6 mL) at 0 °C was charged with LiAlH₄ (1.19 g, 30.9 mmol) and heated at reflux for 48 h. The resulting reaction was cooled to 0 °C, diluted with Et₂O (2.0 mL) and quenched with H₂O (1.2 mL), aqueous 2M NaOH (1.2 mL), and H₂O (3.6 mL). The resulting slurry was washed with Et₂O, dried with MgSO₄, and concentrated *in vacuo* to afford (*S*)-**1.1** as a clear oil (0.423 g, 76%).

Physical State: Clear oil.

TLC: $R_f = 0.10$ (10% MeOH in CH_2Cl_2 , Dragendorff-Munier stain).

$[\alpha]_D^{22} = +34.7$ (c 1.02, CH_2Cl_2).

^1H NMR (600 MHz, CDCl_3) δ 3.43 (s, 1H), 2.84 (t, $J = 8.7$ Hz, 1H), 2.58–2.44 (m, 4H), 2.34 (dd, $J = 14.1, 8.0$ Hz, 1H), 2.27 (dd, $J = 14.5, 9.2$ Hz, 1H), 2.24 (app. bs, 1H), 1.79–1.70 (m, 5H), 1.64–1.56 (m, 2H), 1.49 (app. d, $J = 11.5$ Hz, 1H), 1.41–1.33 (m, 2H), 1.18 (d, $J = 11.9$ Hz, 1H).

^{13}C NMR (150 MHz, CDCl_3) δ 62.7, 60.7, 55.9, 54.6, 40.0, 34.9, 32.4, 28.9, 23.4.

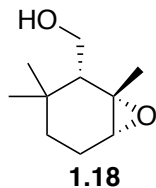
IR (thin film) 3289, 2951, 2870, 2781 cm^{-1} .

HRMS (CI/MeOH) m/z calculated for $\text{C}_{11}\text{H}_{20}\text{N}_2$ ($\text{M} + \text{Na}$) $^+$ 203.1524, found 203.1517.

General CEC Method

Two 1 dram glass vials were capped with a septum, flame dried, flushed with argon, and labeled R and S. THF (0.20 M), diisopropylamine or 1,2-dimethylimidazole (2.0 equiv, 2.0 M solution in THF), and DBU (10 equiv) were added to both vials. To the R vial was added (**R**)-**1.1** (0.10 equiv, 0.28 M solution in THF), and to the S vial (**S**)-**1.1** (0.10 equiv, 0.28 M solution in THF). Each vial was charged with *n*-BuLi (2.2 equiv) at 0 °C, and allowed to stir for 30 min. A solution of epoxide (1.0 equiv, 0.25 M in THF) was added to initiate the reaction, and 0.10 mL aliquots were taken from each vial at 5, 30, 60, and 180 min intervals. The aliquots were partitioned between 1:1 $\text{Et}_2\text{O}:\text{NH}_4\text{Cl}$ (sat. aq.), and the organic layers dried by filtering through a pipette filled with MgSO_4 , and concentrating *in vacuo*. ^1H NMR are taken of both reactions and the conversions examined. See the final two spectra for a sample reaction.

((1*S*,2*R*,6*R*)-1,3,3-trimethyl-7-oxabicyclo[4.1.0]heptan-2-yl)methanol (1.18):

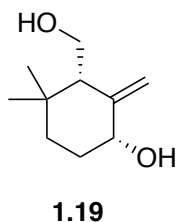


Experimental: Epoxide **1.18** was prepared according to the procedure by Vidari³⁶ on a 5.0 mmol scale (69% yield) from the alkene synthesized by the Overman lab. ¹H and ¹³C NMR spectra matched those previously reported for this compound.³⁶

Physical State: Clear oil.

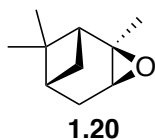
TLC: *R_f* = 0.10 (66% Et₂O in hexanes, Vanillin stain).

(1*R*,3*S*)-3-(hydroxymethyl)-4,4-dimethyl-2-methylenecyclohexanol (1.19):



Experimental: Diol **1.19** was prepared from epoxide **1.18** by the general CEC method (with both LDA and LiDMID as bulk bases). ¹H and ¹³C NMR spectra matched those previously reported for this compound.^{35,36}

(1*R*,2*R*,4*S*,6*R*)-2,7,7-trimethyl-3-oxatricyclo[4.1.1.0^{2,4}]octane (1.20):

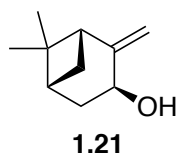


Experimental: Epoxide **1.20** was prepared on 2.9 mmol scale (96% yield) according to the procedure by Crandall.³⁹ ¹H and ¹³C NMR spectra matched those previously reported for this compound.³⁹

Physical State: Clear oil.

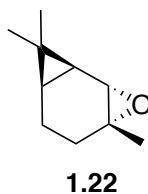
TLC: *R_f* = 0.71 (10% EtOAc in hexanes, Vanillin stain).

(1*R*,3*S*,5*R*)-6,6-dimethyl-2-methylenebicyclo[3.1.1]heptan-3-ol (1.21):



Experimental: Allylic alcohol **1.21** was prepared from epoxide **1.20** by the general CEC method (with both LDA and LiDMID as bulk bases). ¹H and ¹³C NMR spectra matched those previously reported for this compound.

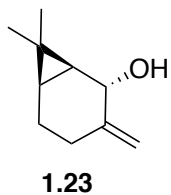
(1*S*,2*S*,4*R*,7*R*)-4,8,8-trimethyl-3-oxatricyclo[5.1.0.0^{2,4}]octane (1.22):



Experimental: Epoxide **1.22** was prepared on 3.7 mmol scale (69% yield) according to the procedure by Palmer.⁴¹ ¹H and ¹³C NMR spectra matched those previously reported for this compound.¹⁶

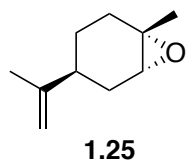
Physical State: Clear oil.

(1*S*,2*S*,6*R*)-7,7-dimethyl-3-methylenebicyclo[4.1.0]heptan-2-ol (1.23):



Experimental: Alcohol **1.23** was prepared by the General CEC Method from epoxide **1.22** (with LDA and LiDMID as the bulk base). ^1H and ^{13}C NMR spectra matched those previously reported for this compound.⁶⁰

(1*S*,4*S*,6*R*)-1-methyl-4-(prop-1-en-2-yl)-7-oxabicyclo[4.1.0]heptane (1.25):

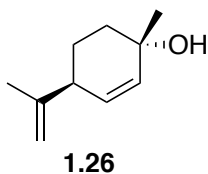


Experimental: Epoxide **1.25** was prepared on 7.6 mmol scale (99% yield) according to the procedure by Singaram.⁴⁰ ^1H and ^{13}C NMR spectra matched those previously reported for this compound.⁴⁰

Physical State: Clear oil.

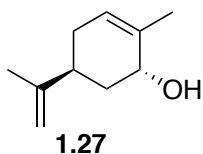
TLC: $R_f = 0.75$ (33% EtOAc in hexanes, Vanillin stain).

(1*S*,4*S*)-1-methyl-4-(prop-1-en-2-yl)cyclohex-2-enol (1.26):



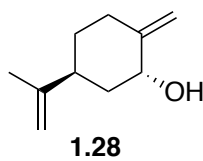
Experimental: Alcohol **1.26** was prepared by the General CEC Method from epoxide **1.25** (with LDA and LiDMID as the bulk base). ^1H and ^{13}C NMR spectra matched those previously reported for this compound.⁶¹

(1*R*,5*S*)-2-methyl-5-(prop-1-en-2-yl)cyclohex-2-enol (1.27):



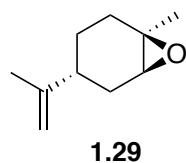
Experimental: Alcohol **1.27** was prepared by the General CEC Method from epoxide **1.25** (with LDA and LiDMID as the bulk base). ^1H and ^{13}C NMR spectra matched those previously reported for this compound.⁶²

(1*R*,5*S*)-2-methylene-5-(prop-1-en-2-yl)cyclohexanol (1.28):



Experimental: Alcohol **1.28** was prepared by the General CEC Method from epoxide **1.25** (with LDA and LiDMID as the bulk base). ^1H and ^{13}C NMR spectra matched those previously reported for this compound.³⁸

(1*S*,4*S*,6*R*)-1-methyl-4-(prop-1-en-2-yl)-7-oxabicyclo[4.1.0]heptane (1.29):

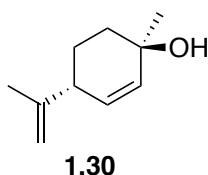


Experimental: Epoxide **1.29** was prepared on 20.0 mmol scale (27% yield) according to the procedure by Singaram.⁴⁰ ^1H and ^{13}C NMR spectra matched those previously reported for this compound.⁴⁰

Physical State: Clear oil.

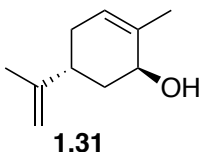
TLC: $R_f = 0.75$ (33% EtOAc in hexanes, Vanillin stain).

(1*S*,4*S*)-1-methyl-4-(prop-1-en-2-yl)cyclohex-2-enol (1.30):



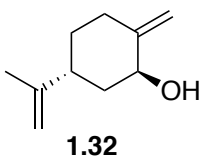
Experimental: Alcohol **1.30** was prepared by the General CEC Method from epoxide **1.29** (with LDA and LiDMID as the bulk base). ^1H and ^{13}C NMR spectra matched those previously reported for this compound.⁶¹

(1*R*,5*S*)-2-methyl-5-(prop-1-en-2-yl)cyclohex-2-enol (1.31):



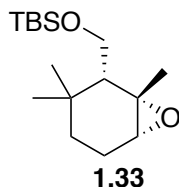
Experimental: Alcohol **1.31** was prepared by the General CEC Method from epoxide **1.29** (with LDA and LiDMID as the bulk base). ^1H and ^{13}C NMR spectra matched those previously reported for this compound.^{42,62}

(1*R*,5*S*)-2-methylene-5-(prop-1-en-2-yl)cyclohexanol (1.32):



Experimental: Alcohol **1.32** was prepared by the General CEC Method from epoxide **1.29** (with LDA and LiDMID as the bulk base). ^1H and ^{13}C NMR spectra matched those previously reported for this compound.³⁸

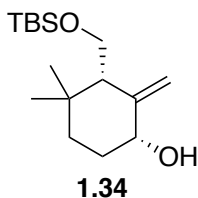
TBS protected epoxy alcohol (1.33):



Experimental: TBS protected alcohol **1.33** was prepared on 0.59 mmol scale from alcohol **1.18** in % yield according to the procedure by Uroos.³⁷ ^1H and ^{13}C NMR spectra matched those previously reported for this compound.³⁷

Physical State: Clear oil.

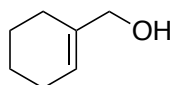
TBS protected allylic alcohol (1.34):



Experimental: Two 1 dram glass vials were capped with a septum, flame dried, flushed with argon, and labeled R and S. THF (0.25 mL, 0.20 M), *n*-BuLi (0.04 mL, 0.1 mmol, 3.4 M solution in hexanes), and DBU (0.08 mL, 0.5 mmol) were added to both vials. To the R vial was added (**R**)-**1.32** (0.23 mL, 0.0050 mmol, 0.28 M solution in THF), and to the S vial (**S**)-**1.32** (0.23 mL, 0.0050 mmol, 0.28 M solution in THF). Each vial was charged with *n*-BuLi (0.04 mL, 0.1 mmol, 3.4 M solution in hexanes) at 0 °C, and allowed to stir for 30 min. A solution of epoxide **1.33**

(0.20 mL, 0.050 mmol, 0.25 M in THF) was added to initiate the reaction, and 0.10 mL aliquots were taken from each vial at 5, 30, 60, and 180 min intervals. The aliquots were partitioned between 1:1 Et₂O:NH₄Cl (sat. aq.), and the organic layers dried by filtering through a pipette filled with MgSO₄, and concentrating *in vacuo*. ¹H NMR are taken of both reactions and the conversions examined. ¹H and ¹³C NMR spectra matched those previously reported for this compound.³⁷

cyclohex-1-en-1-ylmethanol (1.35):



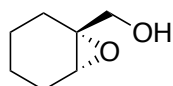
1.35

Experimental: LiAlH₄ (0.24 g, 6 mmol) was suspended in Et₂O (20 mL), and cyclohex-1-enecarbaldehyde (1.15 mL, 10.0 mmol) was added slowly at 0 °C. After stirring for 1 hour the reaction was diluted with Et₂O and quenched with H₂O (20 mL). The sludge was filtered through Celite with additional Et₂O. The layers were separated, and the aq layer was extracted two times with Et₂O. The combined organic layers were washed with sat. aq. Sodium chloride, dried over Na₂SO₄, filtered, and concentrated to afford allylic alcohol **1.35** (1.19 g, quantitative) as a clear oil. ¹H and ¹³C NMR spectra matched those previously reported for this compound.⁶³

Physical State: Clear oil.

TLC: *R_f* = 0.56 (33% Et₂O in hexanes, Vanillin stain).

(1*R*,6*R*)-7-oxabicyclo[4.1.0]heptan-1-ylmethanol (1.36):



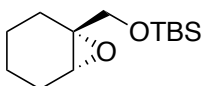
1.36

Experimental: Epoxide **1.36** was prepared by Shi epoxidation (with ketone **1.41**) of alcohol **1.35** on 4.0 mmol scale (546 mg, mixture of 7.3:1 **1.36**:**1.41**).²⁰ Ketone **1.41** and epoxide **1.36** could not be separated by column chromatography, so the mixture was taken forward and purified after protection of the alcohol. ¹H and ¹³C NMR spectra matched those previously reported for this compound.²⁰

Physical State: Clear oil.

TLC: $R_f = 0.38$ (50% Et₂O in hexanes, Vanillin stain).

((1*R*,6*R*)-7-oxabicyclo[4.1.0]heptan-1-ylmethoxy)(*tert*-butyl)dimethylsilane (1.37**):**



1.37

Experimental: A solution of epoxide **1.36** (196 mg, 1.53 mmol) in THF (900 μ L) at rt was charged with imidazole (135 mg, 1.98 mmol) and TBSCl (227 mg, 1.51 mmol). The mixture was stirred for 6.5 h and quenched with H₂O (2.00 mL). The layers were separated and the organic layer washed with sat. aq. NaCl, dried with MgSO₄, filtered, and concentrated to yield 294 mg (81%) of a slight yellow oil. The crude product was purified by column chromatography (1:2 hexane:ethyl acetate) to yield **1.37** (226 mg, 62%) of a clear oil. ¹H and ¹³C NMR spectra matched those previously reported for this compound.⁶⁴

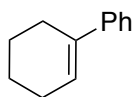
Enantiopurity was determined on the TBDPS protected alcohol which was prepared by the same procedure for **1.37**.

Physical State: Clear oil.

TLC: $R_f = 0.82$ (60% EtOAc in hexanes, Vanillin stain).

SFC: Chiracel AD-H column, 10% *i*-PrOH in hexane, 2.5 mL/min flow, 5 μ L injection, 82% ee.

1-phenyl-1-cyclohexene (1.39):



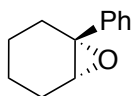
1.39

Experimental: Alkene **1.39** was prepared according to the procedure by Ceylan on 7.6 mmol scale (99% yield).^{Error! Bookmark not defined.} ¹H and ¹³C NMR spectra matched those previously reported for this compound.⁶⁵

Physical State: Clear oil.

TLC: $R_f = 0.69$ (33% Et₂O in hexanes, Vanillin stain).

(1*R*,6*R*)-1-phenyl-7-oxabicyclo[4.1.0]heptane (1.40):



1.40

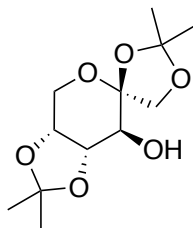
Experimental: Epoxide **1.40** was prepared by Shi epoxidation (with ketone **1.41**) of alkene **1.39**.²⁰ ¹H and ¹³C NMR spectra matched those previously reported for this compound.²⁰

Physical State: Clear oil.

TLC: $R_f = 0.78$ (33% Et₂O in hexanes, Vanillin stain).

HPLC: Chiracel AD column, 1% *i*PrOH in hexane, 1 mL/min flow, 35 μ L injection, 98% ee.

(3*aR*,4'*S*,7*S*,7*aS*)-2,2,2',2'-tetramethyltetrahydrospiro[[1,3]dioxolo[4,5-*c*]pyran-6,4'-[1,3]dioxolan]-7-ol (1.70):

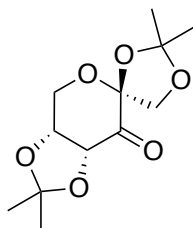


1.70

Experimental: Synthesized in one step from D-fructose according to the procedure by VanderRoest and co-workers.⁶⁶ ¹H and ¹³C NMR spectra matched those previously reported for this compound.^{Error! Bookmark not defined.}

Physical State: Thin, white crystals.

1,2:4,5-Di-O-isopropylidene-D-erythro-2,3-hexodiure-2,6-pyranose (1.41):

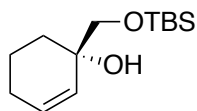


1.41

Experimental: Synthesized from alcohol **1.70** according to the procedure by VanderRoest and co-workers.⁶⁶ ¹H and ¹³C NMR spectra matched those previously reported for this compound.^{Error! Bookmark not defined.}

Physical State: Thick, white crystals.

(S)-1-(((tert)-butyldimethylsilyl)oxy)methyl)cyclohex-2-enol (1.42):



1.42

Experimental: Allylic alcohol **1.42** was prepared by the General CEC Method (with LDA and LiDMID as the bulk base) of epoxide **1.37**.

¹H NMR (500 MHz, CDCl₃) δ 5.89 (app. dt, *J* = 10.2, 7.3 Hz, 1H), 5.59 (app. d, *J* = 10.2 Hz, 1H), 3.48 (d, *J* = 9.6, 1H), 3.44 (d, *J* = 9.6, 1H), 2.67 (s, 1H), 2.12–2.03 (m, 1H), 1.99–1.90 (m, 1H), 1.81–1.66 (m, 2H), 1.64–1.55 (m, 3H), 0.95–0.86 (s, 9H), 0.07 (s, 6H).

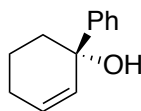
¹³C NMR (150 MHz, CDCl₃)

δ 131.6, 129.3, 69.9, 69.7, 32.6, 25.94, 25.86, 25.54, 19.1, 18.3, –5.4.

IR (thin film) 3476, 3025, 2931, 1473, 1252 cm⁻¹.

HRMS (CI/MeOH) *m/z* calculated for C₁₃H₂₆O₂Si (M + Na)⁺ 265.1600, found 265.1595.

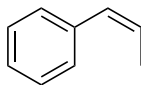
(S)-1,2,3,4-tetrahydro-[1,1'-biphenyl]-1-ol (1.43):



1.43

Experimental: Alcohol **1.43** was prepared by the General CEC Method from epoxide **1.40** (with LDA as the bulk base). ¹H and ¹³C NMR spectra matched those previously reported for this compound.⁶⁷

(Z)-prop-1-en-1-ylbenzene (1.44):



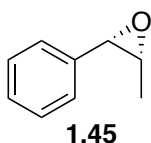
1.44

Experimental: Alkene **1.44** was prepared on 4.3 mmol scale (82% yield) according to the procedure by Liu in >95:5 *cis*-selectivity.⁴⁶ ¹H and ¹³C NMR spectra matched those previously reported for this compound.⁴⁶

Physical State: Brown oil.

TLC: *R_f* = 0.85 (33% Et₂O in hexanes, Vanillin stain).

(2*R*,3*S*)-2-methyl-3-phenyloxirane (1.45):



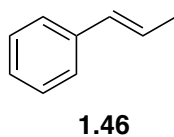
Experimental: Epoxide **1.45** was prepared on 4.3 mmol scale (82% yield) from alkene **1.44** according to the procedure by Jacobsen.⁴⁷ Separation of the product could not be obtained by chiral HPLC, substrate was determined to be 96% ee by optical rotation. ¹H and ¹³C NMR spectra matched those previously reported for this compound.⁶⁸

$[\alpha]_{\text{D}}^{22} = +45.6$ (*c* 0.100, CHCl₃), lit. = $[\alpha]_{\text{D}}^{20} = +47.5$ (*c* 1.17, CHCl₃)⁶⁹

Physical State: Yellow oil.

TLC: *R_f* = 0.49 (33% Et₂O in hexanes, Vanillin stain).

(*E*)-prop-1-en-1-ylbenzene (1.46):

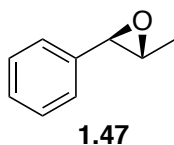


Experimental: Alkene **1.46** was prepared on 4.3 mmol scale (82% yield) according to the procedure by Slauch in >95:5 *trans*-selectivity.⁵⁹ ¹H and ¹³C NMR spectra matched those previously reported for this compound.⁷⁰

Physical State: Clear oil.

TLC: $R_f = 0.83$ (33% Et₂O in hexanes, Vanillin stain).

(2*R*,3*R*)-2-methyl-3-phenyloxirane (1.47):



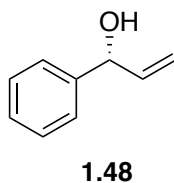
Experimental: Epoxide **1.47** was prepared on 4.3 mmol scale (82% yield) from alkene **1.46** according to the procedure by Shi.²⁰ ¹H and ¹³C NMR spectra matched those previously reported for this compound.²⁰

Physical State: Clear oil.

TLC: $R_f = 0.55$ (25% Et₂O in hexanes, Vanillin stain).

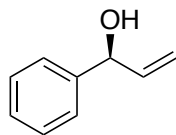
HPLC: AD column, 0.5% *i*-PrOH in hexane, 1 mL/min flow, 100 μ L injection, 89% ee.

(*R*)-1-phenylprop-2-en-1-ol (1.48):



Experimental: Allylic alcohol **1.48** was prepared by the General CEC Method (with LDA and LiDMID as the bulk base) from epoxide **1.45**. ¹H and ¹³C NMR spectra matched those previously reported for this compound.⁷¹

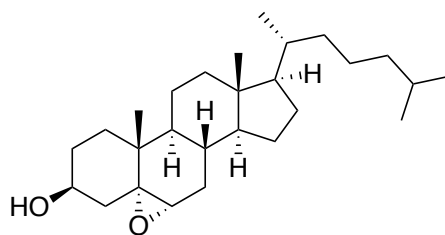
(*S*)-1-phenylprop-2-en-1-ol (1.49):



1.49

Experimental: Allylic alcohol **1.49** was prepared by the General CEC Method (with LDA and LiDMID as the bulk base) from epoxide **1.47**. ^1H and ^{13}C NMR spectra matched those previously reported for this compound.⁷¹

5 α ,6 α -epoxy-cholestan-3 β -ol (1.50):



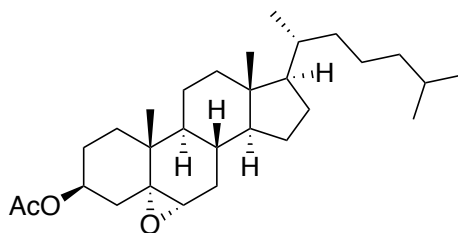
1.50

Experimental: Epoxide **1.50** was prepared on 4.3 mmol scale (82% yield) according to the procedure by Ma.⁴⁹ ^1H and ^{13}C NMR spectra matched those previously reported for this compound.⁴⁹

Physical State: Waxy, white foam.

TLC: $R_f = 0.42$ (50% EtOAc in hexanes, Vanillin stain).

5 α ,6 α -epoxy-cholestan-3 β -yl acetate (1.51):



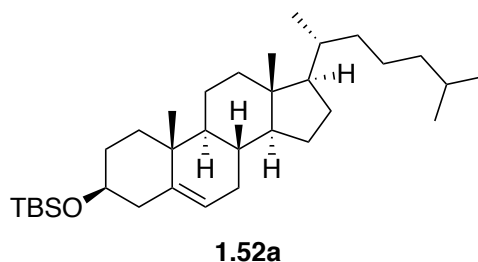
1.51

Experimental: Epoxide **1.51** was prepared on 4.3 mmol scale (82% yield) according to the procedure by Clark.⁷² ¹H and ¹³C NMR spectra matched those previously reported for this compound.⁷²

Physical State: Waxy, white foam.

TLC: $R_f = 0.08$ (50% EtOAc in hexanes, Vanillin stain).

cholestan-5-ene-3 β -yl oxy(*tert*-butyldimethylsilane) (1.52a**):**

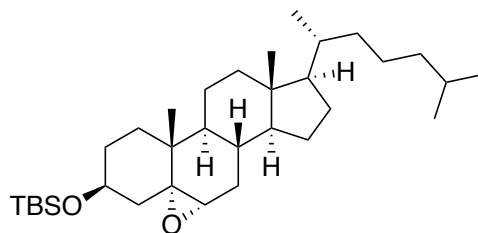


Experimental: To a solution of cholesterol (434 mg, 1.12 mmol) in CH₂Cl₂ (1 mL) was added TBSCl (171 mg, 1.12 mmol) and imidazole (105 mg, 1.46 mmol) at rt. The mixture was stirred for 41 hours before being quenched by the addition of H₂O (4 mL). The layers were separated, and the organic layer washed with additional H₂O. The organic layers were dried with MgSO₄, filtered, and concentrated *in vacuo* to afford TBS protected cholesterol **1.52a** (430 mg, 77%) as a white semi-solid. ¹³C NMR spectra matched those previously reported for this compound.⁷³

Physical State: White semi-solid.

TLC: $R_f = 0.43$ (50% EtOAc in hexanes, Vanillin stain).

5 α ,6 α -epoxy-cholestan-3 β -yl oxy(*tert*-butyldimethylsilane) (1.52**):**



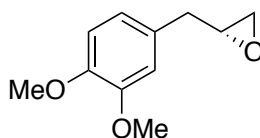
1.52

Experimental: Epoxide **1.50** was prepared on 4.3 mmol scale (82% yield) from TBS protected cholesterol **1.52a** according to the procedure by Ma.⁴⁹ ¹H and ¹³C NMR spectra matched those previously reported for this compound.⁴⁹

Physical State: Waxy, white foam.

TLC: $R_f = 0.88$ (50% EtOAc in hexanes, Vanillin stain).

(R)-2-(3,4-dimethoxybenzyl)oxirane (1.53):



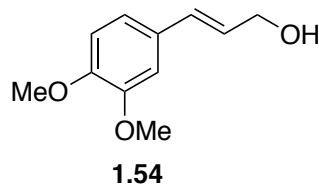
1.53

Experimental: Epoxide **1.53** was prepared on 4.3 mmol scale (82% yield) from methyl eugenol oxide according to the procedure by Jacobsen.⁵² ¹H and ¹³C NMR spectra matched those previously reported for this compound.⁷⁴

Physical State: Light yellow oil.

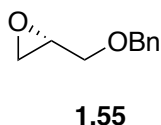
TLC: $R_f = 0.29$ (50% Et₂O in hexanes, KMnO₄ stain).

(R)-2-(3,4-dimethoxybenzyl)oxirane (1.54):



Experimental: Allylic alcohol **1.54** was prepared by the General CEC Method (with LDA) from epoxide **1.53**. ^1H and ^{13}C NMR spectra matched those previously reported for this compound.⁷⁵

(S)-2-((benzyloxy)methyl)oxirane (1.55):

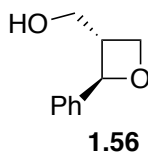


Experimental: Epoxide **1.55** was prepared on 4.3 mmol scale (82% yield) according to the procedure by Carreira.⁵³ ^1H and ^{13}C NMR spectra matched those previously reported for this compound.⁵³

Physical State: Light yellow oil.

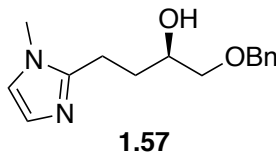
TLC: $R_f = 0.51$ (50% Et_2O in hexanes, KMnO_4 stain).

((2S,3S)-2-phenyloxetan-3-yl)methanol (1.56):



Experimental: Oxetane **1.56** was prepared by the General CEC Method (with LDA) from epoxide **1.55**. ^1H and ^{13}C NMR spectra matched those previously reported for this compound.⁵⁴

(S)-1-(benzyloxy)-4-(1-methyl-1H-imidazol-2-yl)butan-2-ol (1.57):



Experimental: Alcohol **1.57** was prepared by the General CEC Method (with LiDMID) from epoxide **1.55**.

TLC: $R_f = 0.40$ (10% MeOH in CH_2Cl_2 , Vanillin stain).

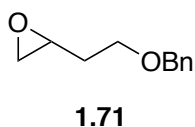
^1H NMR (500 MHz, CDCl_3) δ 7.38–7.27 (m, 5H), 6.90–6.87 (m, 1H), 6.77 (s, 1H), 4.56 (s, 2H), 3.87 (dtd, $J = 8.6, 5.7, 2.7$ Hz, 1H), 3.56 (s, 3H), 3.48 (d, $J = 5.7$ Hz, 2H), 2.90–2.76 (m, 2H), 2.06 (dddd, $J = 10.5, 7.8, 5.6, 3.3$ Hz, 1H), 1.91 (dt, $J = 15.0, 7.3$ Hz, 1H).

^{13}C NMR (125 MHz, CDCl_3) δ 148.3, 138.2, 128.5, 127.8, 127.7, 126.5, 120.5, 74.5, 73.4, 70.0, 32.9, 30.7, 29.8, 23.5.

IR (thin film) 3477, 3025, 2954, 1672, 1472, 1282 cm^{-1} .

HRMS (CI/MeOH) m/z calculated for $\text{C}_{15}\text{H}_{20}\text{N}_2\text{O}_2$ ($\text{M} + \text{Na}$) $^+$ 283.1422, found 283.1419.

2-(2-(benzyloxy)ethyl)oxirane (1.71):

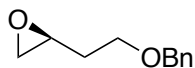


Experimental: To a solution of benzyl protected 3-buten-1-ol (418 mg, 2.58 mmol) in CH_2Cl_2 (15.0 mL) was added *m*-CPBA (904 mg, 5.24 mmol, 70% active peroxide) and the mixture stirred for 14 h, after which the mixture was washed with 2 x 25 mL 0.5 M NaOH. The organic layers were combined, dried with Na_2SO_4 , and concentrated to yield epoxide **1.71** (311 mg, 58%) as a clear oil. ^1H and ^{13}C NMR spectra matched those previously reported for this compound.⁵²

Physical State: Clear oil.

TLC: $R_f = 0.55$ (50% Et₂O in hexanes, Vanillin stain).

(S)-2-(2-(benzyloxy)ethyl)oxirane (1.58):



1.58

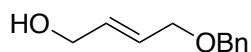
Experimental: Epoxide **1.58** was prepared on 1.7 mmol scale (29% yield) according to the procedure by Jacobsen.⁵² ¹H and ¹³C NMR spectra matched those previously reported for this compound.⁵²

Physical State: Orange oil.

TLC: $R_f = 0.55$ (50% Et₂O in hexanes, Vanillin stain).

HPLC: Chiracel OB-H column, 5% *i*PrOH in hexane, 0.5 mL/min flow, 10 μ L injection, >99% ee.

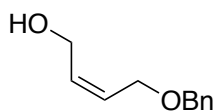
(E)-4-(benzyloxy)but-2-en-1-ol (1.60):



1.60

Experimental: Allylic alcohol **1.60** was prepared by the General CEC Method (with LDA and LiDMID as the bulk base) from epoxide **1.58**. ¹H and ¹³C NMR spectra matched those previously reported for this compound.⁷⁶

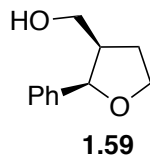
(Z)-4-(benzyloxy)but-2-en-1-ol (1.61):



1.61

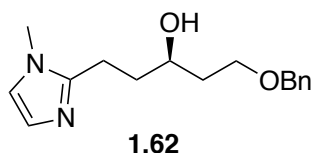
Experimental: Allylic alcohol **1.61** was prepared by the General CEC Method (with LDA and LiDMID as the bulk base) from epoxide **1.58**. ^1H and ^{13}C NMR spectra matched those previously reported for this compound.⁷⁷

((2*R*,3*R*)-2-phenyltetrahydrofuran-3-yl)methanol (1.59):



Experimental: THP **1.59** was prepared by the General CEC Method (with LDA) from epoxide **1.58**. ^1H and ^{13}C NMR spectra matched those previously reported for this compound.⁷⁸

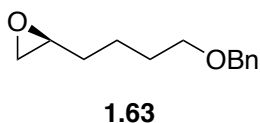
(*R*)-1-(benzyloxy)-5-(1-methyl-1*H*-imidazol-2-yl)pentan-3-ol (1.62):



Experimental: Alcohol **1.62** was prepared by the General CEC Method (with LiDMID) from epoxide **1.58**. Too small a sample after purification of the aliquot to characterize. Crude ^1H NMR showed disappearance of the 2-methyl peak of 1,2-dimethylimidazole which is characteristic of the nucleophilic opened product.

HRMS (CI/MeOH) m/z calculated for $\text{C}_{16}\text{H}_{22}\text{N}_2\text{O}_2$ ($\text{M} + \text{Na}$)⁺ 297.1579, found 297.1579.

(*S*)-2-(4-(benzyloxy)butyl)oxirane (1.63):

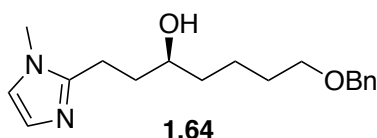


Experimental: Epoxide **1.63** was prepared on 8.4 mmol scale (52% yield) according to the procedure by Jacobsen.⁵² ¹H and ¹³C NMR spectra matched those previously reported for this compound.⁷⁹

Physical State: Brown oil.

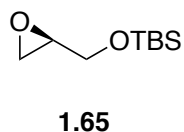
TLC: $R_f = 0.71$ (75% Et₂O in hexanes, Vanillin stain).

(S)-7-(benzyloxy)-1-(1-methyl-1H-imidazol-2-yl)heptan-3-ol (1.64):



Experimental: Alcohol **1.64** was prepared by the General CEC Method (with LiDMID) from epoxide **1.63**. Too small a sample after purification of the aliquot to characterize. Reaction mixture ¹H NMR showed disappearance of the 2-methyl peak of 1,2-dimethylimidazole which is characteristic of the nucleophilic opened product.

(R)-tert-butyldimethyl(oxiran-2-ylmethoxy)silane (1.65):

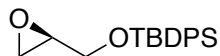


Experimental: Epoxide **1.65** was prepared on 4.3 mmol scale (82% yield) according to the procedure by Crimmins.⁵⁵ ¹H and ¹³C NMR spectra matched those previously reported for this compound.⁵⁵

Physical State:

TLC: $R_f = 0.75$ (50% Et₂O in hexanes, Vanillin stain).

(R)-tert-butyl(oxiran-2-ylmethoxy)diphenylsilane (1.66):



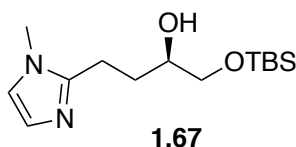
1.66

Experimental: Epoxide **1.66** was prepared on 4.3 mmol scale (82% yield) according to the procedure by Crimmins.⁵⁵ ¹H and ¹³C NMR spectra matched those previously reported for this compound.⁸⁰

Physical State: Clear oil.

TLC: R_f = 0.63 (50% EtOAc in hexanes, Vanillin stain).

(R)-1-((tert-butyldimethylsilyl)oxy)-4-(1-methyl-1H-imidazol-2-yl)butan-2-ol (1.67):



1.67

Experimental: Alcohol **1.67** was prepared by the General CEC Method (with LiDMID). Too small a sample after purification of the aliquot to characterize. Crude ¹H NMR showed disappearance of the 2-methyl peak of 1,2-dimethylimidazole which is characteristic of the nucleophilic opened product.

HRMS (CI/MeOH) m/z calculated for C₁₄H₂₈N₂O₂Si (M + Na)⁺ 307.1818, found 307.1812.

1.9 References:

- (1) Dale, J. A.; Mosher, H. S. *J. Am. Chem. Soc.* **1973**, *95* (2), 512–519.
- (2) Hoye, T. R.; Jeffrey, C. S.; Shao, F. *Nat. Protoc.* **2007**, *2* (10), 2451–2458.
- (3) Flack, H. D.; Bernardinelli, G. *Chirality* **2008**, *20* (5), 681–690.
- (4) Freedman, T. B.; Cao, X.; Dukor, R. K.; Nafie, L. A. *Chirality* **2003**, *15* (9), 743–758.

- (5) Parker, D. *Chem. Rev.* **1991**, *91* (7), 1441–1457.
- (6) Kobayashi, Y.; Hayashi, N.; Kishi, Y. *Org. Lett.* **2002**, *4* (3), 411–414.
- (7) Horeau, A. *Tetrahedron Lett.* **1961**, *2* (15), 506–512.
- (8) Horeau, A. *Tetrahedron Lett.* **1962**, *3* (21), 965–969.
- (9) Sullivan, G. R.; Dale, J. A.; Mosher, H. S. *J. Org. Chem.* **1973**, *38* (12), 2143–2147.
- (10) Vedejs, E.; Jure, M. *Angew. Chem. Int. Ed.* **2005**, *44* (26), 3974–4001.
- (11) Wagner, A. J.; David, J. G.; Rychnovsky, S. D. *Org. Lett.* **2011**, *13* (16), 4470–4473.
- (12) Birman, V. B.; Li, X. *Org. Lett.* **2008**, *10* (6), 1115–1118.
- (13) Wagner, A. J.; Rychnovsky, S. D. *Org. Lett.* **2013**, *15* (21), 5504–5507.
- (14) Wagner, A. J.; Rychnovsky, S. D. *J. Org. Chem.* **2013**, *78* (9), 4594–4598.
- (15) Wagner, A. J.; Miller, S. M.; Nguyen, S.; Lee, G. Y.; Rychnovsky, S. D.; Link, R. D. *J. Chem. Educ.* **2014**, *91* (5), 716–721.
- (16) Miller, S. M.; Samame, R. A.; Rychnovsky, S. D. *J. Am. Chem. Soc.* **2012**, *134* (50), 20318–20321.
- (17) Perry, M. A.; Trinidad, J. V.; Rychnovsky, S. D. *Org. Lett.* **2013**, *15* (3), 472–475.
- (18) Zhang, W.; Loebach, J. L.; Wilson, S. R.; Jacobsen, E. N. *J. Am. Chem. Soc.* **1990**, *112* (7), 2801–2803.
- (19) Katsuki, T.; Sharpless, K. B. *J. Am. Chem. Soc.* **1980**, *102* (18), 5974–5976.
- (20) Wang, Z.-X.; Tu, Y.; Frohn, M.; Zhang, J.-R.; Shi, Y. *J. Am. Chem. Soc.* **1997**, *119* (46), 11224–11235.
- (21) Padwa, A.; Murphree, S. *ARKIVOC iii* (2006), 6–33.
- (22) Asami, M. *Bull. Chem. Soc. Jpn.* **1990**, *63* (3), 721–727.
- (23) Södergren, M. J.; Andersson, P. G. *J. Am. Chem. Soc.* **1998**, *120* (41), 10760–10761.
- (24) Södergren, M. J.; Bertilsson, S. K.; Andersson, P. G. *J. Am. Chem. Soc.* **2000**, *122* (28), 6610–6618.
- (25) Brandt, P.; Norrby, P.-O.; Andersson, P. G. *Tetrahedron* **2003**, *59* (49), 9695–9700.
- (26) Nilsson Lill, S. O.; Arvidsson, P. I.; Ahlberg, P. *Tetrahedron Asymmetry* **1999**, *10* (2), 265–279.

- (27) Thummel, R. P.; Rickborn, B. *J. Am. Chem. Soc.* **1970**, *92* (7), 2064–2067.
- (28) Dinér, P. *Tetrahedron Asymmetry* **2010**, *21* (21–22), 2733–2739.
- (29) Modin, S. A.; Andersson, P. G. *J. Org. Chem.* **2000**, *65* (20), 6736–6738.
- (30) Suzuki, M.; Kimura, Y.; Terashima, S. *Bull. Chem. Soc. Jpn.* **1986**, *59* (11), 3559–3572.
- (31) Brandt, P.; Andersson, P. G. *Synlett* **2000**, *2000* (8), 1092–1106.
- (32) Ram, S.; Spicer, L. D. *Tetrahedron Lett.* **1987**, *28* (5), 515–516.
- (33) Adger, B. M.; O'Farrell, C.; Lewis, N. J.; Mitchell, M. B. *Synthesis* **1987**, *1987* (1), 53–55.
- (34) Ma, G.; Jha, A. *Org. Process Res. Dev.* **2005**, *9* (6), 847–852.
- (35) Serra, S.; Gatti, F. G.; Fuganti, C. *Tetrahedron Asymmetry* **2009**, *20* (11), 1319–1329.
- (36) Luparia, M.; Boschetti, P.; Piccinini, F.; Porta, A.; Zanoni, G.; Vidari, G. *Chem. Biodivers.* **2008**, *5* (6), 1045–1057.
- (37) Uroos, M.; Hayes, C. J. *Org. Lett.* **2010**, *12* (22), 5294–5297.
- (38) Uroos, M.; Lewis, W.; Blake, A. J.; Hayes, C. J. *J. Org. Chem.* **2010**, *75* (24), 8465–8470.
- (39) Crandell, J. K.; Crawley, L. C. *Org. Synth.* **1973**, *53*, 17.
- (40) Chrisman, W.; Camara, J. N.; Marcellini, K.; Singaram, B.; Goralski, C. T.; Hasha, D. L.; Rudolf, P. R.; Nicholson, L. W.; Borodychuk, K. K. *Tetrahedron Lett.* **2001**, *42* (34), 5805–5807.
- (41) Crombie, L.; Crombie, W. M. L.; Jamieson, S. V.; Palmer, C. J. *J. Chem. Soc., Perkin Trans. I* **1988**, No. 5, 1243–1250.
- (42) Suh, Y.-W.; Kim, N.-K.; Ahn, W.-S.; Rhee, H.-K. *J. Mol. Catal. Chem.* **2003**, *198* (1–2), 309–316.
- (43) Stekrova, M.; Kumar, N.; Aho, A.; Sinev, I.; Grünert, W.; Dahl, J.; Roine, J.; Arzumanov, S. S.; Mäki-Arvela, P.; Murzin, D. Y. *Appl. Catal. Gen.* **2014**, *470*, 162–176.
- (44) Pettersen, D.; Amedjkouh, M.; Ahlberg, P. *Tetrahedron* **2002**, *58* (23), 4669–4673.
- (45) Asami, M.; Suga, T.; Honda, K.; Inoue, S. *Tetrahedron Lett.* **1997**, *38* (36), 6425–6428.
- (46) Li, J.; Hua, R.; Liu, T. *J. Org. Chem.* **2010**, *75* (9), 2966–2970.
- (47) Jacobsen, E. N.; Zhang, W.; Muci, A. R.; Ecker, J. R.; Deng, L. *J. Am. Chem. Soc.* **1991**, *113* (18), 7063–7064.

- (48) Salvador, J. A. R.; Hanson, J. R. *J. Chem. Res.* **2002**, 2002 (11), 576–578.
- (49) Ma, E.; Kim, H.; Kim, E. *Steroids* **2005**, 70 (4), 245–250.
- (50) Zhao, Y.-C.; Xiang, Y.-Z.; Pu, L.; Yang, M.; Yu, X.-Q. *Appl. Catal. Gen.* **2006**, 301 (2), 176–181.
- (51) Holland, H. L. *Can. J. Chem.* **1983**, 61 (9), 2165–2170.
- (52) Schaus, S. E.; Brandes, B. D.; Larrow, J. F.; Tokunaga, M.; Hansen, K. B.; Gould, A. E.; Furrow, M. E.; Jacobsen, E. N. *J. Am. Chem. Soc.* **2002**, 124 (7), 1307–1315.
- (53) Jeon, O.-Y.; Carreira, E. M. *Org. Lett.* **2010**, 12 (8), 1772–1775.
- (54) Mordini, A.; Bindi, S.; Pecchi, S.; Degl’Innocenti, A.; Reginato, G.; Serci, A. *J. Org. Chem.* **1996**, 61 (13), 4374–4378.
- (55) Crimmins, M. T.; King, B. W. *J. Am. Chem. Soc.* **1998**, 120 (35), 9084–9085.
- (56) Pangborn, A. B.; Giardello, M. A.; Grubbs, R. H.; Rosen, R. K.; Timmers, F. J. *Organometallics* **1996**, 15 (5), 1518–1520.
- (57) Still, W. C.; Kahn, M.; Mitra, A. *J. Org. Chem.* **1978**, 43 (14), 2923–2925.
- (58) Moffett, B. *Org. Synth.* **1952**, 32, 41.
- (59) Magoon, E. F.; Slauch, L. H. *Tetrahedron* **1967**, 23 (12), 4509–4515.
- (60) Bark, T.; Stoeckli-Evans, H.; Zelewsky, A. von. *J. Chem. Soc., Perkin Trans. I* **2002**, No. 16, 1881–1886.
- (61) Qi, L.; Yamamoto, N.; Meijler, M. M.; Altobelli, L. J.; Koob, G. F.; Wirsching, P.; Janda, K. D. *J. Med. Chem.* **2005**, 48 (23), 7389–7399.
- (62) Fernández-Mateos, A.; Herrero Teijón, P.; Rubio González, R. *Tetrahedron* **2013**, 69 (5), 1611–1616.
- (63) Kimura, M.; Shimizu, M.; Tanaka, S.; Tamaru, Y. *Tetrahedron* **2005**, 61 (15), 3709–3718.
- (64) Gansäuer, A.; Klatte, M.; Brändle, G. M.; Friedrich, J. *Angew. Chem. Int. Ed.* **2012**, 51 (35), 8891–8894.
- (65) Ceylan, M.; Budak, Y.; Gürdere, M. B.; Özdemir, İ.; Finkik, E. *Turk. J. Chem.* **2007**, 31 (6), 647–657.
- (66) Ager, D. J.; Anderson, K.; Oblinger, E.; Shi, Y.; VanderRoest, J. *Org. Process Res. Dev.* **2007**, 11 (1), 44–51.
- (67) Akai, S.; Hanada, R.; Fujiwara, N.; Kita, Y.; Egi, M. *Org. Lett.* **2010**, 12 (21), 4900–4903.

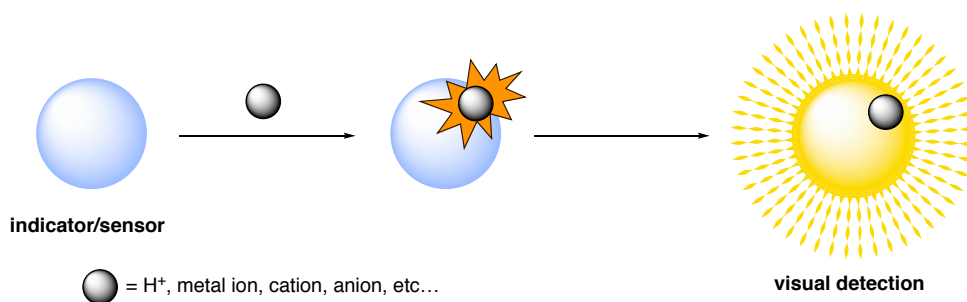
- (68) Tse, M. K.; Bhor, S.; Klawonn, M.; Anilkumar, G.; Jiao, H.; Spannenberg, A.; Döbler, C.; Mägerlein, W.; Hugl, H.; Beller, M. *Chem. – Eur. J.* **2006**, *12* (7), 1875–1888.
- (69) Witkop, B.; Foltz, C. M. *J. Am. Chem. Soc.* **1957**, *79* (1), 197–201.
- (70) Kumar, R.; Sharma, A.; Sharma, N.; Kumar, V.; Sinha, A. K. *Eur. J. Org. Chem.* **2008**, *2008* (33), 5577–5582.
- (71) Pasqua, A. E.; Ferrari, F. D.; Hamman, C.; Liu, Y.; Crawford, J. J.; Marquez, R. *J. Org. Chem.* **2012**, *77* (16), 6989–6997.
- (72) Silvestre, S. M.; Salvador, J. A. R.; Clark, J. H. *J. Mol. Catal. Chem.* **2004**, *219* (1), 143–147.
- (73) Bartoszewicz, A.; Kalek, M.; Stawinski, J. *Tetrahedron* **2008**, *64* (37), 8843–8850.
- (74) Jeyakumar, K.; Chand, D. K. *Synthesis* **2008**, *2008* (5), 807–819.
- (75) Holla, H.; Jenkins, I. D.; Neve, J. E.; Pouwer, R. H.; Pham, N.; Teague, S. J.; Quinn, R. J. *Tetrahedron Lett.* **2012**, *53* (52), 7101–7103.
- (76) Earley, W. G.; Jacobsen, J. E.; Madin, A.; Meier, G. P.; O'Donnell, C. J.; Oh, T.; Old, D. W.; Overman, L. E.; Sharp, M. J. *J. Am. Chem. Soc.* **2005**, *127* (51), 18046–18053.
- (77) Kern, N.; Dombrey, T.; Blanc, A.; Weibel, J.-M.; Pale, P. *J. Org. Chem.* **2012**, *77* (20), 9227–9235.
- (78) Kanomata, K.; Toda, Y.; Shibata, Y.; Yamanaka, M.; Tsuzuki, S.; Gridnev, I. D.; Terada, M. *Chem. Sci.* **2014**, *5* (9), 3515–3523.
- (79) Matsumoto, K.; Usuda, K.; Okabe, H.; Hashimoto, M.; Shimada, Y. *Tetrahedron Asymmetry* **2013**, *24* (2–3), 108–115.
- (80) Huckins, J. R.; de Vicente, J.; Rychnovsky, S. D. *Org. Lett.* **2007**, *9* (23), 4757–4760.
- (81) Griffin, B. A.; Adams, S. R.; Tsien, R. Y. *Science* **1998**, *281* (5374), 269–272.
- (82) Adams, S. R.; Campbell, R. E.; Gross, L. A.; Martin, B. R.; Walkup, G. K.; Yao, Y.; Llopis, J.; Tsien, R. Y. *J. Am. Chem. Soc.* **2002**, *124* (21), 6063–6076.
- (83) Lemieux, G. A.; de Graffenried, C. L.; Bertozzi, C. R. *J. Am. Chem. Soc.* **2003**, *125* (16), 4708–4709.
- (84) Lowry, O. H.; Rosebrough, N. J.; Farr, A. L.; Randall, R. J. *J. Biol. Chem.* **1951**, *193* (1), 265–275.
- (85) Duke, R. M.; Veale, E. B.; Pfeffer, F. M.; Kruger, P. E.; Gunnlaugsson, T. *Chem. Soc. Rev.* **2010**, *39* (10), 3936–3953.

- (86) Yoder, L. *J. Ind. Eng. Chem.* **1919**, *11* (8), 755–755.
- (87) Wang, M.; Leung, K.-H.; Lin, S.; Chan, D. S.-H.; Kwong, D. W. J.; Leung, C.-H.; Ma, D.-L. *Sci. Rep.* **2014**, *4*, 6794.
- (88) Whitehead, T. H.; Wills, C. C. *Chem. Rev.* **1941**, *29* (1), 69–121.
- (89) Bandar, J. S.; Lambert, T. H. *J. Am. Chem. Soc.* **2012**, *134* (12), 5552–5555.
- (90) Inanaga, J.; Hirata, K.; Saeki, H.; Katsuki, T.; Yamaguchi, M. *Bull. Chem. Soc. Jpn.* **1979**, *52* (7), 1989–1993.
- (91) Shiina, I.; Kubota, M.; Oshiumi, H.; Hashizume, M. *J. Org. Chem.* **2004**, *69* (6), 1822–1830.
- (92) Goswami, S.; Das, A. K.; Sen, D.; Aich, K.; Fun, H.-K.; Quah, C. K. *Tetrahedron Lett.* **2012**, *53* (36), 4819–4823.
- (93) Sarmini, K.; Kenndler, E. *J. Biochem. Biophys. Methods* **1999**, *38* (2), 123–137.
- (94) Na Kim, H.; Hee Lee, M.; Jung Kim, H.; Seung Kim, J.; Yoon, J. *Chem. Soc. Rev.* **2008**, *37* (8), 1465–1472.
- (95) Beija, M.; M. Afonso, C. A.; G. Martinho, J. M. *Chem. Soc. Rev.* **2009**, *38* (8), 2410–2433.
- (96) Lee, M. H.; Kim, H. J.; Yoon, S.; Park, N.; Kim, J. S. *Org. Lett.* **2008**, *10* (2), 213–216.
- (97) Yuan, L.; Lin, W.; Feng, Y. *Org. Biomol. Chem.* **2011**, *9* (6), 1723–1726.
- (98) Best, Q. A.; Xu, R.; McCarroll, M. E.; Wang, L.; Dyer, D. J. *Org. Lett.* **2010**, *12* (14), 3219–3221.
- (99) Xue, Z.; Chen, M.; Chen, J.; Han, J.; Han, S. *RSC Adv.* **2013**, *4* (1), 374–378.
- (100) Hofmann, C.; Schuler, S. M. M.; Wende, R. C.; Schreiner, P. R. *Chem Commun* **2014**, *50* (10), 1221–1223.
- (101) Birman, V. B.; Jiang, H. *Org. Lett.* **2005**, *7* (16), 3445–3447.
- (102) Gupta, V. K.; Goyal, R. N.; Sharma, R. A. *Talanta* **2008**, *76* (4), 859–864.
- (103) Zhang, Y.-M.; Lin, Q.; Wei, T.-B.; Wang, D.-D.; Yao, H.; Wang, Y.-L. *Sens. Actuators B Chem.* **2009**, *137* (2), 447–455.
- (104) Sahoo, P. R.; Mishra, P.; Agarwa, P.; Gupta, N.; Kumar, S. *J. Incl. Phenom. Macrocycl. Chem.* **84** (1–2), 163–171.

Chapter 2. Developing a Colorimetric Detection Method for the Competing Enantioselective Conversion Method

2.1 Introduction to Visual Detection

The use of methods to enhance our ability to visually detect microscopic phenomena has long been a vital tool for biologist and chemist alike. From pH indicators to green fluorescent protein (GFP), visual detection methods have changed the way we design and approach scientific problems.¹⁻³ One testament to the power of visual detection methods is Oliver Lowry's colorimetric detection of protein concentration, which is the most cited paper of all time with over 300,000 citations.⁴ Detection methods have allowed scientists to solve problems that were thought to be unsolvable, and scientists have succeeded in pushing boundaries in their research as a result. The goal of these visual detection methods is to represent chemical concentrations or changes with visible signals (Scheme 2.1). Chemical visual detection methods can be broken down into three broad categories: chemical indicators, complexometric indicators, and redox indicators.

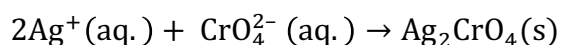


Scheme 2.1: General schematic for a visual detection method.

The most common type of chemical indicators are pH indicators. These molecules are typically weak acids or bases that undergo a color change as the pH of a solution passes a transition point. Anion/cation indicators are a more general type of chemical indicator that elicit

a color change upon exposure to an anion or cation. These are commonly used for the detection of certain anions, such as chloride, acetate, fluoride, and phosphate in aqueous biological and environmental samples.⁵ Chemical indicators can also be used to detect the consumption of a certain reagent through formation of a precipitate. The Mohr method for determining the amount of chloride present in a sample uses potassium chromate as an endpoint. When all the chloride has reacted with silver, a red/brown precipitate forms indicating the endpoint through formation of silver chromate (Equation 2.1):⁶

Equation 2.1: Formation of the Ag_2CrO_4 (s) precipitate in the Mohr method.



Complexometric indicators are used to determine the presence of specific metal ions. These indicators can be specific to a certain metal ion or general for multiple metal ions. These types of indicators are common used to monitor the concentration of metals in environmental samples, or to detect the endpoint when no more ethylenediaminetetraacetic acid (EDTA) is present in solution during titrations.⁷

Redox indicators, or oxidation-reduction indicators, undergo a color change at a specific electrode potential. Redox indicators are broken up into metal-organic complexes and organic redox systems. Redox indicators can also include a proton as part of the electrochemical reaction, separating redox indicators further into pH dependent or pH independent indicators. These indicators are commonly used in analytical chemistry to visualize when enough of an oxidant or reductant has been added.⁸

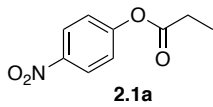
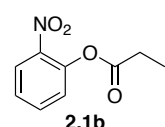
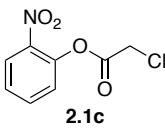
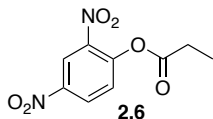
2.2 Introduction to Utilizing Colorimetric Detection in the CEC Method

There are currently three primary means for determining the conversion of reactions using the CEC method: ^1H NMR, mass spectrometry (MS), and thin layer chromatography (TLC). Using ^1H NMR provides a simple analysis and allows one to differentiate between small differences in conversion; however, monitoring CEC reactions by ^1H NMR requires milligram quantities of sample, NMR time, and is typically limited to single sample at one time.^{9,10} Mass spectrometry is very sensitive and can be used to test microgram-sized samples. Additionally, multiple substrate samples can be tested at once as long as there are no overlapping mass peaks.¹¹ Nevertheless, mass spectrometry is limiting as it can be time consuming, requires a method with suitable pseudo-enantiomers of the chiral kinetic resolution catalyst, and is not suited to running >5 compounds at a time. TLC is both sensitive and inexpensive, requiring only a few micrograms of substrate; however, TLC presents difficulties when discriminating small differences in conversion and running screens of ten or more compounds.^{12,13} A colorimetric approach to the current CEC method would remove some of the current limitations of the other monitoring methods. In addition to being able to use mass spectrometry, NMR, or TLC to determine the conversion of the reaction, the observer would be able to identify the configuration of the substrate by simply looking at the color or fluorescence of the reaction. Ideally a colorimetric method would produce very sensitive results with a minimal amount of substrate, not requiring expensive equipment or instrumentation. The goal in developing this method would be to eventually run 96-well plate reactions (or 48 parallel reactions on 48 different substrates), enabling high-throughput screening of biologically active or pharmacological compounds quickly, and inexpensively, without complicated analysis.

Initial experiments into a colorimetric method were conducted by Dr. Alex Wagner and Jonathan David in the Rychnovsky Lab. Unsubstituted aromatic esters do not absorb in the visible region of the UV-VIS spectra. To shift the absorption into the visible region, the tested acyl sources contained a nitro aromatic ester. Compared to the standard CEC reaction with propionic anhydride, use of these aromatic esters results in substantially longer reaction times, hindering the practicality of these esters in a colorimetric method. The most promising result was the 2,4-dinitrophenyl propionate ester **2.6** (entry 10 and 11), which led to acceptable conversions within 26 hours with good selectivity between enantiomers of HBTM (Table 2.1).

Table 2.1: Initial experiments testing different acyl sources (**2.1a–2.1c**, **2.6**) in the CEC reaction of (1*R*,2*S*)-2-phenylcyclohexan-1-ol.

(1*R*,2*S*)-2-phenylcyclohexan-1-ol

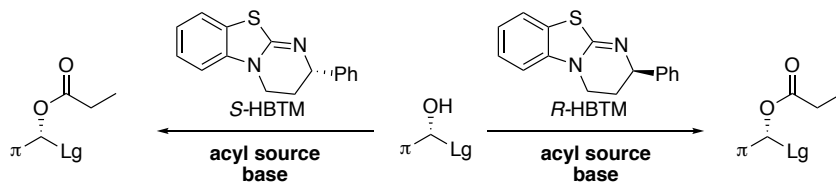
entry	acyl source	time (h)	<i>S</i> -HBTM color (% conversion)	<i>S</i> -HBTM color (% conversion)
1	 2.1a	20	light yellow (0%)	light yellow (0%)
2		46.5	yellow (0%)	yellow (0%)
3		118	bright yellow (47%)	bright yellow (7%)
4	 2.1b	18	bright yellow (1%)	gold yellow (0%)
5		46	bright yellow (5%)	gold yellow (0%)
6		72	bright yellow (9%)	gold yellow (0%)
7	 2.1c	2.2	gold yellow (23%)	gold yellow (11%)
8		43.1	gold yellow (100%)	gold yellow (34%)
9		51.8	gold yellow (100%)	gold yellow (44%)
10	 2.6	2	gold yellow (9%)	gold yellow (0%)
11		26.1	dark gold yellow (26%)	dark gold yellow (2%)

2.3 A Quantitative Approach Using UV-VIS Spectroscopy

UV-VIS spectroscopy is an attractive spectroscopic technique due to the instrument sensitivity, speed of the trials, and possibility of using a 96-well plate to run 48 parallel reactions at once. UV-VIS spectrometers are common in scientific labs and relatively inexpensive compared to other types of spectroscopy, making them ideal for use with the CEC method. The change of the UV-VIS absorbance over the course of the reaction could be used to monitor conversion.

A chromophore is necessary to monitor this change. Currently there are two UV-VIS active species in the CEC reaction: the HBTM catalyst and certain π -groups on the alcohol substrate. The reaction conversion cannot be monitored by a change in the absorbance of HBTM catalyst, since there will be no overall change during the reaction. The substrate alcohol is also a poor chromophore choice since it limits the scope to aromatic alcohols, eliminating the possibility of developing a consistent kinetic method, and introduces the possibility of overlapping UV-VIS absorbance between the starting alcohol and the product ester. Applying the CEC method to UV-VIS spectroscopy required the addition of a new chromophore, either through the base or the acyl source (Scheme 2.2).

Scheme 2.2: Modification of the CEC method to incorporate a chromophore in either the acyl source or the base.



2.4 Aromatic Bases

To test the viability of switching *N,N*-diisopropylethylamine (DIPEA) for an aromatic base, several aromatic bases were analyzed by UV-VIS spectroscopy. Various pyridine, quinoline, imidazole, porphyrin, and miscellaneous substrates were tested (Figure 2.1). Unfortunately, the starting UV-VIS spectra in acetonitrile for these substrates was blue shifted, and upon protonation with aq. 1.0 M HCl or propionic acid the spectra became even more blue shifted. This blue shift, or hypsochromic shift, is a result of the lower energy level of the unexcited state of the *n* orbital, causing an increase in the energy required to affect the *n* to π^* transition. The only exception was the cyclopropenimine base **2.2** which becomes aromatic upon protonation, causing the UV-VIS spectrum to become red shifted ($\lambda_{\text{max}} = 318 \text{ nm}$);¹⁴ however, this falls within the HBTM absorption region (275–325 nm) (Figure 2.2) complicating quantitative UV-VIS analysis.

Some substrates such as 1,2-dimethylimidazole, 2,6-diphenylpyridine, and quinoline showed no change in the UV-VIS spectrum upon addition of either acid, suggesting that the base was not strong enough in polar aprotic solvents. The region of the UV-VIS spectra encountered by the blue shifted bases overlaps with many UV-VIS active compounds, causing the UV-VIS spectra to vary for every new substrate. This would limit any quantitative or kinetic analysis of conversion to be developed, pushing us to examine the possibility of an aromatic acyl source.

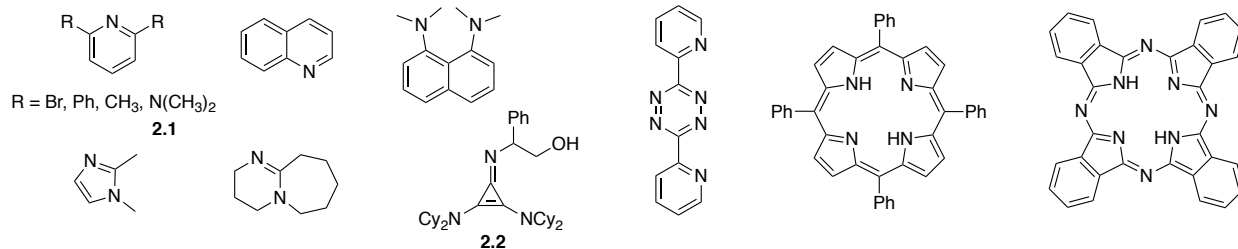
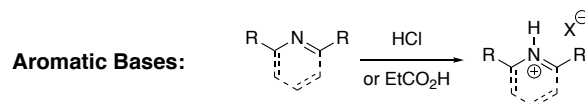


Figure 2.1: Bases tested in UV-VIS in neutral and protonated forms.

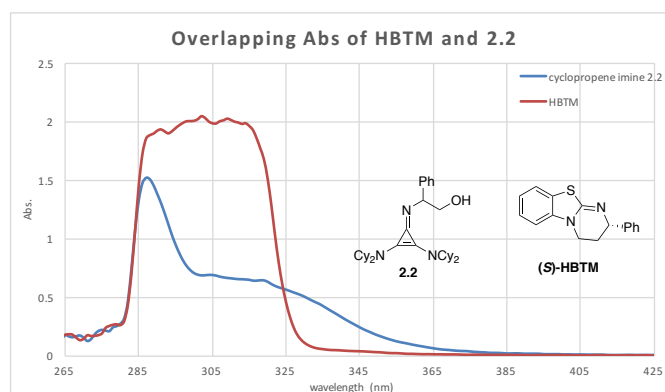


Figure 2.2: Overlap in UV-VIS absorption between cyclopropenimine base **2.2** and (*S*)-HBTM.

2.5 Aromatic Esters and Mixed Anhydrides

Through modification of substituents on an aromatic ring the UV-VIS absorption can be shifted to higher or lower wavelengths. Groups that do not necessarily absorb in the UV-VIS region, but shift the UV-VIS absorption to a different wavelength are called auxochromes. Shifting the absorption to longer wavelengths provides a red shift or bathochromic shift. Electron rich or negatively charged groups tend to have an auxochromic effect on the UV-VIS absorption of the group they are attached to (Figure 2.2).

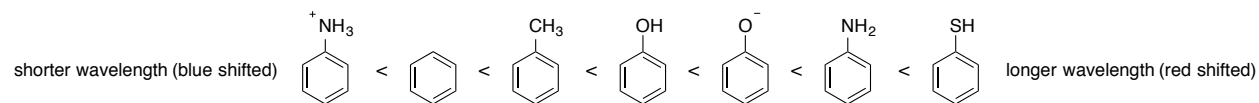
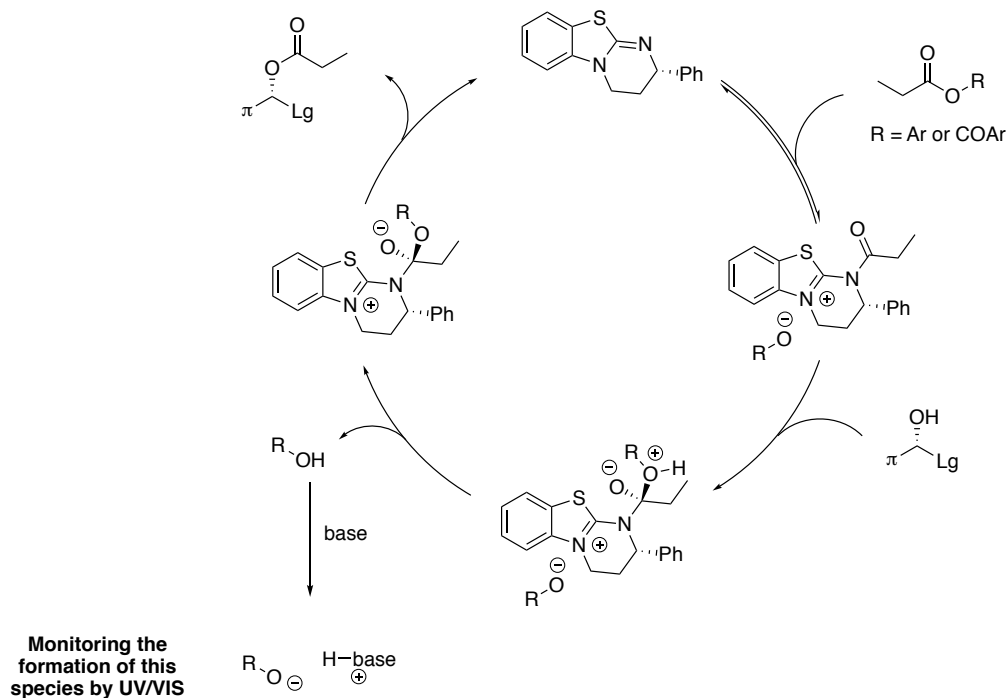


Figure 2.3: Substituent effect on the UV absorption of UV active π systems.

It was envisioned that aromatic mixed anhydrides and esters could act as auxochromic groups after the transfer of the acyl group (Figure 2.3). Upon reaction with HBTM, and subsequently the substrate alcohol, the aromatic portion would be lost as the benzoic acid or phenol. Off cycle, this would then be deprotonated by the base to form trialkylammonium benzoate or trialkylammonium phenoxide (Scheme 2.3). Ideally these negatively charged species would exhibit an auxochromic effect and red shift the UV-VIS spectra of the reaction compared to the starting mixed anhydride or ester. This would allow quantitative monitoring of the product formation by UV-VIS spectroscopy.

Scheme 2.3: Catalytic cycle for HBTM catalyzed acylation of alcohols with an aromatic mixed anhydride or ester.⁹



Mixed anhydrides **2.3**, **2.4** were chosen due to their well-known acylation properties in macrolactonization reactions.^{15,16} Mixed anhydride **2.3** is a variant of 2,4,6-trichlorobenzoyl

chloride (TCBC, Yamaguchi reagent), and is essentially the active mixed anhydride typically formed in the Yamaguchi macrolactonization.¹⁵

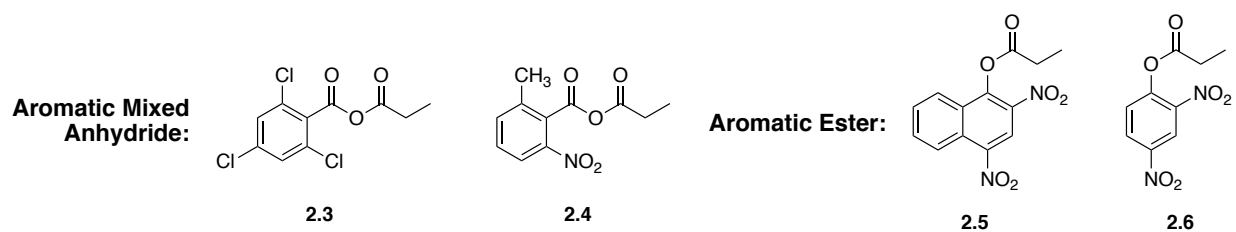


Figure 2.4: Main tested aromatic mixed anhydrides **2.3** and **2.4**, and aromatic esters **2.5** and **2.6** for use in the CEC method.

To determine whether mixed anhydrides would be viable chromophores in the CEC reaction, UV-VIS spectra were taken of the free carboxylic acid, the triethylammonium benzoate, and the mixed anhydride (Figure B1). Trichloro mixed anhydride **2.3** exhibited a bathochromic shift in the UV-VIS spectra upon deprotonation of the free acid (Figure B1). Examining the UV-VIS showed an overlap of mixed anhydride **2.3** with the HBTM absorption region (275–325 nm) (Figure 2.2). This presented issues with developing this technique for use as a kinetics method due to the overlapping peaks. Thus, mixed anhydride **2.3** was abandoned. Mixed anhydride **2.4** was also examined, but the small change in absorption between the anhydride and the benzoate forms was not ideal, prompting us to examine aromatic esters **2.5** and **2.6** as acyl sources.

Drawing from the previous work by Jonathan David and Dr. Alex Wagner in our lab on nitro esters **2.1a** and **2.1b** (Table 2.1), we examined additional nitro species. While the mononitro esters **2.1a** and **2.1b** were not reactive enough for practical use in a CEC method, the dinitro phenyl ester **2.6** showed promising initial results (Table 2.1, entry 10 and 11). Examining the UV-VIS absorption spectra of mononitro esters **2.1a** and **2.1b** in addition to dinitro naphthyl ester **2.5**, it was observed that phenyl ester **2.6** showed a region of absorbance between 400–475 nm in the Et₃N salt without any overlap with the propionate ester or the phenol (Figure 2.5). This

provided ideal conditions for monitoring the reaction and obtaining kinetic data. Dinitro compound **2.6** absorbed in a range without overlapping absorption with HBTM, however to broaden the range of possible substrates it would be desirable to extend the UV-VIS absorption to even longer wavelengths. The extended π -system of dinitronaphthol propionate ester **2.5** decreases the gap between the π and π^* orbitals, shifting the absorption to longer wavelengths (Figure 2.4).

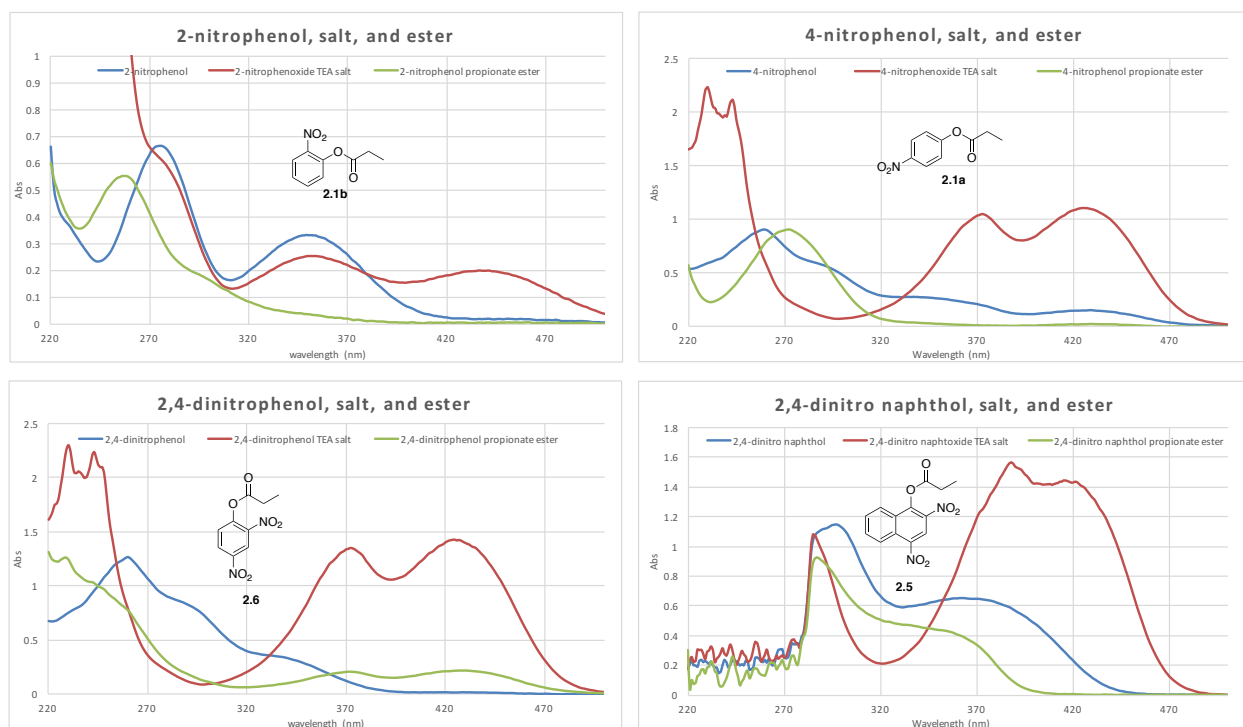


Figure 2.5: UV-VIS spectra of **2.1a**, **2.1b**, **2.5**, and **2.6** as the phenol, Et₃N salt, and propionate ester.

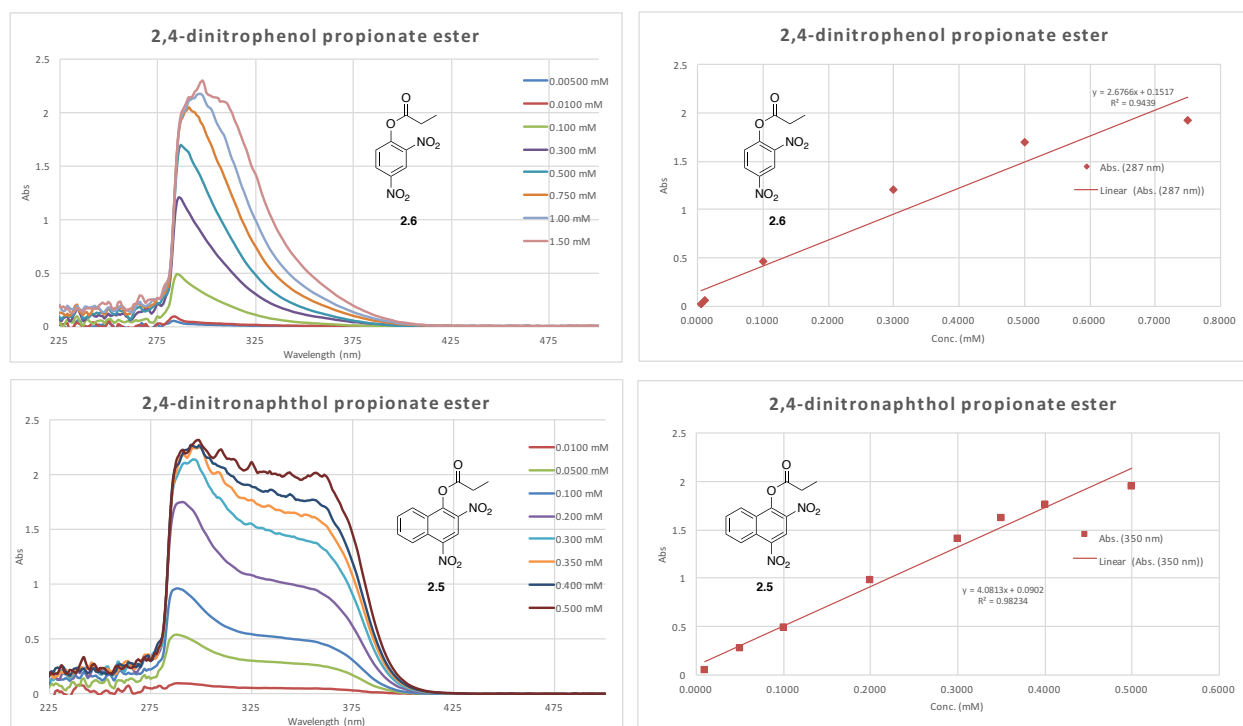


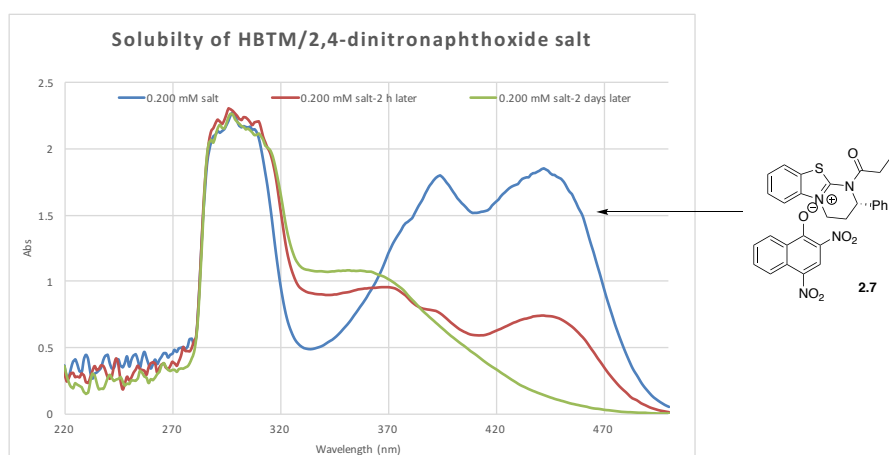
Figure 2.6: UV-VIS traces of propionate esters **2.6** and **2.5** at varying concentrations, and Beer's Law plots of Abs. vs concentration (mM).

Next, concentration studies were performed on compound **2.5** and **2.6** as the propionate ester and the DIPEA salt (Figure 2.6). HBTM and (*S*)-(-)-1-(1-naphthyl)ethanol were also tested to ensure that the UV-VIS spectra would not overlap with compound **2.5** and **2.6** (Figure 2.6, Figure B2). Beer's Law plots of both compounds showed linear trends at lower concentrations; however, at higher concentrations the UV-VIS spectra exhibited a decrease in expected absorption (Figure 2.6).

Next, the acylation characteristics of **2.5** were studied by ^1H NMR. A solution of HBTM and **2.5** in CDCl_3 was allowed to react and then examined by ^1H NMR. When 0.50 equiv. of naphthyl ester **2.5** was used, there was complete transfer of the acyl group to form acylated HBTM salt **2.7**. Using an excess of **2.5** (2.0, 5.0, or 12.0 equiv.) resulted in complete acylation of HBTM (**2.7**). When ester **2.5** was tested using 0.50 equiv. there was a 77% conversion to HBTM

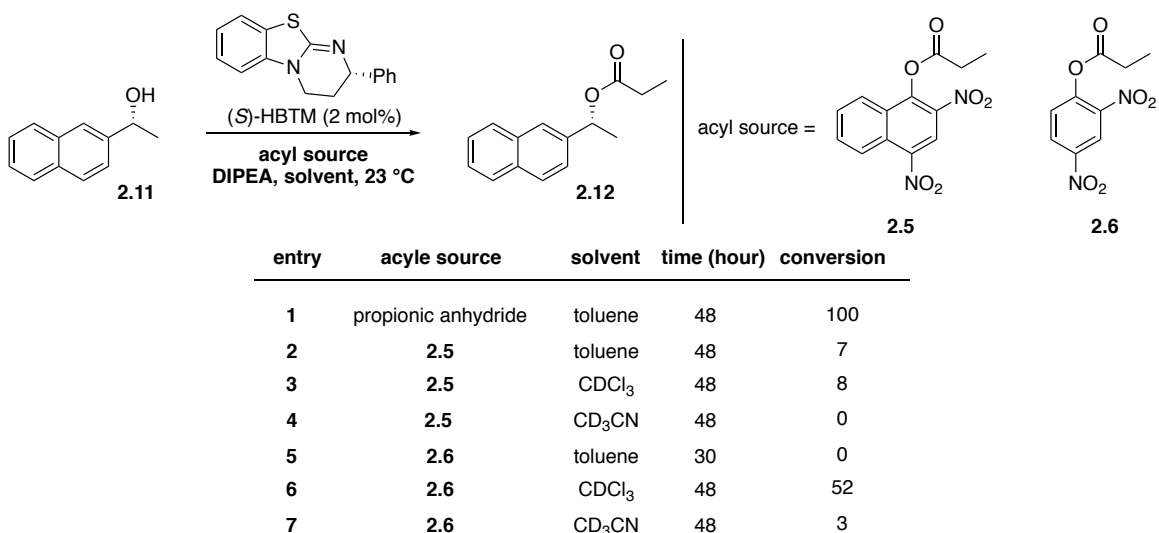
salt **2.8** (Figure B3). These results show that both esters **2.5** and **2.6** are better acylating reagents than propionic anhydride. The standard CEC conditions with propionic anhydride have been shown in kinetic studies by Dr. Alex Wagner to have a $K_{eq} = 0.25$.⁹ It was observed after sitting in the $CDCl_3$ solution that salt **2.7** began to precipitate in the NMR tube. Examining the UV-VIS absorption of salt **2.7** (Figure 2.2) confirmed that it was precipitating out of the cuvette solution as well.

Scheme 2.4: Formation of HBTM salt **2.7** or **2.8** with ester **2.5** and **2.6**, and observation of the precipitating of **2.7** out of solution over time.



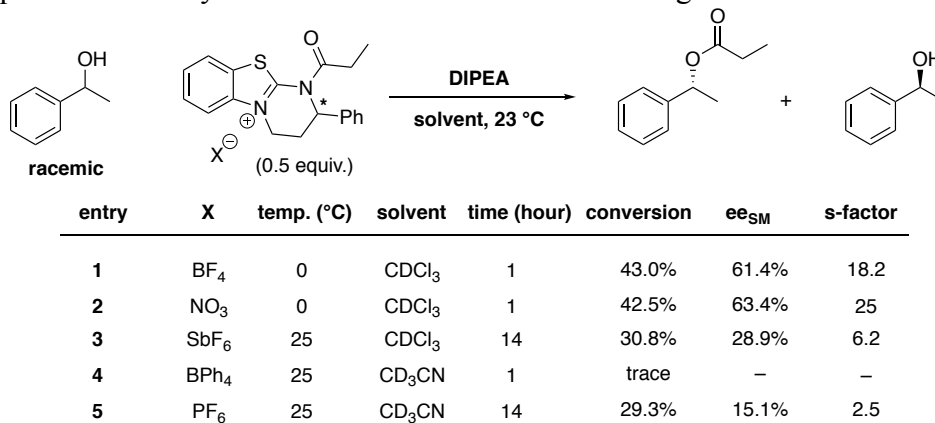
The next step was to use compounds **2.5** and **2.6** in actual CEC reactions and monitor conversion by 1H NMR. The test system used (*S*)-(-)-1-(1-naphthyl)ethanol, which was well behaved, along with the matched catalyst (*S*)-HBTM and DIPEA. Both **2.5** and **2.6** were examined in toluene- d_8 , $CDCl_3$, and CD_3CN . After 48 hours, naphthyl ester **2.5** showed low conversion to the acylated product in any of the tested solvents, while phenyl ester **2.6** showed moderate conversion in $CDCl_3$ (Table 2.2). A control reaction with propionic anhydride showed complete conversion to the acylated product after 48 hours (Table 2.2, entry 1).

Table 2.2: CEC reactions in various solvents with different acyl sources. Conversion monitored by ^1H NMR.



These results were surprising given our recent findings that **2.5** led to higher amounts of acylated HBTM than propionic anhydride, which should result in higher concentrations of activated catalyst and faster reactions. An examination of past work by Dr. Shawn Miller and Dr. Alex Wagner shed light on these results. They studied the effect of different counter ions on the reactivity of the acylated HBTM salt in a kinetic resolution, and they found that there was a dramatic effect on the rate and selectivity depending on the counter ion (Table 2.3).

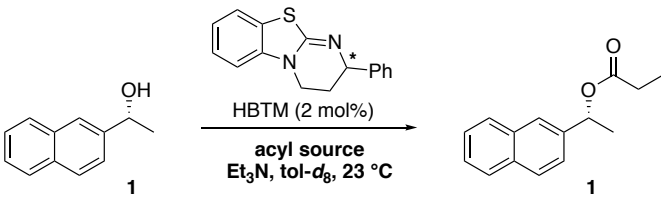
Table 2.3: Effect of HBTM salt counter ion X on the kinetic resolution of racemic secondary alcohol. Experiments run by Dr. Shawn Miller and Dr. Alex Wagner.



This suggested one of two things: that acylated HBTM salts **2.7** and **2.8** that were formed either prevented the alcohol from forming the diastereomeric catalyst substrate pair with the acylated HBTM, or greatly reduced the reactivity by stabilizing the HBTM salt. Analysis of the three HBTM salts that showed greatly reduced reactivity reveals that the anions all contain aromatic moieties (BPh₄, 2,4-dinitrophenyl, or 2,4-dinitronaphthyl). It is possible that the aromatic anions are disrupting the π interaction between the catalyst and the substrate, which has been proposed to account for the reactivity and selectivity.¹⁰ Unfortunately, increasing the amount or concentration of either the HBTM or the acyl source was limited by the intense UV-VIS absorptions. A more reactive stoichiometric acyl source was necessary to monitor the rates of the CEC reactions at the concentrations suitable for UV-VIS spectroscopy.

While the change between the UV-VIS spectrum of the Et₃N salt and the benzoic acid was not drastic for mixed anhydride **2.3**, the 320–390 nm region provided a chance to monitor this acyl source by UV-VIS. Mixed anhydride **2.3** was much more reactive than the esters; side-by-side CEC reactions with propionic anhydride and mixed anhydride **2.3** showed almost identical reactivity (Table 2.4). This result prompted a screen of additional benzoic acids and their benzoate salts (Figure B4). Of the benzoic acids screened, none offered any enlarged region of observation or enhanced spectral properties over 2-methyl-6-nitrobenzoic acid.

Table 2.4: CEC reactions with mixed anhydride **2.3** or propionic anhydride. Conversions determined by ^1H NMR.



entry	acyl source	time (min)	S-HBTM	R-HBTM
1	2.3	90	38 %	2 %
2	propionic acid	90	31 %	6 %

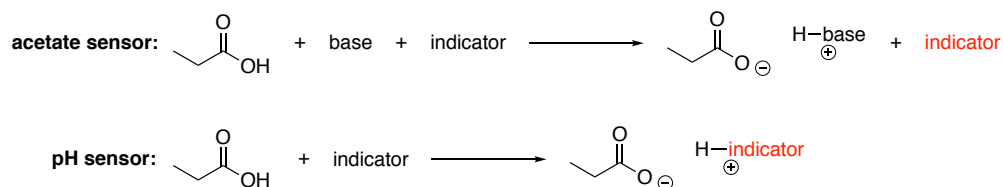
Minimizing solvent evaporation over the course of the reaction is crucial for accurate kinetic measurements. Toluene was an optimal solvent in the CEC reactions due to the high selectivity found by Birman¹⁷ and low volatility compared to CHCl_3 . Unfortunately, the use of toluene required blanking of the UV-VIS before each reaction which was not optimal. While not a large issue for single reactions, if the method were to be expanded to 96-well plates this could present additional problems. Acetonitrile was an attractive solvent choice from a volatility standpoint and the low UV-VIS cutoff (190 nm) compared to toluene (284 nm). Mixed anhydride **2.3** were tested in CEC reactions in acetonitrile alongside propionic anhydride. In toluene both propionic anhydride and mixed anhydride **2.3** went to $\sim 35\%$ conversion over 90 minutes; however, in acetonitrile neither propionic anhydride or the mixed anhydride showed any product formation after 90 minutes for either *S*- or *R*-HBTM. These results led to toluene being chosen as the solvent of choice for further UV-VIS studies.

It was necessary to find the extinction coefficient (ϵ) to relate Abs_{obs} to the concentration of phenoxide salt **2.3**. A Beer's Law plot of absorbance at known concentrations provided ϵ for both **2.3** (ϵ_{MA}) and the phenoxide salt of **2.3** (ϵ_{salt}). (Figure B5–B8). To confirm the rate law with respect to the alcohol, zero-order, first-order, and second-order rate plots were generated. A plot

of $\ln[\text{alcohol}]$ vs time gave a straight fit with $k = -\text{slope}$, confirming that the reaction is first-order in alcohol (Figure B11). The rate constant for each catalyst enantiomer was determined by plotting $1/(1-x)$ vs time ($x = \text{conversion}$). Conversion for both enantiomers of HBTM did not start at 0%, so the conversions were normalized to $t = 0$ equal to 0% conversion. Plotting $1/(1-x)$ vs time for these normalized conversions provided us with rate constants for the reactions with each enantiomer of HBTM (Figure B12). Unfortunately, the relative rates between the two enantiomers were much smaller than those previously seen by Dr. Alex Wagner for this reaction under the same conditions. The expected fast reaction enantiomer of HBTM could be determined using this method; however, the discrepancy in initial absorbance (Abs_0) and thus the percent conversion prevented the use of this method to perform kinetic analyses using either UV-VIS or a plate reader with 96-well plates.

After the setbacks in the quantitative UV-VIS method, we looked to develop a qualitative colorimetric method instead. Two approaches were to develop a sensor that detected the acetate formed in the reaction, or to develop a sensor that detected the change in pH as the reaction progressed and propionic acid is generated (Scheme 2.5).

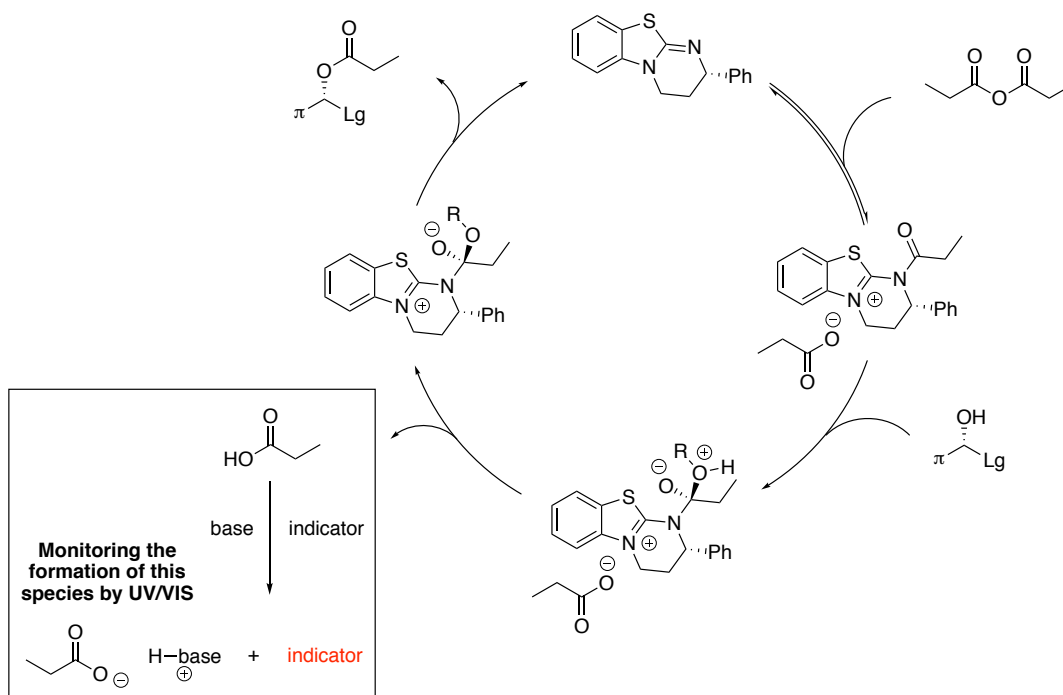
Scheme 2.5: General overview of using an acetate sensor or a pH sensor to detect progression of the CEC reaction by visual color change.



2.6 A Qualitative Approach Using Acetate Sensors

Our initial approach involved the use of a substoichiometric acetate sensor to take advantage of the trialkylammonium propionate that is generated off-cycle in the CEC reactions (Scheme 2.6). Upon formation of the carboxylate, the indicator would change color indicating reaction progress. The extent of conversion could be qualitatively analyzed by examining which reaction was closer to the end color of the acetate sensor.

Scheme 2.6: HBTM catalytic cycle incorporating the use of a pH sensitive indicator.



A wide range of acetate sensors have been studied in the literature; unfortunately, many of these studies were performed in aqueous or polar solvents such as MeCN, DMSO, or DMF. The CEC reactions could not be run in aqueous conditions; however, prior work by Birman had shown that kinetic resolutions with HBTM could be run in MeCN, albeit with reduced *s*-values.¹⁷ Common structural motifs throughout these acetate sensors hydrazones and nitro-substituted aromatic rings, which require highly polar solvents. For solubility, the first acetate sensors that

were studied were naphthylhydrazone **2.13** and quinolinehydrazone **2.14** (Figure 2.7).¹⁸ These compounds were sparingly soluble in most organic solvents, however they somewhat soluble in acetone. Addition of a solution of tetrabutylammonium acetate (TBAA) produced a slightly darker orange color. The change in color for **2.13** and **2.14** was not diagnostic enough to practically distinguish between a high and low conversion CEC reaction. This led to the investigation of several other acetate sensors to discover one that would provide a reasonably diagnostic color change.

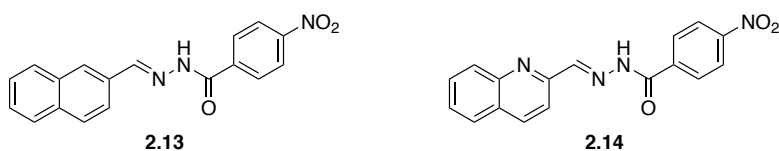
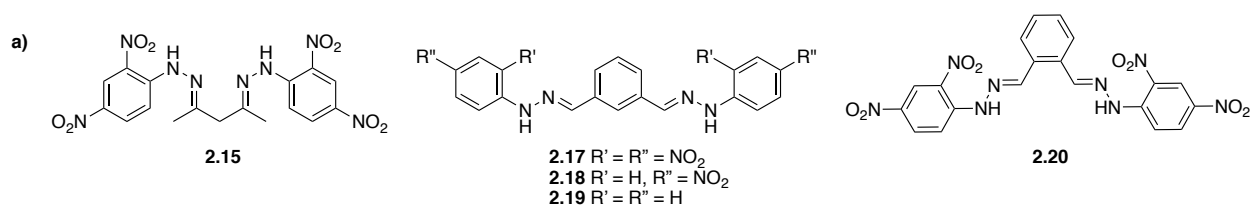


Figure 2.7: Structures of acetate sensors **2.13** and **2.14**.

The next acetate sensors that were tested were symmetrical hydrazones **2.15–2.20** (Table 2.5 a)). The NH protons in sensors **2.15** and **2.19** were not as acidic and no color change was observed upon addition of base or acid; however, the NH protons on other compounds were more acidic and a color change was observed upon addition of a base (DIPEA or DBU) (Table 2.5 b) and 2.5 c)). Addition of propionic acid restored the color to the initial state. Addition of TBAA gave a noticeable change in color for all acetate sensors except **2.18** and **2.19** (Table 2.5 c)) entry 3 and 4). It is possible that the wider angle between the bis-hydrazone groups on **2.18** and **2.19** prevent the intermolecular interactions between the acetate ion and the sensor needed to cause a color change. The change in color when TBAA was added, but not when base/acid were added, was concerning, since the original studies for these acetate sensors all use a tetra-alkyl ammonium acetate salt as the acetate source. Work by Sarmini and Kenndler showed that the pK_a of acetic acid in acetonitrile is 22.3, whereas the pK_a for trialkyl ammonium salts are 18.1; suggesting that the equilibrium favors the carboxylic acid instead of the carboxylate.¹⁹

Table 2.5: a) Tested acetate sensors; Color changes for different acetate sensors in MeCN (b) or toluene (c) upon addition of base, base + acid, or TBAA.



b) entry	acetate sensor	initial	DIPEA	DIPEA+propionic acid	TBAA
1	2.15	yellow	yellow	yellow	red
2	2.17	insoluble	insoluble	insoluble	insoluble
3	2.20	yellow/orange	dark orange	yellow	red

c) entry	acetate sensor	initial	DBU	DBU+propionic acid	TBAA
1	2.15	yellow	dark red	orange	–
2	2.20	yellow	dark purple	yellow	–
3	2.19	faint yellow	faint yellow	faint yellow	faint yellow
4	2.18	yellow	brown	yellow	yellow

Testing acetate sensor **2.20** in different CEC compatible solvents yielded similar results. It is possible that the base deprotonates the sensor causing a color change, and then upon acidification of the solution the sensor is a reprotonated, restoring the original color (Table 2.6). The different solvents did have a slight influence on the colors produced when DBU or DBU/propionic acid were added.

Table 2.6: Solvent screen to see the effect of different solvents on the color of **2.20** when DBU was added or DBU and propionic acid.

entry	solvent	2.20 initial	DBU	DBU+propionic acid
1	toluene	yellow	dark purple	yellow
2	MeCN	yellow/orange	dark purple	yellow
3	acetone	orange	red	orange
4	THF	yellow	dark orange	yellow
5	tert-amyl alcohol	yellow	dark purple	yellow

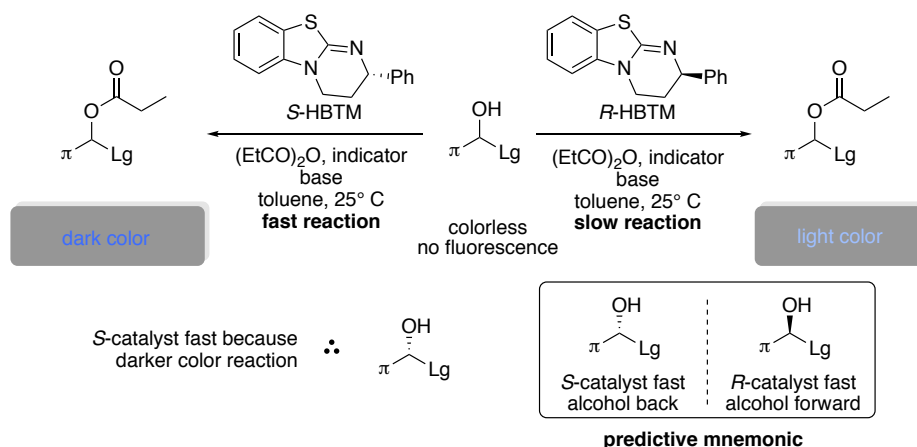
To verify that we were observing a deprotonation/protonation event, compounds **2.15** and **2.20** were examined by ¹H NMR. When DBU was added to the NMR solution of compound **2.15**

no signs of deprotonation of the sensor or protonated DBU were observed. Addition of propionic acid to the solution caused a broadening of the DBU peaks, but no change in the peaks of the acetate sensor. This contrasted with **2.20** which exhibited a shift in the aromatic protons of the sensor when DBU was added, and a return upon addition of propionic acid (Figure A7). Additionally, **2.15** was tested under the acylating conditions of the CEC reactions to see if the sensor would undergo acylation. Over the course of standard CEC reaction (90 min) no change was observed in the spectra, and even after 15 hours, the spectrum was identical. Addition of TBAA to the NMR sample resulted in a drastic change in color from yellow to brown and a loss of the sharp NH peak at 11.15 ppm. The numerous issues encountered with using an acetate sensor led us to pursue using an acid sensitive indicator instead.

2.7 A Qualitative Approach Using Acid Sensitive Indicators

The issues encountered with using a stoichiometric UV-VIS indicator or catalytic acetate sensor led us to examine the viability of using a substoichiometric, acid sensitive indicator in the CEC reaction. As HBTM acylates the alcohol, an equivalent of propionic acid or trialkylammonium propionate is generated. We decided that utilizing an acid/base sensitive indicator could take advantage of this off-cycle process. Ideally the indicator would begin one color/colorless at the beginning of the reaction and distinctly change color throughout the progression of the reaction as more of the acidic species was generated. The faster reacting catalyst/substrate combination would produce more of the acidic species, eliciting a stronger color change, allowing its identification purely on visual inspection (Scheme 2.7).

Scheme 2.7: Reaction scheme for incorporating an acid sensitive indicator to detect the fast reacting catalyst/substrate pair visually.



Initial tests included common pH indicators such as methyl red, bromocresol green, thymol blue, bromothymol blue, rhodamine 6G, neutral red, bromophenol blue, alizarin red, carbol fuchsin, phenol red, and methyl orange. Of those tested, bromocresol green was blue/purple when basic and yellow when propionic acid was added; bromothymol blue was yellow when basic and violet with propionic acid was added; bromophenol blue was purple when basic and yellow when propionic acid was added; and neutral red was yellow when basic and dark orange when propionic acid added. These indicators were then tested to see if these color changes would occur in conditions present during the CEC reaction (Scheme 2.7). Over 1 hour under CEC conditions bromocresol green went from purple to yellow (Figure 2.8), neutral red remained a yellow solution, bromophenol blue went from purple to a lighter purple, and bromothymol blue stayed a yellow solution. While the change in color from beginning to end for bromocresol green was drastic, it unfortunately occurred for both (*R*) and (*S*)-HBTM catalyzed reactions. TLC confirmed a clear difference in conversion between the two enantiomers of catalyst and the (*S*)-(-)-1-(1-naphthyl)ethanol. A control experiment without an alcohol

substrate produced the same color change, suggesting that the color change was not due to protonation of the indicator but instead acylation of the phenol groups on the indicator.

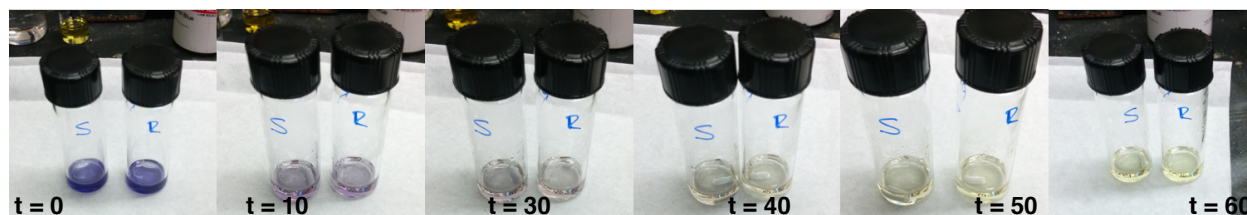


Figure 2.8: Change in color over 60 minutes for both *S*-HBTM (S) and *R*-HBTM (R) catalyzed reactions with (*S*)-(-)-1-(1-naphthyl)ethanol, bromocresol green, propionic anhydride, and DIPEA in toluene.

This knowledge led us to examine other pH sensitive indicators without phenols or primary amines that could be easily acylated. The dyes/indicators tested included: methylene blue, rhodamine 6G, rhodamine B, rhodamine B ethyl ester, sulforhodamine, acid fuchsin, thioflavin T, FD&C blue, neofuchsin standard, brilliant blue G, brilliant blue R, crystal violet, crystal violet lactone, Nile blue A, cresyl violet, xylene cyanole FF, new fuchsin, Nile red, malechite green oxylate, Sudan black B, Sudan red 7B, ponceau S, thioazole yellow G, tetraphenylporphyrin, phthalocyanine, Congo red, primuline, rose bengal, phenothiazine, alizarin yellow, methyl orange, methyl red, and naphthol blue black.

Initial tests were run in CHCl_3 , toluene, and *tert*-amyl alcohol, all solvents which have high *s*-values in HBTM catalyzed kinetic resolutions of alcohols.¹⁷ A solution of the indicator was made basic with either DBU or DIPEA, propionic acid was added to simulate product formation in a CEC reaction, and color changes were monitored. Of the indicators tested rhodamine B, Nile blue A, cresyl violet, brilliant blue G, brilliant blue R, xylene cyanole FF, and new fuchsin exhibited color changes upon addition of propionic acid to the basic solution. Next, each of these indicators were examined for color changes upon the addition of TBAA and under the standard CEC conditions. A base screen with DBU, DIPEA, 2,4-di-*tert*-butylpyridine,

2,2,6,6-tetramethylpiperidine, 1,2-dimethylimidazole, phosphonitrilic chloride, and 1,8-bis(dimethylamino)naphthalene was also run to see if changing the base could affect a different color change (Figure A9). Out of all the bases tested, DBU exhibited the most profound effect between the solution of only sensor and DBU, and the solution when propionic acid was added. Rhodamine B and Nile Blue A exhibited a color change when exposed to simulated CEC conditions (without alcohol) and were selected for testing in actual CEC reactions.

Parallel CEC reactions were set up utilizing DIPEA as the base; one reaction included the alcohol substrate, while the other was a control without alcohol. Both real and control reactions for Rhodamine B and Nile Blue A failed to show any color change over the course of the reaction. The amount of base was reduced six-fold and the reactions repeated; unfortunately, no color change was observed over the course of the reactions. Switching the base from DIPEA to DBU gave similar results for Rhodamine B and Nile Blue A. Treating these reactions with propionic acid provided a color change from light pink to bright pink, however the amount of propionic acid needed to generate the color change was far beyond the amount generated in a CEC reaction. Examining the mechanism for color change in Rhodamine B suggested the reason an excess of propionic acid was needed was due to the equilibrium of the benzoic acid vs the propionic acid. It was hypothesized that by converting the benzoic acid to a benzamide the equilibrium could be shifted to favor to the open, colored form of the molecule (Figure 2.9).

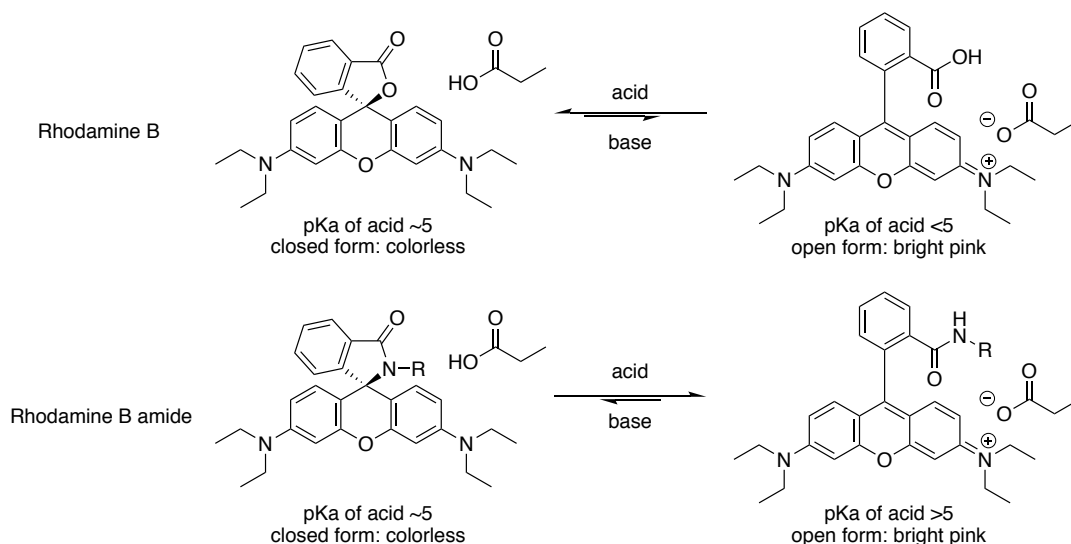


Figure 2.9: Equilibrium positions of Rhodamine B vs a Rhodamine B amide.

Rhodamine based amides have found wide use in research from biological stains to acid and metal based sensors, they provided a range of structural motifs to base our sensor on.^{20,21} Due to the drastic color change with nitro-substituted hydrazines in the acetate study, the first Rhodamine B amide that was synthesized was *p*-NO₂ phenyl hydrazine **2.21** (Figure 2.10). The orange solution turned a dark forest green color upon treatment with DBU. Addition of propionic acid corresponding to 25, 50, 75, and 100% conversion of alcohol to ester in the CEC reaction gradually turned the solution back to orange (Figure 2.10). The change in color at relevant concentrations of propionic acid prompted additional Rhodamine B amides (**2.22–2.24**) to be synthesized and tested (Figure 2.11).

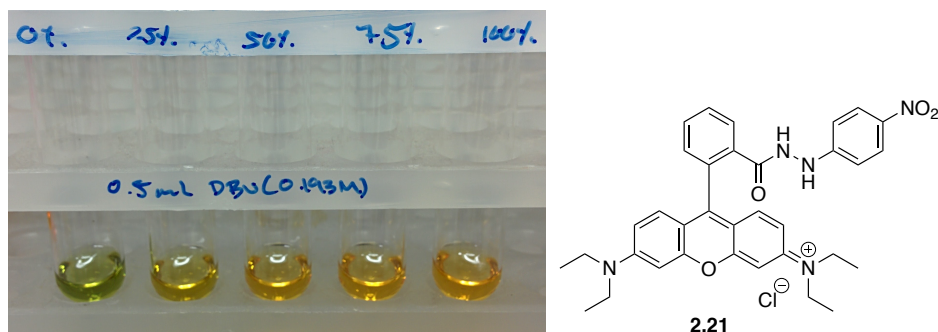


Figure 2.10: Color change exhibited by Rhodamine B hydrazide **2.21**.

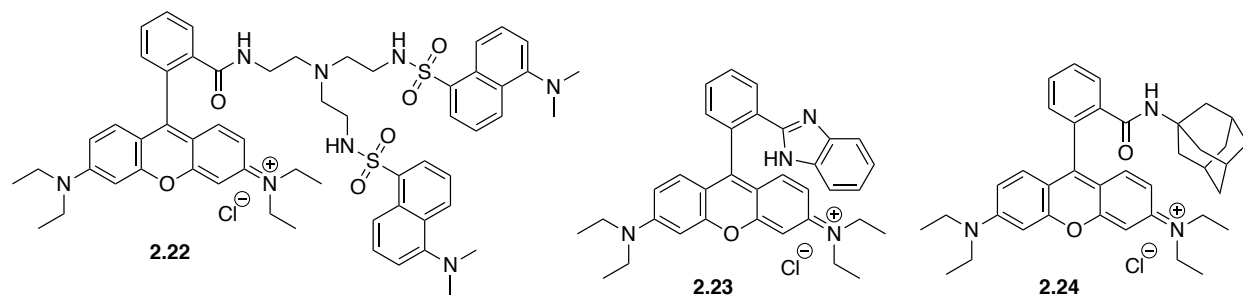


Figure 2.11: Structures of Rhodamine B amides **2.22** and **2.24**; and benzimidazole **2.23**.

Interesting work by Kim used dansyl appended Rhodamine B **2.22** to elicit a fluorescence resonance energy transfer (FRET) response in the presence of metal cations.²² Under basic conditions Rhodamine B **2.22** is a colorless solution with green fluorescence (Figure 2.10 a)). After treatment with a cationic source (M^+ or H^+), the solution turns pink and gives off a pink fluorescence. Unfortunately, after synthesizing and testing indicator **2.22**, it was found that the amount of propionic acid required to cause this change in color and fluorescence was greater than the 30 μmol generated from a CEC reaction at full conversion.

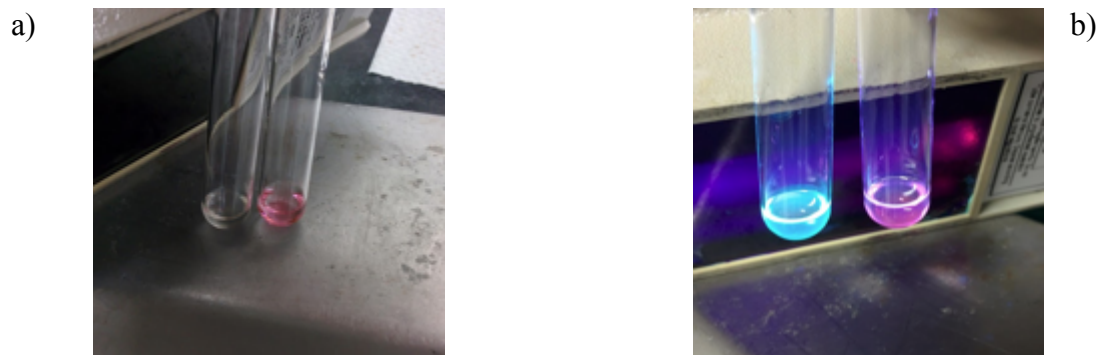


Figure 2.12: a) Basic (left) and acidic (right) forms of indicator **2.22**. b) Fluorescence for basic (left) and acidic (right) forms of indicator **2.22** using a long wave UV lamp (365 nm).

Indicators **2.23** and **2.24** were chosen because of their color change under more basic conditions.^{23–25} The pH range for these sensors is higher than most Rhodamine B amide sensors, allowing for the detection of smaller amounts of propionic acid generated in the CEC reactions.

Benzimidazole **2.23** was previously studied for selective imaging of biological systems at acidic pH (max emission pH 4.5).²⁵ The optimal sensing range for this sensor is pH 4.5–6.5. This benzimidazole, while sensitive to the concentration of propionic acid in a CEC reaction, did not provide the necessary drastic color change needed to distinguish between CEC reactions close in conversion. Work by the Lin group discovered that the pKa of benzamides, such as **2.24**, could be fine-tuned by switching the substituent on the amide. Bulkier groups such as adamantyl and naphthyl cause the spiro lactam to open at higher pH's due to ring-strain.²³ The pH window for adamantyl compound **2.24** was around 5.5–7.5. The indicator turned from a faint pink/tan color with minimal fluorescence to a bright pink solution with bright pink/orange fluorescence (Figure 2.11).

Figure 2.13: a) Compound **2.24** color before and after addition of acid. b) Fluorescence before and after addition of acid.

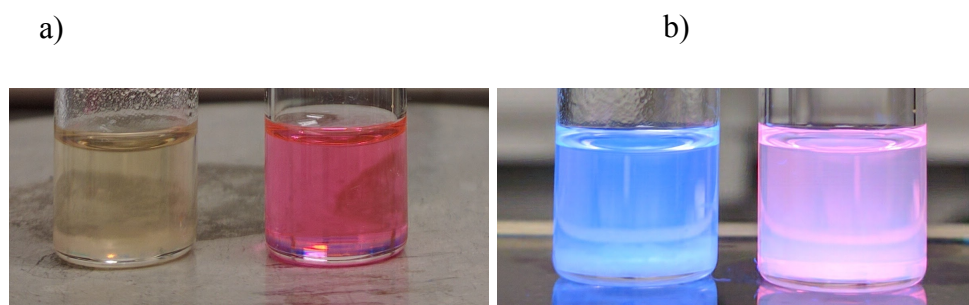
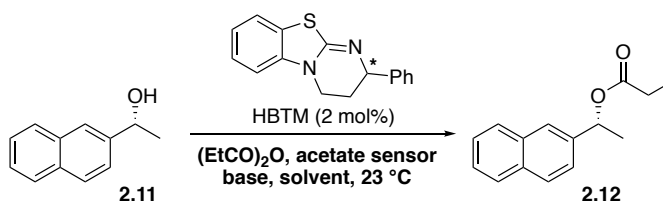


Figure 2.11 also illustrates the ideal color change for a colorimetric CEC method; with no change or slight change with the slow reaction, and a noticeable change for the fast reaction. Adamantyl **2.24** was tested in a CEC reaction with different solvents and bases (Table 2.7). Over the course of the 1 hour reactions, **2.24** exhibited a color change regardless of the base or solvent utilized. Similar to bromocresol green, **2.24** changed colors in the reaction with both *S*- and *R*-HBTM. To determine if the indicator was undergoing acylation to cause the color change an excess of base was added at the end of the CEC reaction. The mixture immediately turned the beige/light pink seen at the beginning of the reaction. If the sensor had been acylated the addition

of base would not have caused a return to the starting color, since the formation of the spiro lactam would have been prohibited without a free proton on nitrogen. Analyzing the reaction by ^1H NMR confirmed that our acetate sensor was not undergoing acylation, but that one of the reaction species was initiating the color change (Figure A13). This color change was independent of the greater amount of propionic acid generated by the faster *S*-HBTM catalyzed reaction. At this point we decided to abandon the project due to the encountered issues.

Table 2.7: CEC reactions with acetate sensors **2.24** and **2.21** under various conditions for 1 hour.

S- and *R*-HBTM catalyzed reactions run side-by-side and colors determined visually.



entry	acetate sensor	base	solvent	starting color		ending color	
				<i>S</i> -HBTM	<i>R</i> -HBTM	<i>S</i> -HBTM	<i>R</i> -HBTM
1	2.24	DIPEA	CHCl_3	light pink	light pink	medium pink	medium pink
2	2.24	DBU	CHCl_3	light pink	light pink	medium pink	medium pink
3	2.24	none	CHCl_3	light pink	light pink	medium pink	medium pink
4	2.24	DIPEA	toluene	light pink	light pink	medium pink	medium pink
5	2.24	DBU	toluene	light pink	light pink	medium pink	medium pink
6	2.24	none	toluene	light pink	light pink	medium pink	medium pink
7	2.21	DIPEA	toluene	yellow	yellow	green	green
8	2.21	DBU	toluene	yellow	yellow	green	green
9	2.21	none	toluene	yellow	yellow	green	green

2.8 Conclusion

While the development of a colorimetric method for either quantitative or qualitative analysis of CEC reactions was ultimately unsuccessful, the many lessons learned along the way may pave the way for future development of a colorimetric CEC method. The initial exploration of mixed anhydrides as an aromatic source allowed for monitoring of the fast and slow reactions; however, the lack of consistent, reliable data for reaction kinetics made this option less attractive. The issues encountered with using acetate sensors, such as solubility of the sensor, lack of color

change without TBAA, and color change distinction led to the pursuit of pH indicators instead. The pH indicators provided the most promise of all the sensors. The ability to run substoichiometric quantities allowed CEC reactions to be run under previously optimized conditions, rather than the dilute concentrations needed for the mixed anhydrides and esters. The pH indicators provided diagnostic color changes, and the structures were easily modified to suit reaction conditions. It should be noted that while the acetate and pH sensors were initially tested as qualitative methods, these indicators could theoretically be monitored by UV-VIS with optimized conditions. The substoichiometric amount of these indicators would be better suited to the UV-VIS detection than stoichiometric mixed anhydrides or esters. The reaction concentration could be optimized independent of the indicator concentration, allowing for concentrated reactions without the need to increase the amount of indicator present.

2.9 Acknowledgement

Candace H. Hart contributed to the testing and synthesis of Rhodamine B amides (**2.21**, **2.22**, **2.23**, and **2.24**). Her research was funded by the UCI Undergraduate Research Opportunity Program (UROP).

2.10 Experimental

General experimental and laboratory conditions

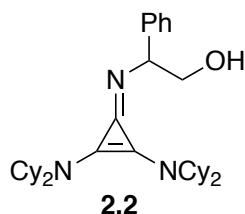
All glassware was flame- or oven-dried and cooled under argon unless otherwise stated. All reactions and solutions were conducted under argon unless otherwise stated. All commercially available reagents were used as received, unless otherwise stated. Toluene (PhMe), tetrahydrofuran (THF), dimethylformamide (DMF), diethyl ether (Et₂O) and dichloromethane

(CH₂Cl₂) were degassed and dried by filtration through activated alumina under vacuum according to the procedure by Grubbs.²⁶ Diisopropylamine (DIPA) and acetonitrile (MeCN) were distilled from CaH₂ prior to use. Thin layer chromatography (TLC) was performed with Millipore 60 F₂₅₄ glass-backed silica gel plates and visualized using potassium permanganate, Dragendorff-Munier, ceric ammonium molybdate (CAM), or vanillin stains. Flash column chromatography was performed according to the method by Still, Kahn, and Mitra²⁷ using Millipore Geduran Silica 60 (40-63 μm). Enantiopure (*S*)-HBTM, (*R*)-HBTM, 2,4-dinitrophenyl propionate, 2-nitrophenyl propionate (**2.9**), 4-nitrophenyl propionate (**2.10**), and (*S*)-(-)-1-(1-naphthyl)ethanol (**2.11**) were previously synthesized by Alex Wagner and generously provided for use.

Instrumentation

All data collected at ambient temperature unless noted. ¹H NMR spectra were taken at 500 or 600 MHz, calibrated using residual NMR solvent or TMS and interpreted on the δ scale. Peak abbreviations are listed: s = singlet, d = doublet, t = triplet, q = quartet, pent = pentet, dd = doublet of doublets, ddd = doublet of doublet of doublets dt = doublet of triplets, ddt = doublet of doublet of triplets, dq = doublet of quartets, m = multiplet, app = apparent, br = broad. ¹³C NMR spectra were taken at 125 MHz, calibrated using the NMR solvent, and interpreted on the δ scale. Melting points were recorded on an Electrothermal Melting Point Apparatus. Electrospray ionization high-resolution mass spectra (ESI-HRMS) were determined by the UC-Irvine Mass Spectrometry Laboratory using the Micromass QTOF2 Mass Spectrometer. UV-Vis spectra were taken on a Thermo Scientific NanoDrop 2000c UV-Vis spectrophotometer in a 1 cm quartz cuvette.

Compound 2.2



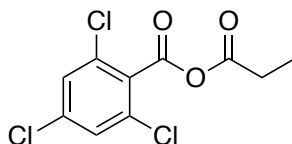
Experimental: *Dicyclohexylamine* was distilled over CaH_2 prior to use. To a solution of tetrachlorocyclopropene (1.38 mL, 11.3 mmol) in CH_2Cl_2 (112 mL) was slowly added dicyclohexylamine (13.4 mL, 67.2 mmol). A cream-colored precipitate formed after a few seconds, and the reaction was stirred for 6 hours. L-phenylalanol (1.90 g, 12.6 mmol) was then added to the reaction mixture and stirred for 21 hours. The mixture was filtered through a plug of Celite and washed with 1.0M HCl (7 x 60 mL). The organic layers were dried with Na_2SO_4 , filtered, and concentrated under reduced pressure to yield the HCl salt **2.2** (7.80 g, 95%) as a light orange solid.

Spectral data was consistent with the literature.¹⁴

Physical State: Light orange solid.

TLC: $R_f = 0.31$ (50% EtOAc in hexanes) (KMnO_4 stain).

Compound 2.3



2.3

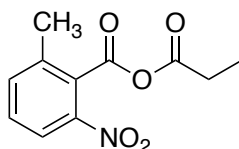
Experimental: To a solution of propionic acid in THF () was added pyridine () and the mixture stirred for 2 minutes. To this solution was added 2,4,6-trichlorobenzoyl chloride () and the mixture was stirred for 3 hours. The reaction mixture was filtered under reduced pressure

through a pad of silica. The residue was rinsed with THF and the filtrate concentrated in vacuo to yield () a white solid.

Spectral data was consistent with the literature.²⁸

Physical State: White solid.

Compound 2.4



2.4

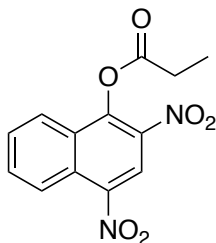
Experimental: To a solution of NaH () in THF (15 mL) at 0 °C was added 6-methyl-2-nitrobenzoic acid (455 mg, 2.50 mmol) in a solution of THF (10 mL). The solution was stirred for 30 min and propionyl chloride was then slowly added to the mixture. The creamy orange solution turned a clear orange color and was stirred for 7 hours. The crude reaction mixture was filtered through Celite and concentrated to yield **2.4** (600 mg, quantitative) as a light brown oil.

Spectral data was consistent with the literature.²⁸

Physical State: Light brown oil.

¹H NMR (500 MHz, CDCl₃, 25 °C) δ 8.05 (d, *J* = 8.0 Hz, 1H), 7.60 (d, *J* = 8.0 Hz, 1H), 7.54 (app. t, *J* = 8.0 Hz, 1H), 2.67 (q, *J* = 7.45 Hz, 2H), 2.51 (s, 3H), 1.23 (t, *J* = 7.50 Hz, 3H).

Compound 2.5



2.5

Experimental: To a flame dried round bottom flask with 60% NaH (640 mg, 16.0 mmol) was added THF (10 mL). A solution of 2,6-dinitronaphthol (1.87 g, 8.00 mmol) in THF (6 mL) was slowly added. An additional 3 mL THF was used to transfer residual 2,6-dinitronaphthol, and the reaction was stirred at 0 °C for 30 minutes, before being allowed to warm to room temperature. After 42 hours at room temperature the mixture was filtered through a pad of Celite. The Celite was rinsed with Et₂O, and the filtrate concentrated to afford crude **2.5**. The solid was triturated three times with Et₂O providing **2.5** (1.644, 71%) as a tan solid.

Physical State: Tan solid.

Melting Point: 101–103 °C.

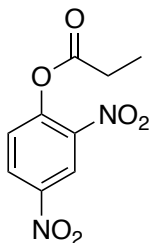
¹H NMR (500 MHz, CDCl₃, 25 °C) δ 8.93 (s, 1 H), 8.67 (d, *J* = 8.63 Hz, 1 H), 8.26 (d, *J* = Hz, 1 H), 7.95 (t, *J* = 7.12 Hz, 1 H), 7.83 (t, *J* = 7.12 Hz, 1 H), 2.93 (q, *J* = 7.48 Hz, 2 H), 1.41 (t, *J* = 7.41 Hz, 3 H).

¹³C NMR (125 MHz, CDCl₃, 25 °C) δ 171.2, 146.2, 143.7, 135.9, 133.4, 129.8, 129.1, 128.0, 124.6, 124.1, 119.8, 29.9, 27.9, 8.9.

IR (thin film): 3093, 2924, 1776, 1585, 1532, 1338, 758 cm⁻¹.

HRMS (ESI) *m/z*: Does not fly.

Compound 2.6



2.6

Experimental: A solution of 60% NaH (1.60g, 40.0 mmol) in THF (60 mL) was added dropwise at 0 °C to a solution of 2,4-dinitrophenol (3.68 g, 20.0 mmol) in THF (15 mL). An additional 5 mL of THF was used to transfer residual 2,4-dinitrophenol. After 30 min propionyl chloride was added and the reaction mixture stirred for 46 hours. The mixture was filtered through Celite and concentrated. The crude **2.6** was triterated with Et₂O and the solvent removed by pipette to yield **2.6** (3.03 g, 63%) as a light yellow solid.

Physical State: Light yellow solid.

Melting Point: 60–65 °C.

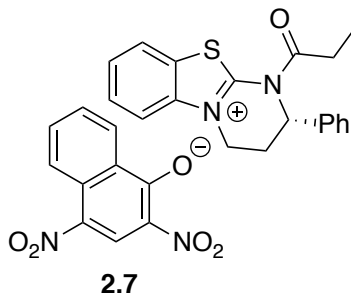
¹H NMR (500 MHz, CDCl₃, 25 °C) δ 8.95 (d, *J* = 2.66 Hz, 1 H), 8.52 (dd, *J* = 8.9, 2.7 Hz, 1 H), 7.48 (d, *J* = 8.9 Hz, 1 H), 2.72 (q, *J* = 7.5 Hz, 2 H), 1.30 (t, *J* = 7.5 Hz, 3 H),

¹³C NMR (125 MHz, CDCl₃, 25 °C) δ 171.3, 149.0, 145.2, 129.2, 126.9, 121.9, 27.8, 8.8.

IR (thin film): 3111, 2996, 1780, 1607, 1531, 1341, 1064 cm⁻¹.

HRMS (ESI) *m/z*: calculated for CHNO (M + NH₄)⁺: 258.0726, found: 258.0715

Compound 2.7

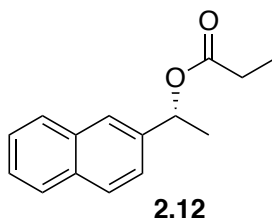


Experimental: (*S*)-HBTM (5.0 mg, 0.019 mmol) was dissolved in CDCl₃ (1.0 mL), mixed with a pipette, and transferred to an NMR tube. The NMR sample was allowed to equilibrate for 10 min in the NMR (CRYO 500) before the ¹H NMR was run. T = 298 K, aq = 3.0 sec, ns = 32.

Physical State: Viscous, orange oil.

¹H NMR (500 MHz, CDCl₃, 25 °C) δ 9.04 (s, 1 H), 8.67 (d, *J* = 8.5 Hz, 1 H), 8.27 (app d, *J* = 8.0 Hz, 1 H), 7.72 (d, *J* = 7.93 Hz, 1 H), 7.59–7.40 (m, 4 H), 7.38–7.15 (m, 6 H), 7.01 (d, *J* = 6.81 Hz, 2 H), 6.18 (d, *J* = 6.81 Hz, 2 H), 7.01 (s, 2 H), 4.68 (d, *J* = 4.66 Hz, 1 H), 3.73 (app t, *J* = 3.72 Hz, 1 H), 3.23–3.06 (m, 2 H), 7.59–7.40 (m, 4 H), 2.72 (d, *J* = 2.70 Hz, 1 H), 2.42–2.30 (m, 1 H), 1.11 (app t, *J* = 6.76 Hz, 3 H).

Compound 2.12



Experimental: A solution of 60% NaH (33.1 mg, 0.730 mmol) in THF (3.0 mL) was added dropwise to a solution of (*S*)-(-)-1-(1-naphthyl)ethanol (50.1 mg, 0.290 mmol) in THF (1.0 mL) at 0 °C. The mixture was slowly warmed to room temperature and stirred for 4 days. The reaction mixture was washed with sat. aq. NaHCO₃ (3 x 1.5 mL) and H₂O (1.5 mL). The organic

layers were dried with MgSO_4 and concentrated under reduced pressure to afford **2.12**. Purification with column chromatography (hexanes to 20% EtOAc in hexanes) provided **2.12** (37.1 mg, %) as a clear oil.

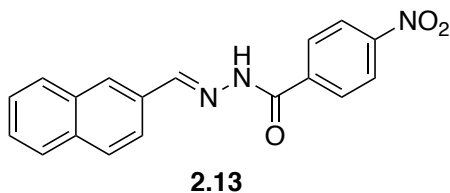
Spectral data was consistent with the literature.²⁹

Physical State: Clear oil.

$^1\text{H NMR}$ (500 MHz, CDCl_3 , 25 °C) δ 7.86–7.80 (m, 4 H), 7.51–7.46 (m, 3 H), 6.07 (q, $J = 6.61$ Hz, 1 H), 2.44–2.33 (m, 2 H), 2.72 (d, $J = 6.65$ Hz, 3 H), 1.16 (d, $J = 7.63$ Hz, 3 H).

TLC: $R_f = 0.57$ (20% EtOAc in hexanes) (Vanillin stain).

Compound 2.13



Experimental: To a solution of 4-nitrophenyl hydrazide (232 mg, 1.28 mmol) and 2-naphthaldehyde (204 mg, 1.28 mmol) in MeOH (21 mL) was added 2-drops of AcOH. The reaction was stirred at 40 hours. The mixture was filtered and the yellow solid washed with cold MeOH. Removal of excess solvent in vacuo afforded **2.13** (408 mg, 99%) as a creamy, yellow solid.

Physical State: Creamy, yellow solid.

Melting Point: 259–260°C.

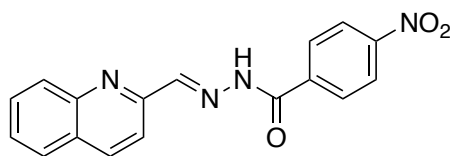
$^1\text{H NMR}$ (500 MHz, $\text{DMSO}-d_6$, 25 °C) δ 12.24 (s, 1 H), 8.63 (s, 1 H), 8.40 (d, $J = 8.58$ Hz, 2 H), 8.21–8.16 (m, 3 H), 8.03–7.93 (m, 4 H), 7.62–7.52 (m, 2 H).

^{13}C NMR (125 MHz, DMSO- d_6 , 25 °C) δ 161.9, 153.5, 149.4, 149.0, 147.4, 138.8, 136.9, 130.8, 130.2, 129.4, 129.0, 128.0, 128.0, 127.5, 123.7, 123.0, 117.5.

IR (thin film): 3421, 3075, 1657, 1600, 1561, 1224, 1343, 1284, 849, 751 cm^{-1} .

HRMS (ESI) m/z : calculated for CHNO ($\text{M} + \text{Na}$) $^+$ 342.0854: , found: 342.0852

Compound 2.14



2.14

Experimental: To a solution of 4-nitrophenyl hydrazide (232 mg, 1.28 mmol) and quinoline-2-carboxaldehyde (200 mg, 1.28 mmol) in MeOH (21 mL) was added 2-drops of AcOH. The reaction was stirred at 4 days. The mixture was filtered and the yellow solid washed with cold MeOH. Removal of excess solvent in vacuo afforded **2.13** (389 mg, 94%) as a tan solid.

Physical State: Tan solid.

Melting Point: 245–247 °C.

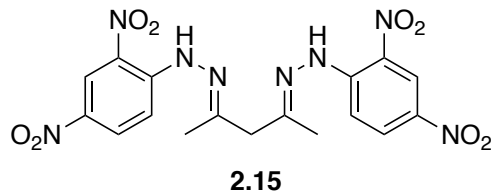
^1H NMR (500 MHz, DMSO- d_6 , 25 °C) δ 12.46 (s, 1 H), 8.63 (s, 1 H), 8.46 (d, J = 8.63 Hz, 1 H), 8.41 (d, J = 8.51 Hz, 2 H), 8.20 (d, J = 8.53 Hz, 2 H), 8.15 (d, J = 8.69 Hz, 1 H), 8.07 (d, J = 8.27 Hz, 1 H), 8.03 (d, J = 8.14 Hz, 1 H), 7.82 (t, J = 7.50 Hz, 2 H), 7.66 (t, J = 7.52 Hz, 2 H).

^{13}C NMR (125 MHz, DMSO- d_6 , 25 °C) δ 161.9, 153.5, 149.4, 149.0, 147.4, 138.8, 136.9, 130.2, 129.4, 129.0, 128.1, 128.0, 127.4, 123.7, 117.5.

IR (thin film): 3431, 3195, 1658, 1602, 1559, 1523, 1345, 1283, 849, 707 cm^{-1} .

HRMS (ESI) m/z : calculated for CHNO ($\text{M} + \text{Na}$) $^+$ 343.0807: , found: 343.0820

Compound 2.15



Experimental: To a solution of 2,4-dinitrophenylhydrazine (884 mg, 4.40 mmol) and acetylacetone (0.20 mL, 2.0 mmol) in MeOH (110 mL) was added 4-drops of AcOH. The solution was heated to reflux for 41 hours. The deep orange precipitate was filtered and washed with cold 10% H₂O in Et₂O. Removal of excess solvent yielded **2.15** (69.4 mg, 8 %) as a yellow solid.

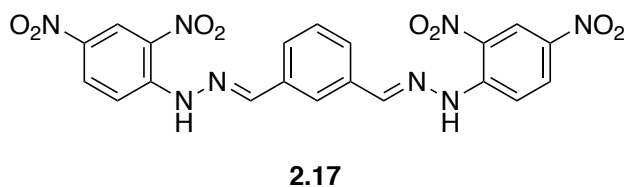
Spectral data was consistent with the literature.³⁰

Physical State: Yellow solid.

¹H NMR (500 MHz, CDCl₃, 25 °C) δ 11.15 (s, 2 H), 9.15 (d, *J* = 2.6 Hz, 2 H), 8.34 (dd, *J* = 9.59, 2.53 Hz, 2 H), 7.94 (d, *J* = 9.55 Hz, 2 H), 3.57 (s, 2 H), 2.17 (s, 6 H).

¹³C NMR (125 MHz, CDCl₃, 25 °C) δ 153.0, 145.1, 138.5, 130.4, 129.7, 123.7, 116.5, 48.5, 16.25.

Compound 2.17



Experimental: To a solution of isophthalaldehyde (135 mg, 1.0 mmol) and 2,4-dinitrophenylhydrazine (324 mg, 1.63 mmol) in EtOH (15 mL) was added a few crystals of *p*-TSOH. The vial was sealed and heated to reflux for 22 hours. The precipitate was filtered off and

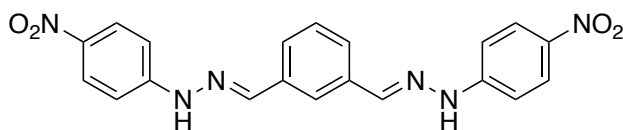
washed with hot EtOH. Residual solvent was removed under reduced pressure to yield **2.17** (366 mg, 74%) as a bright orange solid.

Spectral data was consistent with the literature.³¹

Physical State: Bright orange solid.

¹H NMR (500 MHz, DMSO-*d*₆, 25 °C) δ 11.75 (s, 2H), 8.89 (s, 2H), 8.89–8.79 (m, 2H), 8.44–8.41 (m, 2H), 8.15–8.13 (m, 2H), 7.93–7.91 (m, 2H), 7.64–7.60 (m, 2H).

Compound 2.18



2.18

Experimental: To a solution of isophthalaldehyde (134 mg, 1.0 mmol) and *p*-nitrophenylhydrazine (322 mg, 2.1 mmol) in EtOH (15 mL) was added a few crystals of *p*-TSOH. The vial was sealed and heated to reflux for 22 hours. The precipitate was filtered off and washed with hot EtOH. Residual solvent was removed under reduced pressure to yield **2.17** (195 mg, 48%) as a bright orange solid.

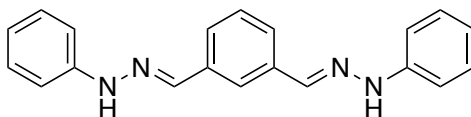
Spectral data was consistent with the literature.³¹

Physical State: Bright orange solid.

¹H NMR (500 MHz, CDCl₃, 25 °C) δ 11.36 (s, 2H), 8.17 (dt, *J* = 9.4, 1.2 Hz, 4H), 8.11 (s, 2H), 8.01 (d, *J* = 1.7 Hz, 1H), 7.77 (dd, *J* = 7.7, 1.6 Hz, 2H), 7.50 (t, *J* = 7.7 Hz, 1H), 7.22 (d, *J* = 8.7 Hz, 4H).

¹³C NMR (125 MHz, CDCl₃, 25 °C) δ 150.5, 141.4, 138.5, 135.3, 129.3, 126.9, 126.2, 124.7, 111.4.

Compound 2.19



2.19

Experimental: To a solution of isophthalaldehyde (134 mg, 1.0 mmol) and phenylhydrazine (227 mg, 2.1 mmol) in EtOH (15 mL) was added a few crystals of *p*-TSOH. The vial was sealed and heated to reflux for 54 hours. The precipitate was filtered off and washed with hot EtOH. Residual solvent was removed under reduced pressure to yield **2.17** (129 mg, 41%) as a bright orange solid.

Physical State: solid.

Melting Point: 203–204 °C.

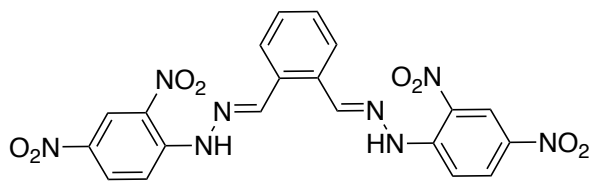
¹H NMR (500 MHz, DMSO-*d*₆, 25 °C) δ 10.38 (s, 2H), 7.90 (s, 2H), 7.84 (d, *J* = 1.7 Hz, 1H), 7.59 (dd, *J* = 7.8, 1.7 Hz, 2H), 7.40 (t, *J* = 7.7 Hz, 1H), 7.27–7.20 (m, 4H), 7.09 (dq, *J* = 7.0, 1.0 Hz, 4H), 6.76 (ddt, *J* = 7.3, 6.4, 1.0 Hz, 2H).

¹³C NMR (125 MHz, DMSO-*d*₆, 25 °C) δ 145.2, 136.2, 136.2, 129.2, 129.0, 124.9, 123.0, 118.8, 112.0.

IR (thin film): 3314, 3053, 1575, 1509, 1485, 1251, 1133, 919, 743 cm⁻¹.

HRMS (ESI) *m/z*: calculated for CHNO (M + Na)⁺ 337.1429; , found: 337.1423

Compound 2.20



2.20

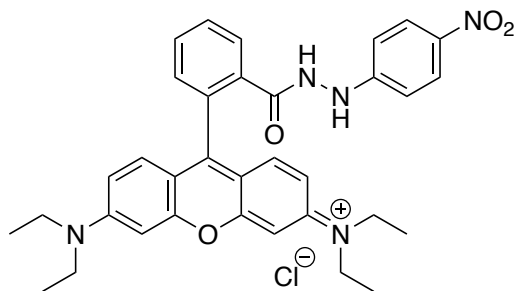
Experimental: To a solution of phthalaldehyde (134 mg, 1.0 mmol) and 2,4-dinitrophenylhydrazine (325 mg, 1.67 mmol) in EtOH (15 mL) was added a few crystals of *p*-TSOH. The vial was sealed and heated to reflux for 22 hours. The precipitate was filtered off and washed with hot EtOH. Residual solvent was removed under reduced pressure to yield **2.17** (324 mg, 65%) as a bright orange solid.

Spectral data was consistent with the literature.³²

Physical State: Bright orange solid.

¹H NMR (500 MHz, CDCl₃, 25 °C) δ 11.81 (s, 1H), 9.19 (s, 1H), 8.91 (d, *J* = 2.6 Hz, 1H), 8.40 (dd, *J* = 9.6, 2.7 Hz, 1H), 8.11 (d, *J* = 9.6 Hz, 1H), 8.04 (dt, *J* = 7.3, 3.6 Hz, 1H), 7.59 (dt, *J* = 7.3, 3.6 Hz, 1H).

Compound 2.21



2.21

Experimental: Carbonyl diimidazole (81 mg, 0.50 mmol) was added to a solution of rhodamine B (240 mg, 0.50 mmol) in CH₂Cl₂ (1.0 mL) and stirred for 90 min. A solution of *p*-nitrophenylhydrazine (77 mg, 0.50 mmol) in CH₂Cl₂ (1.0 mL) was added and the mixture stirred

for another 2 hours. The reaction mixture was washed with H₂O, and the organic layer was concentrated in vacuo to afford **2.21** (309 mg, quantitative) as a viscous, red/purple oil.

Physical State: Viscous, red/purple oil

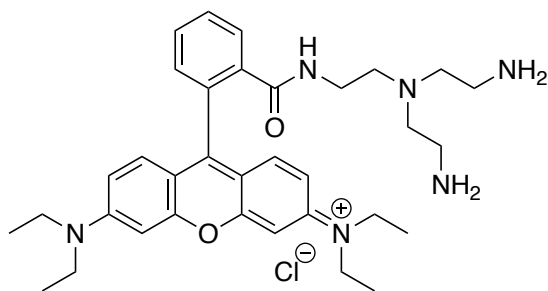
¹H NMR (500 MHz, CDCl₃, 25 °C) δ 8.12 (app d, *J* = 9.01 Hz, 2 H), 8.01 (app d, *J* = 9.01 Hz, 1 H), 7.60 (app dtd, *J* = 25.75, 7.34, 0.93 Hz, 3 H), 7.20 (app d, *J* = 7.55 Hz, 1 H), 7.03 (app d, *J* = 9.11 Hz, 2 H), 6.59 (d, *J* = 8.95 Hz, 2 H), 6.44 (d, *J* = 2.45 Hz, 2 H), 6.34 (dd, *J* = 8.95, 2.45 Hz, 2 H), 3.36 (q, *J* = 7.20 Hz, 8 H), 1.17 (t, *J* = 7.20 Hz, 12 H).

¹³C NMR (125 MHz, CDCl₃, 25 °C) δ 169.9, 154.7, 151.2, 134.7, 133.1, 129.9, 129.40, 129.36, 123.5, 125.6, 123.2, 109.6, 108.4, 97.1, 77.4, 77.1, 76.9, 44.9, 12.6.

IR (thin film): 2972, 1748, 1587, 1337, 1179, 1108, 907, 720 cm⁻¹.

HRMS (ESI) *m/z*: calculated for CHNO (M + H)⁺ 578.27: , found:

Compound 2.25



Experimental: To a solution of Rhodamine B (240 mg, 0.50 mmol) in MeOH (12.5 mL) was added tris(2-aminoethyl)amine (0.15 mL, 1.0mmol). The vial was capped and heated to reflux for 7 days. The solvent was removed under reduced pressure. The sludge was dissolved in CH₂Cl₂ (60 mL) and washed with H₂O (120 mL), 0.50 M HCl (2 x 50 mL). The aqueous layers were made basic with 1.0 M NaOH and extracted with CH₂Cl₂ (3 x 40 mL). The organic layers

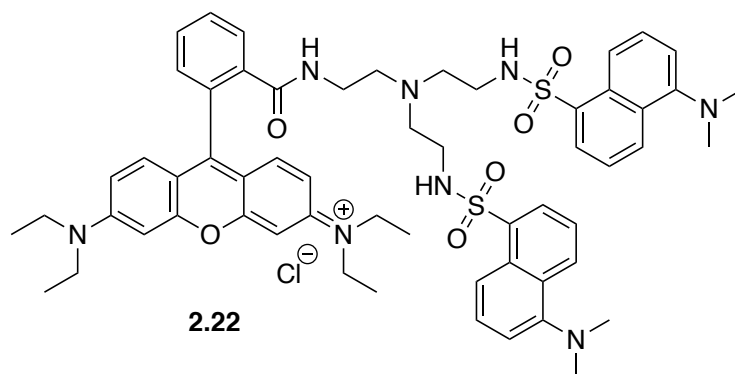
were washed with H₂O, brine, dried with Na₂SO₄, filtered, and concentrated under reduced pressure to yield **2.25** (248 mg, 87%) as a brown oil.

Spectral data was consistent with the literature.²²

Physical State: Brown oil.

¹H NMR (500 MHz, CDCl₃, 25 °C) δ 7.90–7.83 (m, 1H), 7.44 (dt, *J* = 7.2, 3.5 Hz, 2H), 7.12–7.05 (m, 1H), 6.39 (q, *J* = 6.7, 5.8 Hz, 4H), 6.27 (dt, *J* = 11.2, 5.5 Hz, 2H), 3.36–3.30 (m, 8H), 2.56 (d, *J* = 6.7 Hz, 2H), 2.30 (dt, *J* = 65.3, 6.8 Hz, 6H), 1.16 (q, *J* = 6.0, 5.1 Hz, 12H).

Compound 2.22



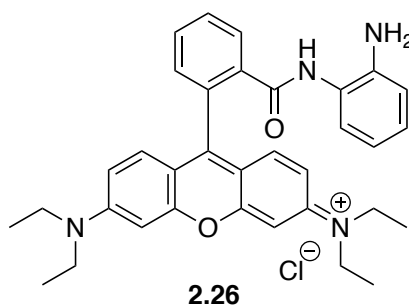
Experimental: To a solution of rhodamine B amide **2.25** (248 mg, 0.430 mmol) in CHCl₃ (16 mL) was added dansyl chloride (262 mg, 0.970 mmol) and Et₃N (0.13 mL, 0.89 mmol). The vial was sealed and heated to 80 °C for 26 hours. The solvent was removed under reduced pressure, and the sludge dissolved in CH₂Cl₂ (100 mL). The mixture was washed with H₂O (3 x 100 mL) and brine (30 mL), then dried with Na₂SO₄, filtered, and concentrated under reduced pressure to yield **2.22** (380 mg, 85%) as a viscous, brown oil.

Spectral data was consistent with the literature.²²

Physical State: Viscous, brown oil.

¹H NMR (500 MHz, CDCl₃, 25 °C) δ 8.46 (dd, *J* = 8.7, 3.8 Hz, 4H), 8.17 (d, *J* = 7.2 Hz, 2H), 8.07 (d, *J* = 7.2 Hz, 1H), 7.53–7.39 (m, 7H), 7.10 (d, *J* = 7.0 Hz, 1H), 7.04 (d, *J* = 7.5 Hz, 2H), 6.69 (d, *J* = 5.5 Hz, 2H), 6.39–6.33 (m, 4H), 6.20 (dd, *J* = 9.0, 2.5 Hz, 2H), 3.31 (hept, *J* = 7.4 Hz, 12H), 2.81 (s, 12H), 2.69 (q, *J* = 5.4 Hz, 4H), 2.10 (t, *J* = 5.2 Hz, 4H), 1.85 (t, *J* = 5.4 Hz, 2H), 1.14 (t, *J* = 6.9 Hz, 12H).

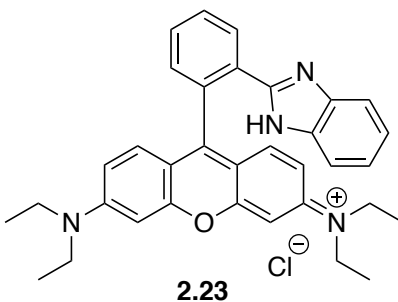
Compound 2.26



Experimental: Rhodamine B (116 mg, 0.250 mmol), EDC•HCl (52 mg, 0.28 mmol), DMAP (6 mg, 0.05 mmol) were added to a vial followed by dry CH₂Cl₂ (1.0 mL). The mixture was stirred for 30 minutes before addition of diaminobenzene (30 mg, 0.28 mmol). The reaction mixture was stirred for 48 hours. The volatiles were removed under reduced pressure, and the crude product purified by column chromatography (CH₂Cl₂ to 20% MeOH in CH₂Cl₂) afforded **2.26** (116 mg, quantitative) as a purple oil.

Physical State: Purple oil.

Compound 2.23

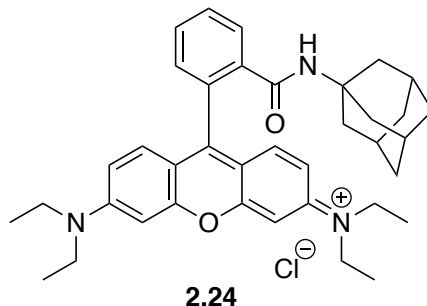


Experimental: A solution of **2.26** (116 mg, 0.250 mmol) in THF (1.0 mL) was added slowly to a 0 °C suspension of LiAlH₄ (16 mg, 0.38 mmol) in THF (1.0 mL). An additional 0.5 mL THF was used to transfer any remaining rhodamine B to the reaction vessel. The vial was warmed to rt and the reaction stirred until completion by TLC. The reaction mixture was quenched with 1-butanol, and H₂O was added. The aqueous layer was extracted with additional 1-butanol and the layers separated. The organic layers were dried over Na₂SO₄, filtered, and concentrated to afford **2.23**. Purification by column chromatography (CH₂Cl₂ to 10% MeOH in CH₂Cl₂) afforded **2.23** (42 mg, 33%) as a sticky, brown oil.

Physical State: Sticky, brown oil.

¹H NMR (500 MHz, CDCl₃, 25 °C) δ 8.11 (d, *J* = 7.6 Hz, 1H), 7.80 (d, *J* = 8.1 Hz, 1H), 7.59–7.51 (m, 2H), 7.48 (t, *J* = 7.5 Hz, 1H), 7.38 (td, *J* = 7.6, 1.4 Hz, 1H), 7.28–7.19 (m, 3H), 7.19–7.13 (m, 1H), 7.02 (t, *J* = 7.6 Hz, 1H), 6.95 (td, *J* = 7.7, 1.6 Hz, 2H), 6.64 (dd, *J* = 8.9, 1.5 Hz, 2H), 6.49 (t, *J* = 2.0 Hz, 2H), 6.31–6.29 (m, 2H), 6.15 (dd, *J* = 8.9, 2.2 Hz, 1H), 6.10 (dd, *J* = 8.0, 1.7 Hz, 1H), 3.32 (dd, *J* = 4.7, 2.5 Hz, 8H), 1.14 (t, *J* = 1.6 Hz, 12H).

Compound 2.24



Experimental: All glassware was flame-dried and the reactions run under an atmosphere of argon with dry solvents. A solution of rhodamine B (240 mg, 0.500 mmol) in CH₂Cl₂ (5 mL) was cooled to 0 °C and oxalyl chloride (0.060 mL, 0.65 mmol) was added. One-drop of DMF was added and the reaction stirred at 0 °C for 5 min. The reaction mixture was warmed to room temperature and stirred for an additional 45 min. The volatiles were removed under reduced pressure and the dark pink sludge dissolved in CH₂Cl₂ (2.2 mL). Adamantyl amine (98 mg, 0.65 mmol) was added in one portion, followed by Et₃N (0.11 mL, 0.75 mmol). The reaction was stirred overnight and halted with the addition of H₂O (0.5 mL) and brine (1.0 mL). The layers were separated and the aqueous layer extracted with CH₂Cl₂ (3 x 2 mL). The organic layers were washed with aqueous 1.0 M NaOH and the layers separated. The aqueous layers were extracted with CH₂Cl₂ (3 x 2 mL). The organic layers were dried with Na₂SO₄, filtered, and concentrated in vacuo to afford **2.24** (153 mg, 53%) as a pink solid.

Spectral data was consistent with the literature.²³

Physical State: Pink solid.

¹H NMR (500 MHz, CDCl₃, 25 °C) δ 7.79–7.72 (m, 1H), 7.31–7.25 (m, 2H), 6.83–6.76 (m, 1H), 6.63 (d, *J* = 8.8 Hz, 2H), 6.35 (d, *J* = 2.6 Hz, 2H), 6.27 (dd, *J* = 8.8, 2.6 Hz, 2H), 3.34 (q, *J* = 7.1 Hz, 8H), 2.15 (d, *J* = 3.0 Hz, 6H), 1.88 (t, *J* = 3.3 Hz, 3H), 1.49 (t, *J* = 11.7 Hz, 6H), 1.17 (t, *J* = 7.0 Hz, 12H).

2.11 References:

- (1) Griffin, B. A.; Adams, S. R.; Tsien, R. Y. *Science* **1998**, *281* (5374), 269–272.
- (2) Adams, S. R.; Campbell, R. E.; Gross, L. A.; Martin, B. R.; Walkup, G. K.; Yao, Y.; Llopis, J.; Tsien, R. Y. *J. Am. Chem. Soc.* **2002**, *124* (21), 6063–6076.
- (3) Lemieux, G. A.; de Graffenried, C. L.; Bertozzi, C. R. *J. Am. Chem. Soc.* **2003**, *125* (16), 4708–4709.
- (4) Lowry, O. H.; Rosebrough, N. J.; Farr, A. L.; Randall, R. J. *J. Biol. Chem.* **1951**, *193* (1), 265–275.
- (5) Duke, R. M.; Veale, E. B.; Pfeffer, F. M.; Kruger, P. E.; Gunnlaugsson, T. *Chem. Soc. Rev.* **2010**, *39* (10), 3936–3953.
- (6) Yoder, L. *J. Ind. Eng. Chem.* **1919**, *11* (8), 755–755.
- (7) Wang, M.; Leung, K.-H.; Lin, S.; Chan, D. S.-H.; Kwong, D. W. J.; Leung, C.-H.; Ma, D.-L. *Sci. Rep.* **2014**, *4*, 6794.
- (8) Whitehead, T. H.; Wills, C. C. *Chem. Rev.* **1941**, *29* (1), 69–121.
- (9) Wagner, A. J.; Rychnovsky, S. D. *Org. Lett.* **2013**, *15* (21), 5504–5507.
- (10) Wagner, A. J.; David, J. G.; Rychnovsky, S. D. *Org. Lett.* **2011**, *13* (16), 4470–4473.
- (11) Miller, S. M.; Samame, R. A.; Rychnovsky, S. D. *J. Am. Chem. Soc.* **2012**, *134* (50), 20318–20321.
- (12) Wagner, A. J.; Rychnovsky, S. D. *J. Org. Chem.* **2013**, *78* (9), 4594–4598.
- (13) Wagner, A. J.; Miller, S. M.; Nguyen, S.; Lee, G. Y.; Rychnovsky, S. D.; Link, R. D. *J. Chem. Educ.* **2014**, *91* (5), 716–721.
- (14) Bandar, J. S.; Lambert, T. H. *J. Am. Chem. Soc.* **2012**, *134* (12), 5552–5555.
- (15) Inanaga, J.; Hirata, K.; Saeki, H.; Katsuki, T.; Yamaguchi, M. *Bull. Chem. Soc. Jpn.* **1979**, *52* (7), 1989–1993.
- (16) Shiina, I.; Kubota, M.; Oshiumi, H.; Hashizume, M. *J. Org. Chem.* **2004**, *69* (6), 1822–1830.
- (17) Birman, V. B.; Li, X. *Org. Lett.* **2008**, *10* (6), 1115–1118.
- (18) Goswami, S.; Das, A. K.; Sen, D.; Aich, K.; Fun, H.-K.; Quah, C. K. *Tetrahedron Lett.* **2012**, *53* (36), 4819–4823.

- (19) Sarmini, K.; Kenndler, E. *J. Biochem. Biophys. Methods* **1999**, *38* (2), 123–137.
- (20) Na Kim, H.; Hee Lee, M.; Jung Kim, H.; Seung Kim, J.; Yoon, J. *Chem. Soc. Rev.* **2008**, *37* (8), 1465–1472.
- (21) Beija, M.; M. Afonso, C. A.; G. Martinho, J. M. *Chem. Soc. Rev.* **2009**, *38* (8), 2410–2433.
- (22) Lee, M. H.; Kim, H. J.; Yoon, S.; Park, N.; Kim, J. S. *Org. Lett.* **2008**, *10* (2), 213–216.
- (23) Yuan, L.; Lin, W.; Feng, Y. *Org. Biomol. Chem.* **2011**, *9* (6), 1723–1726.
- (24) Best, Q. A.; Xu, R.; McCarroll, M. E.; Wang, L.; Dyer, D. J. *Org. Lett.* **2010**, *12* (14), 3219–3221.
- (25) Xue, Z.; Chen, M.; Chen, J.; Han, J.; Han, S. *RSC Adv.* **2013**, *4* (1), 374–378.
- (26) Pangborn, A. B.; Giardello, M. A.; Grubbs, R. H.; Rosen, R. K.; Timmers, F. J. *Organometallics* **1996**, *15* (5), 1518–1520.
- (27) Still, W. C.; Kahn, M.; Mitra, A. *J. Org. Chem.* **1978**, *43* (14), 2923–2925.
- (28) Hofmann, C.; Schuler, S. M. M.; Wende, R. C.; Schreiner, P. R. *Chem Commun* **2014**, *50* (10), 1221–1223.
- (29) Birman, V. B.; Jiang, H. *Org. Lett.* **2005**, *7* (16), 3445–3447.
- (30) Gupta, V. K.; Goyal, R. N.; Sharma, R. A. *Talanta* **2008**, *76* (4), 859–864.
- (31) Zhang, Y.-M.; Lin, Q.; Wei, T.-B.; Wang, D.-D.; Yao, H.; Wang, Y.-L. *Sens. Actuators B Chem.* **2009**, *137* (2), 447–455.
- (32) Sahoo, P. R.; Mishra, P.; Agarwa, P.; Gupta, N.; Kumar, S. *J. Incl. Phenom. Macrocycl. Chem.* **84** (1–2), 163–171.

Chapter 3. Introduction to the *Lycopodium* Alkaloids

3.1 Introduction

The *Lycopodium* alkaloids are isolated from the *Lycopodium* family of club mosses. These evergreen mosses are named after the club-shaped strobili at the tips of the moss-like branches.¹ The *Lycopodium* alkaloids feature a diverse group of over 250 complex natural products. Some of these compounds possess interesting biological activity, including potent and selective inhibition of acetylcholinesterase (AChE).² These molecules contain quinolizine, pyridine, and pyridone type motifs, which can pose synthetic challenges when examined in conjunction with the caged, polycyclic cores of these alkaloids. These molecules are divided into four classes, which are named after a respective *Lycopodium* alkaloid within that class: the lycopodine class, the lycodine class, the fawcettimine class, and the miscellaneous class (Figure 3.1). Any *Lycopodium* alkaloids lacking the lycodine, lycopodine, or fawcettimine cores belong to the miscellaneous class.

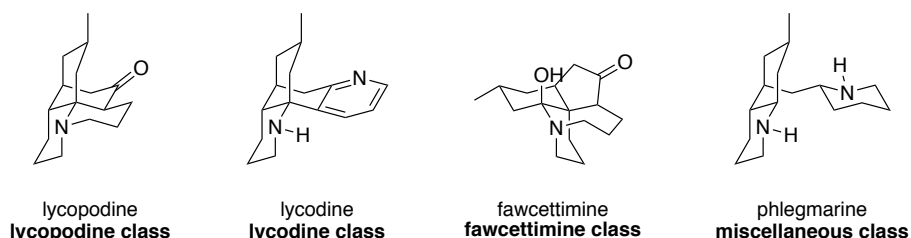


Figure 3.1: Representative compounds from the four classes of *Lycopodium* alkaloids.

Of interest to our group, and many other laboratories, are fastigiatine (**3.1**), himeradine A (**3.2**), and lyconadin D (**3.3**) and E (**3.4**) from the lycodine class, along with lyconadin A–C (**3.5–3.7**) from the miscellaneous class (Figure 3.2). The biological activity of (+)-fastigiatine (**3.1**) has not been assessed; however, similar members of the family such as himeradine A (**3.2**) have been shown by Kobayashi and co-workers to have modest *in vitro* cytotoxicity against murine

lymphoma L1210 cells ($IC_{50} = 10 \mu\text{g/mL}$).³ Unfortunately, additional studies by Kobayashi on the related lyconadin D and E (**3.3** and **3.4** respectively) showed no significant biological activity.⁴

In initial studies, lyconadin A (**3.5**) was shown to exhibit cytotoxicity against murine lymphoma L1210 and human epidermoid carcinoma KB cells ($IC_{50} = 0.46 \mu\text{g/mL}$ and $1.7 \mu\text{g/mL}$ respectively);⁵ however, lyconadin B (**3.6**) did not show cytotoxicity ($IC_{50} > 10 \mu\text{g/mL}$) when tested against these cell lines.⁶ Both lyconadin A (**3.5**) and B (**3.6**) were however shown to enhance expression of nerve growth factors (NGF) in 1321N1 human astrocytoma cells, which has applications in various neurodegenerative diseases.^{6,7} Even though the Waters,⁸ Fukuyama,⁹ and Dai¹⁰ labs have reported the natural product synthesis of lyconadin C (**3.7**), to the best of our knowledge, no biological testing has been performed. The structural complexity of these molecules, along with the potential to be drug candidates for neurodegenerative diseases, make the chemical synthesis of these molecules and their analogues attractive targets.

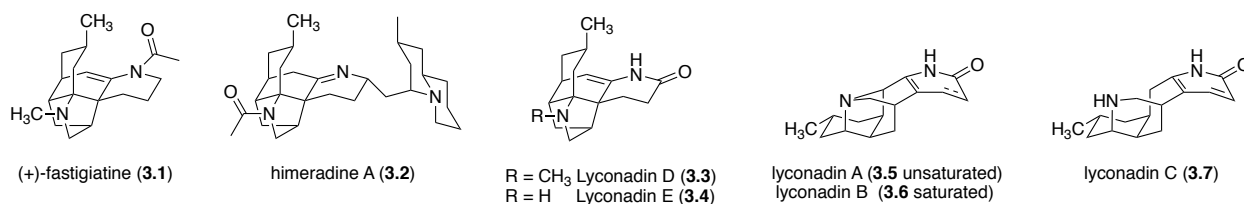


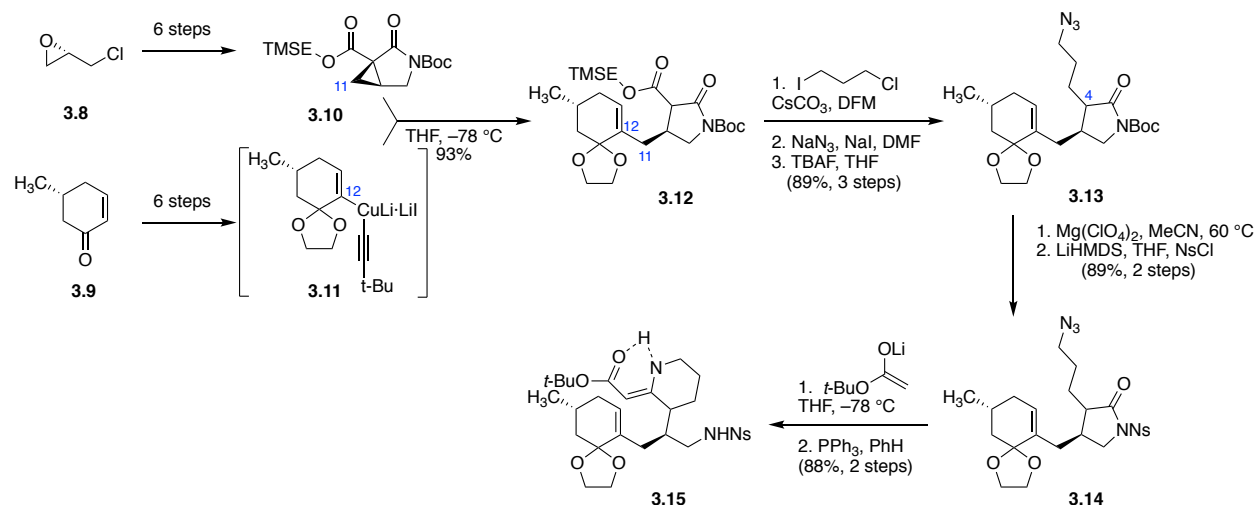
Figure 3.2: *Lycopodium* alkaloids of interest to the Rychnovsky laboratory.

3.2 Highlights of Shair's Synthesis of (+)-Fastigiatine

Shair and co-workers reported the first total synthesis of (+)-fastigiatine **3.1** in 2010.^{11,12} Their approach was part of a unified strategy to synthesizing several of the *Lycopodium* alkaloids. The overall synthesis was accomplished in 19 steps from commercially available (*S*)-epichlorohydrin **3.8**. Ring opening of cyclopropane **3.10** with cuprate **3.11** afforded 1,3-

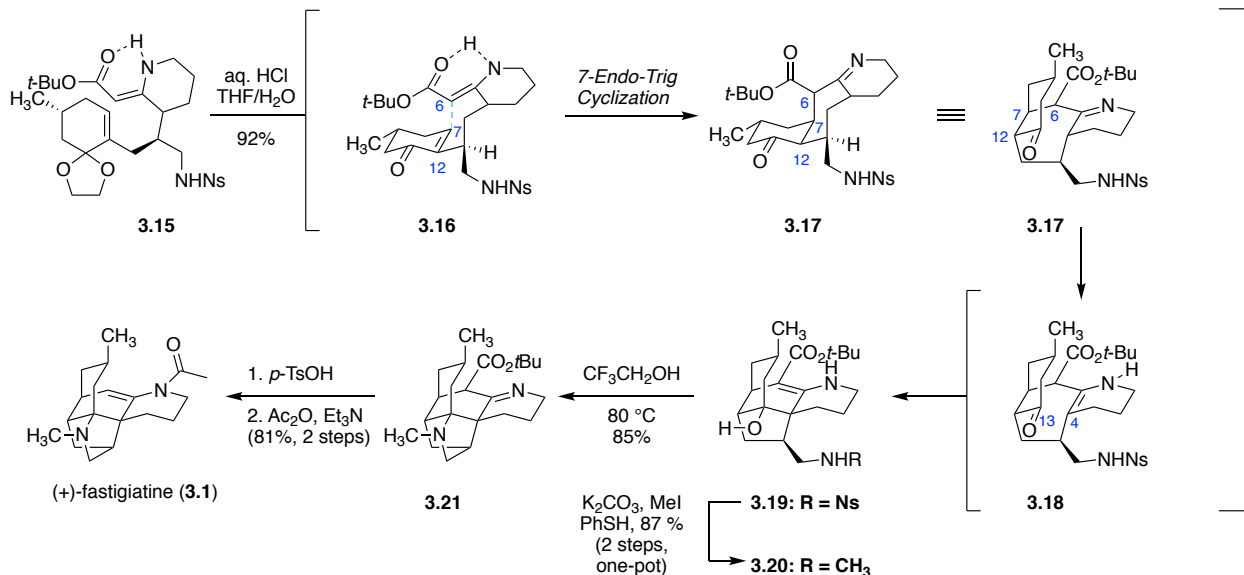
dicarbonyl **3.12**. Alkylation, S_N2 displacement of the chloride with azide, and decarboxylative cleavage of the TMSE ester furnished azide **3.13** in excellent yield. Protecting group manipulation, followed by addition of the lithium enolate of *tert*-butyl acetate and Staudinger reduction of the azide provided key intermediate **3.15**.

Scheme 3.1: Synthesis of enamine **3.15** by Shair.



Upon exposure to aqueous HCl, **3.15** underwent ketal deprotection (**3.16**), *7-endo-trig* cyclization to form the seven-membered ring (**3.17**), and spontaneous transannular aldol (C13–C4 bond) to form **3.19** (Scheme 3.2). While the transannular aldol product was unexpected, heating **3.20** in the presence of 2,2,2,-trifluoroethanol promoted a retro-aldol, reforming the C13 ketone and prompting the desired *in situ* condensation with the primary amine. A transannular Mannich reaction on the resultant iminium ion constructed the key C13–C4 bond and the desired core structure **3.21**. Final manipulation afforded (+)-fastigiatine **3.1** in 15 steps from cyclopropane **3.10**.

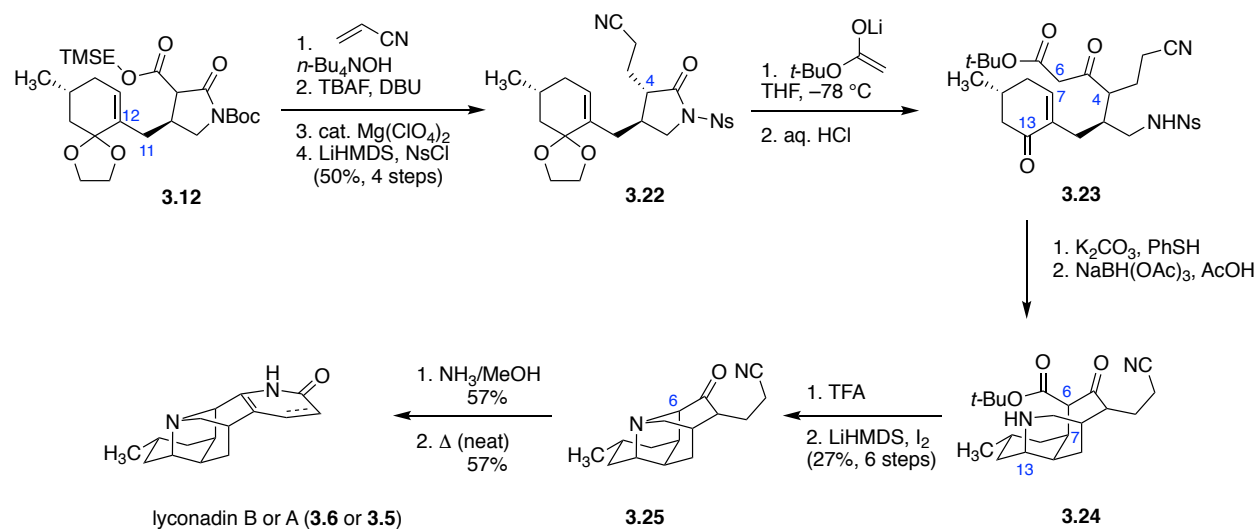
Scheme 3.2: Endgame to (+)-fastigiatine **3.1** by Shair.



3.3 Highlights of Shair's Synthesis of Lyconadin A and B

In a similar manner to the synthesis of (+)-fastigiatine **3.1** (Scheme 3.2), Shair and co-workers utilized intermediate **3.12** to construct the core of lyconadin A and B (Scheme 3.3).¹¹ The pendant nitrile that would form the pyridone ring was installed *via* conjugate addition to acrylonitrile. Decarboxylation of the TMSE ether with TBAF and replacement of the Boc protecting group afforded *N*-nosyl lactam **3.22**. Ring opening of the lactam (**3.23**) with the lithium enolate of *tert*-butyl acetate was carried over from the fastigiatine synthesis (Scheme 3.1). Addition of K₂CO₃ followed by PhSH yielded the tricyclic imine, which was subsequently reduced forming **3.24**. Following decarboxylation of the *tert*-butyl ester, the N–C6 bond was formed by addition of iodine to C6 and ring closure (**3.25**) analogous to Sarpong's syntheses of lyconadin A (Scheme 3.7).^{13,14} Heating nitrile **3.25** in NH₃/MeOH promoted the formation of lyconadin B **3.6**. Trace amounts of lyconadin A **3.5** were observed in this reaction, and heating of neat lyconadin B **3.6** in the presence of trace oxygen delivered lyconadin A **3.5**.

Scheme 3.3: Final steps of Shair's synthesis of lyconadin A (**3.5**) and B (**3.6**) from **3.12**.

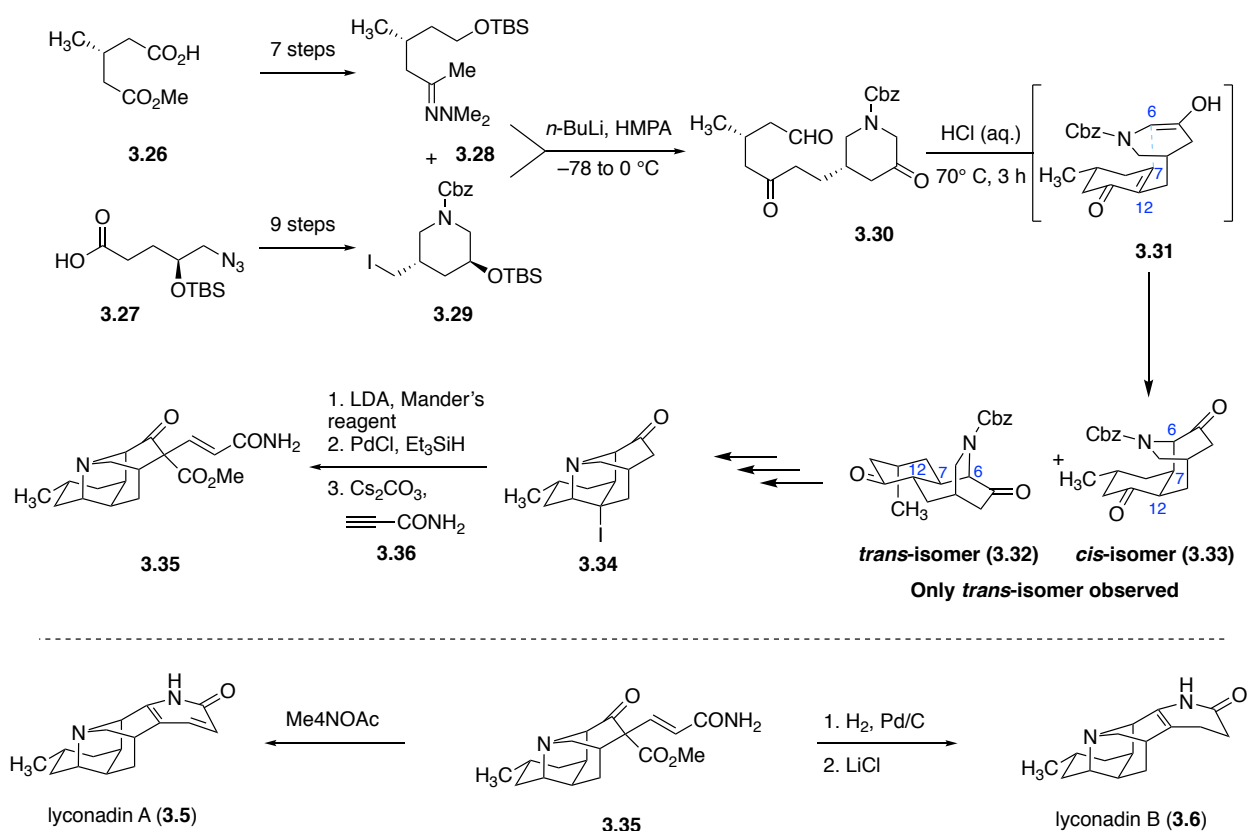


3.4 Highlights of Smith's Synthesis of Lyconadin A and B

The first synthesis of lyconadin A **3.5** was completed by Smith and Beshore in 2007 utilizing hydrazone **3.28** and iodide **3.29** (Scheme 3.4).^{15,16} Construction of hydrazone **3.28** was completed in seven steps from (–)-methyl (*R*)-3-methylglutarate (**3.26**). Iodide **3.29** was formed in 9 steps from azide **3.27** utilizing an asymmetric aldol reaction and S_N2 cyclization. Coupling of **3.28** and **3.29** *via* displacement of the iodide, followed by primary OTBS deprotection and oxidation yielded aldehyde **3.30**. Acidic conditions resulted in the aldol condensation, as well as *in situ* enolization and conjugate addition to form the C6–C7 bond (**3.31**). Unfortunately, the desired *cis*-isomer **3.33** was not observed. The undesired *trans*-isomer **3.32** was carried forward; however, multiple functional group manipulations were required to form the lyconadin core **3.34**. Tetracycle **3.34** was elaborated into tricarbonyl **3.35** by acylation with Mander's reagent, reductive iodide removal, and conjugate addition into propiolamide (**3.36**). Lyconadin A **3.5** was formed by a one-pot decarboxylation, olefin isomerization, and condensation of **3.35** with

Me₄NOAc. Hydrogenation of **3.35**, followed by treatment with LiCl afforded lyconadin B **3.6** by a similar decarboxylation/cyclization strategy.

Scheme 3.4: Synthesis of lyconadin A or B (**3.5** or **3.6**) by Smith.

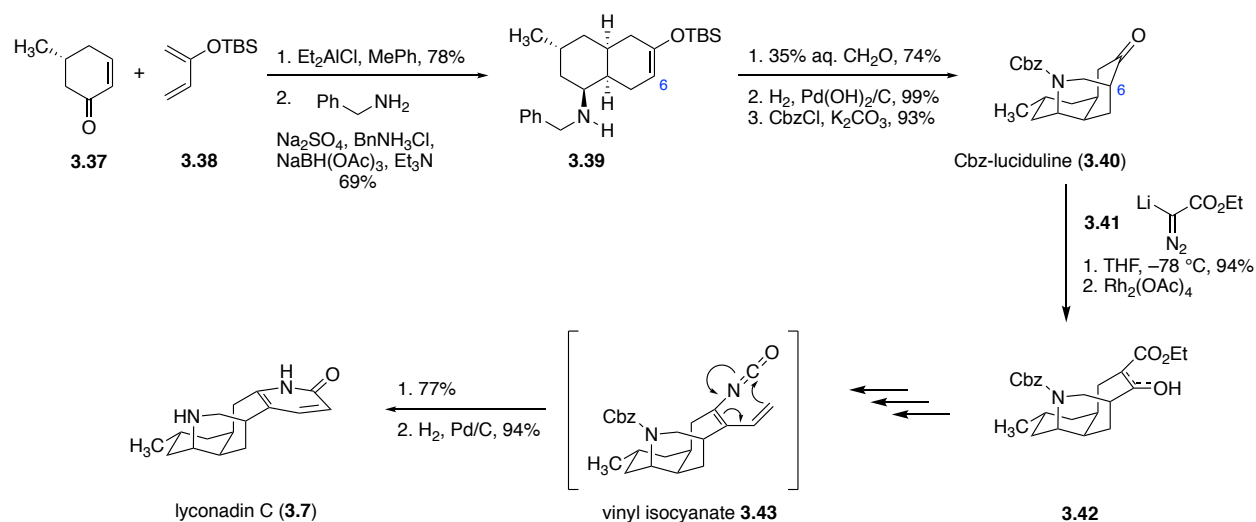


3.5 Highlights of Waters's Synthesis of Lyconadin C

In their synthesis of lyconadin C (**3.7**), Waters's and co-workers set the foundation for the Diels-Alder reaction that our group would use in our synthesis of (+)-fastigiatine (**3.1**).¹⁷ Enone **3.37** can be accessed in 4 steps from (+)-pulegone.^{18,19} The diastereoselective Diels-Alder between enone **3.37** and siloxydiene **3.38** formed the decalone core, which underwent reductive amination with benzylamine to form **3.39** (Scheme 3.5). Condensation of the amine onto formaldehyde promoted an intramolecular Mannich-type ring closure between C6 and the iminium ion. Replacement of the benzyl group with the Cbz protection group provided Cbz-

luciduline **3.40**.²⁰ Addition of the lithiated ethyl diazoacetate (**3.41**) to the ketone, and ring-expansion of the diazoalcohol with $\text{Rh}_2(\text{OAc})_4$ gave the seven-membered β -keto ester **3.42**. In four-steps this intermediate was transformed into vinyl isocyanate **3.43**, which underwent 6π -electrocyclization to form the desired pyridone. Removal of the Cbz group afforded lyconadin C **3.7** in 12 overall steps.

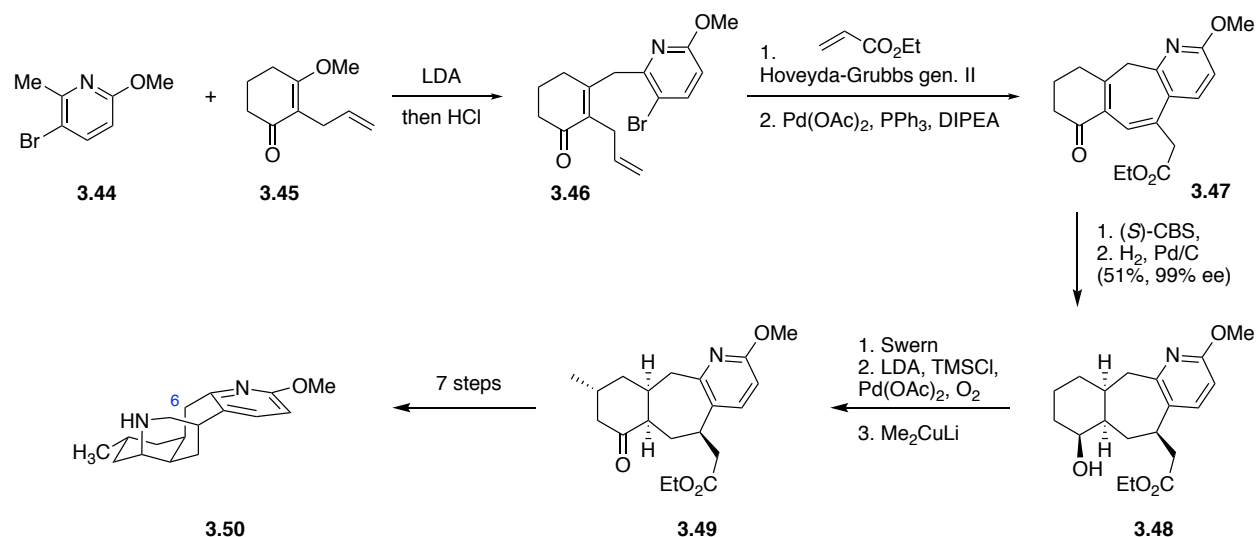
Scheme 3.5: Synthesis of lyconadin C **3.7** by Waters.



3.6 Highlights of Sarpong's Synthesis of Lyconadin A

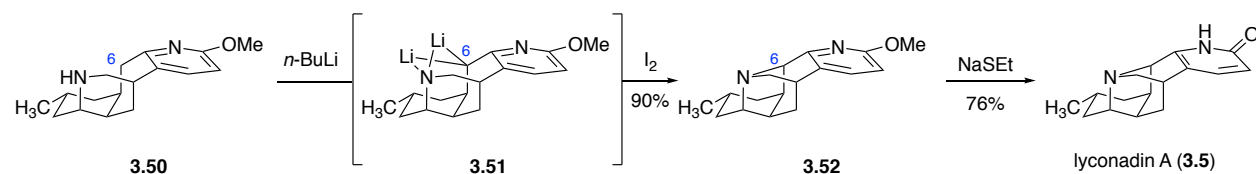
The Sarpong research group has published two syntheses of lyconadin A (**3.5**), a racemic route in 2008 and an asymmetric route in 2009.^{10,11} The asymmetric route began with a Stork–Danheiser reaction between **3.44** and **3.45** to form enone (**3.46**). A sequence of cross metathesis followed by a Heck reaction formed the seven-membered ring **3.47**. In two key steps, the enantioselectivity was conferred using a Corey-Bakshi-Shibata (CBS) reduction of the carbonyl and diastereoselective hydrogenation of the diene to afford alcohol **3.48** in 99% ee. It took three steps to install the β -methyl group (**3.49**), and another seven steps to reach tetracycle **3.50**.

Scheme 3.6: Synthesis of tetracycle **3.50** in Sarpong's synthesis of lyconadin A **3.5**.



The key final C–N bond formation at C6 was accomplished by treatment of tetracycle **3.50** with two equivalents of *n*-BuLi to form dianion **3.51**, which was oxidized to **3.52** upon addition of iodine (Scheme 3.7). Cleavage of the methyl ether with NaSEt revealed the pyridone of lyconadin A **3.5**.

Scheme 3.7: C–N bond formation and methyl cleavage to form lyconadin A **3.5**.

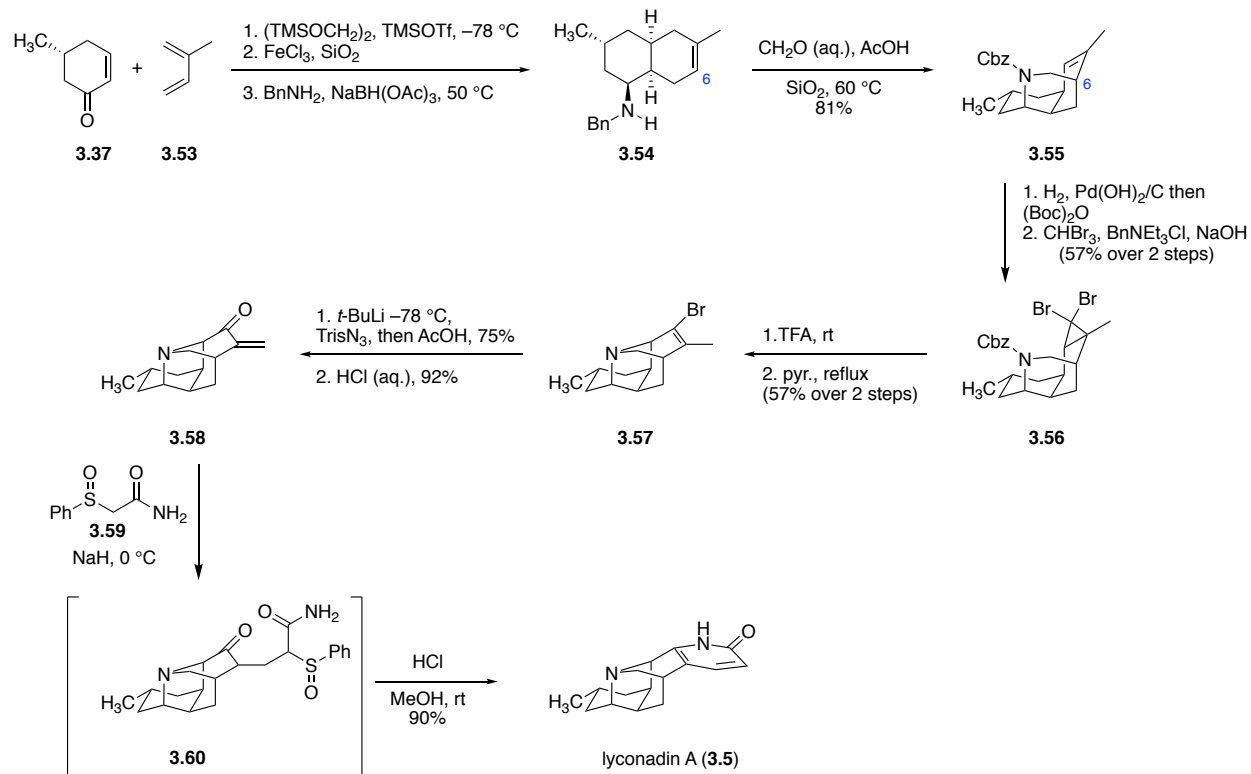


3.7 Highlights of Fukuyama's Synthesis of Lyconadin A–C

Similar to many of the other lycopodium alkaloid syntheses, Fukuyama's total synthesis of lyconadin A **3.5** began with enone **3.37**.²¹ However, unlike other syntheses, the ketone was protected as the ketal in a one-pot acetal formation/Diels-Alder process (Scheme 3.8).²² Deprotection of the ketal and reductive amination with benzylamine constructed the decalin core **3.54**. The aza-Prins reaction of **3.54** with formaldehyde constructed tricycle **3.55** in 81% yield.

The benzyl group was replaced as the *N*-Boc, and the alkene underwent cyclopropanation to dibromide **3.56** under phase-transfer conditions. *N*-Boc cleavage in TFA and refluxing in pyridine delivered tetracycle **3.57**. Lithium-halogen exchange and treatment with trisyl azide, followed by release of nitrogen under acidic conditions furnished enone **3.58**. The enolate of **3.59** was generated with NaH, and underwent Michael addition into enone **3.58** to form sulfoxide **3.60**. Lyconadin A **3.5** was formed upon treatment of sulfoxide **3.60** with methanolic HCl to afford the cyclization and sulfoxide elimination. Overall the synthesis was accomplished in 12% overall yield and 15 steps from (+)-pulegone.

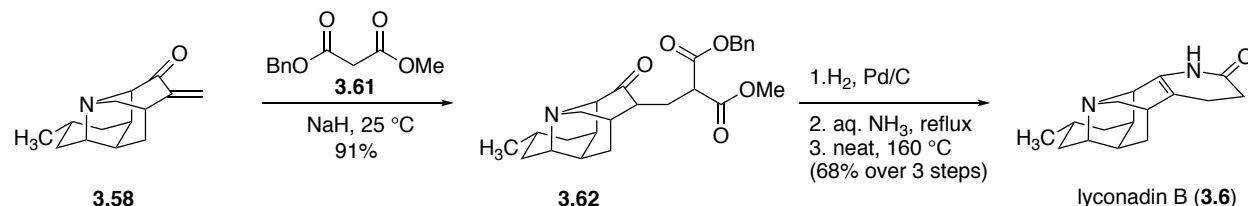
Scheme 3.8: Fukuyama's synthesis of lyconadin A **3.5**.



The Fukuyama group later published their efforts towards lyconadin A–C in 2013.⁹ The synthesis of lyconadin B (**3.6**) was identical to their original lyconadin A (**3.5**) synthesis until intermediate **3.58** (Scheme 3.9). Instead of using sulfoxide **3.59**, benzyl methyl malonate **3.61** was used instead. Benzyl ester **3.62** underwent a debenzoylation/decarboxylation, instead of the

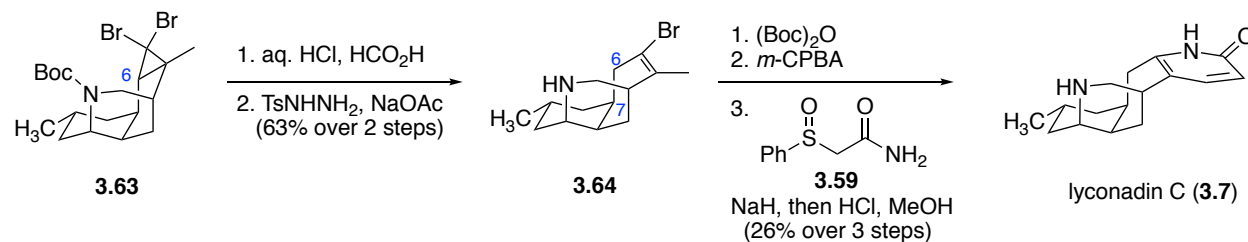
sulfoxide elimination utilized for lyconadin A **3.5** (Scheme 3.8). Conversion of the methyl ester to the amide through refluxing in aqueous ammonia, and heating the neat mixture induced dehydration to furnish lyconadin B **3.6**.

Scheme 3.9: Synthesis of lyconadin B **3.6** by Fukuyama.



Fukuyama and co-workers had to modify their approach since lyconadin C **3.7** lacks the C–N bond at C6 found in lyconadin A (**3.5**) and B (**3.6**). Unfortunately, attempts to undergo the ring expansion with the *N*-Boc, Ts, or Ns protected amine to prevent this bond formation were unsuccessful. It was found that under acidic conditions dibromocyclopropane **3.63** underwent expansion to the seven-membered ring without C–N bond formation, presumably due to protection the amine as the ammonium salt (Scheme 3.10). Selective diimide reduction of the less hindered C7/C6 alkene afforded **3.64**. *N*-Boc protection and oxidation furnished an enone similar to **3.58**, without the N–C6 bond. A similar Michael addition/sulfoxide elimination with **3.59** used in the original lyconadin A (**3.5**) (Scheme 3.8) synthesis afforded lyconadin C **3.7** (Scheme 3.10).

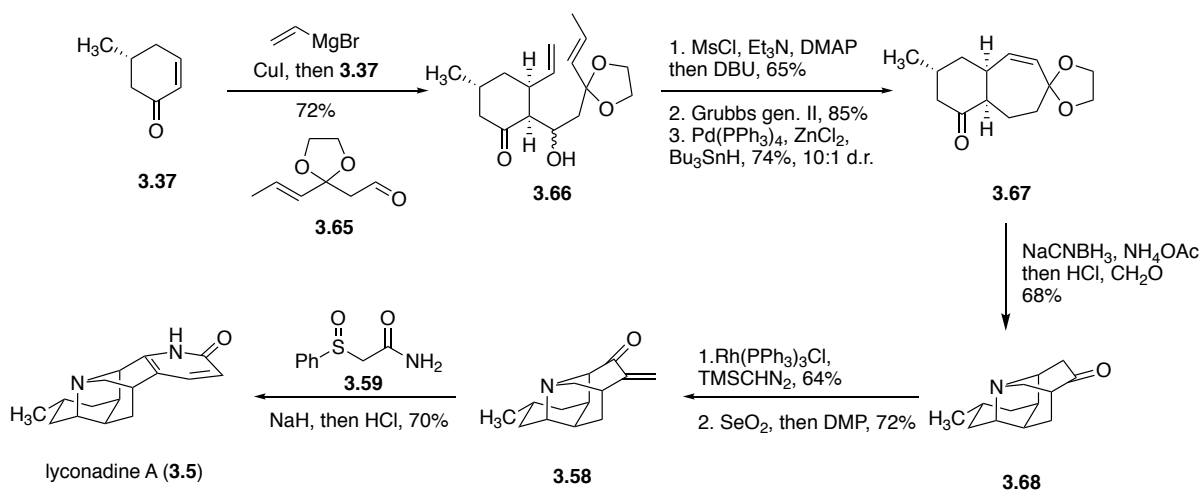
Scheme 3.10: Synthesis of lyconadin C (**3.7**) by Fukuyama.



3.8 Highlights of Dai's Synthesis of Lyconadin A and C

The Dai synthesis of lyconadin A (**3.5**) and C (**3.7**) commenced with conjugate addition of the vinyl cuprate to **3.37**, followed by trapping of the resultant enolate with aldehyde **3.65** to form **3.66** (Scheme 3.11). The alcohol was eliminated to form the exocyclic enone, and the seven-membered ring was closed *via* ring-closing metathesis. Chemo- and stereoselective reduction of the enone afforded the *cis*-6,7-fused ring system in **3.67**. This compound was used as a branching point for lyconadin A (**3.5**) and C (**3.7**). For the synthesis of lyconadin A (**3.5**), the key C–N bond formation in **3.68** was achieved through reductive amination onto the ketone **3.67**, followed by formal [4 + 2] cyclization between the iminium ion of formaldehyde and the enolic diene. Ketone **3.68** was converted to enone **3.58** through a Lebel olefination,¹⁶ allylic oxidation, and alcohol oxidation sequence. Dai then utilized the Fukuyama pyridone synthesis with **3.59** (Scheme 3.8) to complete the synthesis of lyconadin A (**3.5**).

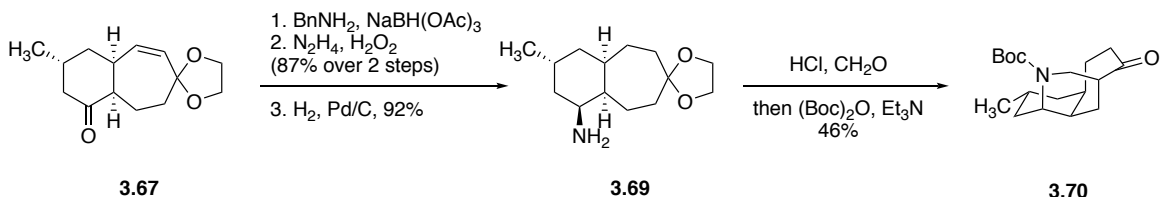
Scheme 3.11: Dai's synthesis of lyconadin A (**3.5**) and C (**3.7**).



Lyconadin C was synthesized beginning with intermediate **3.67** (Scheme 3.12). Reductive amination with benzylamine, diimide reduction of the alkene, and debenzylation of the amine furnished amine **3.69**. Upon treatment with formaldehyde and acid, **3.69** underwent a Mannich

reaction, and the resulting secondary amine was protected as the *N*-Boc (**3.70**). Compound **3.70** was elaborated to lyconadin C (**3.7**) using similar approach to lyconadin A (Scheme 3.11, compound **3.68**).

Scheme 3.12: Transformation of **3.67** to **3.70** *en route* to lyconadin C (**3.7**).



3.9 Conclusion

These previous syntheses are only a representative sample of the work on *Lycopodium* alkaloids. Other molecules in the four classes have garnered synthetic interest as well due to the interesting biological activity and the ever-increasing biological data. The synthesis of the *Lycopodium* alkaloids has led to the development of numerous strategies for forming 7-membered rings and caged, polycyclic compounds. The work of Shair, Fukuyama, and Dai in developing unified routes to a number of these alkaloids, has inspired our group in our endeavors towards a unified approach to these complex molecules.

3.10 References:

- (1) Ma, X.; Gang, D. R. *Nat. Prod. Rep.* **2004**, *21* (6), 752–772.
- (2) Tang, X.-C.; De Sarno, P.; Sugaya, K.; Giacobini, E. *J. Neurosci. Res.* **1989**, *24* (2), 276–285.
- (3) Morita, H.; Hirasawa, Y.; Kobayashi, J. 'ichi. *J. Org. Chem.* **2003**, *68* (11), 4563–4566.
- (4) Ishiuchi, K.; Kubota, T.; Ishiyama, H.; Hayashi, S.; Shibata, T.; Mori, K.; Obara, Y.; Nakahata, N.; Kobayashi, J. *Bioorg. Med. Chem.* **2011**, *19* (2), 749–753.

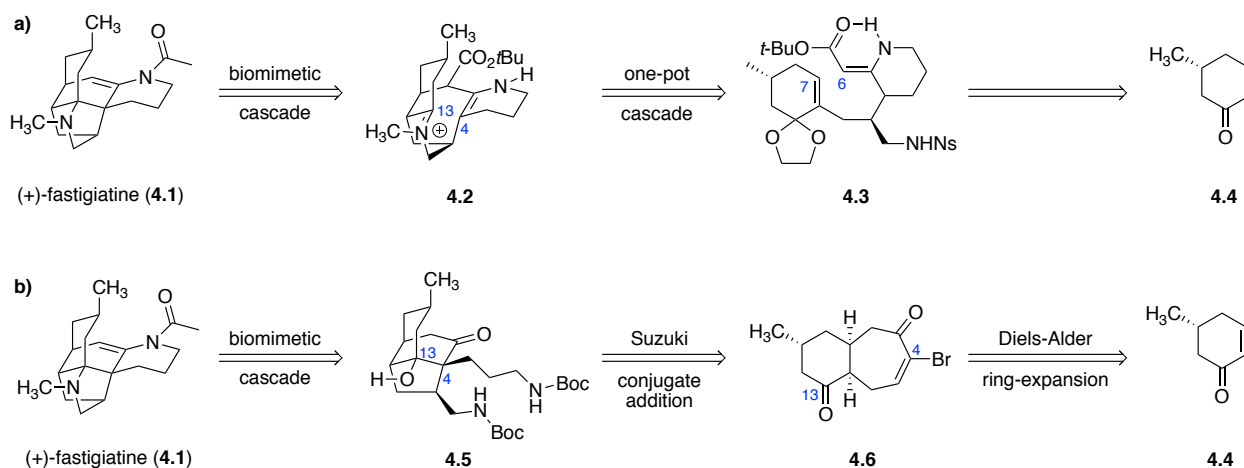
- (5) Kobayashi, J. Ichi; Hirasawa, Y.; Yoshida, N.; Morita, H. *J. Org. Chem.* **2001**, *66* (17), 5901–5904.
- (6) Ishiuchi, K.; Kubota, T.; Hoshino, T.; Obara, Y.; Nakahata, N.; Kobayashi, J. *Bioorg. Med. Chem.* **2006**, *14* (17), 5995–6000.
- (7) Yang, Y.; Dai, M. *Synlett* **2014**, *25* (15), 2093–2098.
- (8) Cheng, X.; Waters, S. P. *Org. Lett.* **2013**, *15* (16), 4226–4229.
- (9) Nishimura, T.; Unni, A. K.; Yokoshima, S.; Fukuyama, T. *J. Am. Chem. Soc.* **2013**, *135* (8), 3243–3247.
- (10) Yang, Y.; Haskins, C. W.; Zhang, W.; Low, P. L.; Dai, M. *Angew. Chem. Int. Ed.* **2014**, *53* (15), 3922–3925.
- (11) Lee, A. S.; Liao, B. B.; Shair, M. D. *J. Am. Chem. Soc.* **2014**, *136* (38), 13442–13452.
- (12) Liao, B. B.; Shair, M. D. *J. Am. Chem. Soc.* **2010**, *132* (28), 9594–9595.
- (13) Bisai, A.; West, S. P.; Sarpong, R. *J. Am. Chem. Soc.* **2008**, *130* (23), 7222–7223.
- (14) West, S. P.; Bisai, A.; Lim, A. D.; Narayan, R. R.; Sarpong, R. *J. Am. Chem. Soc.* **2009**, *131* (31), 11187–11194.
- (15) Beshore, D. C.; Smith, A. B. *J. Am. Chem. Soc.* **2007**, *129* (14), 4148–4149.
- (16) Beshore, D. C.; Smith, A. B. *J. Am. Chem. Soc.* **2008**, *130* (41), 13778–13789.
- (17) Samame, R. A.; Owens, C. M.; Rychnovsky, S. D. *Chem. Sci.* **2015**, *7* (1), 188–190.
- (18) Nangia, A.; Prasuna, G. *Synth. Commun.* **1994**, *24* (14), 1989–1998.
- (19) Kozak, J. A.; Dake, G. R. *Angew. Chem. Int. Ed.* **2008**, *47* (22), 4221–4223.
- (20) Cheng, X.; Waters, S. P. *Org. Lett.* **2010**, *12* (2), 205–207.
- (21) Nishimura, T.; Unni, A. K.; Yokoshima, S.; Fukuyama, T. *J. Am. Chem. Soc.* **2011**, *133* (3), 418–419.
- (22) Chatgililoglu, C.; Crich, D.; Komatsu, M.; Ryu, I. *Chem. Rev.* **1999**, *99* (8), 1991–2070.
- (23) Lebel, H.; Guay, D.; Paquet, V.; Huard, K. *Org. Lett.* **2004**, *6* (18), 3047–3050.

Chapter 4. A Computationally Inspired Approach to the Total Synthesis of (+)-Fastigiatine

4.1 Introduction

The *Lycopodium* alkaloids contain a rich synthetic history, which has attracted the interest of many synthetic laboratories (see Chapter 3 for representative syntheses). Of particular interest to both the Shair¹ and Rychnovsky² groups is (+)-fastigiatine **4.1** from the lycodine class of *Lycopodium* alkaloids.³ This densely functionalized molecule has inspired biomimetic cascade cyclizations as a way to forge key bond formations. Similar intramolecular Mannich reactions were initially reported by Stork and Heathcock in their respective syntheses of lycopodine and lycodine, and have provided the inspiration for the biomimetic cascades found in the two (+)-fastigiatine syntheses (Scheme 4.1).

Scheme 4.1: Retrosynthetic analysis of the a) Shair and b) Rychnovsky synthesis of (+)-fastigiatine **4.1**.



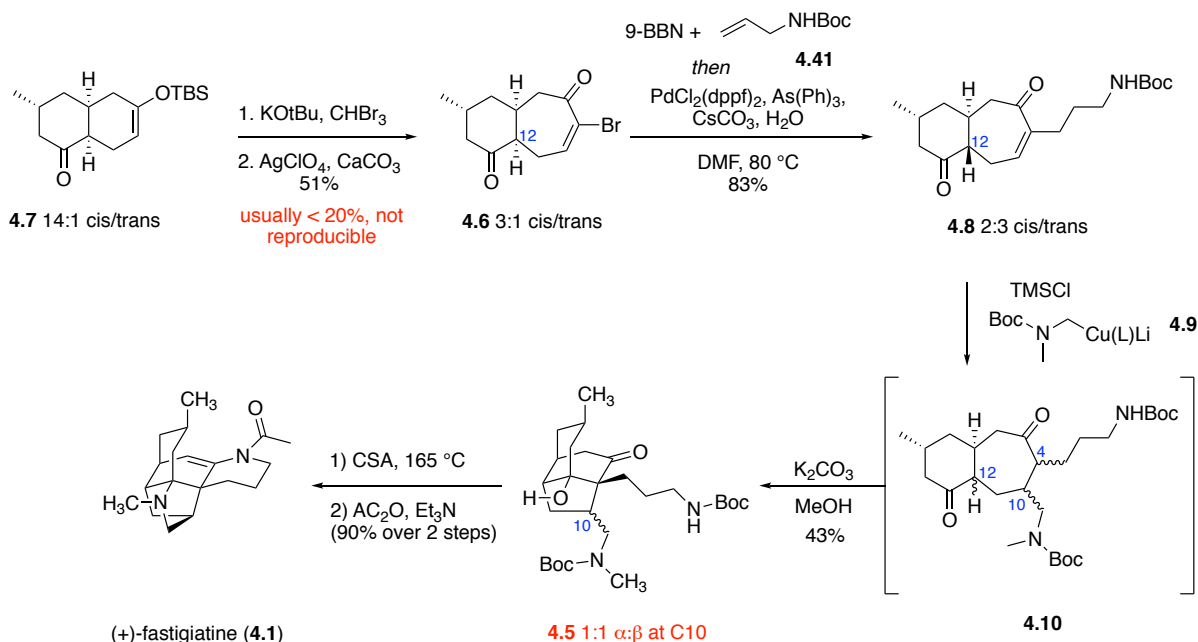
The first synthesis of (+)-fastigiatine **4.1** was performed by Shair and co-workers in 2010.¹ It utilized a key biomimetic cascade to forge the key C13–C4 bond. Formation of the precursor to iminium **4.2** was made possible through an acid-promoted ketal deprotection, *7-endo-trig*

cyclization, and spontaneous transannular aldol starting from vinylogous urethane **4.3**. Enone **4.4**, derived in 4 steps from (+)-pulegone,^{4,5} was the common starting material for both syntheses. Recently, our group published a highly concise, six step total synthesis of (+)-fastigiatine from enone **4.4** (Scheme 4.2).² While our route also took advantage of the biomimetic cascade to form the C13–C4 bond, we envisioned *cis*-fused bicyclo[5.4.0]undecane **4.6** as a key intermediate that could be not only used to synthesize (+)-fastigiatine **4.1**, but other members of the *Lycopodium* alkaloids.

4.2 1st Generation Synthesis of (+)-Fastigiatine

At six overall steps, our initial synthesis was extremely concise (Scheme 4.2); however, the decalin ring expansion (**4.7–4.6**) and the conjugate addition were problematic steps. Work by Dr. Renzo Samame to optimize the ring expansion was plagued by low yields and the generation of a mixture of C12 epimers **4.6** due to the acidity of the α -keto protons. Attempts to drive the equilibrium to *cis*-fused **4.6** or **4.8** under basic conditions were ultimately unsuccessful, and in all cases favored the *trans*-fused system. In addition to scrambling the stereochemistry at C12, the *trans*-fused **4.8** also provided no substrate-controlled facial selectivity during the subsequent cuprate reaction due to the accessibility of both faces of the enone. These issues drastically reduced the amount of usable material Jacob and myself were able to carry through the synthetic route. In order to mitigate these issues we devised a 2nd generation approach.

Scheme 4.2: 1st generation synthesis of (+)-fastigiatine.



4.3 2nd Generation Synthesis of (+)-Fastigiatine: A Computationally Inspired Approach

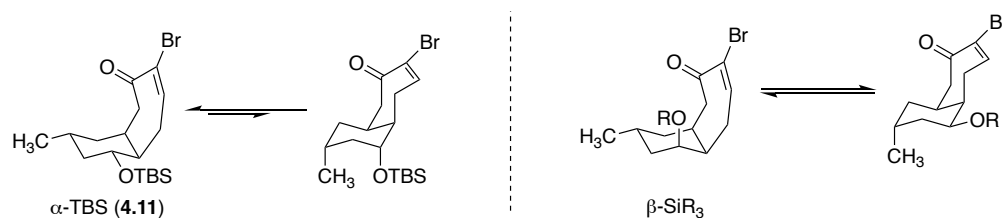
By utilizing a slightly modified approach, we were confident that we could solve both our problems in our initial synthesis. Masking of the C13 ketone mitigated the problematic C12 proton throughout the synthesis. Epimerization of the C12 position occurred during the ring expansion step, so it was chosen to reduce the decalone **4.7** to the alcohol before this step. Reduction of **4.7** can occur from either the convex or concave face of the molecule, producing two epimeric alcohols. Previous work by Dr. Renzo Samame had shown that reduction of decalone **4.7** provided a 1.0:1.5 ratio of α : β -alcohols (Table 4.4). The ability to generate both epimers was desired for our upcoming studies.

While the stereochemistry of the alcohol at C13 is inconsequential, we were interested in using this stereochemistry to affect the upcoming conjugate addition reaction. We were

particularly interested in protecting the axial β -alcohol, which we believed might induce a cyclohexane ring-flip due the steric bulk of the protecting group. This conformational change would place the silyl ether in the equatorial position, blocking the bottom face of the enone. We envisioned this would allow for increased diastereoselectivity in the conjugate addition *via* substrate control. With this strategy in mind, preliminary DFT calculations were performed on the simplified α - and β -protected alcohols **4.11**–**4.14** (Appendix Chapter 4), rather than the cross coupled structures (**4.19**, **4.27**, and **4.28**).

The computations showed that the α -alcohol **4.11** placed the methyl and protected alcohol equatorial, exposing the bottom, undesired, face of the enone to nucleophilic attack (Table 4.1, entry 1). We were pleased to see the calculations indicate a preference for the axial β -alcohol to undergo a ring-flip when larger protecting groups were introduced (TIPS **4.13** and TBDPS **4.14**) (Table 4.1, entries 3 and 4). The ring flipped compounds block the bottom face of the enone, which might allow for diastereoselective conjugate addition from the desired top face.

Table 4.1: Computational studies on the conformation of alcohols **4.11**–**4.14**. DFT basis set: B3LYP/6-31G(d).

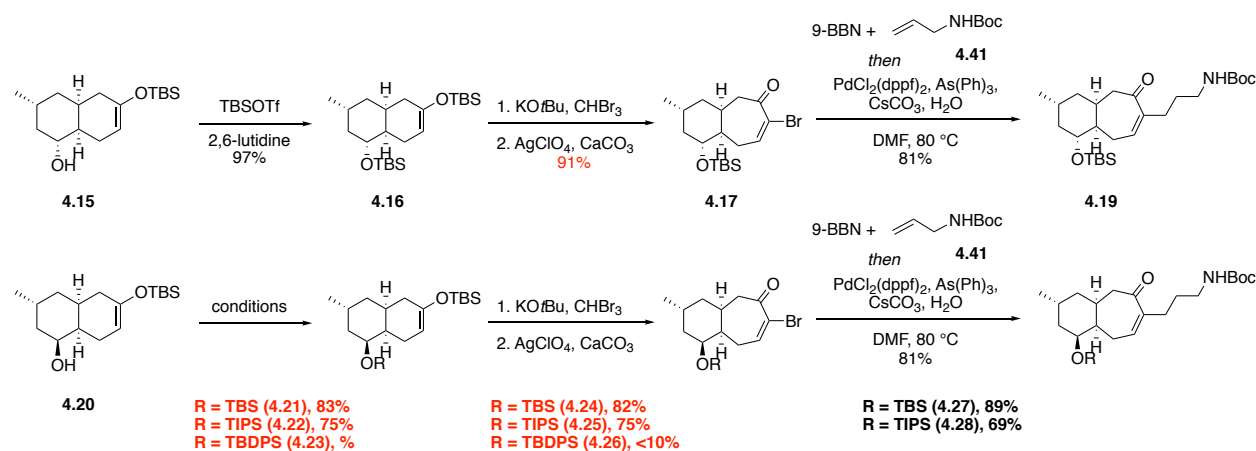


entry	protected alcohol	ring flip by ¹ H NMR?	favored conformation by computation calculations
1	α -TBS (4.11)	no	equatorial methyl (0.44 kcal)
2	β -TBS (4.12)	no	equatorial methyl (0.44 kcal)
3	β -TIPS (4.13)	no	axial methyl (1.29 kcal)
4	β -TBDPS (4.14)	yes	axial methyl (1.20 kcal)

To test our hypothesis that the use of a bulky α - or β -protected alcohol could induce a conformation change, modified routes to enones **4.19**, **4.27**, and **4.28** were developed. Our screen

of hydride sources (Table 4.4) indicated that reduction of decalone **4.7** using sodium borohydride provided a useable mixture of both α - and β -alcohols (**4.15** and **4.20**, respectively), which could be easily separated by column chromatography. The α -alcohol was taken forward as the TBS ether **4.16**, while the β -alcohol was protected as the TBS (**4.21**), TIPS (**4.22**), and TBDPS (**4.23**) ethers (Scheme 4.3).

Scheme 4.3: Synthesis of α - or β -protected alcohols **4.19**, **4.27**, and **4.28**.

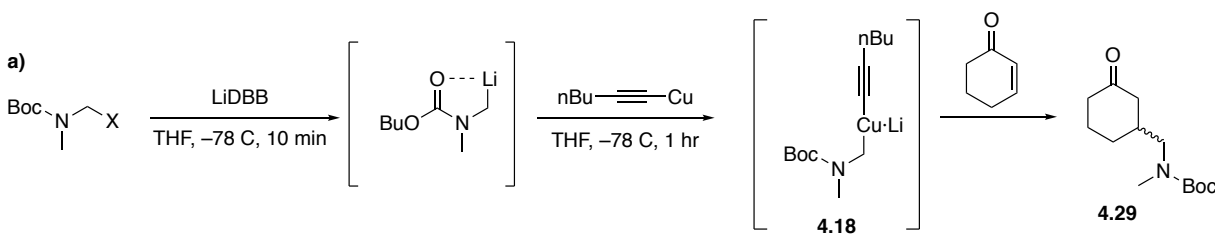


The ring expansion of decalone **4.7** was low yielding in our first generation synthesis of fastigiatine (**4.1**). We believe this is due to deprotection of the enoxysilane to form the 1,5-diketone, which can produce a variety of unidentifiable retro-Michael/Grob-type fragmentation byproducts. The use of freshly distilled bromoform and sublimed potassium *tert*-butoxide were crucial to minimizing decomposition; however, yields were typically well below the reported 50%. The protected alcohols were expected to contain fewer decomposition pathways due to the removal of any acidic α -keto protons. Satisfyingly, the treatment of enoxysilanes (**4.16**, **4.21**–**4.23**) under the ring expansion conditions afforded significantly improved yields of bromoenone **4.17**, **4.24**–**4.26** (Scheme 4.3). Unfortunately, the base-sensitivity of the TBDPS ether led to low yields of **4.26** under the basic reaction conditions, and it was decided that **4.26** would not be carried forward in the sequence. Suzuki cross coupling of the remaining silyl-protected

bromo-enones (**4.17**, **4.24**, and **4.25**) afforded desired enones **4.19**, **4.27**, and **4.28** in moderate to excellent yield.⁶ With the appropriate enones in hand, we turned our attention to the conjugate addition.

Our previous synthesis of (+)-fastigiatine **4.1** utilized the novel aminomethylene cuprate reagent **4.18** in the conjugate addition.² This reagent was generated by reductive lithiation of the phenyl sulfide **4.30** with LiDBB,⁷ followed by transmetalation to the alkyl cuprate (Scheme 4.4).⁸ This process was complex and time-consuming, generally requiring multiple days to complete even a single reaction. These reactions were also extremely sensitive due to the use of LiDBB, and rigorous schlenk conditions were necessary. For these reasons, we decided to investigate a more robust way to install the aminomethylene unit.

Scheme 4.4: a) Generation and conjugate addition of organocuprate **4.18** with cyclohex-2-en-1-one. b) Effect of X group on 1,4- vs 1,2-addition to cyclohex-2-en-1-one.

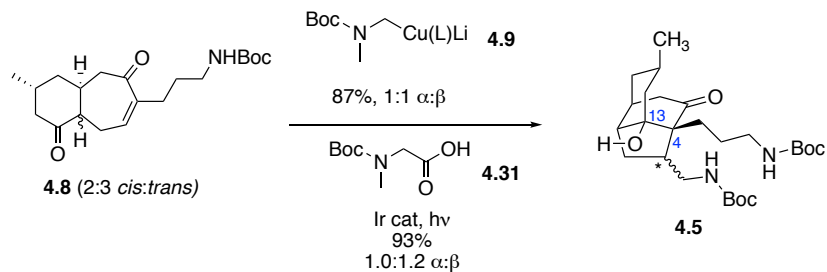


entry	X	addition products	
		1,4	1,2
1	CN	0%	42%
2	Cl	trace	0%
3	SPh (4.30)	89%	0%

We were inspired by the recent work of the Overman and MacMillan groups demonstrating the use of nucleophilic radicals in conjugate additions.⁹ Using amino acids, the α -amino radical

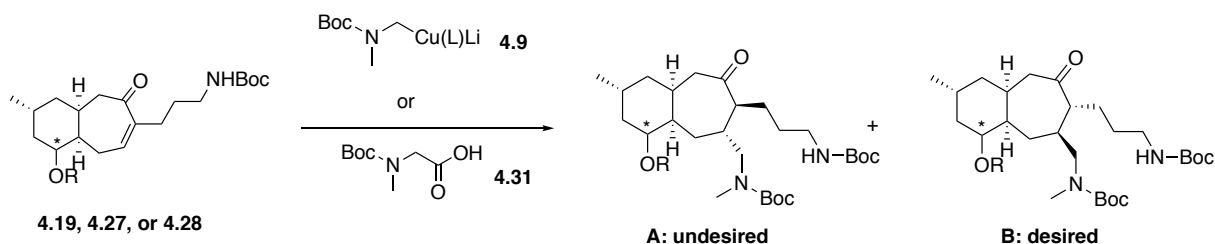
can be generated by photoredox initiated, *in situ* radical decarboxylation with readily available iridium catalysts. This photoredox catalyzed system utilizes easily accessible starting materials, mild reaction conditions, short setup/reaction times, and simplified purification.

Scheme 4.5: Formation of tricycle **4.5** under organocuprate or photochemical conditions.



An initial proof-of-concept was carried out between glycine derivative **4.31** and enone **4.8**. We chose enone **4.8** as our model substrate to ensure that no drastic conformational changes would occur, allowing a more direct comparison between the cuprate conjugate addition and the photochemical conjugate addition. Gratifyingly, the conjugate addition was successful, affording the desired 1,4-adduct **4.5** in 93% yield. The radical conjugate addition provided a 1.0:1.2 dr, which was comparable to the 1.0:1.0 dr that was achieved using the organocuprate (Scheme 4.5). This result prompted us to attempt the photochemical addition on the protected C13 alcohols **4.19**, **4.27**, and **4.28**.

Table 4.2: Comparison between the organocuprate and photochemical conjugate addition on protected alcohols **4.19**, **4.27**, and **4.28**.



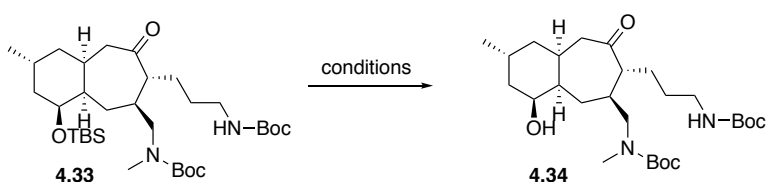
entry	compound	method	%yield	dr A:B
1	α -TBS (4.19)	cuprate	82	4:1
2	β -TBS (4.27)	cuprate	69	1.0:2.5
3	β -TBS (4.27)	photochemical	67	1.0:2.5
4	β -TIPS (4.28)	photochemical	87	1:5

In Dr. Renzo Samame's original studies of the α -TBS alcohol **4.19** undergoing the conjugate addition with the organocuprate, this substrate displayed a preference for nucleophilic attack from the convex face. This provided a 4:1 ratio favoring the undesired α -diastereomer **4.32**, and we decided to abandon further studies with the α -TBS alcohol **4.19** under photochemical conditions (Table 4.2). The β -TBS alcohol **4.27** underwent addition to the desired concave face in a 1.0:2.5 α : β ratio for both the organocuprate and the photochemical addition. This preference for the β -approach helped to initially validate our computational model, and the β -TIPS alcohol **4.28** was tested to see if we could indeed improve the diastereoselectivity through a conformational change. The TIPS ether **4.28** provided the conjugate addition product in an excellent 1:5 ratio of diastereomers, with addition to the concave face being highly favored. This result confirmed the addition of a sterically bulky group forces the compound to undergo a ring flip, blocking the concave face and favoring the convex face.

The two conjugate addition diastereomers are inseparable by flash chromatography, and the *N*-Boc groups complicate spectroscopic characterization and 2D NMR correlations due to a complex mixture of rotamers. Attempts to improve the spectra at elevated temperatures were

unsuccessful; fortunately, the carbamate moieties are weakly UV active (273 nm), and diastereomeric ratios of the crude reaction mixtures could be obtained by HPLC analysis. To confirm the identity of the diastereomers, each product was carried through the deprotection and oxidation until they converged with the previously reported intermediates **4.5a** and **4.5b** (Scheme 4.6).

Table 4.3: Optimization of conditions for deprotection of TBS alcohol **4.33**.

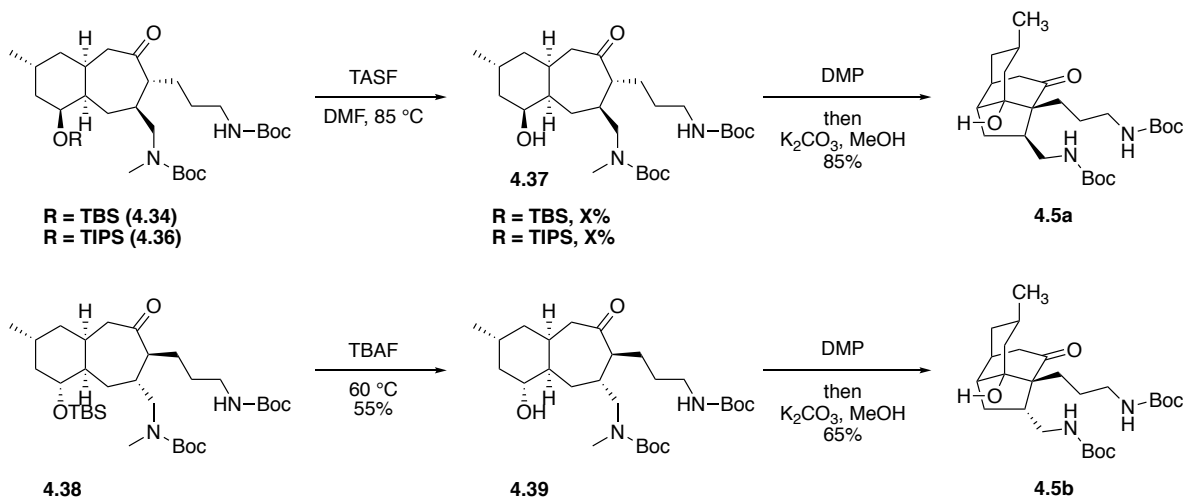


entry	conditions	temp. (°C)	%yield 4.34
1	TBAF	60	45
2	CSA	50	decomp.
3	aq. HF-CH ₃ CN	25	decomp.
4	HF-pyridine	25	41
3	TASF	25	NR
4	TASF	85	only 4.34

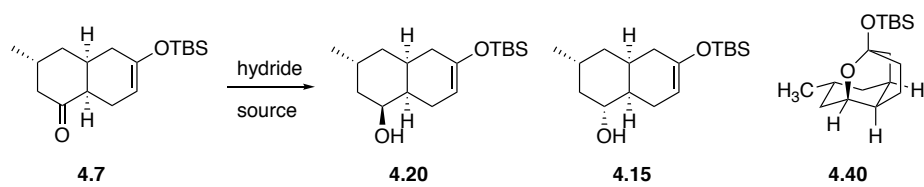
The deprotection-oxidation sequence needed to be optimized due to the unexpectedly difficult silyl deprotection (Table 4.3). Presumably the sterically hindered environment around the axial alcohol prevented facile deprotection, resulting in several low-yielding attempts at silyl deprotection. Deprotection with TBAF at room temperature was sluggish and provided no reaction; however, heating to 60 °C provided some deprotected product **4.34**, as well as unidentifiable byproducts. Deprotection with camphorsulfonic acid was also attempted, however while partial deprotection was observed, a significant amount of mono- or bis-cleavage of the *N*-Boc groups was also present. This was observed when **4.33** was treated with HF in acetonitrile. HF-pyridine was selective for silyl cleavage, unfortunately the yields were still quite low. The

anhydrous fluoride source, TASF, has been reported to be both mild and efficient at cleaving sterically hindered silyl groups.¹⁰ When treated with TASF in THF at room temperature, alcohol **4.33** showed no reaction after 48 hours; fortunately, switching the solvent to DMF and heating the mixture to 85 °C provided clean deprotection of the silyl group.

Scheme 4.6: Transformation of silyl alcohols **4.34**, **4.36**, and **4.38** to tricycles **4.5a** and **4.5b**.



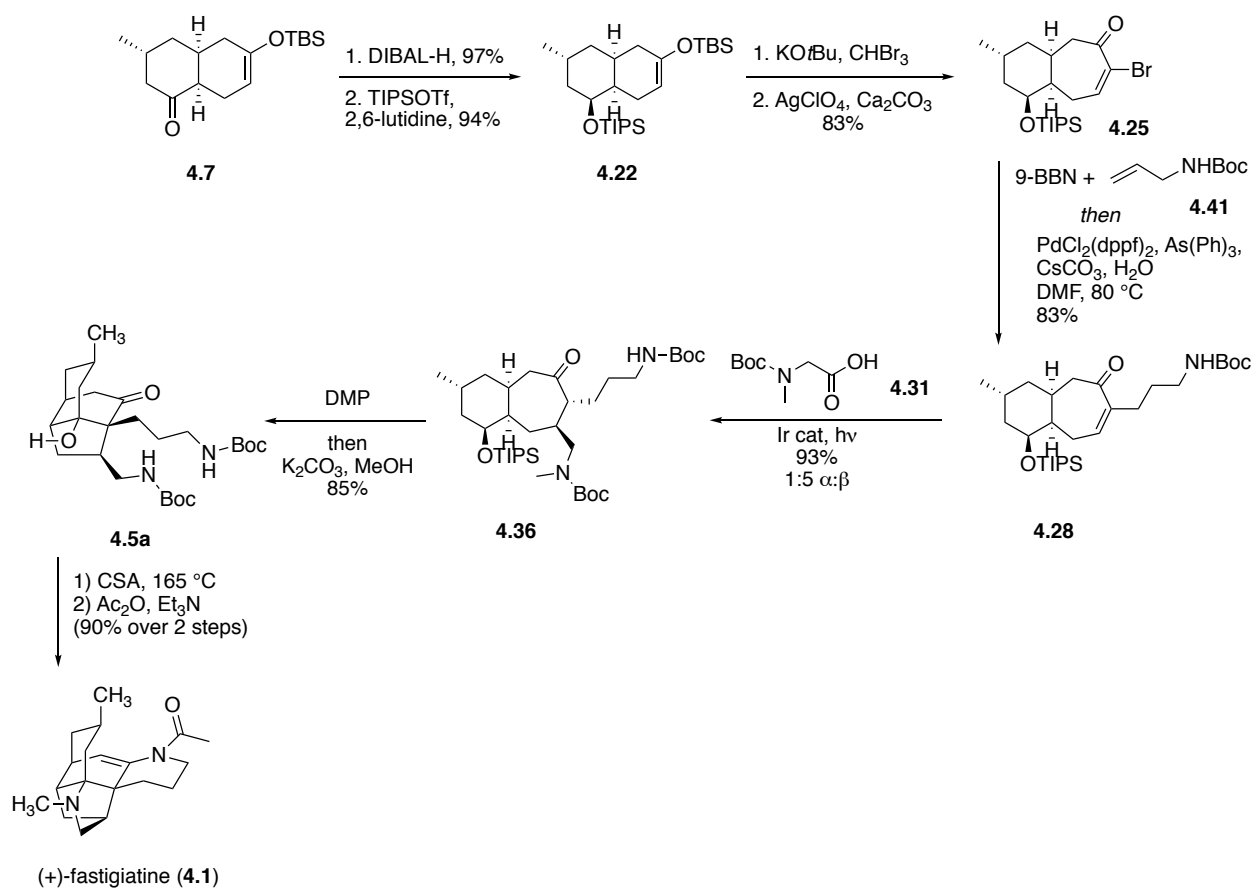
Our optimized conditions provided deprotection of the TIPS and TBS ethers **4.36** and **4.34** in X and X% yield, respectively. Generation of known tricycle **4.5a** was performed with a one-pot oxidation-aldol sequence, which provided confirmation that the major diastereomer of the conjugate addition was in fact the desired product. Generation of the epimer **4.5b** through the α -TBS alcohol **4.38** also confirmed that the α -TBS alcohol generated the undesired diastereomer in the conjugate addition step.

Table 4.4: Screening of various hydride sources for the reduction of decalone **4.7**.

entry	hydride source	ratio of reduction products		
		4.20	4.15	4.40
1	NaBH ₄	1.5	1	0
2	LiAlH(OC ₄ H ₉) ₃	3	1	0
3	L-Selectride	0	1	11
4	DIBAL-H	16	0	0

Our work during the conjugate addition studies confirmed that the axial β -alcohol was our desired epimer. Fortunately, careful selection of the hydride source allowed us to control the amount of equatorial vs axial alcohol (Table 4.3). Interestingly, while no side products were observed with treatment of decalone **4.7** with NaBH₄ or LiAlH(OC₄H₉)₃, treatment with L-Selectride induced a spontaneous transannular cyclization of the axial alcohol onto the enoxysilane, producing the caged tricyclic ketal **4.40** (Table 4.3). Reduction of decalone **4.7** with DIBAL-H provided an excellent 16:1 dr. While reduction with DIBAL-H provided a mixture of **4.20** and **4.40**, the alcohol could be coaxed into cyclization through extended stirring of the quenched reaction mixture. We were concerned that formation of the ketal **4.40** would present issues in later steps due to the possibility of reopening the ketal to two possible alkene regioisomers. Fortunately, treatment of ketal **4.40** with excess silyl triflate in the presence of 2,6-lutidine opened the ketal, affording excellent yields of the desired protected alcohols **4.21** or **4.22** as a single regioisomer. Interestingly, protection of the C13 alcohol was significantly faster when the caged ketal was reopened compared to the rate of protection on the free alcohol (0.25–2 hours vs overnight). The protected alcohols **4.21** and **4.22** were also much cleaner and could be carried on to subsequent steps without purification.

Scheme 4.7: Overall route for 2nd-generation (+)-fastigiatine synthesis.



4.4 Conclusions

Our 2nd-generation synthetic route of (+)-fastigiatine readily provides gram-scale quantities of late stage intermediates. We have also successfully resolved the low-yielding steps that plagued our original synthesis, improving both the yield and the diastereoselectivity of our synthesis. The finding that reduction of the C13 carbonyl, and thus removal of the acidic α -proton, allowed us to improve the yield of ring expansion and cross coupling step was critical in allowing us to bring forward gram-scale quantities of material. This allowed us to readily test our hypothesis regarding the ability to induce a ring flip and block the undesired face during the conjugate addition step. By switching from an organocuprate to a photochemical conjugate

addition, we could not only boost the yield, but the practicality of this transformation as well. We were also gratified to discover that formation of the caged tricycle **4.40** allowed us to access protected alcohols **4.21** and **4.22** in higher yields and purities. Our lab is currently utilizing our discoveries on this project in the syntheses of other members of the *Lycopodium* alkaloids.

4.5 Experimental Contributions

Initial work for this project was performed by Dr. Renzo Samame. Gregory Suryn and Jacob DeForest carried the project forward to fruition. Gregory Suryn performed most of the optimization and early sequence reactions, while Jacob DeForest was crucial in the late stage transformations.

4.6 Experimental

I. General experimental and laboratory conditions

All glassware was flame- or oven-dried and cooled under argon unless otherwise stated. All reactions and solutions were conducted under argon unless otherwise stated. All commercially available reagents were used as received, unless otherwise stated. Toluene (PhMe), tetrahydrofuran (THF), dimethylformamide (DMF), diethyl ether (Et₂O) and dichloromethane (CH₂Cl₂) were degassed and dried by filtration through activated alumina under vacuum according to the procedure by Grubbs.²⁸ Diisopropylamine (DIPA), acetonitrile (MeCN), 1,3-Dimethyl-3,4,5,6-tetrahydro-2-pyrimidinone (DMPU) were distilled from CaH₂ prior to use. All reactions involving LiDBB were conducted with glass stirbars. Thin layer chromatography (TLC) was performed with Millipore 60 F₂₅₄ glass-backed silica gel plates and visualized using potassium permanganate, Dragendorff-Munier, ceric ammonium molybdate (CAM) or vanillin

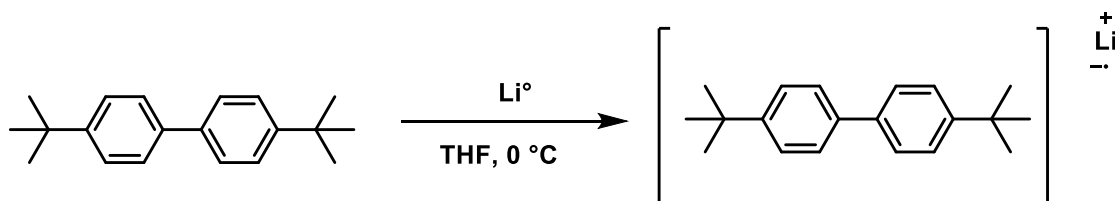
stains. Flash column chromatography was performed according to the method by Still, Kahn, and Mitra²⁹ using Millipore Geduran Silica 60 (40-63 μm).

II. Instrumentation

All data collected at ambient temperature unless noted. ^1H NMR spectra were taken at 500 or 600 MHz, calibrated using residual NMR solvent or TMS and interpreted on the δ scale. Peak abbreviations are listed: s = singlet, d = doublet, t = triplet, q = quartet, pent = pentet, dd = doublet of doublets, ddd = doublet of doublet of doublets dt = doublet of triplets, ddt = doublet of doublet of triplets, dq = doublet of quartets, m = multiplet, app = apparent, br = broad. ^{13}C NMR spectra were taken at 125 MHz, calibrated using the NMR solvent, and interpreted on the δ scale.

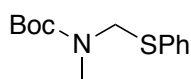
Some samples were analyzed above room temperature to minimize line broadening due to rotamers.

General procedure for preparation of LiDBB stock solution.



Experimental: A round-bottom flask equipped with a glass stir bar was charged with 4,4'-di-*tert*-butylbiphenyl (1.00 g, 3.76 mmol) and the flask was flame-dried under vacuum until 4,4'-di-*tert*-butylbiphenyl melted, at which point it was cooled to room temperature under argon. The DBB was then dissolved in THF (7.5 mL) and cooled to 0 °C. Lithium wire (365 mg, 52.6 mmol, 14 equiv) was rinsed and cut into small pieces in a 20 mL scintillation vial filled with hexanes. Several pieces of lithium were also scraped with a razor to ensure a fresh surface before transferring to the DBB solution. Dry THF was added and the solution vigorously stirred to give a dark green solution within 2-3 min. The mixture was stirred for 5 h at 0 °C to produce lithium di-*tert*-butylbiphenyl (LiDBB) at full molarity (0.4 M).

***tert*-butyl methyl((phenylthio)methyl)carbamate (4.30):**



4.30

Experimental: Dry toluene (149 mL) was added to a 500 mL round-bottom flask containing *tert*-butyl methyl carbamate (5.86 g, 0.044 mol, 1 equiv), paraformaldehyde (1.55 g, 0.051 mol, 1.15 equiv) and magnesium sulfate (15 g) at room temperature. After five minutes, TMSCl (16.9 mL, 0.134 mol, 3 equiv) was added dropwise via syringe. The solution was allowed to stir for 15

min, then thiophenol (5.07 mL, 0.025 mol, 1.1 equiv) was added and the resulting mixture was allowed to stir until starting material was consumed as observed by TLC. After 5 h, the crude reaction mixture was filtered, concentrated, and purified via chromatography (15% EtOAc in hexanes) to afford product **4.30** (10.62 g, 94%) as a crystalline white solid.

Physical State: Crystalline white solid.

Melting Point: 60–63 °C.

¹H NMR (500 MHz, CDCl₃, 65 °C) δ 7.49 (d, *J* = 7.0 Hz, 1H), 7.31–7.20 (m, 3H), 4.75 (s, 2H), 2.90 (s, 3H), 1.33 (s, 9H).

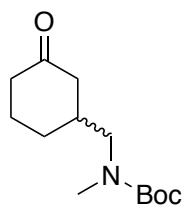
¹³C NMR (125 MHz, CDCl₃, 65 °C) δ 155.0, 134.5, 133.4, 129.0, 127.6, 80.2, 55.5, 33.3, 28.3.

IR (thin film): 2972, 2929, 1699, 1478, 1443, 1389, 1265, 1230, 1172, 1133, 1052, cm⁻¹.

HRMS (ESI) *m/z*: calculated for C₁₃H₁₉NO₂SNa (M + Na)⁺: 276.1034, found: 276.1029.

TLC: R_f = 0.42 (20% EtOAc in hexanes) (KMnO₄ stain).

***tert*-butyl methyl((3-oxocyclohexyl)methyl)carbamate (4.29):**



4.29

A round bottom flask containing **4.30** (211 mg, 0.83 mmol) and 1,10-phenanthroline (2-3 crystals) was dried by azeotroping three times with freshly distilled benzene. The flask was then equipped with a glass stir bar and THF (15 mL) was introduced under Ar. The mixture was cooled to -78 °C and *n*-BuLi/hexanes (2-3 M) was added until a brown dark color persisted (~0.3–0.4 mL). This procedure was performed to quench adventitious proton sources. LiDBB (4.7 mL, 1.86 mmol, 2.2 equiv) was then added dropwise over 10 min at -78 °C until a dark-

green color persisted, and the mixture was allowed to stir for 20 min. A separate flask containing 1-hexynyl copper (240 mg, 1.67 mmol) and tetrahydrofuran (3 mL) was cooled to $-78\text{ }^{\circ}\text{C}$ and trimethyl phosphite (0.44 mL, 3.75 mmol) was introduced; the mixture was stirred until a clear solution developed. The resulting homogeneous solution was added via syringe to the organolithium reagent down the flask wall over 3 min and stirring was continued for 1 h to produce **4.18** as deep red solution. Cyclohex-2-en-1-one (40 mg, 0.42 mmol) was dissolved in THF (0.3 mL) and freshly distilled TMSCl (263 μL , 2.08 mmol), and added to the solution containing the organocuprate. The resulting mixture was stirred at $-78\text{ }^{\circ}\text{C}$ for 24 h and quenched with 10% concentrated ammonium hydroxide/saturated ammonium chloride (20 mL), followed by warming to room temperature. After 1 h, the organic layer was separated and the aqueous layer were extracted with ethyl acetate (3 x 20 mL). The organic layers were combined, dried with Na_2SO_4 , filtered, and concentrated under vacuum. The resulting mixture was filtered through a plug silica (20% CH_2Cl_2 in hexanes) to remove excess of 4,4'-di-*tert*-butylbiphenyl, at which point ethyl acetate was used to flushed the plug. The solvent was removed under vacuum, then re-purified by column chromatography (25% EtOAc/hexanes) to afford **4.29** (89.2 mg, 89%) as a colorless oil.

Physical State: colorless oil.

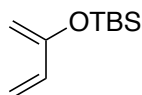
^1H NMR (500 MHz, CDCl_3) δ 3.24–3.03 (m, 2H), 2.84–2.74 (m, 3H), 2.39–2.28 (m, 2H), 2.27–2.18 (m, 1H), 2.11–1.90 (m, 3H), 2.67 (s, 3H), 1.88–1.75 (m, 1H), 1.67–1.53 (m, 1H), 1.40 (s, 9H), 1.38–1.27 (m, 1H).

^{13}C NMR (125 MHz, CDCl_3) δ 211.3, 210.9, 156.2, 155.8, 79.8, 79.6, 54.5, 53.9, 45.8, 45.7, 41.5, 38.5, 38.1, 35.2, 29.1, 28.5, 25.3, 25.2.

HRMS (ESI) m/z : calculated for $\text{C}_{13}\text{H}_{23}\text{NO}_3\text{Na}$ ($\text{M} + \text{Na}$) $^+$: 264.1576, found: 264.1572.

TLC: $R_f = 0.33$, (25 % EtOAc in Hexanes, CAM stain).

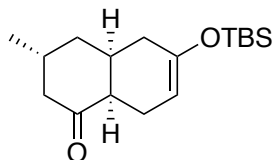
(buta-1,3-dien-2-yloxy)(*tert*-butyl)dimethylsilane (4.42):



4.42

Experimental: A one-liter round bottom was charged with diisopropylamine (19.9 mL, 142 mmol) and THF (225 mL), and cooled to 0 °C. Once cool, nBuLi (2.3 M, 61.8 mL, 142.25 mmol) was added via cannula. The mixture was stirred for 10 minutes, then cooled down to -78 °C. Once cool, a solution of methyl vinyl ketone (10.71 mL, 128.5 mmol) in THF (250 mL) was added dropwise over 30 minutes via cannula. After addition was complete, the mixture was allowed to stir for ten minutes, then DMPU (9.0 mL, freshly distilled over CaH₂) was added dropwise over 5-10 minute period, and stirred for 10 minutes. Next, a solution of TBSCl (29.0 g, 192.75 mmol) in THF (90 mL) was added via cannula over 30 minutes. After the addition was complete, the reaction mixture was warmed to 0 °C and stirred for 20 minutes, then warmed to room temperature and stirred for 3 hours. Upon completion, the reaction was diluted with pentane (250 mL) and 1M acetic acid (250 mL). The layers were separated, and the aqueous layer extracted with pentane (150 mL). The organics were combined and washed with H₂O (2 x 100 mL) and brine (1 x 200 mL), and dried with Na₂SO₄, filtered, and concentrated under reduced pressure to afford a pale yellow oil. Purification by chromatography (100% pentane) afforded the desired diene **4.42** (8.0 g, 34%) as a clear, colorless oil. The spectral data matched those reported in the literature.^{1,2}

Decalone (4.7):



4.7

Experimental: A round-bottom flask was charged with (+)-5-methylcyclohex-2-en-1-one (**4.4**) (2.01 g, 18.26 mmol) and 2-*tert*-butyldimethylsiloxy-1,3-butadiene (**4.42**) (4.68 g, 25.44 mmol) and purged 4 times via vacuum/argon cycles. Dry toluene (75 mL) was added and the solution was cooled to 0 °C. Diethyl aluminum chloride (19.1 mL, 1.0 M in toluene, 19.1 mmol) was then added dropwise over a 10 min period. The resulting mixture was allowed to reach room temperature with stirring. After 1.5 h, the mixture was cooled to 0 °C and quenched by the rapid addition of sat. aq. NaHCO₃ (250 mL) and 10% potassium sodium tartrate (20 mL). The aqueous layer was separated and extracted with Et₂O (3 x 200 mL). The combined organic layers were washed with saturated NaHCO₃ (3 x 200 mL), brine (3 x 200 mL), dried over Na₂SO₄ and concentrated under reduced pressure. Volatile materials were removed under high vacuum (ca. 1 Torr) overnight to afford the desired product **4.7** (4.91 g, 91%) as light yellow oil. If desired, product can be purified by column chromatography (10% EtOAc/hexanes).

Physical State: Viscous, colorless oil

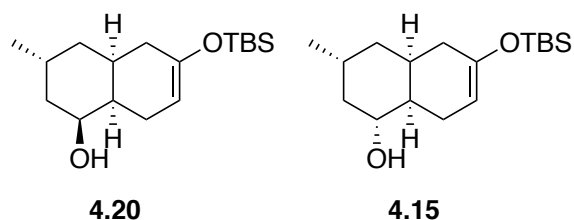
¹H NMR (500 MHz, CDCl₃) δ 4.81–4.78 (m, 1H), 2.61 (t, *J* = 5.8 Hz, 1H), 2.57–2.48 (m, 2H), 2.39 (ddd, *J* = 13.5, 4.8, 2.0 Hz, 1H), 2.25–2.17 (m, 1H), 2.20–1.95 (m, 2H), 1.86 (app. dd, *J* = 8.0, 1.5 Hz, 2H), 1.80 (d, *J* = 14.5 Hz, 1H), 1.64 (ddd, *J* = 13.5, 11.5, 4.0 Hz, 1H), 1.03 (d, *J* = 6 Hz, 3H), 0.89 (s, 9H), 0.11 (s, 3H), 0.08 (s, 3H).

¹³C NMR (125 MHz, CDCl₃) δ 211.1, 148.2, 102.0, 49.7, 47.0, 38.2, 36.1, 31.9, 30.8, 25.9, 22.6, 22.2, 18.1, -4.1, -4.4.

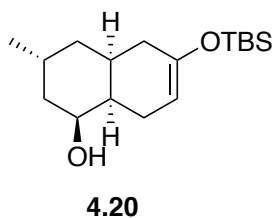
HRMS (ESI) *m/z* calculated for C₁₇H₃₁O₂Si (M + H)⁺: 295.2093, found: 295.2095.

TLC: $R_f = 0.60$ (10% EtOAc in hexanes, CAM Stain).

β -decalin alcohol (4.20) and α -decalin alcohol (4.15):



Experimental: To a solution of decalone **4.7** (2.95 g, 10.03 mmol) in absolute ethanol (33 mL, 0.3 M) at 0 °C was added sodium borohydride (1.89 g, 50.13 mmol) in three portions over 30 minutes. Upon completion as observed by TLC, the reaction mixture was partitioned between EtOAc (50 mL) and H₂O (50 mL) and allowed to reach room temperature. The organic layer was separated and the aqueous layer was extracted with EtOAc (3 x 50 mL). The combined organic layers were washed with brine, dried over Na₂SO₄ and concentrated *in vacuo* to give a colorless oil. Purification by column chromatography (10% EtOAc in hexanes) afforded a mixture of separable diastereomers **4.20** and **4.15** (2.79 g, 94%) as yellow oil (~1.4:1 *ax/eq* mixture of C13 epimers).



¹H NMR (500 MHz, CDCl₃) δ 4.86 (app s, 1H), 3.99 (app s, 1H), 2.41–2.27 (m, 1H), 2.22–2.13 (m, 1H), 2.12–2.01 (m, 4H), 1.98–1.87 (m, 1H), 1.85–1.73 (m, 1H), 1.65–1.67 (m, 1H), 1.27–1.12 (m, 1H), 0.94 (d, $J = 6.5$ Hz, 3H), 0.91 (s, 9H), 0.12 (d, $J = 5.1$ Hz, 6H).

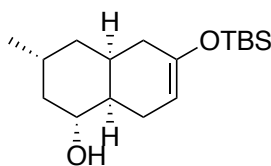
^{13}C NMR (125 MHz, CDCl_3) δ 151.8, 102.1, 72.8, 39.7, 37.2, 34.9, 31.0, 26.0, 21.6, 18.2, -4.1, -4.2.

IR (thin film) 3393, 2926, 2856, 1674, 1462, 1378, 1250, 1192, 1176, 1084, 1013, 881, 834, 777, 679 cm^{-1} .

HRMS (ESI) m/z calculated for $\text{C}_{17}\text{H}_{32}\text{O}_2\text{SiNa}$ ($\text{M} + \text{Na}$) $^+$: 319.2069, found: 319.2061.

TLC: 0.41 (10% EtOAc in hexanes, CAM Stain).

$[\alpha]_D^{24} = +29$ (c 2.94, CHCl_3).



^1H NMR (500 MHz, CDCl_3) δ 4.77 (app d, $J = 5.7$ Hz, 1H), 3.57 (ddd, $J = 15.2, 10.6, 4.5$ Hz, 1H), 2.42 (dd, $J = 17.6, 5.8$ Hz, 1H), 2.23–2.16 (m, 1H), 2.15–2.08 (m, 1H), 1.98 (app d, $J = 11.6$ Hz, 2H), 1.86–1.76 (m, 2H), 1.52 (d, $J = 14.0$, 2H), 1.45 (ddd, $J = 10.9, 5.4$ Hz, 1H), 1.31–1.24 (br s, 1H), 1.18 (td, $J = 13.3, 4.8$ Hz, 1H), 0.93 (d, $J = 6.6$ Hz, 3H), 0.91 (s, 9H), -0.12 (d, $J = 5.8$ Hz, 6H).

^{13}C NMR (125 MHz, CDCl_3) δ 141.1, 101.7, 67.7, 54.1, 45.1, 41.8, 39.1, 33.7, 31.7, 26.6, 25.9, 24.2, 22.5, 18.2, -4.1, -4.3.

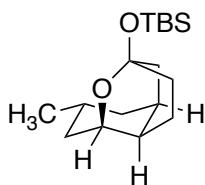
IR (thin film) 3373, 2926, 1701, 1666, 1513, 1463, 1365, 1250, 1171, 1103, 1058, 835, cm^{-1} .

HRMS (ESI) m/z calculated for $\text{C}_{17}\text{H}_{32}\text{O}_2\text{SiNa}$ ($\text{M} + \text{Na}$) $^+$: 319.2069, found: 319.2076.

TLC: $R_f = 0.31$ (10% EtOAc in hexanes, CAM stain).

$[\alpha]_D^{24} = -4.0$ (c 1.57, CHCl_3).

Caged tricyclic ketal (4.40):

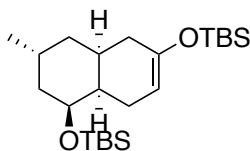


4.40

Experimental: Decalone **4.7** (692 mg, 2.35 mmol) was dissolved in DCM (7.83 mL) and cooled to $-78\text{ }^{\circ}\text{C}$. In a separate flask, DIBAL-H (1M in PhMe, 8.23 mL, 8.23 mmol) was cooled to $-78\text{ }^{\circ}\text{C}$. Once cool, the DIBAL-H was added dropwise to the decalone solution, and the resulting mixture stirred for 24 hours. Upon completion, sat. aq. Rochelles salt (20 mL) and NaHCO_3 (20 mL) was added, followed by additional DCM (20 mL). The mixture was warmed to room temperature, and stirred vigorously for 1 hour. The layers were separated, and the aqueous layer extracted with DCM (3 x 50 mL). The organic layers were combined, dried over Na_2SO_4 , filtered, and concentrated. Purification by column chromatography (10% EtOAc:hexanes) afforded **4.40** as a white solid (675 mg, 97%).

Physical state: White solid.

β -TBS alcohol (4.22):



4.22

To a solution of **4.20** (1.48 g, 5.0 mmol) in CH_2Cl_2 (7.1 mL) at $-78\text{ }^{\circ}\text{C}$ was added 2,6-lutidine (1.16 mL, 9.98 mmol, 2 equiv), followed by dropwise addition of neat TBSOTf (1.38 mL, 5.99

mmol, 1.2 equiv). The mixture was stirred for 8 h, and the reaction was quenched by the addition of Et₃N (0.84 mL, 5.99 mmol, 1.2 equiv) then NaHCO₃ (15 mL) at -78 °C. The solution was warmed to room temperature, where the organic layer was separated and the aqueous layer was extracted with CH₂Cl₂ (3 x 15 mL). The combined organic layers were washed with brine, dried over Na₂SO₄ and concentrated *in vacuo* to give a yellow oil. Purification by column chromatography (5% CH₂Cl₂ in hexanes) gave product **4.22** (1.98 g, 97%) as a clear oil.

Physical State: Clear, colorless oil.

¹H NMR (500 MHz, CDCl₃) δ 4.77 (s, 1H), 3.94 (dt, *J* = 8.9, 4.2, 1H), 2.23–2.12 (m, 1H), 2.09–1.98 (m, 4H), 1.88–1.78 (br. s, 2H), 1.69 (ddd, *J* = 13.9, 9.5, 5.1 Hz, 1H), 1.61 (ddd, *J* = 14.1, 10.5, 4.7 Hz, 1H), 1.28 (dt, *J* = 13.6, 3.8 Hz, 1H), 1.06 (dt, *J* = 13.3, 4.1 Hz, 1H), 0.97 (d, *J* = 7.3 Hz, 3H), 0.90 (s, 9H), 0.86 (s, 9H), 0.11 (s, 6H), 0.01 (s, 6H).

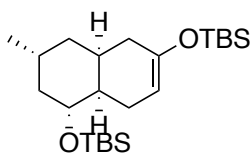
¹³C NMR (125 MHz, CDCl₃) δ 151.2, 149.2, 109.7, 102.3, 68.5, 41.3, 38.7, 36.0, 35.5, 34.8, 30.6, 30.4, 28.3, 26.13, 26.06, 25.9, 20.5, 18.9, 18.4, 18.32, 18.26, 18.2, 15.9, 7.03, 6.98, 5.3, -4.0, -4.3, -4.4, -4.5, -4.6.

IR (thin film) 2955, 2911, 1673, 1461, 1360, 1255, 1180, 1152, 1097, 1068, 1005, 963, 892, 859, 835, 773, 745 cm⁻¹.

HRMS (ESI) *m/z* calculated for C₂₃H₄₆O₂Si₂H (M + H)⁺: 411.3115, found: 411.3128.

TLC: R_f = 0.36 (5% CH₂Cl₂ in hexanes, CAM stain).

α-TBS alcohol (4.16):



4.16

Experimental: To a solution of **4.15** (286 mg, 0.97 mmol) in CH₂Cl₂ (1.4 mL) at -78 °C was added 2,6-lutidine (0.22 mL, 1.93 mmol, 2 equiv) followed by dropwise addition of neat TBSOTf (0.29 mL, 1.26 mmol, 1.3 equiv). The mixture was stirred for 7 h, at which point the reaction was quenched through addition of Et₃N (0.17 mL, 1.26 mmol, 1.3 equiv) then NaHCO₃ (5 mL) at -78 °C. The solution was warmed to room temperature, where the organic layer was separated and the aqueous layer was extracted with CH₂Cl₂ (3 x 5 mL). The combined organic layers were washed with brine, dried over Na₂SO₄ and concentrated *in vacuo* to give a yellow oil. Purification by column chromatography (5% CH₂Cl₂ in hexanes) gave the product **4.16** (364 mg, 92%) as a clear oil.

Physical State: Clear, colorless oil.

¹H NMR (500 MHz, CDCl₃) δ 4.76–4.72 (m, 1H), 3.58–3.50 (m, 1H), 2.37 (dd, *J* = 16.2, 5.6 Hz, 1H), 2.21–2.13 (m, 2H), 2.06–1.93 (m, 2H), 1.88–1.72 (m, 3H), 1.52–1.45 (m, 2H), 1.15 (td, *J* = 12.8, 4.5 Hz, 1H), 1.00–0.95 (m, 6H), 0.94–0.85 (m, 16H), 0.70–0.62 (m, 4H), 0.12 (d, *J* = 9.3 Hz, 2H), 0.03 (s, 6H).

¹³C NMR (125 MHz, CDCl₃) δ 149.0, 102.2, 101.6, 68.4, 45.4, 41.8, 39.2, 33.7, 31.7, 26.5, 26.1, 25.9, 24.4, 22.6, 18.3, 18.2, 7.0, 5.2, -3.9, -4.0, -4.3, -4.5, -4.6.

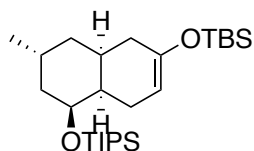
IR (thin film) 2954, 2910, 1670, 1461, 1362, 1250, 1170, 1100, 1090, 1065, 1001, 961, 895, 831, 771, 744 cm⁻¹.

HRMS (ESI) *m/z* calculated for C₂₃H₄₆O₂Si₂H (M + H)⁺: 411.3115, found: 411.3132.

TLC: R_f = 0.24 (5% CH₂Cl₂ in hexanes, CAM stain).

[α]_D²⁴ = -8.0 (*c* 1.80, CHCl₃).

β-TIPS alcohol (4.23):



4.23

Experimental: To a solution of ketal **4.20** (470 mg, 1.59 mmol) in DCM (5.3 mL) was added 2,6-lutidine (0.56 mL, 4.77 mmol) at room temperature, and the mixture cooled to -78 °C. Once cool, neat TIPSOTf (0.855 ml, 3.18 mmol) was added dropwise with vigorous stirring. The reaction was stirred for 20 minutes, at which point sat. aqueous NaHCO₃ (10 mL) was added, and the reaction allowed to warm to room temperature. The layers were then separated, and the aqueous layer extracted with DCM (3 x 20 mL), the organic layers combined, dried with Na₂SO₄, and concentrated in vacuo. The crude oil was then placed under hi-vac overnight to afford pure **4.23** as a clear, colorless oil (675 mg, 94%).

¹H NMR (500 MHz, CDCl₃) δ 4.84 (app t, *J* = 2.5 Hz, 1H), 4.10 (dt, *J* = 11.5, 4.5 Hz, 1H) 2.35 (br d, *J* = 14.5 Hz, 1H), 2.14–1.98 (m, 5H), 1.74 (ddd, *J* = 13.2, 11.4, 5.4 Hz, 1H), 1.68–1.58 (m, 2H), 1.44 (br d, *J* = 13.1 Hz, 1H), 1.11–0.98 (m, 25H), 0.91 (s, 9H), 0.12 (d, *J* = 2.3 Hz, 6H).

¹³C NMR (125 MHz, CDCl₃) δ 148.8, 102.8, 69.7, 39.4, 35.9, 32.5, 29.3, 27.8, 26.0, 19.7, 18.37, 18.36, 18.35, 18.2, 12.6, -4.1.

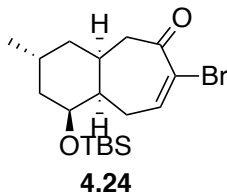
IR (thin film) 2928, 2891, 2864, 1675, 1463, 1377, 1251, 1193, 1099, 879, 834, 776 cm⁻¹.

HRMS (ESI) *m/z* calculated for C₂₆H₅₂O₂Si (M + H)⁺: 453.3584, found: 453.3579.

TLC: R_f = 0.80 (15% EtOAc in hexanes, KMnO₄ Stain).

[α]_D²⁴ = -2.67 (*c* 0.965, CHCl₃).

β-TBS bromoenone (4.24):



Experimental: To a solution of enoxysilane **4.21** (1.24 g, 3.03 mmol) in petroleum ether (16 mL, dried over MgSO_4) at $-20\text{ }^\circ\text{C}$ was added sublimed $\text{KO}t\text{-Bu}$ (1.02 g, 9.08 mmol) in one portion, followed by freshly distilled bromoform (0.79 mL, 9.08 mmol) dropwise. The reaction mixture was allowed to stir at $-20\text{ }^\circ\text{C}$ until starting material was consumed as observed by TLC. After 1h, the mixture was poured into 12 mL of water. The organic layer was separated and the aqueous layer was extracted with EtOAc (3 x 20 mL). The combined organic layers were dried over Na_2SO_4 and concentrated in vacuo. The residue was dissolved in acetone (33 mL), followed by the addition of calcium carbonate (1.51 g, 15.14 mmol) and silver perchlorate monohydrate (3.14 g, 15.14 mmol). The mixture was stirred at $25\text{ }^\circ\text{C}$ overnight, during which time a dark precipitate developed. The next morning, the reaction was quenched by the addition of Et_3N (2.11 mL, 15.14 mmol) and silica gel (~1.0 g), and the mixture concentrated in vacuo. The resulting crude mixture was vacuum filtered through a plug of silica using Et_2O as the eluent. Evaporation of the solvent, followed by subsequent re-purification by column chromatography (10% EtOAc in hexanes) gave the product **4.24** (0.96 g, 82%) as a pale yellow oil.

Physical State: Pale yellow oil.

$^1\text{H NMR}$ (500 MHz, CDCl_3) δ 7.23 (dd, $J = 9.8, 4.8$ Hz, 1H), 3.89–3.84 (m, 1H) 3.05 (dd, $J = 15.5, 11.0$ Hz, 1H), 2.58 (ddd, $J = 15.7, 11.1, 4.7$ Hz, 1H), 2.51 (dd, $J = 16.0, 3.0$ Hz, 1H), 2.37 (ddd, $J = 15.8, 9.7, 4.3$ Hz, 1H), 2.24–2.1(m, 1H), 1.95–1.85 (m, 1H), 1.80 (dt, $J = 10.3, 4.4$ Hz, 1H), 1.70–1.62 (m, 1H), 1.56 (dt, $J = 13.7, 3.9$ Hz, 1H), 1.31 (ddd,

$J = 13.8, 9.0, 5.3$ Hz, 1H), 1.20 (ddd, $J = 12.0, 8.8, 2.8$ Hz, 1H), 0.91 (d, $J = 7$ Hz, 3H), 0.85 (s, 9H), 0.02 (s, 3H), -0.02 (s, 3H).

$^{13}\text{C NMR}$ (125 MHz, CDCl_3) δ 197.8, 145.9, 125.6, 69.9, 47.0, 40.7, 40.4, 38.6, 31.0, 28.1, 26.0, 23.4, 21.1, 18.1, -4.4, -4.8.

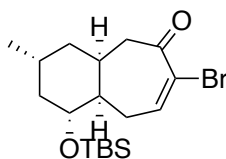
IR (thin film) 2952, 2926, 2852, 1681, 1462, 1253, 1059, 834, 735 cm^{-1} .

HRMS (ESI) m/z calculated for $\text{C}_{18}\text{H}_{31}\text{BrO}_2\text{Si}$ ($\text{M} + \text{NH}_4$) $^+$: 404.1620, found: 411.1613.

TLC: $R_f = 0.34$ (40% CH_2Cl_2 in hexanes, CAM Stain).

$[\alpha]_D^{24} = +45$ (c 0.9, CHCl_3).

α -TBS bromoenone (**4.17**):



4.17

Experimental: To a solution of enoxysilane **4.16** (364 g, 0.89 mmol) in petroleum ether (4.7 mL, dried over MgSO_4) at -20 $^\circ\text{C}$ was added sublimed $\text{KO}t\text{-Bu}$ (297 mg, 2.66 mmol) in one portion, followed by freshly distilled bromoform (0.23 mL) dropwise. The reaction mixture was allowed to stir at -20 $^\circ\text{C}$ until starting material was consumed as observed by TLC. After 1.5 h, the mixture was poured into water (5 mL). The organic layer was separated and the aqueous layer was extracted with EtOAc (3 x 5 mL). The combined organic layers were combined, dried over Na_2SO_4 , filtered, and concentrated in vacuo. The residue was dissolved in acetone (9.9 mL), followed by the addition of calcium carbonate (444 mg, 4.44 mmol) and silver perchlorate monohydrate (3.14 g, 15.14 mmol). The mixture was stirred at 25 $^\circ\text{C}$ overnight, during which time a dark precipitate developed. The next morning, the reaction was quenched by the addition

of Et₃N (0.62 mL, 4.44 mmol) and silica gel (~0.5 g), and the mixture concentrated in vacuo.

The resulting solids were vacuum filtered through a plug of silica using Et₂O as the eluent.

Evaporation of the solvent, followed by subsequent re-purification by column chromatography (10% EtOAc in hexanes) gave bromoenone **4.17** (311 mg, 91%) as a pale yellow oil.

Physical State: Pale yellow oil.

¹H NMR (500 MHz, CDCl₃) δ 7.16 (dd, *J* = 9.3, 6.2 Hz, 1H), 3.47 (td, *J* = 10.6, 4.4 Hz, 1H), 2.78 (ddd, *J* = 15.3, 9.0, 5.8 Hz, 1H), 2.63 (dd, *J* = 17.0, 11.0 Hz, 1H), 2.46 (app d, 15.5 Hz, 1H), 2.33–2.26 (m, 1H), 2.09 (ddd, *J* = 14.9, 10.3, 6.3 Hz, 1H), 1.85–1.79 (m, 1H), 1.73 (tt, *J* = 9.5, 6.3 Hz, 1H), 1.57 (dd, *J* = 13.5, 2.0 Hz, 1H), 1.51–1.39 (m, 1H), 1.30–1.19 (m, 2H), 1.06 (q, *J* = 11.7 Hz, 1H), 0.91 (d, *J* = 6.5 Hz, 1H), 0.88 (s, 9H), 0.06 (s, 3H), 0.04 (s, 1H).

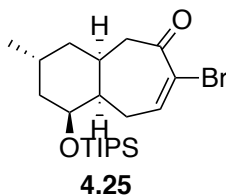
¹³C NMR (125 MHz, CDCl₃) δ 197.7, 143.9, 126.0, 73.6, 45.4, 44.2, 41.6, 40.6, 32.8, 32.3, 26.9, 26.0, 22.3, 18.2, -3.6, -4.5.

IR (thin film) 2957, 2925, 2852, 1681, 1456, 1253, 1101, 1064, 834, 772 cm⁻¹.

HRMS (ESI) *m/z* calculated for C₁₈H₃₁BrO₂Si (M + NH₄)⁺: 404.1620, found: 411.1623.

TLC: R_f = 0.28 (40% CH₂Cl₂ in hexanes, CAM Stain).

β-TIPS bromoenone (4.25):



Experimental: To a solution of enoxysilane **4.22** (675 mg, 1.49 mmol) in petroleum ether (7.45 mL, dried over MgSO₄) at -40 °C was added sublimed KO^t-Bu (502 mg, 4.47 mmol) in one portion, followed by freshly distilled bromoform (0.39 mL, 4.47 mmol) dropwise. The reaction

mixture was allowed to stir at $-40\text{ }^{\circ}\text{C}$ until starting material was consumed as observed by TLC. Once complete, the reaction mixture filtered through celite, and washed with excess petroleum ether. The mixture was then transferred to a separator funnel, and washed with 20 mL of water. The organic layer was dried over Na_2SO_4 and concentrated under vacuo. The residue was dissolved in acetone (7.45 mL), to this solution was added calcium carbonate (745 mg, 7.45 mmol) and silver perchlorate monohydrate (1.54 g, 7.45 mmol), and the mixture was stirred at $25\text{ }^{\circ}\text{C}$ overnight, during which time a dark precipitate developed. The mixture was quenched by the addition of Et_3N (1.04 mL, 7.45 mmol) and silica gel ($\sim 1.0\text{ g}$), and the mixture concentrated under vacuo. The resulting crude mixture was flushed through a plug of silica using Et_2O . Purification by column chromatography gave the product **4.25** (475 mg, 75%) as a yellow oil.

Physical State: yellow oil.

$^1\text{H NMR}$ (500 MHz, CDCl_3) δ 7.33 (dd, $J = 9.8, 3.6\text{ Hz}$, 1H), 4.09 – 4.03 (m, 1H), 2.74 – 2.60 (m, 3H), 2.42 (ddd, $J = 17.1, 10.5, 3.5\text{ Hz}$, 1H), 2.28 (ddt, $J = 14.6, 9.7, 5.0\text{ Hz}$, 1H), 2.04 (m, 1H), 1.93 (m, 1H), 1.63 – 1.56 (m, 1H), 1.48 (ddd, $J = 13.8, 9.5, 4.5\text{ Hz}$, 1H), 1.44 – 1.28 (m, 3H), 1.03 (s, 17H), 0.97 (app d, $J = 7.4\text{ Hz}$, 5H).

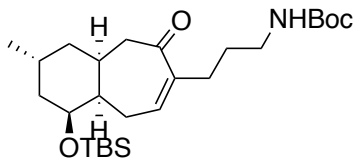
$^{13}\text{C NMR}$ (126 MHz, CDCl_3) δ 196.6, 148.2, 125.8, 68.5, 48.2, 44.6, 38.0, 35.7, 30.6, 25.8, 25.7, 19.5, 18.20 (3C), 18.16 (3C), 12.5 (3C).

HRMS (ESI) m/z calculated for $\text{C}_{21}\text{H}_{37}\text{BrO}_2\text{SiNa}$ ($\text{M} + \text{Na}$) $^+$: 451.1644, 453.1626, found 451.1624, 453.1604.

IR (thin film): 2891, 2866, 1689, 1462, 882 cm^{-1} .

$[\alpha]_{\text{D}}^{23} = +23.8$ (c 1.0, CHCl_3).

β -TBS enone (4.27):



4.27

Experimental: All solvents were subjected to *three* freeze-pump-thaw cycles before use in this reaction, and were used within one week. To a solution of *tert*-butyl allylcarbamate **4.41** (239 mg, 1.51 mmol) in THF (2.5 mL) was added a solution of 9-BBN (0.5 M in THF, 4.3 mL, 2.13 mmol) at room temperature. After stirring for 4 h, the solution was treated with water (365 μ L, 20.25 mmol) and stirred for 20 min. In a separate Schlenk flask was added bromo enone **4.24** (391 mg, 1.01 mmol), Cs₂CO₃ (725 mg, 2.23 mmol), AsPh₃ (124 mg, 0.41 mmol), and Pd(dppf)Cl₂ (296 mg, 0.41 mmol), and the atmosphere purged via high-vacuum/argon cycles (4x) before addition of DMF (6.5 mL). The resulting mixture was then stirred for 15 min before the borane solution was added in one portion. The reaction was heat to 80 °C, at which point the mixture turned black. After heating for 4 hours, the reaction was cooled to room temperature, diluted with Et₂O (15 mL), and filtered through a plug of neutral alumina. Concentration in vacuo followed by purification via flash column chromatography (15% EtOAc in hexanes) afforded enone **4.27** (419 mg, 89%) as a colorless oil.

Physical State: colorless oil.

¹H NMR (500 MHz, CDCl₃) δ 6.39–6.21 (m, 1H), 4.80–4.55 (br. s, 1H), 3.88–3.83 (m, 1H), 3.09–3.02 (br. s, 2H), 2.91–2.84 (m, 1H), 2.52–2.42 (m, 1H), 2.33–2.27 (m, 1H), 2.26–2.21 (m, 1H), 2.20–2.10 (m, 1H), 1.94–1.86 (m, 1H), 1.73–1.67 (m, 1H), 1.65–1.60 (m, 1H), 1.56–1.49 (m, 3H), 1.41 (s, 9H), 1.31–1.23 (m, 1H), 1.21–1.14 (m, 1H), 0.91 (d, 7.0 Hz, 3H), 0.84 (s, 9H), 0.00 (s, 3H), -0.02 (s, 3H).

^{13}C NMR (125 MHz, CDCl_3) δ 206.7, 156.2, 142.5, 140.6, 79.1, 70.0, 48.6, 41.7, 40.2, 40.1, 38.3, 31.1, 29.9, 29.7, 28.6, 26.0, 25.9, 23.9, 21.0, 18.2, -4.4, -4.7.

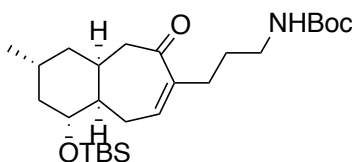
IR (thin film) 3362, 2925, 2857, 1694, 1515, 1451, 1410, 1388, 1364, 1299, 1251, 1166, 1105, 1050, 636, 775, 676 cm^{-1} .

HRMS (ESI/) m/z calculated for $\text{C}_{26}\text{H}_{47}\text{NO}_4\text{SiNa}$ ($\text{M} + \text{Na}$) $^+$: 488.3172, found: 488.3174.

TLC: R_f = 0.31 (15% EtOAc in hexanes, CAM Stain)

$[\alpha]_D^{23} = +34$ (c 0.83, CHCl_3)

α -TBS enone (4.19)



4.19

Experimental: All solvents were subjected to **three** freeze-pump-thaw cycles before use in this reaction, and were used within one week. To a solution of *tert*-butyl allylcarbamate **4.41** (131 mg, 0.830 mmol) in THF (1.4 mL) was added a solution of 9-BBN (0.50 M in THF, 2.3 mL, 1.2 mmol) at room temperature. After stirring for 4 h, the solution was treated with water (199 μL , 11.1 mmol) and allowed to stir for 20 min. A separate Schlenk flask was charged with bromo enone **4.17** (214 mg, 0.550 mmol), Cs_2CO_3 (397 mg, 1.22 mmol), AsPh_3 (50 mg, 0.17 mmol), and $\text{Pd}(\text{dppf})\text{Cl}_2$ (122 mg, 0.170 mmol), and the atmosphere was purged via high-vacuum/argon cycles (4x) before addition of DMF (3.6 mL). The resulting mixture was then stirred for 15 min before the borane solution was added. The reaction was heated to 80 $^\circ\text{C}$ for 4 hours, during which time the mixture turned black. After completion, the mixture was cooled to room temperature, diluted with Et_2O (15 mL), and filtered through a plug of neutral alumina.

Concentration in vacuo followed by purification via flash column chromatography (15% EtOAc in hexanes) afforded the desired enone **4.19** (209.0 mg, 81%) as a colorless oil.

Physical State: Clear, colorless oil

¹H NMR (500 MHz, CDCl₃) δ 6.38–6.33 (m, 1H), 4.70–4.62 (br s, 1H), 3.46 (td, *J* = 10.6, 4.4 Hz, 1H), 3.11–3.04 (m, 2H), 2.70 (ddd, *J* = 14.7, 9.8, 6.0 Hz, 1H), 2.52 (dd, *J* = 17.3, 11.6 Hz, 1H), 2.35–2.27 (m 1H), 2.26–2.19 (m, 2H), 2.17–2.09 (m, 1H), 2.01–1.93 (m, 1H), 1.82–1.76 (m, 1H), 1.67–1.59 (m, 1H), 1.58–1.50 (m, 4H), 1.43 (s, 9H), 1.22 (dt, *J* = 13.0, 5.2 Hz, 1H), 0.99 (q, *J* = 11.8 Hz, 1H), 0.90 (d, *J* = 6.6 Hz, 3H), 0.88 (s, 9H), 0.05 (s, 3H), 0.03 (s, 3H)

¹³C NMR (125 MHz, CDCl₃) δ 207.0, 156.2, 142.6, 137.8, 79.2, 74.0, 46.7, 44.4, 41.7, 40.8, 40.2, 32.9, 30.6, 30.0, 29.7, 28.6, 27.0 26.0, 22.4, 18.2, –3.6, –4.5

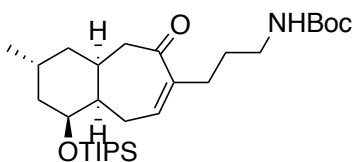
IR (thin film) 3373, 2926, 1701, 1665, 1512, 1463, 1364, 1249, 1171, 1103, 774 cm⁻¹

HRMS (ESI) *m/z* calculated for C₂₆H₄₇NO₄SiNa (M + Na)⁺: 488.3172, found: 488.3181

TLC: R_f = 0.30 (15% EtOAc in hexanes, CAM Stain)

[α]_D²³ = +22 (*c* 1.14, CHCl₃)

β-TIPS enone (4.28):



4.28

Experimental: All solvents were subjected to **three** freeze-pump-thaw cycles before use in this reaction, and were used within one week. To a solution of *tert*-butyl allylcarbamate **4.41** (61.2 mg, 0.390 mmol) in THF (0.65 mL) was added a solution of 9-BBN (0.50 M in THF, 1.09 mL, 0.550 mmol) at room temperature. After stirring for 4 h, the solution was treated with water (94

μL , 5.2 mmol) and stirred for 20 min. A separate Schlenk flask was charged with bromo enone **4.25** (111 mg, 0.260 mmol), Cs_2CO_3 (186 mg, 0.570 mmol), AsPh_3 (24 mg, 0.078 mmol), and $\text{Pd}(\text{dppf})\text{Cl}_2$ (64 mg, 0.078 mmol), and the flask purged via high-vacuum/argon cycles (4x) before addition of DMF (1.6 mL). The resulting mixture was then stirred for 15 min before the borane solution was added. The reaction was heated to 80 °C for 6 hours, during which time the mixture turned black. After completion, the mixture was cooled to room temperature, diluted with Et_2O (5 mL) and filtered through a plug of neutral alumina. Concentration in *vacuo* followed by purification via flash column chromatography (15% EtOAc in hexanes) afforded the desired enone **4.28** (90.0 mg, 69%) as a colorless oil.

Physical State: Clear, colorless oil.

^1H NMR (500 MHz, CDCl_3) δ 6.59 (dd, $J = 8.9, 2.5$ Hz, 1H), 4.70 (br s, 1H), 4.07 – 4.01 (m, 1H), 3.14 – 2.98 (m, 2H), 2.63 – 2.51 (m, 2H), 2.46 (dd, $J = 12.7, 5.6$ Hz, 1H), 2.36 – 2.29 (m, 1H), 2.28 – 2.15 (m, 3H), 2.08 – 1.99 (m, 1H), 1.87 – 1.80 (m, 1H), 1.61 – 1.50 (m, 4H), 1.43 (s, 12H), 1.36 – 1.29 (m, 2H), 1.01 (app d, $J = 3.8$ Hz, 18H), 0.97 (d, $J = 7.2$ Hz, 3H).

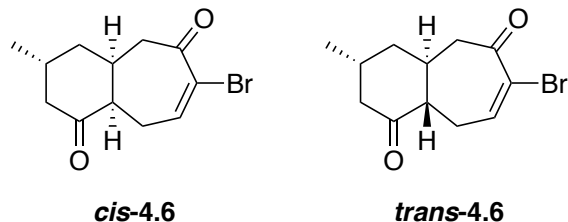
^{13}C NMR (126 MHz, CDCl_3) δ 156.1, 143.8, 143.3, 128.5, 77.4, 68.5, 49.8, 45.8, 40.0, 37.9, 35.4, 30.7, 29.9, 28.6 (3C), 26.6, 23.6, 19.4, 18.2 (6C), 12.5 (3C).

IR (thin film): 3381, 2866, 1714, 1667, 1173 cm^{-1} .

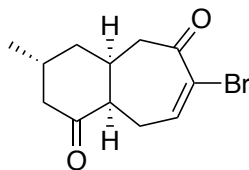
HRMS (ESI) m/z calculated for $\text{C}_{29}\text{H}_{53}\text{NO}_4\text{SiNa}$ ($\text{M} + \text{Na}$) $^+$: 530.3641, found: 530.3632.

$[\alpha]_{\text{D}}^{23} = +26.6$ (c 1.0, CHCl_3).

Bromo-enones (*cis*-4.6) and (*trans*-4.6):



Experimental: To a solution of decalone **4.7** (1.210 g, 4.120 mmol) in petroleum ether (110 mL, dried over MgSO_4) at $-20\text{ }^\circ\text{C}$ was added sublimed potassium *tert*-butoxide (1.390 g, 12.37 mmol) in 3 portions. The heterogeneous mixture turned yellow within 2 min. After 2 min, freshly distilled bromoform (1.08 mL, 12.4 mmol) was added dropwise in petroleum ether (20 mL) over 4 min. The reaction mixture was allowed to stir at $-20\text{ }^\circ\text{C}$ until starting material was consumed as observed by TLC. After 45 min, the mixture was removed from the cooling bath and filtered through a silica plug with 25% EtOAc in petroleum ether. The filtrate was concentrated under vacuum and the resulting yellow oil was dissolved in acetone (45 mL), followed by the addition of calcium carbonate (2.060 g, 20.63 mmol) and silver perchlorate monohydrate (1.850 g, 8.250 mmol). The reaction was allowed to stir at $25\text{ }^\circ\text{C}$ for 9 h, during which time a dark precipitate developed. The reaction was quenched by addition of Et_3N (1.15 mL, 8.25 mmol) and silica gel (1.5 g), and the mixture concentrated in vacuo. The resulting crude mixture was vacuum filtered through a plug of silica using Et_2O . The solvent was evaporated, and the crude material re-purified via chromatography (15% to 25% EtOAc in hexanes) to afford a mixture of diastereomers ***cis*-4.6** and ***trans*-4.6** (570.0 mg, 51%) as yellow oil ($\sim 3:1$ *cis/trans* mixture of C-12 epimers). A small sample of the mixture was purified by MPLC to separate the *cis* and *trans* isomers for characterization.



cis-4.6

Physical State: Yellow oil.

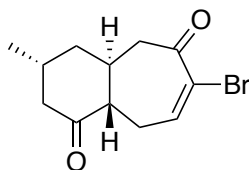
¹H NMR (500 MHz, CDCl₃) δ 7.24 (dd, *J* = 10.5, 4.8 Hz, 1H), 2.75–2.65 (m, 3H), 2.57–2.46 (m, 3H), 2.4 (dd, *J* = 16.3, 10.3 Hz, 1H), 2.07 (t, *J* = 12.8 Hz, 1H), 1.97–1.87 (m, 1H), 1.84 (dt, *J* = 13.5, 3.3 Hz, 1H), 1.75 (ddd, *J* = 14.8, 11.5, 4.3 Hz, 1H), 1.05 (d, *J* = 6.5 Hz, 1H).

¹³C NMR (125 MHz, CDCl₃) δ 209.8, 195.7, 144.1, 125.6, 49.7, 47.4, 45.3, 39.4, 34.7, 29.9, 27.0, 22.1.

IR (thin film) 3444, 2955, 2924, 1705, 1685, 1600, 1452, 1379, 1231, 1111, 1041, 916 cm⁻¹.

HRMS (ESI) *m/z* calculated for C₁₂H₁₅BrO₂Na (M + Na)⁺: 293.0153, found: 293.0161.

TLC: R_f = 0.33 (20% EtOAc in hexanes, CAM Stain).



trans-4.6

Physical State: Yellow oil.

¹H NMR (500 MHz, CDCl₃) δ 7.22 (dd, *J* = 8.3, 4.3 Hz, 1H), 2.92 (dd, *J* = 14.0, 6.0 Hz, 1H), 2.87–2.78 (m, 1 H), 2.60 (dd, *J* = 14.0, 5.5 Hz, 1H), 2.53–2.36 (m, 3H), 2.27–2.21 (m, 1H), 2.18 (d, *J* = 13 Hz, 1H), 1.94 (td, *J* = 13.0, 4.8 Hz, 1H), 1.68 (d, *J* = 14.5 Hz, 1H), 0.98 (d, *J* = 7 Hz, 1H).

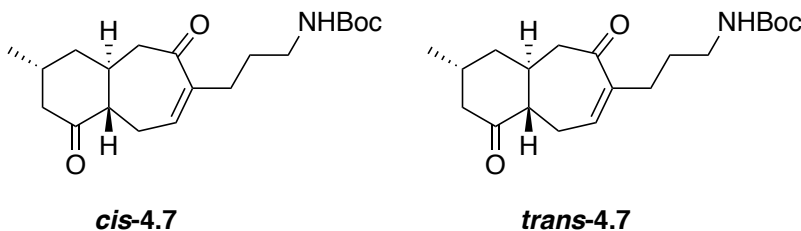
¹³C NMR (125 MHz, CDCl₃) δ 209.4, 195.3, 145.3, 125.9, 54.9, 48.0, 46.9, 38.3, 35.6, 29.8, 28.4, 20.0.

IR (thin film) 3437, 2957, 2826, 1602, 1711, 1687, 1459, 1385, 1238, 1090, 912 cm^{-1} .

HRMS (ESI) m/z calculated for $\text{C}_{12}\text{H}_{15}\text{BrO}_2\text{Na}$ ($\text{M} + \text{Na}$)⁺: 293.0153, found: 293.0161.

TLC: R_f = 0.32 (20% EtOAc in hexanes, CAM Stain).

Enones (*cis*-4.7) and (*trans*-4.7):



Experimental: All solvents were subjected to **three** freeze-pump-thaw cycles before use in this reaction, and were used within one week. To a solution of *tert*-butyl allylcarbamate **4.41** (402 mg, 2.56 mmol) in THF (4.3 mL) was added a solution of 9-BBN (0.50 M in THF, 7.2 mL, 3.6 mmol) at room temperature. After stirring for 4 h, the solution was treated with water (615 μL , 34.1 mmol) and allowed to stir for 20 min. A separate Schlenk flask was charged with bromo enone *cis*-**4.6** and *trans*-**4.6** (~3:1) (461 mg, 1.71 mmol), Cs_2CO_3 (1.22 g, 3.76 mmol), AsPh_3 (157 mg, 0.510 mmol), and $\text{Pd}(\text{dppf})\text{Cl}_2$ (375 mg, 0.510 mmol), and the flask was purged via high-vacuum/argon cycles (4x) before addition of DMF (11 mL). The resulting mixture was then stirred for 15 min before the borane solution was added in one portion. The subsequent mixture was heated to 80 $^\circ\text{C}$ for 4 hours, at which point the solution turned black. Upon completion, the reaction was cooled to room temperature, diluted with Et_2O (15 mL), and filtered through a plug of neutral alumina. Concentration *in vacuo* followed by purification via flash column chromatography (30% to 40% EtOAc in hexanes) afforded inseparable diastereomers (494.0 mg, 83%) *cis*-**4.7** and *trans*-**4.7** as a colorless oil (~ 2:3 *cis/trans* epimers at C-12).

Physical State: Colorless oil.

¹H NMR (600 MHz, CDCl₃) δ 6.50–6.40 (m, 1H), 4.67–4.55 (br s, 1H), 3.13–3.01 (app m, 2H), 2.83–2.73 (m, 1H), 2.66–2.60 (m, 0.5H), 2.59–2.54 (m, 1H), 2.49–2.40 (m, 2.5H), 2.34–2.25 (m, 2.5H), 2.20–2.11 (m, 2H), 2.03 (t, *J* = 12.5 Hz, 0.5H), 1.97–1.87 (m, 1H), 1.82–1.75 (m, 0.5H), 1.73–1.69 (m, 0.5H), 1.68–1.64 (m, 1H), 1.54 (p, *J* = 5.9 Hz, 2H), 1.42 (s, 9H), 1.02 (d, *J* = 6.5 Hz, 1.5H), 0.97 (d, *J* = 7.0, Hz, 1.5H).

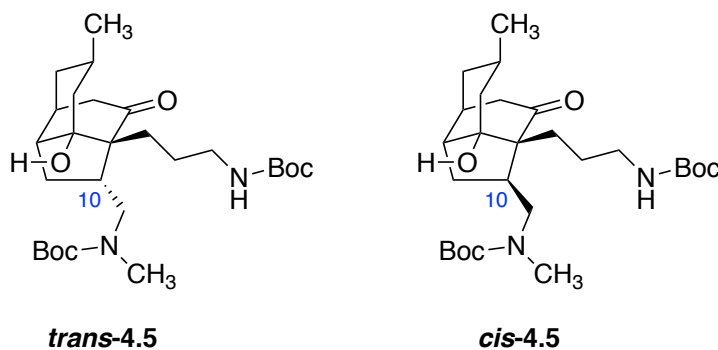
¹³C NMR (125 MHz, CDCl₃) δ 211.1, 210.5, 204.6, 204.1, 156.2, 142.6, 139.5, 138.4, 79.3, 55.6, 53.3, 49.8, 49.1, 48.0, 47.04, 46.99, 40.5, 40.1, 39.5, 39.0, 38.3, 36.0, 34.8, 30.5, 29.99, 29.97, 29.92, 29.6, 28.6, 26.7, 25.6, 22.1, 20.1.

IR (thin film) 3373, 2953, 2921, 2881, 1708, 1664, 1517, 1454, 1391, 1252, 1173, 875 cm⁻¹.

HRMS (ESI) *m/z* calculated for C₂₀H₃₁NO₄Na (M + Na)⁺: 372.2151, found: 372.2157.

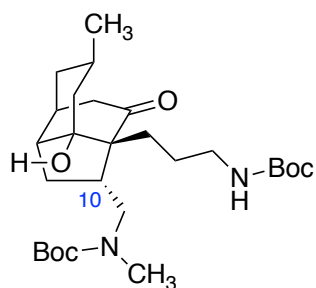
TLC: R_f = 0.32 (40% EtOAc in hexanes, CAM Stain).

Aldol tricycle (*trans*-4.5) and (*cis*-4.5):



Experimental: A round bottom flask containing **4.30** (0.620 g, 2.44 mmol) and 1,10-phenanthroline (2–3 crystals) was dried by azeotroping three times with freshly distilled benzene. The flask was then equipped with a glass stir bar and THF (27 mL) was introduced under argon. The mixture was cooled to –78 °C and *n*-BuLi (2.3M in hexanes) was added dropwise until a brown dark color persisted. This procedure was performed to quench adventitious proton sources.

LiDBB (0.4 M, 12.8 mL, 5.12 mmol) was then added dropwise over 10 min at $-78\text{ }^{\circ}\text{C}$ until a dark-green color persisted, and the mixture was allowed to stir for 20 min. In a separate flask containing 1-hexynyl copper (0.710 g, 4.94 mmol) and tetrahydrofuran (6.2 mL) was added trimethyl phosphite (1.8 mL, 15 mmol), and the mixture stirred at room temperature until a clear solution developed. The resulting homogeneous solution was chilled to $-78\text{ }^{\circ}\text{C}$, at which point it was added via syringe to the organolithium reagent down the flask wall over 3 min, and stirred for 1 h to produce **4.18** as deep red solution. The carbamate *cis*-**4.7** and *trans*-**4.7** (213 mg, 0.610 mmol) was dissolved in THF (0.5 mL), freshly distilled TMSCl (0.39 mL, 3.0 mmol) was added, then the mixture added directly to the organocuprate solution. The resulting mixture was stirred at $-78\text{ }^{\circ}\text{C}$ for 24 h, at which point it was quenched by the addition 10% concentrated ammonium hydroxide/saturated ammonium chloride (120 mL), followed by warming to room temperature. After 1 h, the organic layers were separated and the aqueous layers were extracted with ethyl acetate (3 x 40 mL). The organic layers were combined, dried with Na_2SO_4 , filtered, and concentrated under vacuum. The resulting mixture was filtered through a plug silica (20% CH_2Cl_2 in hexanes) to remove excess 4,4'-di-*tert*-butylbiphenyl, at which point ethyl acetate was used elute the remaining desired material. The ethyl acetate was subsequently evaporated, and the crude mixture taken up in methanol (15 mL). Potassium carbonate (627 mg, 4.54 mmol) was added, and the suspension mixed vigorously for 4 hr. After completion, the solids were filtered and the solvent evaporated, at which point the crude residue was purified by chromatography (20% to 40% EtOAc/hexanes gradient), to deliver tricycle *trans*-**4.7** (126.1 mg, 42%) and its C10 epimer *cis*-**4.7** (134.5 mg, 45%) as a colorless oil.



***trans*-4.5**

Physical State: Colorless oil.

¹H NMR (500 MHz, tol-d₈, 85 °C) δ 4.46–4.37 (br s, 1H), 3.42–3.27 (br s, 1H), 3.10 (m, 2H), 2.77–2.72 (m, 1H), 2.71–2.68 (m, 1H), 2.67 (s, 3H), 2.63–2.52 (m, 1H), 2.25 (ddd, $J = 13.5, 11.2, 7.6$ Hz, 1H), 2.01 (d, $J = 17.5$ Hz, 1H), 1.87 (app d, $J = 13.6$ Hz, 1H), 1.85–1.80 (m, 1H), 1.76–1.67 (m, 1H), 1.66–1.56 (m, 5H), 1.45 (s, 18H), 1.37–1.29 (m, 2H), 1.12–1.00 (br s, 1H), 0.86 (q, $J = 13.7$ Hz, 2H), 0.70 (d, $J = 6.5$ Hz, 3 H).

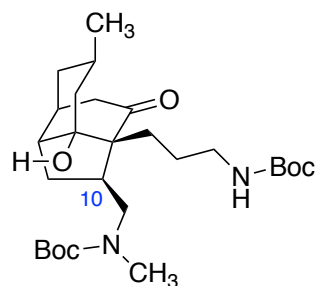
¹³C NMR (125 MHz, CDCl₃, 25 °C) δ 213.5, 213.3, 156.5, 156.3, 155.8, 80.1, 79.6, 79.3, 65.4, 48.4, 48.0, 47.1, 43.7, 43.2, 43.0, 42.7, 41.8, 41.1, 35.5, 35.3, 34.5, 34.2, 32.1, 29.9, 29.8, 29.6, 28.7, 28.6, 26.0, 25.5, 24.5, 22.9, 22.5, 14.3.

IR (thin film) 3364, 2962, 2925, 1686, 1519, 1482, 1451, 1393, 1367, 1247, 1043, 771 cm⁻¹.

HRMS (ESI) m/z calculated for C₂₇H₄₆N₂O₆Na (M + Na)⁺: 517.3254, found: 517.3261.

TLC: R_f = 0.34 (44 % EtOAc in Hexanes, CAM stain).

[α]_D²⁴ = -74 (*c* 1.23, CHCl₃).



***cis*-4.5**

Physical State: Colorless oil.

¹H NMR (500 MHz, *tol-d*₈, 85 °C) δ 4.51–4.43 (br s, 1H), 3.75 (dd, *J* = 13.3, 11.3 Hz, 1H), 3.17 (dd, *J* = 13.8, 4.3 Hz, 1H), 3.12–3.05 (m, 2H), 2.71 (s, 3H), 2.29 (dd, *J* = 16.5, 8.0 Hz, 1H), 2.17 (ddd, *J* = 12.8, 7.0, 5.3 Hz, 1H), 2.03–1.96 (m, 1H), 1.91–1.85 (m, 1H), 1.79 (d, *J* = 16.5 Hz, 1H), 1.74 (dd, *J* = 14.0, 4.5 Hz, 1H), 1.69–1.64 (m, 1H), 1.61–1.51 (m, 4H), 1.46 (s, 9H), 1.43 (s, 9H), 1.34–1.26 (m, 3H), 1.06–1.00 (br s, 1H), 0.83 (td, *J* = 12.8, 3.0 Hz, 1H), 0.73 (t, *J* = 13.0 Hz, 1H), 0.65 (d, *J* = 6.0 Hz, 3H), 0.51–0.43 (br s, 1H).

¹³C NMR (125 MHz, CDCl₃, 25 °C) δ 214.4, 214.2, 156.8, 156.4, 156.22, 83.9, 83.8, 79.75, 79.66, 79.12, 79.06, 65.2, 65.1, 52.6, 51.7, 48.0, 43.0, 42.1, 41.9, 41.3, 40.7, 35.4, 35.3, 34.9, 32.1, 31.9, 31.6, 29.9, 29.8, 29.5, 28.6, 25.6, 22.9, 22.7, 21.8, 14.3.

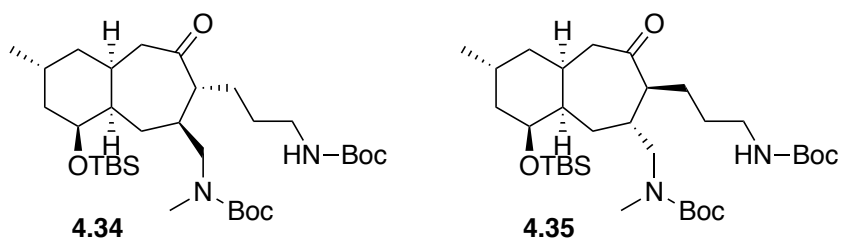
IR (thin film) 3380, 2957, 2920, 1961, 1514, 1456, 1393, 1252, 1168, 1033, 876, 771 cm⁻¹.

HRMS (ESI) *m/z* calculated for C₂₇H₄₆N₂O₆Na (M + Na)⁺: 517.3254, found: 517.3234.

TLC: R_f = 0.38 (44 % EtOAc in Hexanes, CAM stain).

[α]_D²⁴ = -41 (*c* 1.82, CHCl₃).

β-TBS Ketone (4.34) and (4.35):



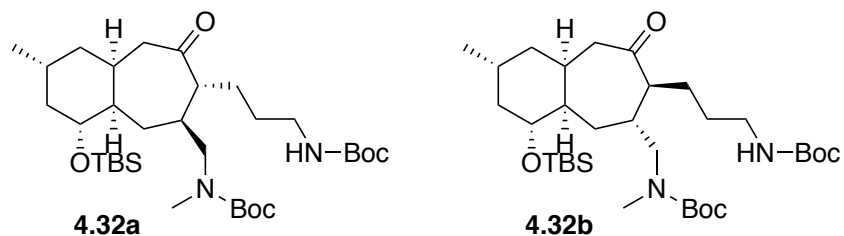
Experimental: A round bottom flask containing **4.30** (304.5 mg, 1.200 mmol) and 1,10-phenanthroline (2–3 crystals) was dried by azeotroping three times with freshly distilled benzene. The flask was then equipped with a glass stir bar and THF (19 mL) was introduced under argon.

The mixture was cooled to $-78\text{ }^{\circ}\text{C}$ and *n*-BuLi (2.3M in hexanes) was added dropwise until a brown dark color persisted. This procedure was performed to quench adventitious proton sources. LiDBB (0.4M, 6.0 mL, 2.4 mmol) was then added dropwise over 10 min at $-78\text{ }^{\circ}\text{C}$ until a dark-green color persisted, and the mixture was allowed to stir for 20 min. In a separate flask containing 1-hexynyl copper (346.5 mg, 2.410 mmol) and tetrahydrofuran (3.0 mL) was added trimethyl phosphite (0.854 mL, 7.22 mmol), and the mixture stirred at room temperature until a clear solution developed. The resulting homogeneous solution was chilled to $-78\text{ }^{\circ}\text{C}$, at which point it was added via syringe to the organolithium reagent down the flask wall over 3 min, and stirred for 1 h to produce **4.18** as deep red solution. The carbamate **4.27** (140 mg, 0.301 mmol) was dissolved in THF (0.20 mL), freshly distilled TMSCl (0.189 mL, 1.5 mmol) was added, then the mixture added directly to the organocuprate solution. The resulting mixture was stirred at $-78\text{ }^{\circ}\text{C}$ for 24 h, at which point it was quenched by the addition 10% concentrated ammonium hydroxide/saturated ammonium chloride (20 mL), followed by warming to room temperature. After 1 h, the organic layers were separated and the aqueous layers were extracted with ethyl acetate (3 x 15 mL). The organic layers were combined, dried with Na_2SO_4 , filtered, and concentrated under vacuum. The resulting mixture was filtered through a plug silica (20% CH_2Cl_2 in hexanes) to remove excess 4,4'-di-*tert*-butylbiphenyl, at which point ethyl acetate was used elute the remaining desired material. The solvent was evaporated, and the crude residue purified by chromatography (20% EtOAc/hexanes) to deliver an inseparable mixture of diastereomers **4.34** and **4.35** (110 mg, 60%).

TLC: Minor diastereomer: $R_f = 0.69$ (30% EtOAc in hexanes, CAM stain)

Major diastereomer: $R_f = 0.62$ (30 % EtOAc in hexanes, CAM stain)

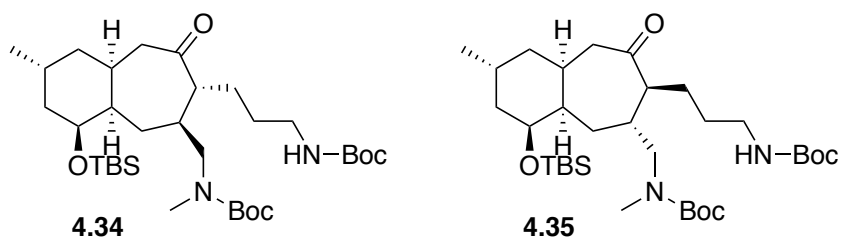
α -TBS Ketone (4.32a) and (4.32b):



Experimental: A round bottom flask containing **4.30** (152.3 mg, 0.6020 mmol) and 1,10-phenanthroline (2–3 crystals) was dried by azeotroping three times with freshly distilled benzene. The flask was then equipped with a glass stir bar and THF (12 mL) was introduced under argon. The mixture was cooled to $-78\text{ }^{\circ}\text{C}$ and *n*-BuLi (2.3M in hexanes) was added dropwise until a brown dark color persisted. This procedure was performed to quench adventitious proton sources. LiDBB (0.4M, 3.0 mL, 1.2 mmol) was then added dropwise over 10 min at $-78\text{ }^{\circ}\text{C}$ until a dark-green color persisted, and the mixture was allowed to stir for 20 min. In a separate flask containing 1-hexynyl copper (173.3 mg, 1.203 mmol) and tetrahydrofuran (1.5 mL) was added trimethyl phosphite (0.427 mL, 3.61 mmol), and the mixture stirred at room temperature until a clear solution developed. The resulting homogeneous solution was chilled to $-78\text{ }^{\circ}\text{C}$, at which point it was added via syringe to the organolithium reagent down the flask wall over 3 min, and stirred for 1 h to produce **4.18** as deep red solution. The carbamate **4.19** (70 mg, 0.150 mmol) was dissolved in THF (0.25 mL), freshly distilled TMSCl (94.5 μL , 0.750 mmol) was added, then the mixture added directly to the organocuprate solution. The resulting mixture was stirred at $-78\text{ }^{\circ}\text{C}$ for 24 h, at which point it was quenched by the addition 10% concentrated ammonium hydroxide/saturated ammonium chloride (15 mL), followed by warming to room temperature. After 1 h, the organic layers were separated and the aqueous layers were extracted with ethyl acetate (3 x 10 mL). The organic layers were combined, dried with Na_2SO_4 , filtered, and

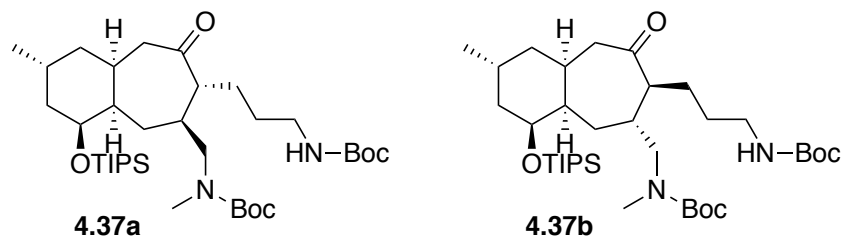
concentrated under vacuum. The resulting mixture was filtered through a plug silica (20% CH₂Cl₂ in hexanes) to remove excess 4,4'-di-*tert*-butylbiphenyl, at which point ethyl acetate was used elute the remaining desired material. The solvent was evaporated, and the crude residue purified by chromatography (20% EtOAc/hexanes) to deliver an inseparable mixture of diastereomers **4.32a** and **4.32b** (74 mg, 81%).

β-TBS Ketone (4.34) and (4.35):



Experimental: The enone **4.27** (116 mg, 0.250 mmol), K₂HPO₄ (142 mg, 0.825 mmol), Ir[dF(CF₃)ppy]₂(dtbbpy)PF₆ (5.6 mg, 0.0050 mmol), and carboxylic acid **4.31** (142 mg, 0.750 mmol) were added to a flame-dried dram vial, followed by the addition of DMF (0.63 mL). Argon was bubbled through the mixture for 15 minutes, then the vial was sealed, and irradiated with blue LED lights (2 x 24W) for 24 hours. Once complete, MeOH (1 mL) and K₂CO₃ (1 scoop) was added and allowed to stir for 30 minutes, followed by the addition of H₂O (1 mL). The mixture was extracted with DCM (3 x 3 mL), the organic layers combined, dried over Na₂SO₄, and concentrated in vacuo. Purification by column chromatography (20% EtOAc:hexanes) afforded **4.34** and **4.35** as a clear, colorless oil, as an indistinguishable mixture of diastereomers and rotamers (106.0 mg, 69%).

β-TIPS Ketone (4.37a) and (4.37b):

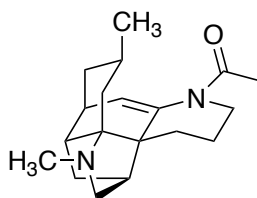


Experimental: The enone **4.28** (100 mg, 0.200 mmol), K_2HPO_4 (114 mg, 0.66 mmol), $Ir[dF(CF_3)ppy]_2(dtbbpy)PF_6$ (4.5 mg, 0.0040 mmol), and carboxylic acid **4.31** (114 mg, 0.600 mmol) were added to a flame-dried dram vial, followed by the addition of DMF (0.5 mL). Argon was bubbled through the mixture for 15 minutes, then the vial was sealed, and irradiated with blue LED lights (2 x 24W) for 24 hours. Once complete, MeOH (1 mL) and K_2CO_3 (1 scoop) was added and allowed to stir for 30 minutes, followed by the addition of H_2O (1 mL). The mixture was extracted with DCM (3 x 3 mL), the organic layers combined, dried over Na_2SO_4 , and concentrated in vacuo. Purification by column chromatography (20% EtOAc:hexanes) afforded **X** as a clear, colorless oil, as an indistinguishable mixture of diastereomers and rotamers (113.0 mg, 87%).

TLC: Minor diastereomer: $R_f = 0.48$ (25% EtOAc in hexanes, CAM stain)

TLC: Major diastereomer: $R_f = 0.41$ (25% EtOAc in hexanes, CAM stain).

(+)-fastigiatine (4.1):



(+)-fastigiatine (**4.1**)

Experimental: A 10 mL Schlenk flask was charged with tricycle *cis*-**4.5** (57.1 mg, 0.120 mmol) and purged three times with argon/vacuum. Freshly distilled and degassed 1,2-dichlorobenzene

(5.9 mL) was introduced and the solution cooled to 0 °C, at which point (+)-10-camphorsulfonic acid (402.5 mg, 1.730 mmol) was added. The reaction was removed from the ice bath and warmed to 165 °C in a sealed atmosphere for 1 h. The mixture was cooled to 0 °C, quenched with saturated NaHCO₃ (5 mL) and extracted with CHCl₃ (2 x 5 mL). The combined organic layers were dried over Na₂SO₄ and concentrated to remove CHCl₃. To the resulting solution were added Et₃N (0.16 mL, 1.2 mmol) and Ac₂O (0.11 mL, 1.2 mmol), and the mixture was stirred for 5 h. The reaction was quenched by addition of methanol (2 mL). Concentration under vacuum and purification by silica gel chromatography (gradient 1% to 10% MeOH in CHCl₃ with 0.5% ammonium hydroxide) afforded (+)-fastigiatine **4.1** (34.6 mg, 90% yield) as a white crystalline solid. The data for the synthetic natural product matched that reported by Shair.⁴

Physical State: White, crystalline solid.

¹H NMR (500 MHz, CDCl₃, 25 °C) δ 5.19 (d, *J* = 5.5 Hz, 1H), 3.82 (dt, *J* = 11.5, 6.0 Hz, 1H), 3.30–3.21 (m, 2H), 2.42–2.37 (m, 1H), 2.32 (s, 3H), 2.19 (d, *J* = 9.0 Hz, 1H), 2.18–2.16 (m, 1H), 2.15 (s, 3H), 2.07 (br app d, *J* = 14.5 Hz, 1H), 2.06–1.96 (m, 1H), 1.93–1.89 (m, 1H), 1.81–1.72 (m, 1H), 1.68 (dd, *J* = 14.0, 4.5 Hz, 1H), 1.63–1.53 (m, 3H), 1.43–1.32 (m, 2H), 1.20 (app t, *J* = 12.0 Hz, 1H), 1.02 (app dt, *J* = 12.8, 3.3 Hz, 1H), 0.91 (d, 6.5 Hz, 3H).

¹³C NMR (125 MHz, CDCl₃, 25 °C) δ 170.5, 139.6, 123.6, 65.7, 60.0, 55.4, 45.9, 45.8, 40.6, 38.7, 37.8, 35.4, 35.0, 34.3, 25.9, 23.4, 22.7, 22.0, 21.6.

HRMS (ESI) *m/z* calculated for C₁₉H₂₈N₂ONa (M + Na)⁺: 323.2099, found: 323.2106.

TLC: R_f = 0.33 (10 % MeOH in CHCl₃, UV or KMnO₄).

[α]_D²⁴ = +310 (*c* 1.32, CHCl₃).

References:

- ¹ (a) Gerard, R. V.; MacLean, D. B.; Fagianni, R.; Lock, C. *J. Can. J. Chem.* **1986**, *64*, 943–949.
- (b) Gerard, R. V.; MacLean, D. B. *Phytochemistry* **1986**, *25*, 1143–1150.
- ² Ishiuchi, K.; Kubota, T.; Ishiyama, H.; Hayashi, S.; Shibata, T.; Mori, K.; Obara, Y.; Nakahata, N.; Kobayashi, J. *Bioorg. Med. Chem.* **2011**, *19*, 749.
- ³ H. Morita, Y. Hirasawa and J. Kobayashi, *J. Org. Chem.*, **2003**, *68*, 4563–4566.
- ⁴ (a) Liao, B. B.; Shair, M. D. *J. Am. Chem. Soc.*, **2010**, *132*, 9594–9595. (b) Lee, A. S.; Liao, B. B.; Shair, M. D.; *J. Am. Chem. Soc.*, **2014**, *136*, 13442–13452.
- ⁵ Heathcock, C. H.; Kleinman E. F.; Binkley, E. S. *J. Am. Chem. Soc.*, **1982**, *104*, 1054–1068.
- ⁶ Samame, R. A.; Owens, C. M.; Rychnovsky, D. R. *Chem. Sci.*, **2015**, DOI: 10.1039/c5sc03262h.
- ⁷ (a) Oppolzer, W.; Petrzilka, M. *Helv. Chim. Acta*, **1978**, *61*, 2755–2762. (b) Caine, D.; Procter K.; Cassell, R. A. *J. Org. Chem.*, **1984**, *49*, 2647–2648.
- ⁸ Mutti, F.; Daubie, C.; Decalogne, F.; Fournier, R.; Rossie, P. *Tetrahedron Lett.*, **1996**, *37*, 3125–3128.
- ⁹ After screening several conditions, it was found that elimination proceeded in higher yields when conducted neat.
- ¹⁰ Cheng, X.; Waters, S. P. *Org. Lett.*, **2010**, *12*, 205–207.
- ¹¹ (a) Amice, P.; Blanco, L.; Conia, J. M.; *Synthesis*, **1976**, 196–197. (b) P. Hudson, Pairaudeau, G.; Parsons, P. J.; Jahans, A. W.; Drew, M. G. *Tetrahedron Lett.*, **1993**, *34*, 7295–7298.
- ¹² (a) Anderson, J. C.; Blake, A. J.; Graham, J. P.; Wilson, C. *Org. Biomol. Chem.*, **2003**, *1*, 2877–2885. (b) Chavan, S. P.; Sharma, A. K. *Synlett*, **2001**, 667–669.
- ¹⁴ Tsunoda, T.; Suzuki, M.; Noyori, R. *Tetrahedron Lett.*, **1980**, *21*, 1357–1358.
- ¹⁵ Hanessian, S.; Pan, J.; Carnell, A.; Bouchard, H.; Lesage, L. *J. Org. Chem.*, **1997**, *62*, 465–473.
- 15(a) Reese, C. B.; Shaw, A. *J. Am. Chem. Soc.*, **1970**, *92*, 2566–2568. (b) Xiao, Q.; Ren, W. W.; Chen, Z.-X.; Sun, T.W.; Li, Y.; Ye, Q.D.; Gong, J. X.; Meng, F. K.; You, L.; Liu, Y. F.; Zhao, M. Z.; Xu, L. M.; Shan, Z. H. Y.; Shi, Y. F.; Chen, J. H.; Yang, Z. *Angew. Chem., Int. Ed.*, **2011**, *50*, 7373–7377.
- ¹⁶ Lee, K.; Lee, J.; Lee, P. H. *J. Org. Chem.* **2002**, *67*, 8265–8268. (b) Lee, K.; Kim, H.; Mo, J.; Lee, P. H. *Chem.–Asian J.* **2011**, *6*, 2147–2157. (c) Koszinowski, K. *J. Am. Chem. Soc.* **2010**, *132*, 6032–6040.
- ¹⁷ (a) Miyaura, N.; Ishiyama, T.; Sasaki, H.; Ishikawa, M.; Satoh, M.; Suzuki, M. *J. Am. Chem. Soc.*, **1989**, *111*, 314–321. (b) Bradshaw, B.; Luque-Corredera, C.; Saborit, G.; Cativiela, C.; Dorel, R.; Bo, C.; Bonjoch, J. *Chem.–Eur. J.*, **2013**, *19*, 13881–13892. (c) Chemler, S. R.; Trauner, D.; Danishefsky, S. J. *Angew. Chem. Int. Ed.*, **2001**, *40*, 4544–4568.
- ¹⁸ Nagata, W.; Yoshioka, M. *Org. React.*, **2005**, *25*, 255–476.

- ¹⁹ LiDBB is an arene radical anion reducing agent first described by Freeman: Freeman, P. K.; Hutchinson, L. L. *J. Org. Chem.* **1980**, *45*, 1924–1930.
- ²⁰ Corey developed the use of alkynes as nontransferable ligands for curates chemistry: Corey, E. J.; Beames, D. J. *J. Am. Chem. Soc.* **1972**, *94*, 7210–7211.
- ²¹ Wolckenhauer, S. A.; Rychnovsky, S. D. *Org. Lett.* **2004**, *6*, 2745–2748.
- ²² Guijarro, D.; Yus, M. *Tetrahedron*, **1994**, *50*, 3447–3452.
- ²³ This new reagent was prepared from the corresponding alkyl chloride **4.53**. See supporting information.
- ²⁴ Hong, B.; Li, H.; Wu, J.; Zhang, J.; Lei, X. *Angew. Chem. Int. Ed.*, **2015**, *54*, 1011–1015.
- ²⁵ Stork, G.; Kretchmer, R. A.; Schlessinger, R. A. *J. Am. Chem. Soc.*, **1968**, *90*, 647–1648.
- ²⁶ Chu, L.; Ohta, C.; Zuo, Z.; MacMillan, D. W. C.; *J. Am. Chem. Soc.*, **2014**, *136*, 10886–10889.
- ²⁷ Prier, C. K.; Rankic, D. A.; MacMillan, D.W.C. *Chem. Rev.*, **2013**, *113*, 5322–5363.
- ²⁸ A. Pangborn, M. Giardello, R. Grubbs, R. Rosen, F. Timmers *Organometallics* **1996**, *15*, 1518–1520.
- ²⁹ W. Still, M. Khan, A. Mitra *J. Org. Chem.* **1978**, *43*, 2923–2925.
- ³⁰ R. K. Dieter, C. W. Alexander, L. E. Nice *Tetrahedron*, 2000, **56**, 2767–2778.
- ³¹ Yoon, U, C.; Jin, Y. X.; Oh, S. W.; Park, C. H.; Park, J. H.; Campana, C. F.; Cai, X.; Duesler, E. N.; Mariano, P. S. *J. Am. Chem. Soc.* **2003**, *125*, 10664–10671.

4.7 References:

- (1) Liau, B. B.; Shair, M. D. *J. Am. Chem. Soc.* **2010**, *132* (28), 9594–9595.
- (2) Samame, R. A.; Owens, C. M.; Rychnovsky, S. D. *Chem. Sci.* **2015**, *7* (1), 188–190.
- (3) Ma, X.; Gang, D. R. *Nat. Prod. Rep.* **2004**, *21* (6), 752–772.
- (4) Nangia, A.; Prasuna, G. *Synth. Commun.* **1994**, *24* (14), 1989–1998.
- (5) Kozak, J. A.; Dake, G. R. *Angew. Chem. Int. Ed.* **2008**, *47* (22), 4221–4223.
- (6) Chemler, S. R.; Trauner, D.; Danishefsky, S. J. *Angew. Chem. Int. Ed.* **2001**, *40* (24), 4544–4568.
- (7) Freeman, P. K.; Hutchinson, L. L. *J. Org. Chem.* **1980**, *45* (10), 1924–1930.
- (8) Corey, E. J.; Beames, D. J. *J. Am. Chem. Soc.* **1972**, *94* (20), 7210–7211.
- (9) Chu, L.; Ohta, C.; Zuo, Z.; MacMillan, D. W. C. *J. Am. Chem. Soc.* **2014**, *136* (31), 10886–10889.
- (10) Middleton, W. *Org. Synth.* **1986**, *64*, 221.

Chapter 5. Progress Towards a Unified Approach to Lyconadin A–E

5.1 Introduction

Following the synthesis of (+)-fastigiatine (**5.1**),¹ our lab developed an ongoing synthetic interest towards a unified approach to a number of the *Lycopodium* alkaloids, including himeridine A (**5.2**) and lyconadins E/D (**5.6–5.7**) from the lycodine class, as well as lyconadins A–C (**5.3–5.5**) from the miscellaneous class (Figure 5.1). We believed a similar bromoenone intermediate (Figure 5.1) utilized in our first and second generation (+)-fastigiatine syntheses, could serve as an ideal platform for elaboration into the other synthetic targets. It was anticipated that we would need to utilize reductive amination chemistry similar to the syntheses of lyconadins A–C by Waters,² Fukuyama,^{3,4} and Dai (Chapter 3);⁵ however, much of the other chemistry would draw inspiration from our (+)-fastigiatine syntheses.

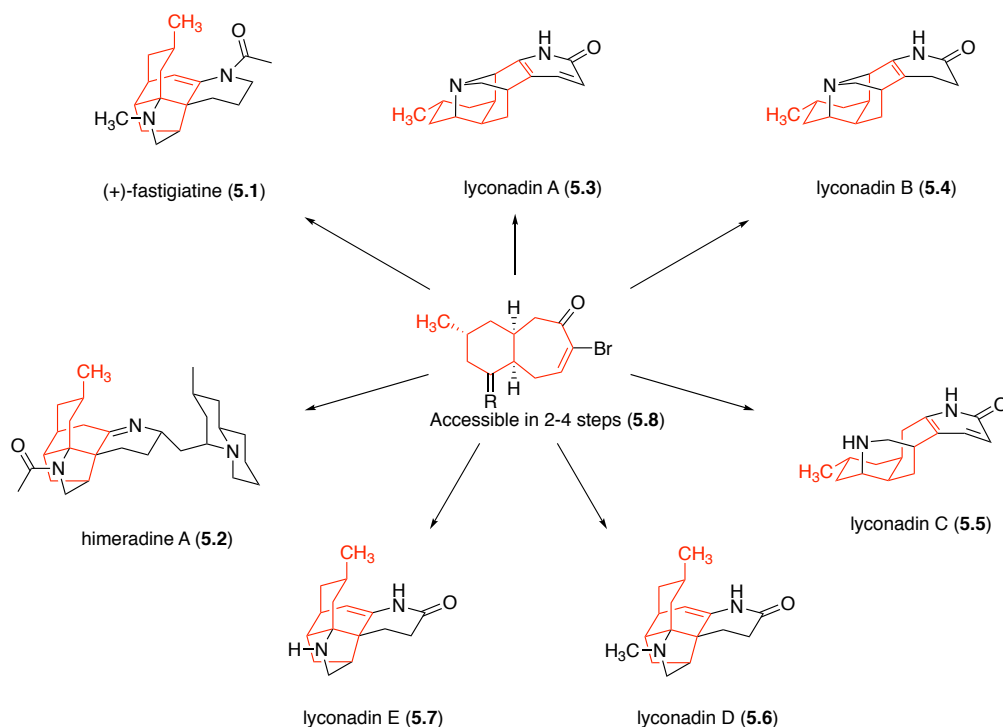
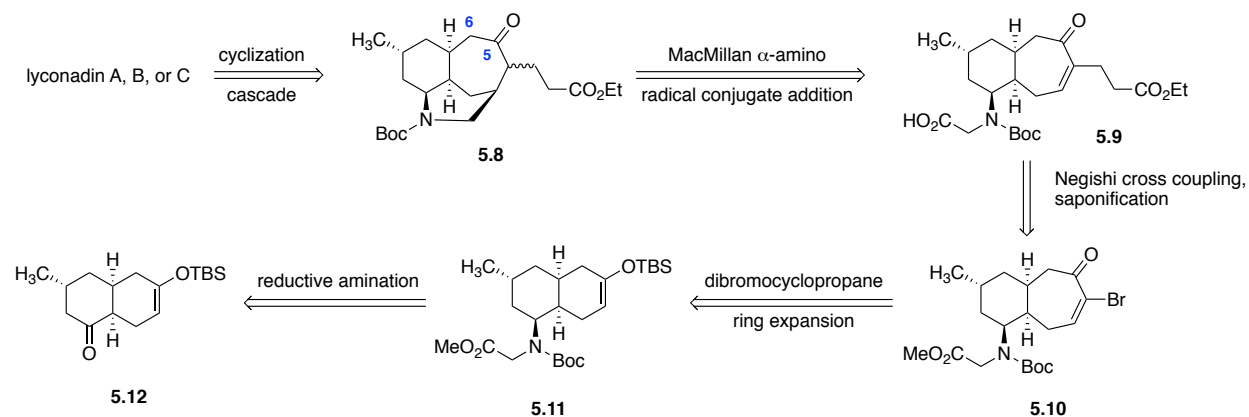


Figure 5.1: Unified synthesis of *Lycopodium* alkaloids via bromoenone.

5.2 Retrosynthetic Analysis

Lyconadins A–C (**5.3–5.5**) were chosen as our initial targets to demonstrate our unified approach to the miscellaneous *Lycopodium* alkaloids. Lyconadins A–C (**5.3–5.5**) can be formed from cyclization of **5.8** with an *in situ* formed amide onto the C5 ketone. Lyconadin A (**5.3**) and B (**5.4**) would require transannular closure of the secondary amine onto C6 prior to the amide formation. A key step in the synthesis is formation of tricycle **5.8**, which we envisioned constructing utilizing the α -amino radical conjugate addition chemistry developed by the MacMillan group.⁶ Negishi cross-coupling of bromoenone **5.10** with the appropriate organozinc bromide would afford enone **5.9**. This in turn could be generated through dibromocyclopropanation and Ag-promoted ring expansion of **5.11**. Decalin **5.11** could be generated from **5.12** through a diastereoselective reductive amination with glycine methyl ester. Ketone **5.12** has previously been synthesized by our group *en route* to (+)-fastigiatine (**5.1**).¹

Scheme 5.1: Initial retrosynthetic analysis of lyconadins A, B, and C (**5.3–5.5**).



Our initial investigation into the reductive amination and the cross-coupling steps proved to be challenging. Reductive amination using the HCl salt of glycine methyl ester was moderate in yield (28–46%), even over extended time periods (Table 5.1, entry 1). Previous work by Waters's has shown the reductive amination with methylamine to be a high yielding reaction; in

our hands this reaction also cleanly provided amine **5.14** in 96% over 18 hours (Table 5.1, entry 2). Additional conditions were tested to determine whether more electron rich amines would improve the formation of product. The attempt to form the primary amine through Ti(OiPr)₄ mediated reductive amination with ammonia in methanol resulted in a complex mixture of products.⁷ Work by Menche has shown anilines to be competent amine sources for the reductive amination of ketones.⁸ This reaction relies on catalytic quantities of thiourea as a hydrogen bond donor to activate the imine, followed by transfer hydrogenation by the Hantzsch ester. Unfortunately, their substrate scope does not include any cyclic or sterically hindered ketones. When attempted on ketone **5.12**, a mixture of three inseparable diastereomers were formed, presumably from the epimerization at C10 on ketone **5.12** and formation of both epimers of amine **5.16** during the transfer hydrogenation (Table 5.1, entry 4). A primary alcohol could serve as a carboxylic acid precursor for the α -amino radical conjugate addition later in our synthesis. TBS protected ethanolamine initially provided a moderate 50% yield of **5.17**; however, the use of fresh NaBH(OAc)₃ increased the yield to 72% (Table 5.1, entries 5 and 6).

Table 5.1: Screening of conditions and partners for the reductive amination of ketone **5.12**.

entry	compound	RNH ₂	conditions	temp. (°C)	solvent	time (hour)	yield (%)
1	5.13	HCl·H ₂ NCH ₂ CO ₂ Me	NaBH(OAc) ₃ , Na ₂ SO ₄ , Et ₃ N	25	1,2-DCE	48	46
2	5.14	HCl·H ₂ NCH ₃	NaBH(OAc) ₃ , Na ₂ SO ₄ , Et ₃ N	25	1,2-DCE	18	96
3	5.15	NH ₃ (MeOH)	Ti(OiPr) ₄ then NaBH ₄	25	CDCl ₃	6/41	complex mixture
4	5.16	H ₂ NC ₆ H ₄ pOMe	Hantzsch ester, thiourea, 5Å MS	50	toluene	7 (days)	complex mixture
5	5.17	H ₂ NCH ₂ CH ₂ OTBS	NaBH(OAc) ₃ , Na ₂ SO ₄ , Et ₃ N	25	1,2-DCE	69	50
6	5.17	H ₂ NCH ₂ CH ₂ OTBS	NaBH(OAc) ₃ , Na ₂ SO ₄ , Et ₃ N	25	1,2-DCE	41	72

After formation of the amine, *N*-Boc protection (**5.19**) proved to be challenging. Attempts to protect **5.17** as the *N*-Boc amine were low yielding (20%, 83% brsm), even under prolonged

reaction time. Using stoichiometric DMAP and excess (Boc)₂O to optimize the yields when protecting **5.17** resulted in a slight improvement, but the results were still suboptimal. Recent work on an alternative route for (+)-fastigiatine (**5.1**) by our laboratory has shown both protection and deprotection of the alcohol at the equivalent position to be challenging, typically requiring forcing conditions. Examining alternative procedures for Boc protection led us to attempt the protection in an ultrasonic bath. These conditions were developed for accelerated Boc protection of amino acids that typically require extended reaction times.⁹ Using this procedure, *N*-Boc protection improved from 54% to 85%, and reaction times were reduced from 24 hours to only 2 hours. The use of ultrasound routinely provides *N*-Boc protected amine **5.19** in 85% to 99% yield.

With optimal conditions for the reductive amination and protection identified, we proceeded with the ring-expansion to form bromoenone **5.10**. The initial attempt on the ring expansion with protected amine **5.13** was low yielding, providing a mixture of bromoenone **5.10** as an inseparable mixture with additional species. Ring expansion with **5.19** led to bromoenone **5.20** in 84% crude yield. This reaction had previously given our lab variable yields depending on the quality of potassium *tert*-butoxide and substrate used, and the ring expansion of **5.19** proved to be no exception. Purified yields ranged from 25% to 48%, with freshly sublimed potassium *tert*-butoxide and freshly distilled CHBr₃ necessary for moderate yields. To test the cross coupling in the next step without exhausting precious material, we decided to screen conditions on model systems (2-bromocyclohept-2-en-1-one **5.21** or 2-bromocyclohex-2-en-1-one **5.22**).

Our initial approach involved a Negishi cross coupling between **5.21** and commercially available organozinc bromide **5.23**. Several palladium catalysts and ligands were screened, however none of these conditions cleanly afforded the desired coupling product **5.24**. Small

amounts 1,2 and 1,4-addition of the organozinc reagent were commonly observed by ESI mass spectrometry. All reactions returned starting enone **5.21** after prolonged reaction time, with $\text{Pd}_2(\text{dba})_3$ and tricyclohexylphosphine (PCy_3) affording 1,4-addition as the only identifiable product by ESI mass spectrometry (Table 5, entry 5).

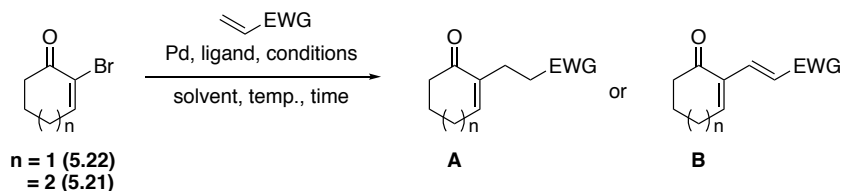
Table 5.2: Conditions for Negishi cross coupling of **5.21** with organozinc bromide **5.23**. Detection of 1,2/1,4-addition and **5.24**¹⁰ by ESIMS.

Reaction scheme: **5.21** + **5.23** (BrZn-CH₂-CH=CH₂-CO₂Et) → **5.24** (1,4-addition product). Conditions: Pd, ligand, 25 °C, time.

entry	Pd source	ligand	time (hours)	product
1	$\text{Pd}(\text{PPh}_3)_2\text{Cl}_2$	none	62	5.21 + 1,2/1,4-addn
2	$\text{Pd}_2(\text{dba})_3$	tris-(2-furyl)phosphine	62	5.21 + 1,2/1,4-addn
3	$\text{Pd}(\text{PPh}_3)_4$	none	62	5.21 + small amount of 5.24
5	$\text{Pd}_2(\text{dba})_3$	PCy_3	14	1,4-addn
6	$\text{Pd}_2(\text{dba})_3$	AsPh_3	84	5.21 + complex mixture
7	$\text{Pd}_2(\text{dba})_3$	DPEPhos	84	5.21 + small amount of 5.24
8	$\text{Ni}(\text{acac})_2$	none	28	5.21

We next explored Heck or reductive Heck conditions to couple **5.21** with ethyl acrylate or acrylonitrile (Table 5.3). The reductive Heck reactions with either ethyl acrylate (Table 5.3, entry 1) or acrylonitrile (Table 5.3, entry 2) afforded cyclohept-2-en-1-one exclusively. Attempts to couple **5.21** or **5.22** via a standard Heck reaction also resulted in dehalogenation (Table 5.3, entries 3 and 4). Previous success protecting **5.17** under ultrasonic conditions prompted us to try the Heck coupling in ionic liquid $[\text{emim}][\text{BF}_4]$ utilizing ultrasound. Unfortunately, no reactivity occurred and the starting bromoenone was returned.

Table 5.3: Screened conditions for the reductive Heck (product **A**) or Heck (product **B**) reactions of bromoenones **5.21** or **5.22** with ethyl acrylate or acrylonitrile.



entry	n	product	EWG	conditions	temp. (°C)	solvent	time (hour)	product (% yield)
1	2	A	CO ₂ Et	HCO ₂ Na, Bu ₄ NCl, Pd(OAc) ₂	25	DMF	48	cyclohept-2-en-1-one
2	2	A	CN	HCO ₂ Na, Bu ₄ NCl, Pd(OAc) ₂	25	DMF	48	cyclohept-2-en-1-one
3	2	B	CN	Pd(OAc) ₂ , PPh ₃ , K ₂ CO ₃ , Bu ₄ NCl	50	DMF/H ₂ O	9	cyclohex-2-en-1-one
4	1	B	CN	Pd(PPh ₃) ₄ , Et ₃ N	70	MeCN	9	cyclohex-2-en-1-one
5	1	B	CN	Pd(OAc) ₂ , NaOAc,)))	25	[emim][BF ₄]	3	returned 5.22

We next examined the Suzuki coupling due to our group's previous success utilizing the Suzuki coupling in the synthesis of (+)-fastigiatine (**5.1**).¹ The presence of the pyridone in the lyconadin structures required a modification to the coupling of *N*-Boc allyl amine previously used in our laboratory's synthesis of (+)-fastigiatine (**5.1**). Boron homoenolates formed with borohydrides and α,β -unsaturated carbonyls, or nitriles, have been shown to undergo 1,4-reduction rather than hydroboration of the alkene.¹¹ Nitriles are typically reduced twice, forming a stable borazine (**5.25**), which forced us to look for an alternative coupling partner (Figure 5.2).

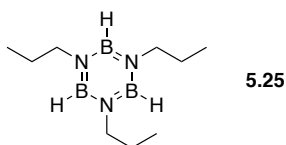


Figure 5.2: Borazine **5.25** formed from reduction of acrylonitrile with BH₃·THF.

While hydroboration with organoboranes is not possible with α,β -unsaturated compounds, β -organoboron compounds can be formed through the copper-catalyzed conjugate addition of diboron reagents.^{12,13} These boron homoenolates are competent partners in a variety of Suzuki cross coupling reactions. Unfortunately, their use with α -halo enones is limited. The

most relevant precedent is the coupling of trifluoroborate homoenolates with 2-bromo-3-methylcyclopent-2-en-1-one by Molander.^{14,15} Formation of trifluoroborate homoenolate of acrylonitrile (**5.26**) and Suzuki coupling with 2-bromocyclohept-2-en-1-one **5.21** failed to afford any of the desired product **5.28a** (Table 5.4, entry 5). The β -boration of acrylonitrile with B_2Pin_2 gave coupling partner **5.27**, which was then used in the Suzuki cross coupling reaction. Screening of a variety of conditions led to low yields of the product in all cases (Table 5.4). The use of THF as a solvent, or a cosolvent, led to the formation of an additional alkene isomer **5.28b**. Different bases led to differing amounts of isomer formation; however, formation of any alkene isomer would be detrimental to carrying out the α -amino radical conjugate addition in subsequent steps.

Table 5.4: Screen of conditions for the Suzuki coupling of bromoenone **5.21** and pinacol boronic ester **5.27**.

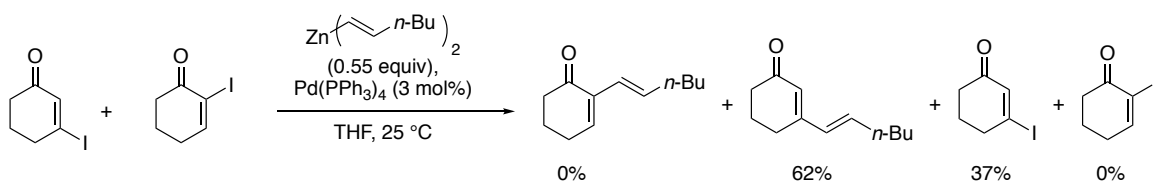
entry	conditions	temp. (°C)	solvent	time (hour)	Ratio 5.28a:5.28b (% yield)
1	$PdCl_2(dppf)_2$, $(Ph)_3As$, $CsCO_3$	80	DMF/THF	5	1.0:0.84 (23)
2	$PdCl_2(dppf)_2$, $(Ph)_3As$, $CsCO_3$	80	DMF	4	1:0 (13) ^a
3	$PdCl_2(dppf)_2$, $(Ph)_3As$, KOH , H_2O	80	THF	9	1.0:6.3 (28)
4	$PdCl_2(dppf)_2$, $(Ph)_3As$, $KOtBu$, H_2O	80	THF	5	1.0:2.1 (27)
5	5.26 , $Pd(OAc)_2$, $RuPhos$, K_2CO_3	85	toluene/ H_2O	4	(0) ^b

a: Cyclohept-2-en-1-one also seen. *b:* Reaction run with trifluoroborate **5.26** instead of BPin **5.27**.

The mixture of products formed with the sp^2 - sp^3 Suzuki coupling conditions led us to attempt sp^2 - sp Sonogashira coupling to mitigate possible scrambling of the enone (Table 5.5). We chose to couple bromoenone **5.21** with TBDPS protected propargyl alcohol **5.29**. The coupling reaction with THF as the solvent returned starting bromoenone **5.21** (Table 5.5, entry 1),

while use of DMF afforded trace amounts of product **5.31** (Table 5.5, entry 2). Concurrently, our lab had been successful in boosting the yields of Sonogashira reactions on two separate projects. Jacob DeForest, *en route* to himeridine A, found that the use of propargyl alcohol, instead of the protected propargyl alcohol, improved the yield of a Sonogashira coupling with 2-bromopyridine. Unfortunately, these conditions cleanly afforded debromination of **5.22** to give cyclohex-2-en-1-one. Prior work by Negishi has shown in a competition experiment with β -haloenones that α -haloenones are sluggish to react and typically lead to dehalogenation under cross-coupling conditions (Scheme 5.2).

Scheme 5.2: Competition experiment between α -haloenones and β -haloenones in a Negishi cross coupling.



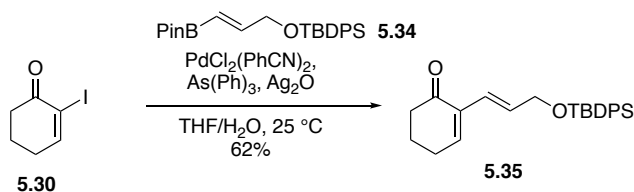
Sarah Block had higher yields and cleaner reactions by switching from a bromoaniline to an iodoaniline in a Sonogashira coupling during her synthesis of tyrosine reactive cross-linkers. Using her conditions, **5.31** was formed in 60% yield when using 2-iodocyclohex-2-en-1-one **5.30**.

Table 5.5: Screening of conditions for the Sonogashira coupling of **5.22** or **5.30** with various propargyl alcohols.

entry	X	product	R	conditions	temp. (°C)	solvent	time (hour)	product (% yield)
1	Br	5.31	TBDPS	Pd(PPh ₃) ₄ , CuI, DIPEA	60	THF	44	returned 5.22
2	Br	5.31	TBDPS	Pd(PPh ₃) ₄ , CuI, Et ₃ N	50	DMF	44	trace amount of 5.31
3	Br	5.32	H	Pd(PPh ₃) ₄ , CuI	25 to 60	Et ₃ N	44	cyclohex-2-en-1-one
4	I	5.31	TBDPS	Pd(PPh ₃) ₄ , CuI	25	Et ₃ N	19	5.31 (60)
5	I	5.33		Pd(dba) ₃ , P(2-furyl) ₃	0 to 25	DMF/THF	3	cyclohex-2-en-1-one

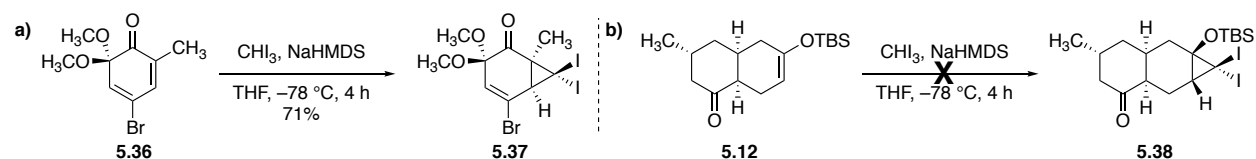
In addition to the sp^2 - sp Sonogashira coupling with iodoenone **5.30**, the sp^2 - sp^2 Suzuki coupling with pinacol boronic ester **5.34** also proceeded in moderate yields (Scheme 5.2). However, the additional π -bonds may present issues during the α -amino radical conjugate addition. Attempts to selectively hydrogenate the exocyclic alkene to alleviate these issues were unsuccessful. While the successes of the cross coupling with **5.30** were promising, they required the formation of the iodoenone before the cross coupling step in our synthesis.

Scheme 5.3: Suzuki coupling of **5.30** with pinacol boronate ester **5.34**.



While the dibromocyclopropanation/ring expansion step is well-precedented in the literature, the analogous version with iodine is scarcely known. Initially, we envisioned converting the bromide to an iodide prior to the cross coupling. The use of aromatic substitution chemistry developed by Buchwald¹⁶ or traditional Finkelstein conditions¹⁷ were ultimately unsuccessful in converting the bromide to the iodide, resulting in debromination and unreacted starting material, respectively. If the bromoenone could not be converted to the iodoenone, it would be necessary to install the iodine during the cyclopropanation/ring expansion sequence. To our knowledge, the closest precedent is work by the Herzon lab using iodoform and NaHMDS to form the diiodocyclopropane **5.36** on an α , β , δ , γ -unsaturated ketone **5.37** (Scheme 1.4 a).¹⁸ Using these conditions with decalone **5.12** failed to afford any diiodocyclopropane or ring expanded product **5.38** (Scheme 5.4).

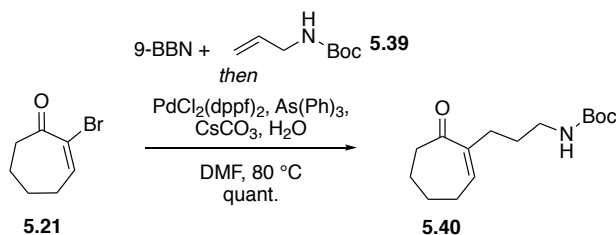
Scheme 5.4: a) Precedent by Herzon lab.¹⁸ b) Attempt to diiodocyclopropanate ketone **5.12**.



Due to the scarce literature precedent for the diiodocyclopropanation, we attempted to modify an ultrasound-promoted dichlorocyclopropanation with CCl_4 and magnesium. CCl_4 was replaced with CI_4 , unfortunately this resulted in decomposition of ketone **5.12**, failing to provide any of the desired product **5.38**.¹⁹ With generation of the iodoenone ultimately unsuccessful, we decided to revise our approach to the cross coupling by revisiting the Suzuki coupling between our bromoenone **5.21** and Boc protected allylamine **5.39**.

5.3 Revised Synthetic Approach

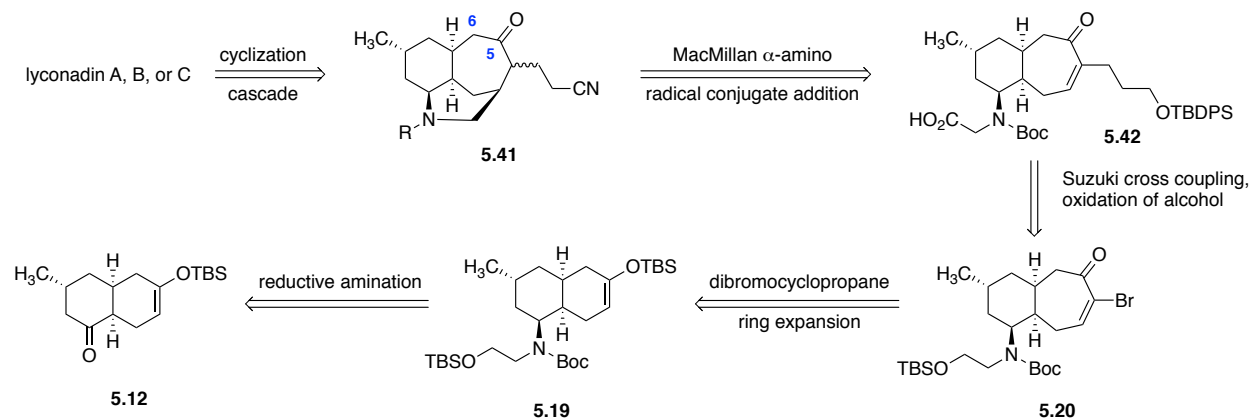
Scheme 5.5: Suzuki cross-coupling between *N*-Boc allylamine **5.39** and bromoenone **5.21**.



The Suzuki coupling conditions featured in the synthesis of (+)-fastigiatine (**5.1**) were reproduced with bromoenone **5.21** and *N*-Boc protected allylamine **5.39**, affording a quantitative yield of the coupling product (**5.40**). This led us to revise our synthetic approach. Initial attempts to oxidize the amine to the amide by Dr. Renzo Samame in our lab led to a mix of oxidation products. Rather than selectively oxidize the amine, we decided to base our strategy on work by Zhao utilizing the oxidation of primary alcohols to nitriles with H_4NOAc , catalytic TEMPO, and $\text{PhI}(\text{OAc})_2$. The pendant nitrile could then be converted to the amide which could cyclize onto

the ketone, forming the dihydropyridone ring in lyconadins B, D, and E (**5.4**, **5.6–5.7**). This cyclization utilizing the nitrile has been demonstrated previously in Shair's recent synthesis of lyconopodium A and B (**5.3–5.4**).²⁰ Our findings in our reductive amination studies, as well as our cross coupling studies, led to a revised retrosynthetic approach (Scheme 5.).

Scheme 5.6: Revised retrosynthesis of lyconadins A–C (**5.3–5.5**).



The cyclization of the secondary amine onto C6 and the amide onto the C5 ketone remains from our previous retrosynthetic route, with a nitrile replacing the ethyl ester as the amide surrogate. An approach based on tricycle **5.41** would utilize the previous α -amino radical conjugate addition; however, the carboxylic acid precursor (**5.42**) would be generated from oxidation of the primary TBS protected alcohol **5.20**. The Suzuki coupling of TBDPS protected allyl alcohol **5.43** would replace the Negishi coupling. Bromoenone **5.20** would be generated using the dibromocyclopropanation/ring expansion of decalin **5.19**. Reductive amination of **5.12** with TBS protected ethanolamine would afford **5.19**.

Initial model studies on **5.22** for the Suzuki coupling of TBDPS allyl alcohol **5.43** highlighted the optimization of the conditions performed by Dr. Renzo Samame. Attempts under conditions by Trost provided only minor amounts of **5.44** (Table 5.6, entries 1 and 2),²¹ while the conditions used for our lab's synthesis of (+)-fastigiatine (**5.1**) afforded **5.44** in 64% yield on the

model substrate (Table 5.6 entry 3). These conditions, when applied to the actual bromoenone **5.20**, provided the Suzuki product **5.42** in 54% yield.

Table 5.6: Screening of conditions for the Suzuki coupling of **5.22** with allyl alcohol **5.43**.

entry	conditions	temp. (°C)	solvent	time (hour)	product (% yield)
1	PdCl ₂ (dppf) ₂ , K ₃ PO ₄ , H ₂ O	55	THF	18	trace 5.44
2	PdCl ₂ (dppf) ₂ , K ₃ PO ₄ , H ₂ O	55	THF	28	trace 5.44
3	PdCl ₂ (dppf) ₂ , AsPh ₃ , CsCO ₃ , H ₂ O	80	DMF/THF	14	5.44 (64%)
4	PdCl ₂ (dppf) ₂ , AsPh ₃ , CsCO ₃ , H ₂ O,)))	30	DMF/THF	4	5.44 (42%)

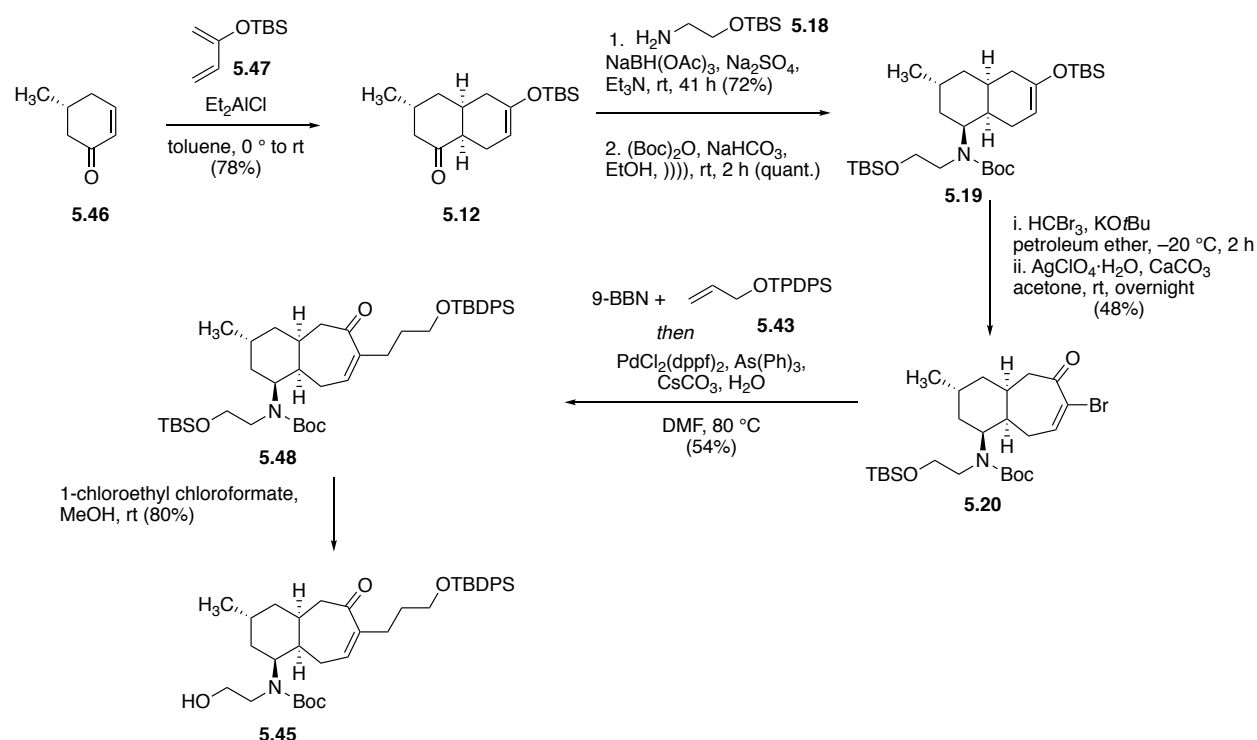
5.4 Current Progress

The most advanced intermediate prepared to date is primary alcohol **5.45**. A co-worker in our laboratory, Dr. Navendu Jana, has taken over the project, and is investigating the oxidation and cyclization steps. The Diels-Alder between **5.46** and **5.47** routinely provides decalone **5.12** in >60% yield. While reductive amination of **5.12** with amino alcohol **5.18** has been optimized to afford yields of **5.17** >60%, prolonged reaction times are still required. Ultrasonic conditions have greatly enhanced the Boc protection yield and reaction time, yielding **5.19** in >90% yield in 2 hours. The dibromocyclopropanation/ring expansion step is sensitive to the purity of reagents used, however 40–50% yields of bromoenone **5.20** can be routinely achieved. After extensive screening of various cross coupling conditions, the Suzuki cross coupling between **5.20** and **5.43** was determined to be optimal. Selective deprotection of the primary TBS protected alcohol (**5.48**) in the presence of the primary TBDPS protected alcohol was achieved through the use of anhydrous HCl generated *in situ* (**5.45**).²² Unfortunately, in an attempt to oxidize the primary

alcohol **5.45** to the carboxylic acid **5.42**,²³ the vial fell into an oil bath and the product was lost.

Currently, our lab is working to show the viability of the intramolecular α -amino radical conjugate addition in the next step.

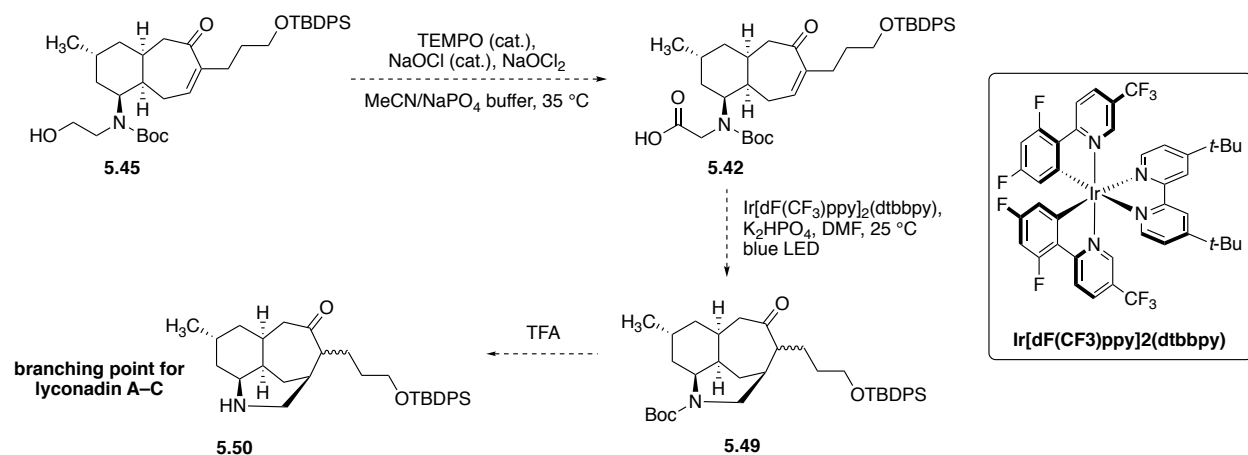
Scheme 5.7: Current progress towards the total synthesis of lyconadins A–C (**5.3–5.5**).



5.5 Future Directions

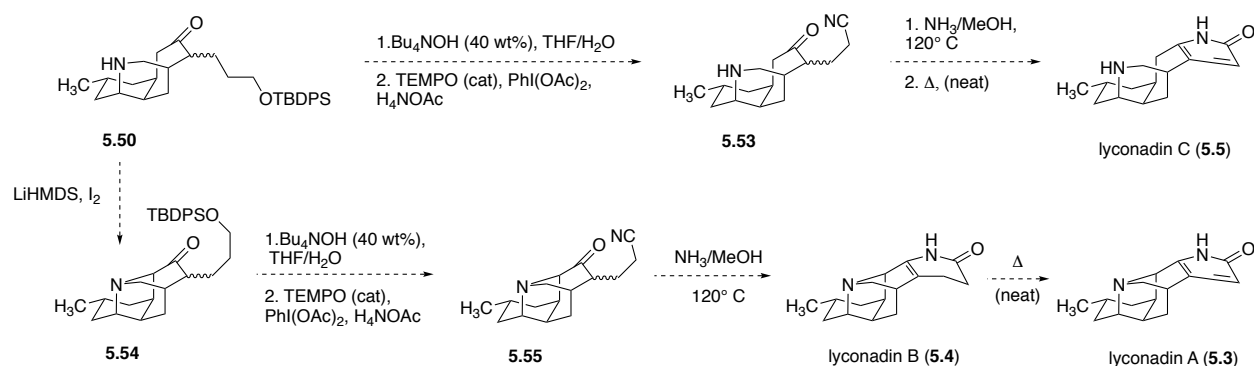
Currently the synthesis is three steps from the branching point for lyconadins A, B, and C (Scheme 5.7). Oxidation of primary alcohol **5.45** yields carboxylic acid **5.42**. Under photoredox conditions, the generated α -amino radical is poised to undergo the conjugate addition from the correct face of the enone (**5.49**). This intramolecular process should be completely diastereoselective compared to the intermolecular addition for (+)-fastigiatine (**5.1**). *N*-Boc deprotection provides the branching point (**5.50**) between lyconadins A and B, and lyconadin C.

Scheme 5.8: Steps until the branching point, tricycle **5.50**.



Nitrile **5.53** can be formed through deprotection of the primary alcohol and oxidation up to the nitrile. Amide formation and in situ cyclization to the dihydropyridone, followed by heating provides lyconadin C. Lyconadins A and B can be formed through a similar route after cyclization of the amine onto C6 (**5.54**). In the synthesis of lyconadins A and B, Shair performed this cyclization through α -iodination with LiHMDS and I₂.²⁰ Shair's synthesis at this step contained a pendent nitrile compared to our TBDPS protected alcohol (**5.54**). Deprotection of the alcohol and oxidation to nitrile **5.55** provides a direct intercept of Shair's synthesis. *In situ* formation of the amide through ammonia in methanol, and cyclization to the dihydropyridone affords lyconadin B (**5.4**). Heating lyconadin B affords lyconadin A (**5.3**), presumably through autoxidation with trace oxygen in the reaction vessel. Shair performed these last two steps in a moderate 57% yield for each.

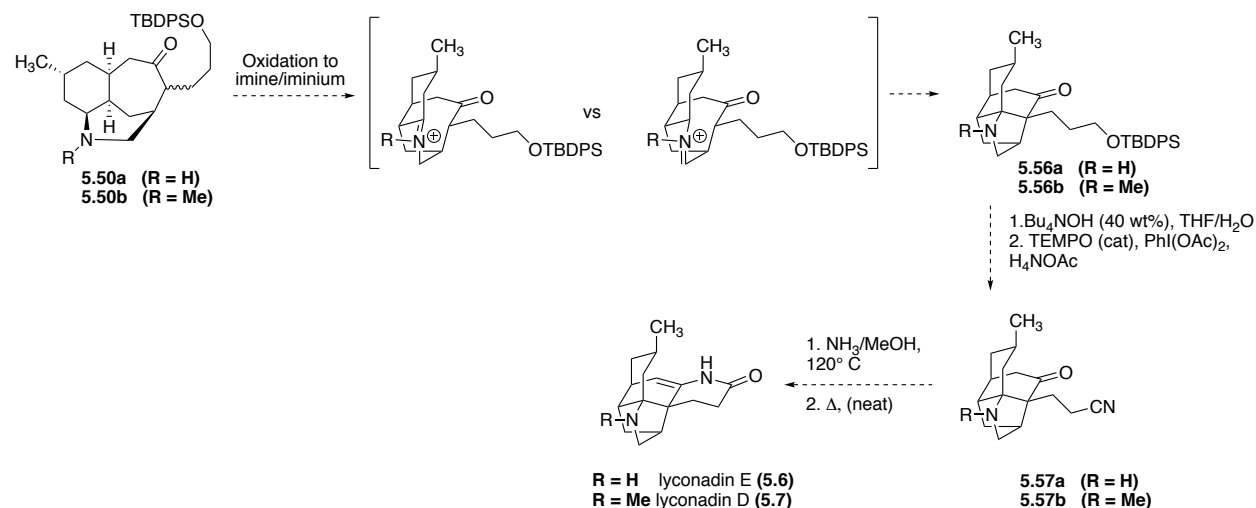
Scheme 5.9: End game for lyconadins A/B and C (5.3–5.5).



Ideally, tricycle **5.50** could also be used to synthesize lyconadins D and E (Scheme 5.9).

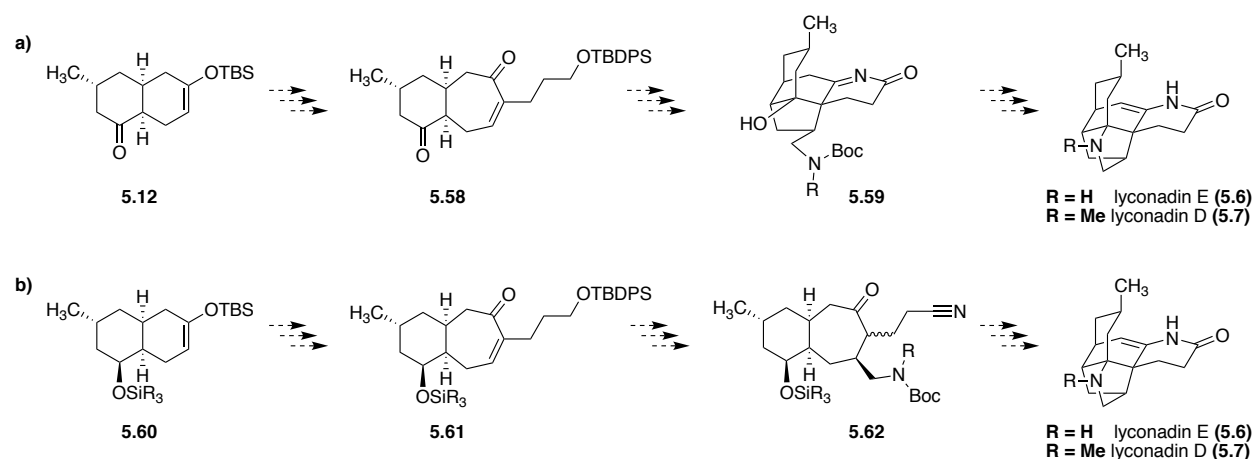
Oxidation of **5.50a** or **5.50b** should cause a spontaneous transannular Mannich on the imine or iminium, as seen in our lab's synthesis of (+)-fastigiatine. Competing oxidation to form the aldimine vs the ketimine is projected to be an issue; unfortunately, due to the highly-strained nature of this complex intermediate, the selectivity for the ketimine over the aldimine would most likely be determined experimentally. Fortunately, since **5.50a** is already being synthesized *en route* to lyconadins A–C, this step could be attempted without requiring additional synthetic endeavors.

Scheme 5.10: Endgame for the synthesis of lyconadins D or E (5.6, 5.7) from tricyclic **5.50**.



Since lyconadins D and E are members of the lycodine structural class of *Lycopodium* alkaloids, they could be accessed through a similar route to our 1st or 2nd-generation synthesis of (+)-fastigiatine (Scheme 5.10). The key difference would be the use of TBDPS protected allyl alcohol (**5.43**) in the Suzuki cross coupling step. This protected alcohol would provide the handle to oxidize to the nitrile (**5.62**), which would be used as the amide surrogate to form the dihydropyridone found in lyconadin D and E.

Scheme 5.11: a) Key intermediates in the synthesis of lyconadins D or E utilizing the 1st-generation or b) a 2nd-generation (+)-fastigiatine synthesis.



5.6 Conclusions

Our current synthetic progress has reached intermediate **5.45**. Importantly, conditions for the reductive amination, Boc protection, and Suzuki coupling have been determined—steps that proved more challenging than originally anticipated. Intermediate **5.45** is one step away from the pivotal α -amino radical conjugate addition step, and two steps away from tricycle **5.50** which will provide access to lyconadins A–C. Tricycle **5.50** theoretically also affords access to lyconadins D and E as well; however, these previously unsynthesized molecules will most likely be synthesized through a route similar to (+)-fastigiatine. Overall, our synthetic strategy allows

for a unified approach to a wide range of members of both the lycodine and miscellaneous family of Lycopodium alkaloids.

5.7 Experimental

General experimental and laboratory conditions

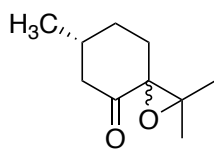
All glassware was flame- or oven-dried and cooled under argon unless otherwise stated. All reactions and solutions were conducted under argon unless otherwise stated. All commercially available reagents were used as received, unless otherwise stated. Toluene (PhMe), tetrahydrofuran (THF), dimethylformamide (DMF), diethyl ether (Et₂O) and dichloromethane (CH₂Cl₂) were degassed and dried by filtration through activated alumina under vacuum according to the procedure by Grubbs.²⁴ Diisopropylamine (DIPA) and acetonitrile (MeCN) were distilled from CaH₂ prior to use. Thin layer chromatography (TLC) was performed with Millipore 60 F₂₅₄ glass-backed silica gel plates and visualized using potassium permanganate, Dragendorff-Munier, ceric ammonium molybdate (CAM), or vanillin stains. Flash column chromatography was performed according to the method by Still, Kahn, and Mitra²⁵ using Millipore Geduran Silica 60 (40–63 μm). Bromoenone **5.22** was previously synthesized by Jacob DeForest and generously provided for use (spectra were consistent with literature reports).²⁶ *N*-Boc allylamine **5.39** was previously synthesized by Sarah Block and generously provided for use (spectra were consistent with literature reports).²⁷

Instrumentation

All data collected at ambient temperature unless noted. ¹H NMR spectra were taken at 500 or 600 MHz, calibrated using residual NMR solvent or TMS and interpreted on the δ scale. Peak abbreviations are listed: s = singlet, d = doublet, t = triplet, q = quartet, pent = pentet, dd =

doublet of doublets, ddd = doublet of doublet of doublets dt = doublet of triplets, ddt = doublet of doublet of triplets, dq = doublet of quartets, m = multiplet, app = apparent, br = broad. ^{13}C NMR spectra were taken at 125 MHz, calibrated using the NMR solvent, and interpreted on the δ scale. Melting points were recorded on an Electrothermal Melting Point Apparatus. Electrospray ionization high-resolution mass spectra (ESI-HRMS) were determined by the UC-Irvine Mass Spectrometry Laboratory using the Micromass QTOF2 Mass Spectrometer.

(6*R*)-2,2,6-trimethyl-1-oxaspiro[2.5]octan-4-one (5.63):



5.63

Experimental: A two-neck round bottom flask was fitted with an addition funnel, and (+)-pulegone (72.3 g, 0.475 mol) and MeOH (363 mL) were added. The solution was cooled to 0 °C for 10 min, and 30% H₂O₂ (181 mL, 1.77 mol) was added dropwise over 5 min. A solution of KOH (55 g, 0.97 mol) in H₂O (181 mL) was transferred to the addition funnel and added dropwise over 15 min. The reaction mixture was stirred for 30 min at 0 °C before warming to rt and stirring for an additional 4 hours. The reaction was poured into a separatory funnel with sat. aq. sodium chloride (750 mL) and extracted with Et₂O (3 x 750 mL). The organic layers were washed with additional sat. aq. sodium chloride (450 mL), dried over Na₂SO₄, filtered, and concentrated under reduced pressure to afford epoxide **5.63** (57.0 g, 71%) as a mixture of diastereomers.

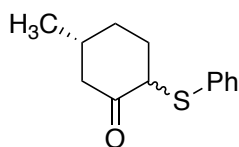
Spectral data was consistent with the literature.^{28,29}

Physical State: Faint, yellow oil.

$^1\text{H NMR}$ (500 MHz, CDCl_3 , 25 °C) δ 2.62 (dt, $J = 13.6, 3.1$ Hz, 1H), 2.43 (d, $J = 2.4$ Hz, 5H), 2.20 (td, $J = 13.5, 4.4$ Hz, 2H), 2.09–1.72 (m, 10H), 1.44 (d, $J = 2.4$ Hz, 8H), 1.23 (d, $J = 7.0$ Hz, 7H), 1.08 (t, $J = 7.2$ Hz, 8H).

TLC: $R_f = 0.15$ (12% EtOAc in hexanes, KMnO_4).

(5*R*)-5-methyl-2-(phenylthio)cyclohexan-1-one (5.64):



5.64

Experimental: All glassware was flame dried and under an argon atmosphere. Dry solvents were all dispensed into the flame dried round bottom flask and kept under argon. To a 2 L, two-neck round bottom flask with 400 mL addition funnel was added NaH (31.56 g, 788.7 mmol) and THF (350 mL), then the mixture was cooled to 0 °C for 10 minutes. In a separate 1 L round bottom flask with THF (350 mL) was added PhSH (67.5 mL, 357 mmol). This solution was then cannula transferred to the addition funnel, and the solution was slowly added (2–3 drops/s) to the two-neck flask over 1.5 hours with vigorous stirring. Crude pulegone oxide **5.63** (44.23 g, 262.9 mmol) was transferred to a 500 mL round bottom flask with THF (245 mL). The solution was then cannula transferred to the addition funnel and added slowly (2 drops/sec) over 1.5 hours. The reaction mixture was warmed to room temperature and allowed to stir for 2 hours before being heated to reflux for 24 hours. After completion by TLC, the mixture was cooled to 0 °C. A solution of sat. aq. ammonium chloride (800 mL) was added slowly *via* addition funnel to keep the internal temperature below 15 °C. The biphasic mixture was then transferred to a separatory funnel and the layers separated. The aqueous layer was extracted with Et₂O (3 x 250 mL). The organic layers were washed with sat. aq. sodium chloride (2 x 250 mL), dried with Na₂SO₄,

filtered, and concentrated to yield sulfide **X** (40.15 g, 69%) as a mixture of inseparable diastereomers.

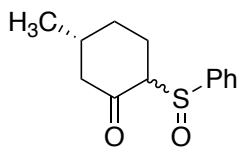
Spectral data was consistent with the literature.^{28,29}

Physical State: Viscous, orange oil.

¹H NMR (500 MHz, CDCl₃, 25 °C) δ (mixture of diastereomers) 7.43–7.37 (m, 3H), 7.31–7.21 (m, 5H), 3.86 (ddd, J = 11.3, 5.8, 1.3 Hz, 1H), 3.74–3.70 (m, 0.5H), 2.79 (dd, J = 13.7, 12.2 Hz, 0.5H), 2.69 (ddd, J = 13.1, 4.0, 2.0 Hz, 1H), 2.33 (dddd, J = 13.6, 5.8, 4.8, 3.7 Hz, 1H), 2.28–2.18 (m, 1.2H), 2.20–2.06 (m, 1.7H), 2.06–1.87 (m, 3H), 1.78 (dtd, J = 13.6, 11.4, 3.7 Hz, 1.2H), 1.73–1.65 (m, 1.3H), 1.45–1.35 (m, 1.3H), 1.22–1.19 (m, 0.5H), 1.05 (d, J = 6.6 Hz, 1.5H), 1.02 (d, J = 6.5 Hz, 3H).

TLC: R_f = 0.67 (40% EtOAc in hexanes, KMnO₄).

(5*R*)-5-methyl-2-(phenylsulfinyl)cyclohexan-1-one (5.65):



5.65

Experimental: A mechanical stirrer was used to prevent the stalling due to buildup of solid precipitate. A solution of sulfide **5.64** (45.1 g, 205 mmol) in MeOH (511 mL) was cooled to 0 °C, and a solution of NaIO₄ (43.8 g, 205 mmol) in H₂O (205 mL) was added in one portion. The ice bath was removed, and the reaction stirred at rt for 8 hours. The salts were removed by filtering, and the salts were rinsed with CH₂Cl₂ (300 mL) to remove any residual product. Sat. aq. sodium chloride (100 mL) was added to aid in separation. The aqueous layer was extracted with CH₂Cl₂ (3 x 300 mL). The organic layers were combined and washed with sat. aq. sodium sulfite

(200 mL) and sat. aq. sodium chloride (300 mL). The organic layers were dried over Na₂SO₄, filtered, and concentrated to yield sulfoxide **5.65** (49.6 g, quantitative) as a mixture of four diastereomers.

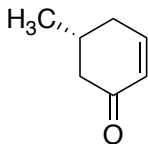
Spectral data was consistent with the literature.^{28,29}

Physical State: Golden oil.

¹H NMR (600 MHz, CDCl₃, 25 °C) δ 7.68 (dd, *J* = 6.6, 3.0 Hz, 1H), 7.66–7.63 (m, 2H), 7.59–7.54 (m, 2H), 7.53–7.44 (m, 8H), 3.66 (ddd, *J* = 11.4, 5.8, 1.1 Hz, 1H), 3.38–3.29 (m, 2H), 2.60 (dq, *J* = 14.5, 4.9 Hz, 1H), 2.55–2.47 (m, 3H), 2.24 (dd, *J* = 14.0, 10.2 Hz, 1H), 2.17–1.88 (m, 5H), 1.85–1.77 (m, 2H), 1.45 (d, *J* = 6.9 Hz, 1H), 1.43–1.28 (m, 2H), 1.07 (d, *J* = 6.7 Hz, 3H), 1.03–0.96 (m, 6H).

TLC: R_f = 0.19 (40% EtOAc in hexanes, KMnO₄).

(*R*)-5-methylcyclohex-2-en-1-one (5.46):



5.46

Experimental: CaCO₃ (3.16 g, 31.5 mmol) was added to a solution of sulfoxide **5.65** (7.43 g, 31.5 mmol) in CCl₄ (42 mL), and the atmosphere exchanged for argon. The mixture was heated to reflux for 20 hours. After cooling to rt, the mixture was diluted with CH₂Cl₂ (50 mL) and filtered through a pad of Celite. The Celite was rinsed with additional CH₂Cl₂. The organics were combined and dried with Na₂SO₄, filtered, and concentrated to provide crude enone **5.46** (20.8 g) as a golden oil. Cooling the oil in a freezer crystallized the sulfinic acid byproduct, which could be removed by filtration. Purification by column chromatography (plug of silica with hexanes to

20% EtOAc), followed by collection of the product and additional purification by column chromatography (hexanes to 10% EtOAc) afforded pure enone **5.46** (typical yields 30–50%) as a golden oil.

Spectral data was consistent with the literature.^{28,29}

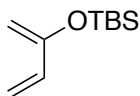
Physical State: Golden oil.

¹H NMR (500 MHz, CDCl₃, 25 °C) δ 6.96 (ddd, *J* = 10.1, 5.6, 2.6 Hz, 1H), 6.02 (ddt, *J* = 10.1, 2.9, 1.1 Hz, 1H), 2.48 (ddt, *J* = 15.8, 3.6, 0.9 Hz, 1H), 2.42 (dddt, *J* = 18.6, 5.7, 4.5, 1.3 Hz, 1H), 2.28–2.17 (m, 1H), 2.12 (dd, *J* = 15.7, 12.3 Hz, 1H), 2.04 (ddt, *J* = 19.4, 9.7, 2.8 Hz, 1H), 1.07 (d, *J* = 6.5 Hz, 3H).

¹³C NMR (125 MHz, CDCl₃) δ 200.2, 150.0, 129.8, 46.5, 34.2, 30.5, 21.4.

TLC: R_f = 0.52 (40% EtOAc in hexanes, KMnO₄).

(buta-1,3-dien-2-yloxy)(*tert*-butyl)dimethylsilane (5.47):



5.47

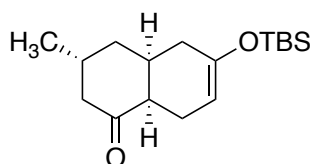
Experimental: A 1 L round bottom flask was charged with diisopropylamine (19.9 mL, 142 mmol) and THF (225 mL), and cooled to 0 °C. Once cool, *n*-BuLi (2.3 M, 61.8 mL, 142 mmol) was added via cannula. The mixture was stirred for 10 minutes, then cooled down to –78 °C. Once cool, a solution of methyl vinyl ketone (10.71 mL, 128.5 mmol) in THF (250 mL) was added dropwise over 30 minutes via cannula. After addition was complete, the mixture was allowed to stir for ten minutes, then DMPU (9.0 mL, freshly distilled over CaH₂) was added dropwise over 5–10 minute period, and stirred for 10 minutes. Next, a solution of TBSCl (29.0 g, 193 mmol) in THF (90 mL) was added via cannula over 30 minutes. After the addition was

complete, the reaction mixture was warmed to 0 °C and stirred for 20 minutes, then warmed to room temperature and stirred for 3 hours. Upon completion, the reaction was diluted with pentane (250 mL) and 1M acetic acid (250 mL). The layers were separated, and the aqueous layer extracted with pentane (150 mL). The organics were combined and washed with H₂O (2 x 100 mL) and sat. aq. sodium chloride (200 mL), and dried with Na₂SO₄, filtered, and concentrated under reduced pressure to afford a pale yellow oil. Purification by chromatography (100% pentane) afforded the desired diene **5.47** (8.0 g, 34%) as a clear, colorless oil. Spectral data was consistent with the literature.^{30,31}

Physical State: Clear, colorless oil.

¹H NMR (500 MHz, CDCl₃, 25 °C) δ 6.20 (dd, *J* = 16.9, 10.5 Hz, 1H), 5.52 (ddt, *J* = 17.0, 1.9, 0.6 Hz, 1H), 5.08 (dddd, *J* = 10.5, 2.1, 1.5, 0.8 Hz, 1H), 4.35–4.31 (m, 2H), 0.98 (s, 9H), 0.18 (s, 6H).

Decalone (5.12):



5.12

Experimental: A round-bottom flask was charged with (+)-5-methylcyclohex-2-en-1-one (**5.46**) (2.01 g, 18.3 mmol) and 2-*tert*-butyldimethylsilyloxy-1,3-butadiene (**5.47**) (4.68 g, 25.4 mmol) and purged four times via vacuum/argon cycles. Dry toluene (75 mL) was added and the solution was cooled to 0 °C. Diethyl aluminum chloride (19.1 mL, 1.0 M in toluene, 19.1 mmol) was then added dropwise over a 10 min period. The resulting mixture was allowed to reach room temperature with stirring. After 1.5 h, the mixture was cooled to 0 °C and quenched by the rapid

addition of sat. aq. NaHCO₃ (250 mL) and 10% potassium sodium tartrate (20 mL). The aqueous layer was separated and extracted with Et₂O (3 x 200 mL). The combined organic layers were washed with saturated NaHCO₃ (3 x 200 mL), sat. aq. sodium chloride (3 x 200 mL), dried over Na₂SO₄ and concentrated under reduced pressure. Volatile materials were removed under high vacuum (ca. 1 Torr) overnight to afford the desired product **5.12** (4.91 g, 91%) as light yellow oil. If desired, product can be purified by column chromatography (10% EtOAc/hexanes).

Physical State: Viscous, colorless oil

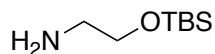
¹H NMR (500 MHz, CDCl₃) δ 4.81–4.78 (m, 1H), 2.61 (t, *J* = 5.8 Hz, 1H), 2.57–2.48 (m, 2H), 2.39 (ddd, *J* = 13.5, 4.8, 2.0 Hz, 1H), 2.25–2.17 (m, 1H), 2.20–1.95 (m, 2H), 1.86 (app dd, *J* = 8.0, 1.5 Hz, 2H), 1.80 (d, *J* = 14.5 Hz, 1H), 1.64 (ddd, *J* = 13.5, 11.5, 4.0 Hz, 1H), 1.03 (d, *J* = 6 Hz, 3H), 0.89 (s, 9H), 0.11 (s, 3H), 0.08 (s, 3H).

¹³C NMR (125 MHz, CDCl₃) δ 211.1, 148.2, 102.0, 49.7, 47.0, 38.2, 36.1, 31.9, 30.8, 25.9, 22.6, 22.2, 18.1, –4.1, –4.4.

HRMS (ESI) *m/z* calculated for C₁₇H₃₁O₂Si (M + H)⁺: 295.2093, found: 295.2095.

TLC: R_f = 0.60 (10% EtOAc in hexanes, CAM stain).

2-((*tert*-butyldimethylsilyl)oxy)ethan-1-amine (**5.18**):



5.18

Experimental: To a solution of ethanolamine (1.51 mL, 25.0 mmol) and imidazole (3.40 g, 50.0 mmol) in CH₂Cl₂ (27 mL) was added a solution of TBSCl (3.96 g, 26.3 mmol) in CH₂Cl₂ (10 mL) slowly over 5 min. After stirring for 18 hours the reaction was stopped by addition of H₂O (25 mL). The layers were separated, and the aqueous layer extracted with CH₂Cl₂ (2 x 25 mL). The

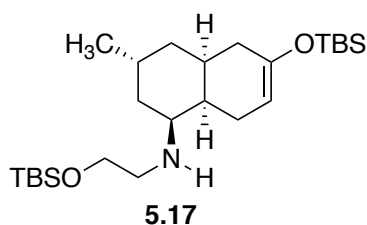
organic layers were dried over MgSO₄, the salts filtered off, and the solvent removed in vacuo to afford **5.18** (5.49 g, quantitative) as a light yellow oil.

Spectral data was consistent with the literature.³²

Physical State: Light yellow oil.

¹H NMR (500 MHz, CDCl₃, 25 °C) δ 3.65 (t, *J* = 5.3 Hz, 2H), 3.07 (s, 2H), 2.81 (t, *J* = 5.3 Hz, 2H), 0.90 (s, 9H), 0.07 (s, 6H).

Amino decalin (5.17):



Experimental: Ketone **5.12** (50 mg, 0.17 mmol) was weighed into a 1-dram vial and Na₂SO₄ (74 mg, 0.51 mmol) was added. A solution of amine **5.18** (92 mg, 0.51 mmol) in 1,2-DCE (0.52 mL) was added to the vial, and the atmosphere changed to argon. NaBH(OAc)₃ (54 mg, 0.26 mmol) was added and the reaction mixture stirred for 43 hours. The mixture was quenched by addition of aq. 1.0 M NaOH (2.8 mL), and the layers separated. The aqueous layer was extracted with CH₂Cl₂ (3 x 2 mL), and the organic layers washed with brine. After drying over MgSO₄, the organic layers were filtered and concentrated. The crude yellow oil was purified by column chromatography (hexanes to 50% EtOAc in hexane) to afford **5.17** (39.6 mg, 51%) as a light yellow oil.

Physical State: Light yellow oil.

¹H NMR (500 MHz, CDCl₃, 25 °C) δ 4.80 (d, *J* = 4.7 Hz, 1H), 3.70 (t, *J* = 5.4 Hz, 2H), 2.87 (d, *J* = 11.3 Hz, 1H), 2.74 (dt, *J* = 11.5, 5.6 Hz, 1H), 2.65 (dt, *J* = 11.5, 5.2 Hz, 1H), 2.36 (br. d, *J* =

13.5 Hz, 1H), 1.90 (br. s, 1H), 1.66 (td, $J = 12.9, 5.1$ Hz, 2H), 1.60–1.43 (m, 3H), 1.36 (br. d, $J = 12.9$ Hz, 1H), 1.09 (d, $J = 13.3$ Hz, 1H), 1.03 (d, $J = 7.3$ Hz, 3H), 0.91 (s, 9H), 0.89 (s, 9H), 0.12 (s, 6H), 0.06 (s, 6H).

^{13}C NMR (125 MHz, CDCl_3 , 25 °C) δ 149.3, 102.3, 62.7, 49.0, 36.28, 35.2, 29.9, 29.6, 26.1, 26.0, 19.9, 18.5, 18.2, 0.2, -4.10, -4.13, -5.06, -5.09.

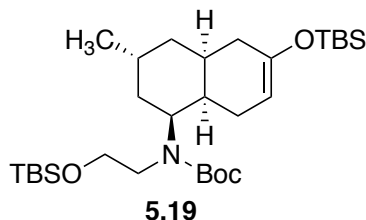
IR (thin film): 2954, 1673, 1467, 1254, 729 cm^{-1} .

HRMS (ESI) m/z : calculated for CHNO ($\text{M} + \text{Na}$) $^+$: , found:

$[\alpha]_{\text{D}}^{24} = -20.8$ (c 1.1, CHCl_3).

TLC: $R_f = 0.36$ (30% EtOAc in hexanes, stain).

***N*-Boc amino decalin (5.19):**



Experimental: To a solution of amine **5.17** (169 mg, 0.370 mmol) in EtOH (1.0 mL) was added NaHCO_3 (36 mg, 0.43 mmol). A solution of $(\text{Boc})_2\text{O}$ (127 mg, 0.560 mmol) in EtOH (0.85 mL) was transferred to the reaction mixture, and the vial was topped with a septum with a vent needle. The mixture was sonicated in an ultrasound bath for 2 hours. The mixture was then filtered through Celite and concentrated *in vacuo* to afford enoxysilane **5.19** (188 mg, 91%) as a clear oil. *If needed, excess $(\text{Boc})_2\text{O}$ can be decomposed by addition of a few crystals of DMAP and sonicating the mixture for 30 min. Purification by column chromatography (hexanes to 50% EtOAc in hexane) yields pure 1.*

Physical State: Clear oil.

¹H NMR (500 MHz, CDCl₃, 25 °C) δ 4.78 (dt, *J* = 4.8, 2.1 Hz, 1H), 4.34–4.10 (m, 1H), 3.66 (td, *J* = 9.1, 4.7 Hz, 1H), 3.50 (s, 1H), 3.44–3.30 (m, 1H), 3.01 (dt, *J* = 14.8, 7.5 Hz, 1H), 2.43–2.34 (m, 1H), 2.27–2.06 (m, 4H), 2.00 (td, *J* = 13.2, 5.5 Hz, 1H), 1.81–1.71 (m, 1H), 1.68–1.54 (m, 3H), 1.46 (s, 9H), 1.08 (d, *J* = 7.4 Hz, 3H), 0.89 (d, *J* = 7.7 Hz, 18H), 0.10 (s, 6H), 0.04 (s, 6H).

¹³C NMR (125 MHz, CDCl₃, 25 °C) δ 156.0, 149.2, 101.8, 79.6, 62.6, 53.2, 46.7, 37.2, 36.1, 32.3, 30.3, 30.0, 29.94, 29.91, 28.8, 28.3, 26.2, 26.0, 19.7, 19.3, 18.6, 18.3, -4.08, -4.14, -5.0.

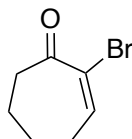
IR (thin film): 2954, 2855, 1690, 1471, 1363, 1251, 1144, 833 cm⁻¹.

HRMS (ESI) *m/z*: calculated for CHNO (M + Na)⁺: , found:

$[\alpha]_D^{24} = -33.6$ (*c* 1.00, CHCl₃).

TLC: R_f = 0.83 (40% EtOAc in hexanes, stain).

2-bromocyclohept-2-en-1-one (5.21):



5.21

Experimental: A solution of bromine (0.54 mL, 1.0 mmol) in CH₂Cl₂ (25 mL) was slowly added over 1 hour to a 0 °C solution of cyclohept-2-en-1-one (1.15 mL, 1.00 mmol) in CH₂Cl₂ (25 mL). After 1 hour Et₃N (2.53 mL, 16.7 mmol) was slowly added over 8 min, and the reaction allowed to warm to room temperature. The reaction mixture was quenched with 1.0 M HCl (aq.) and the layers separated. The organic layer was washed with sat. aq. sodium chloride (18 mL), dried over Na₂SO₄, the salts filtered, and the solvent removed in vacuo to yield **5.21**. Purification by column chromatography (hexanes to 30% EtOAc in hexanes) provided pure **5.21** (825 mg, 43%) as a golden oil.

Spectral data was consistent with the literature.²⁶

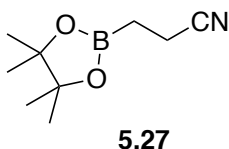
Physical State: Golden oil.

¹H NMR (500 MHz, CDCl₃, 25 °C) δ 7.33 (t, *J* = 6.6 Hz, 1H), 2.76–2.69 (m, 2H), 2.48–2.40 (m, 2H), 1.88–1.76 (m, 4H).

¹³C NMR (125 MHz, CDCl₃, 25 °C) δ 196.4, 148.2, 127.1, 41.5, 29.5, 24.9, 21.4.

TLC: R_f = 0.24 (15% EtOAc in hexanes, vanillin stain).

3-(3,3,4,4-tetramethyl-1λ3,2,5-bromadioxolan-1-yl)propanenitrile (5.27):



Experimental: CuCl (3.5 mg, 0.033 mmol), NaO*t*-Bu (9.5 mg, 0.099 mmol), and DPEPhos (18.1 mg, 0.033 mmol) were added to a flame dried vial under argon. The vial was purged with argon, and THF (1.0 mL) was added. After stirring for 30 min a solution of B₂Pin₂ (295 mg, 1.16 mmol) in THF (1.0 mL) was added, and the mixture was stirred for an additional 30 min. Acrylonitrile (0.07 mL, 1.0 mmol), MeOH (0.11 mL), and THF (0.7 mL) were added, and the reaction mixture stirred for 15 hours. The resultant slurry was filtered through Celite, washed with EtOAc, dried over Na₂SO₄, and concentrated under reduced pressure. Purification with column chromatography (hexanes to 20% EtOAc in hexanes) afforded **5.27** (129 mg, 71%) as a clear oil.

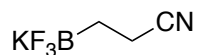
Spectral data was consistent with the literature.³³

Physical State: Clear oil.

¹H NMR (500 MHz, CDCl₃, 25 °C) δ 2.40 (t, *J* = 7.8 Hz, 2 H), 1.25 (s, 12 H), 1.17 (t, *J* = 8.0 Hz, 2 H).

TLC: $R_f = 0.39$ (5% EtOAc in CH_2Cl_2 , Hanessian's stain).

3-(trifluoro- λ 4-boraneyl)propanenitrile, potassium salt (5.26):



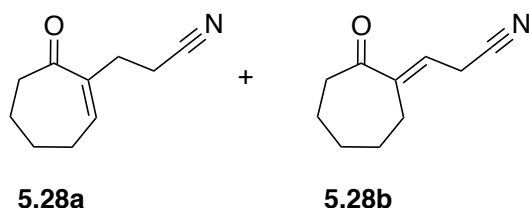
5.26

Experimental: A solution of sat. aq. KHF_2 (0.9 mL, 4.0 mmol) was added dropwise to a solution of **5.27** (181 mg, 1.00 mmol) in MeCN (5 mL). After stirring for 22 hours, the volatiles were removed under reduced pressure. The resultant slurry was triturated with hot acetone and filtered through a plug of cotton to remove the inorganic salts. The solution was concentrated until 1–2 mL of acetone remained, and Et_2O was added to precipitate out the solids. The remainder of the solvent was removed *in vacuo* to yield **5.26** (107 mg, 66%) as a white solid. Spectral data was consistent with the literature.^{14,34}

Physical State: White solid.

$^1\text{H NMR}$ (500 MHz, CDCl_3 , 25 °C) δ 2.57 (t, $J = 8.5$ Hz, 2H), 0.88 (s, 2H).

3-(7-oxocyclohept-1-en-1-yl)propanenitrile (5.28a) and (E)-3-(2-oxocycloheptylidene)propanenitrile (5.28b):



5.28a

5.28b

Experimental: Representative procedure that provided the greatest amount of product, with minimal amount of enone isomerization. All solvents were degassed prior to use, and the reaction was run under an atmosphere of argon. A solution of bromoenone **5.21** (29 mg, 0.15

mmol) in DMF (0.5 mL) was transferred to a Schlenk flask. Another 0.5 mL DMF was used to transfer any remaining **5.21** from the original vial to the Schlenk flask. The Schlenk flask was degassed with three vacuum/argon cycles before PdCl₂(dppf)₂ (37 mg, 0.045 mmol), AsPh₃ (14 mg, 0.045 mmol), and Cs₂CO₃ (112 mg, 0.330 mmol) were added. Another degassing with three vacuum/argon cycles was performed, and the mixture was stirred for 15 minutes. To a separate container was added **5.27** (43 mg, 0.23 mmol) and THF (0.5 mL). This container was degassed with three vacuum/argon cycles before transferring the contents to the Schlenk flask. An additional 0.5 mL THF was used to transfer any remaining **5.27** to the Schlenk flask from the separate container. The reaction was heated to 80 °C for 6 hours before being cooled back to rt. The mixture was filtered through a plug of silica with Et₂O and concentrated. The slurry was taken up in a 1:1 mixture of Et₂O to H₂O and extracted three times with Et₂O. The organic layers were washed three times with H₂O, dried over MgSO₄, filtered, and concentrated under reduced pressure. The crude product was purified by column chromatography (hexanes to 40% EtOAc in hexanes) to afford an inseparable mixture of alkene isomers **5.28a** and **5.28b** (5.6 mg, 23%) as a yellow oil.

Spectral data was consistent with the literature.¹⁰

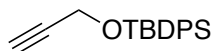
Physical State: Yellow oil.

¹H NMR (600 MHz, CDCl₃, 25 °C) δ major alkene isomer (**5.28a**): δ 6.78 (t, *J* = 6.3 Hz, 1H), 2.65–2.59 (m, 2.9H), 2.53 (br. s, 4H), 2.48–2.44 (m, 2H), 1.87–1.73 (m, 5.9H).

minor alkene isomer (**5.28b**): δ 6.57 (t, *J* = 6.3 Hz, 0.29H), 2.43–2.39 (m, 0.9H).

TLC: R_f = 0.41 (33% EtOAc in hexanes, Hanessian's stain).

***tert*-butyldiphenyl(prop-2-yn-1-yloxy)silane (5.29):**



5.29

Experimental: A solution of propargyl alcohol (0.52 mL, 8.9 mmol) in CH₂Cl₂ (1.5 mL) was added to a solution of TBDPSCl (2.6 mL, 9.8 mmol) and imidazole (669 mg, 9.81 mmol) in CH₂Cl₂ (8 mL) and stirred for 36 hours. The reaction mixture was diluted with Et₂O and H₂O before being transferred to a separatory funnel. The layers were separated and the aqueous layer was extracted with Et₂O (3 x 20 mL). The organic layers were washed with brine, dried over MgSO₄, filtered, and concentrated. Purification by column chromatography (hexanes to 15% EtOAc in hexanes) afforded protected alcohol **5.29** (2.08 g, 79%) as a clear oil.

Spectral data was consistent with the literature.³⁵

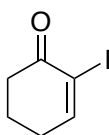
Physical State: Clear oil.

¹H NMR (500 MHz, CDCl₃, 25 °C) δ 7.73–7.68 (m, 4H), 7.45–7.35 (m, 6H), 2.41 (app. d, *J* = 2.40 Hz, 2H), 2.41 (app. t, *J* = 2.40 Hz, 1H), 1.07 (s, 9H).

¹³C NMR (125 MHz, CDCl₃, 25 °C) δ 135.8, 133.2, 130.0, 128.0, 82.2, 73.2, 52.79, 26.9, 19.4.

TLC: R_f = 0.64 (5% EtOAc in hexanes, KMnO₄ stain).

2-iodocyclohex-2-en-1-one (5.30):



5.30

Experimental: K₂CO₃ (1.67 g, 12.0 mmol) was added to a solution of cyclohex-2-en-1-one (0.970 mL, 10.0 mmol) in 1:1 THF/H₂O (25 mL each). DMAP (246 mg, 2.0 mmol) was added, followed by I₂ (1.91 g, 15.0 mmol). After 17 hours, the reaction mixture was diluted with 100

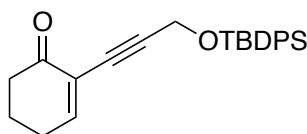
mL EtOAc, washed with sat. aq. Na₂SO₃ (70 mL), and the layers separated. The organic layer was dried with MgSO₄, filtered, and concentrated to yield **5.30** (955 mg, 42%) as an orange solid. Spectral data was consistent with the literature.³⁶

Physical State: Orange solid.

¹H NMR (500 MHz, CDCl₃, 25 °C) δ 7.76 (td, *J* = 4.4, 2.3 Hz, 1H), 2.68–2.59 (m, 2H), 2.43 (qd, *J* = 5.2, 4.4, 3.0 Hz, 2H), 2.08 (ddt, *J* = 10.5, 4.4, 2.7 Hz, 2H).

TLC: R_f = 0.50 (30% EtOAc in hexanes, KMnO₄ stain).

2-(3-((*tert*-butyldiphenylsilyl)oxy)prop-1-yn-1-yl)cyclohex-2-en-1-one (5.31):



5.31

Experimental: To a flame dried 1-dram vial was weighed enone **5.30** (35 mg, 0.16 mmol), alkyne **5.29** (65 mg, 0.21 mmol), CuI (6.2 mg, 0.032 mmol), and PdCl₂(PPh₃)₂ (22 mg, 0.032 mmol). The vial was degassed with three vacuum/argon cycles and Et₃N (0.32 mL) added. After 19 hours the volatiles were removed under reduced pressure. The slurry was redissolved in CH₂Cl₂ and H₂O and extracted three times with CH₂Cl₂. The organic layers were washed with brine, dried over MgSO₄, filtered, and concentrated. Purification by column chromatography (hexanes to 15% EtOAc in hexanes) afforded a mixture of **5.29** and enone **5.31** (37 mg, 60%) as a yellow oil.

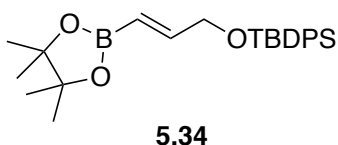
Physical State: Yellow oil.

¹H NMR (500 MHz, CDCl₃, 25 °C) δ 7.72–7.62 (m, 9H), 7.42–7.29 (m, 15H), 7.09 (t, *J* = 4.4 Hz, 1H), 6.81 (t, *J* = 6.0 Hz, 1H), 4.52 (d, *J* = 6.0 Hz, 2H), 4.36 (s, 2H), 2.51–2.45 (m, 2H), 2.41 (q, *J* = 5.7 Hz, 2H), 1.99 (dq, *J* = 8.1, 6.1 Hz, 2H), 1.06–0.99 (m, 20H).

IR (thin film): 3070, 2929, 2855, 1589, 1427, 1109, 700 cm⁻¹.

TLC: R_f = 0.59 (30% EtOAc in hexanes, KMnO₄ stain).

(*E*)-tert-butyl diphenyl((3-(4,4,5,5-tetramethyl-1,3,2-dioxaborolan-2-yl)allyl)oxy)silane (5.34):



Experimental: Alkyne **5.29** (300 mg, 1 mmol) was added to a flame dried vial, and the vial degassed with three vacuum/argon cycles. CH₂Cl₂ (0.5 mL) and pinacol borane (0.16 mL, 1.1 mmol) were added dropwise, followed by Cp₂ZrHCl (26 mg, 0.10 mmol). The reaction mixture was stirred at rt for 46 hours. The reaction mixture was diluted with H₂O (2 mL) and extracted with Et₂O (3 x 3 mL). The organic layers were washed with sat. aq. sodium chloride (4 mL), dried over MgSO₄, filtered, and concentrated. Purification by column chromatography (hexanes to 30% EtOAc in hexanes) afforded **5.34** (121 mg, 28%) as a clear oil.

Spectral data was consistent with the literature.³⁷

Physical State: Clear oil.

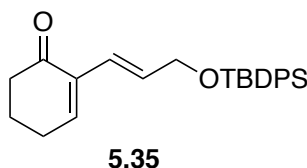
¹H NMR (500 MHz, CDCl₃, 25 °C) δ 7.67 (app. dd, *J* = 6.43, 1.44 Hz, 4H), 7.43–7.34 (m, 6H), 6.68 (dt, *J* = 6.43, 1.44 Hz, 4H), 5.95 (dt, *J* = 17.9, 2.1 Hz, 1H), 4.27 (dd, *J* = 3.2, 2.2 Hz, 2H), 1.29 (s, 12H), 1.06 (s, 9H).

¹³C NMR (125 MHz, CDCl₃, 25 °C) δ 151.9, 135.7, 135.1, 133.6, 129.8, 127.9, 114.1, 83.4, 77.5, 65.2, 64.81, 27.0, 25.0, 25.0, 24.7.

IR (thin film): 3071, 2857, 1644, 1339, 1109, 700 cm^{-1} .

TLC: $R_f = 0.50$ (5% EtOAc in hexanes, KMnO_4 stain).

(E)-2-(3-((tert-butyl)phenyl)silyloxy)prop-1-en-1-yl)cyclohex-2-en-1-one (5.35):



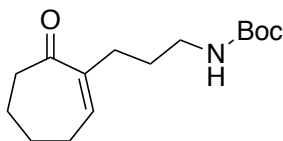
Experimental: All solvents were degassed prior to use, and the reaction was run under an atmosphere of argon. To a Schlenk flask was added enone **5.30** (42 mg, 0.18 mmol) $\text{PdCl}_2(\text{PhCN})_2$ (14 mg, 0.036 mmol), AsPh_3 (24 mg, 0.072 mmol), and Ag_2O (67 mg, 0.29 mmol) were added. The Schlenk flask was degassed with three vacuum/argon cycles. A solution of boronic ester **5.34** (121 mg, 0.286 mmol) in THF (0.8 mL), along with H_2O (0.1 mL) were added to the Schlenk flask. The reaction was stirred at rt for 23 hours. The reaction mixture was quenched with 1 mL sat. aq. NH_4Cl and stirred for 1 hour. The layers were separated, and the aqueous layer was extracted with Et_2O (3 x 2 mL). The organic layers were washed with H_2O (2 x 2 mL) and sat. aq. sodium chloride (2 mL). The organic layers were dried over MgSO_4 , filtered, and concentrated. Purification by column chromatography (hexanes to 30% EtOAc in hexanes) afforded **5.34** (45 mg, 62%) as a light yellow, viscous oil.

Physical State: Light yellow, viscous oil.

$^1\text{H NMR}$ (500 MHz, CDCl_3 , 25 $^\circ\text{C}$) δ 7.68 (dt, $J = 6.6, 1.5$ Hz, 6H), 7.43–7.35 (m, 11H), 6.93 (t, $J = 4.4$ Hz, 1H), 6.45 (app. dd, $J = 15.9, 0.7$ Hz, 1H), 6.29 (dt, $J = 15.9, 4.9$ Hz, 1H), 4.28 (d, $J = 4.0$ Hz, 2H), 2.43 (dd, $J = 11.5, 6.4$ Hz, 4H), 1.99 (pent, $J = 6.1$ Hz, 2H), 1.07 (s, 9H).

TLC: $R_f = 0.55$ (30% EtOAc in hexanes, KMnO_4 stain).

***tert*-butyl (3-(7-oxocyclohept-1-en-1-yl)propyl)carbamate (5.40):**



5.40

Experimental: *All solvents were degassed prior to use, and the reaction was run under an atmosphere of argon.* To a solution of *N*-Boc allylamine **5.39** (60 mg, 0.38 mmol) and THF (0.63 mL) in a Schlenk flask was added 0.50 M 9-BBN (1.1 mL, 0.55 mmol) slowly at rt. The mixture was stirred for 4 hours before H₂O (0.09 mL, 5 mmol) was added. PdCl₂(dppf)₂ (61 mg, 0.075 mmol), AsPh₃ (23 mg, 0.075 mmol), and Cs₂CO₃ (181 mg, 0.550 mmol) were added to a separate Schlenk flask, and the Schlenk flask was degassed with four vacuum/argon cycles. A solution of bromoenone **5.28** (47 mg, 0.25 mmol) in DMF (0.8 mL) was transferred to the second Schlenk flask. Another 0.9 mL DMF was used to transfer any remaining **5.28** from the original vial to the Schlenk flask. The Schlenk flask was again degassed with three vacuum/argon cycles, and the mixture was stirred for 15 minutes. The solution of organoborane was transferred to the second Schlenk flask and the reaction was heated to 80 °C for 4 hours before being cooled back to rt. The mixture was filtered through a plug of silica with Et₂O and concentrated. The slurry was taken up in a 1:1 mixture of Et₂O to H₂O and extracted three times with Et₂O. The organic layers were washed three times with H₂O and once with brine, dried over MgSO₄, filtered, and concentrated under reduced pressure. The crude product was purified by column chromatography (hexanes to 60% EtOAc in hexanes) to afford enone **5.40** (60 mg, quantitative) as a slight yellow oil.

Physical State: Slight yellow oil.

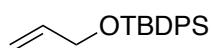
¹H NMR (500 MHz, CDCl₃, 25 °C) δ 6.54 (t, *J* = 6.0 Hz, 1H), 3.15 – 3.00 (m, 2H), 2.61 – 2.54 (m, 2H), 2.38 (q, *J* = 5.8 Hz, 2H), 2.25 (t, *J* = 7.4 Hz, 2H), 1.74 (dq, *J* = 18.5, 6.4 Hz, 4H), 1.56 (pent., *J* = 7.0 Hz, 2H), 1.44 (s, 9H).

¹³C NMR (125 MHz, CDCl₃, 25 °C) δ 205.4, 177.0, 143.1, 143.0, 134.2, 72.8, 72.0, 43.7, 42.8, 42.4, 40.1, 36.4, 30.33, 29.7, 28.6, 28.4, 27.7, 25.2, 22.8, 21.6, 20.7, 20.2, 17.7.

IR (thin film): 3358, 2929, 1688, 1519, 1365, 1249, 1165 cm⁻¹.

HRMS (ESI) *m/z*: calculated for CHNO (M + H)⁺: 268.1913, found: 268.1901

(allyloxy)(*tert*-butyl)diphenylsilane (5.43):



5.43

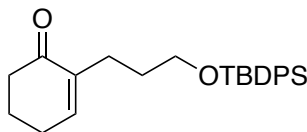
Experimental: To a solution of imidazole (656 mg, 9.60 mmol) in DMF (6.6 mL) was added allyl alcohol (0.54 mL, 8.0 mmol), followed by dropwise addition of TBDPSCl (2.3 mL, 8.8 mmol). The mixture was stirred at rt for 3 hours before being poured into a separatory funnel. H₂O (15 mL) was added and extracted with Et₂O (3 x 15 mL). The organic layers were washed with H₂O (4 x 10 mL) followed by sat. aq. sodium chloride (10 mL). The organic layers were dried over MgSO₄, filtered, and concentrated. The crude product was purified by column chromatography (hexanes to 60% EtOAc in hexanes) to afford enone **5.43** (2.82 g, quantitative) as a clear oil.

Spectral data was consistent with the literature.³⁸

Physical State: Clear oil.

¹H NMR (500 MHz, CDCl₃, 25 °C) δ 7.72–7.68 (m, 4H), 7.47–7.36 (m, 6H), 5.94 (ddt, *J* = 17.1, 10.5, 4.3 Hz, 1H), 5.39 (dt, *J* = 17.1, 2.0 Hz, 1H), 5.13 (dt, *J* = 10.5, 1.8 Hz, 1H), 4.23 (dt, *J* = 3.8, 1.6 Hz, 2H), 1.08 (s, 9H).

2-(3-((*tert*-butyldiphenylsilyl)oxy)propyl)cyclohex-2-en-1-one (5.44):



5.44

Experimental: *All solvents were degassed prior to use, and the reaction was run under an atmosphere of argon.* To a solution of TBDPS allyl alcohol **5.43** (116 mg, 0.380 mmol) and THF (0.6 mL) in a Schlenk flask was added 0.50 M 9-BBN (1.1 mL, 0.55 mmol) slowly at rt. The mixture was stirred for 4 hours before H₂O (0.09 mL, 5 mmol) was added. PdCl₂(dppf)₂ (61 mg, 0.075 mmol), AsPh₃ (24 mg, 0.075 mmol), and Cs₂CO₃ (182 mg, 0.550 mmol) were added to a separate Schlenk flask, and the atmosphere degassed with four vacuum/argon cycles. A solution of bromoenone **5.28** (44 mg, 0.25 mmol) in DMF (0.8 mL) was transferred to the second Schlenk flask. Another 0.3 mL DMF was used to transfer any remaining **5.28** from the original vial to the Schlenk flask. The Schlenk flask was again degassed with three vacuum/argon cycles, and the mixture was stirred for 15 minutes. The solution of organoborane was transferred to the second Schlenk flask and the reaction was heated to 80 °C for 3 days before being cooled back to rt. The mixture was filtered through a plug of silica with Et₂O and concentrated. The slurry was taken up in a 1:1 mixture of Et₂O to H₂O and extracted three times with Et₂O. The organic layers were washed three times with H₂O and once with brine, dried over MgSO₄, filtered, and concentrated under reduced pressure. The crude product was purified by column chromatography (hexanes to 60% EtOAc in hexanes) to afford enone **5.40** (63 mg, 64%) as a slight yellow oil.

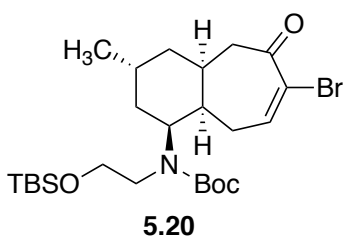
Spectral data was consistent with the literature.³⁹

Physical State: Slight yellow oil.

¹H NMR (500 MHz, CDCl₃, 25 °C) δ 7.73–7.70 (m, 2H), 7.66 (dd, *J* = 7.9, 1.5 Hz, 4H), 7.43–7.35 (m, 9H), 6.65 (t, *J* = 4.1 Hz, 1H), 3.64 (t, *J* = 6.4 Hz, 2H), 2.44–2.35 (m, 4H), 1.98–1.90 (m, 2H), 1.90–1.83 (m, 2H), 1.71–1.63 (m, 2H), 1.54 (ddd, *J* = 8.6, 7.3, 4.9 Hz, 2H), 1.06 (d, *J* = 10.4 Hz, 14H).

TLC: *R*_f = 0.38 (15% EtOAc in hexanes, KMnO₄ stain).

Bromoeneone (5.20):



Experimental: To a solution of enoxysilane **5.19** (89 mg, 0.16 mmol) in petroleum ether (0.85 mL, dried over MgSO₄) at –20 °C was added sublimed KO^t-Bu (54 mg, 0.48 mmol) in one portion, followed by freshly distilled bromoform (0.05 mL, 0.5 mmol) dropwise. The reaction mixture was allowed to stir at –20 °C until starting material was consumed as observed by TLC. After 1.5 h, the mixture was poured into water (1 mL). The organic layer was separated and the aqueous layer was extracted with EtOAc (3 x 1 mL). The combined organic layers were combined, dried over Na₂SO₄, filtered, and concentrated in vacuo. The residue was dissolved in acetone (1.1 mL), followed by the addition of calcium carbonate (87 mg, 0.80 mmol) and silver perchlorate monohydrate (141 mg, 0.64 mmol). The mixture was stirred at 25 °C overnight, during which time a dark precipitate developed. The next morning, the reaction was quenched by the addition of Et₃N (0.15 mL, 0.80 mmol) and silica gel (70 mg), and the mixture concentrated *in vacuo*. The resulting solids were vacuum filtered through a plug of silica using EtOAc as the eluent. Evaporation of the solvent, followed by subsequent re-purification by column

chromatography (hexanes to 20% EtOAc in hexanes) gave bromoenone **5.20** (41 mg, 48%) as a pale, yellow oil.

Physical State: Pale, yellow oil.

¹H NMR (500 MHz, CDCl₃, 25 °C) δ 7.29 (dd, *J* = 9.5, 2.6 Hz, 1H), 4.03 (d, *J* = 13.4 Hz, 1H), 3.73–3.61 (m, 2H), 3.42 (s, 1H), 3.12 (dt, *J* = 14.0, 7.1 Hz, 1H), 2.77–2.68 (m, 1H), 2.42–2.28 (m, 4H), 2.21 (dd, *J* = 17.6, 9.4 Hz, 2H), 1.84 (s, 1H), 1.06 (d, *J* = 7.3 Hz, 3H), 0.89 (s, 9H), 0.05 (s, 6H).

¹³C NMR (125 MHz, CDCl₃, 25 °C) δ 195.4, 155.5, 148.9, 126.2, 80.1, 62.1, 53.4, 49.3, 47.7, 33.8, 31.4, 30.9, 29.9, 28.7, 28.0, 26.2, 25.8, 18.6, 18.2, 0.2, -3.4, -5.08, -5.10.

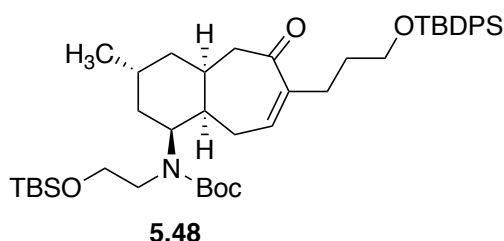
IR (thin film): 2954, 2856, 1688, 1460, 1365, 1250, 1146, 1099, 834 cm⁻¹.

HRMS (ESI) *m/z*: calculated for CHNO (M + Na)⁺: , found:

[α]_D²⁴ = -7.42 (*c* 0.950, CHCl₃).

TLC: R_f = 0.41 (15% EtOAc in hexanes, KMnO₄ stain).

Enone (5.48):



Experimental: All solvents were degassed prior to use, and the reaction was run under an atmosphere of argon. To a solution of TBDPS allyl alcohol **5.43** (39 mg, 0.12 mmol) and THF (0.2 mL) in a Schlenk flask was added 0.50 M 9-BBN (0.35 mL, 0.17 mmol) slowly at rt. The mixture was stirred for 4 hours before H₂O (0.03 mL, 2 mmol) was added. PdCl₂(dppf)₂ (21 mg, 0.024 mmol), AsPh₃ (9 mg, 0.03 mmol), and Cs₂CO₃ (62 mg, 0.18 mmol) were added to a

separate Schlenk flask, and the atmosphere degassed with four vacuum/argon cycles. A solution of bromoenone **5.20** (43 mg, 0.080 mmol) in DMF (0.5 mL) was transferred to the second Schlenk flask. The Schlenk flask was again degassed with three vacuum/argon cycles, and the mixture was stirred for 10 minutes. The solution of organoborane was transferred to the second Schlenk flask and the reaction was heated to 80 °C for 19 hours before being cooled back to rt. The mixture was filtered through a plug of silica with Et₂O as the eluent. The slurry was taken up in Et₂O (3 mL), H₂O (3 mL) added, and the aqueous layer extracted with Et₂O (3 x 3mL). The organic layers were dried over MgSO₄, filtered, and concentrated under reduced pressure. Purification by column chromatography (hexanes to 15% EtOAc in hexanes) afforded enone **5.48** (63 mg, 64%) as a clear oil.

Physical State: Clear oil.

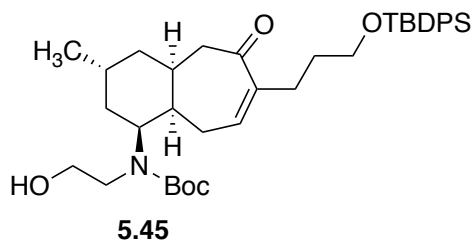
¹H NMR (500 MHz, CDCl₃, 25 °C) δ 7.68–7.62 (m, 4H), 7.45–7.34 (m, 6H), 6.44 (d, *J* = 8.1 Hz, 1H), 4.02 (br d, *J* = 11.7 Hz, 1H), 3.73–3.55 (m, 4H), 3.46 (br s, 1H), 3.11 (dt, *J* = 14.1, 7.1 Hz, 1H), 2.47 (dd, *J* = 10.6, 5.8 Hz, 1H), 2.43–2.13 (m, 7H), 2.07 (dd, *J* = 17.6, 8.9 Hz, 1H), 1.64–1.57 (m, 3H), 1.40 (s, 9H), 1.04 (s, 9H), 0.89 (s, 9H), 0.07–0.02 (m, 6H).

¹³C NMR (125 MHz, CDCl₃, 25 °C) δ 203.9, 155.6, 144.2, 142.8, 135.8, 135.8, 134.2, 134.2, 129.7, 127.8, 79.8, 63.5, 53.4, 50.6, 34.0, 32.0, 31.6, 30.9, 29.9, 29.5, 28.7, 28.2, 27.1, 26.2, 24.0, 19.43, 18.6, 18.3, 0.2, –5.05, –5.08.

HRMS (ESI) *m/z*: calculated for C₄₄H₆₉NO₅Si₂ (M + Na)⁺: 770.4612, found: 770.4604.

TLC: R_f = 0.62 (15% EtOAc in hexanes, KMnO₄ stain).

Alcohol (5.45):



Experimental: Enone **5.48** (26 mg, 0.035 mmol) was weighed into a vial and the atmosphere was changed to argon. A freshly made stock solution of 1-chloroethyl chloroformate (0.10 mL, 0.011 M) was added to the vial, and the reaction was monitored by TLC. After 21 hours the reaction was quenched by addition of sat. aq. NaHCO₃ (0.5 mL), and the aqueous layer was extracted with Et₂O (3 x 2 mL). The organic layers were dried over MgSO₄, filtered, and concentrated. Purification by column chromatography (hexanes to 15% EtOAc in hexanes) afforded enone **5.45** (18 mg, 80%) as a clear oil.

Crude material was taken on without purification to next step.

Physical State: Clear oil.

¹H NMR (500 MHz, CDCl₃, 25 °C) δ 7.65 (dtd, *J* = 6.7, 4.1, 3.6, 1.6 Hz, 4H), 7.43–7.35 (m, 7H), 6.44 (d, *J* = 7.7 Hz, 1H), 4.02 (dt, *J* = 14.0, 4.0 Hz, 1H), 3.76–3.58 (m, 6H), 3.25 (dt, *J* = 14.7, 4.8 Hz, 1H), 2.47 (app dt, *J* = 10.3, 5.6, 4.5 Hz, 1H) 2.42–2.15 (m, 8H), 2.08 (dd, *J* = 17.7, 8.8 Hz, 1H), 1.61 (dq, *J* = 8.9, 6.5, 4.7 Hz, 3H), 1.51–1.43 (m, 3H), 1.40 (s, 11H), 1.26 (d, *J* = 2.5 Hz, 3H), 1.08–1.02 (m, 14H).

HRMS (ESI) *m/z*: calculated for C₃₈H₅₅NO₅Si (M + Na)⁺: 656.3747, found: 656.3750.

TLC: R_f = 0.29 (33% EtOAc in hexanes, KMnO₄ stain).

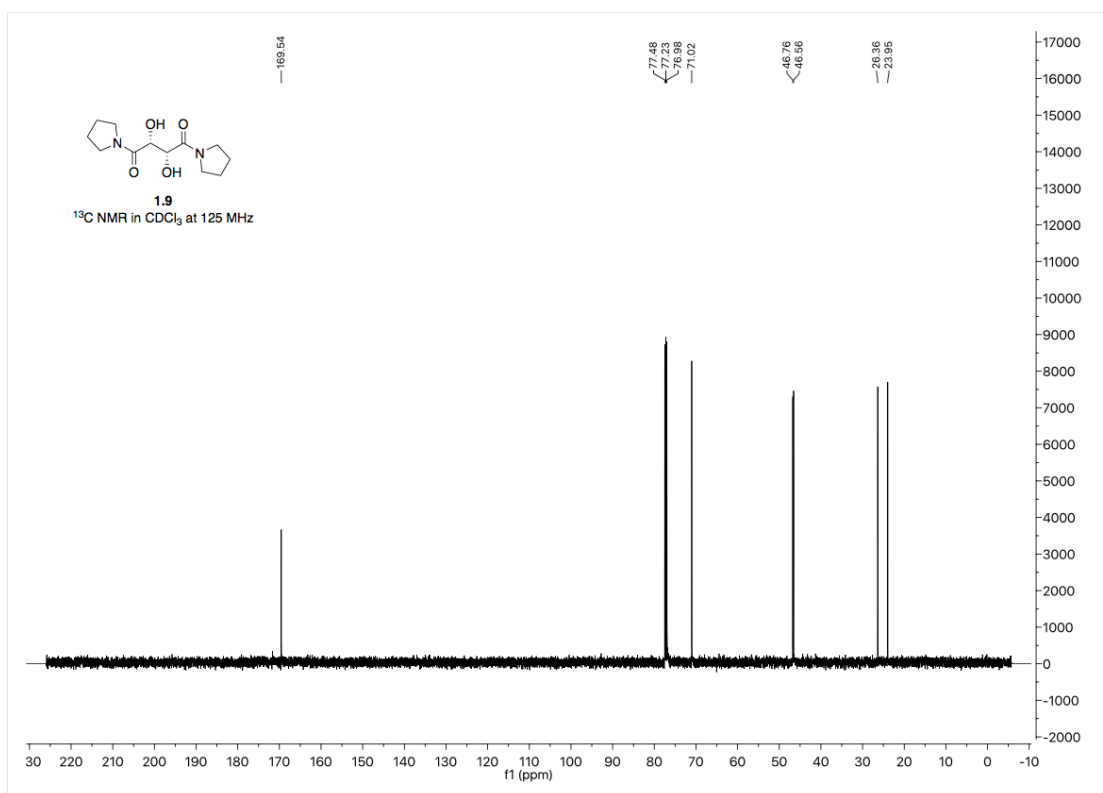
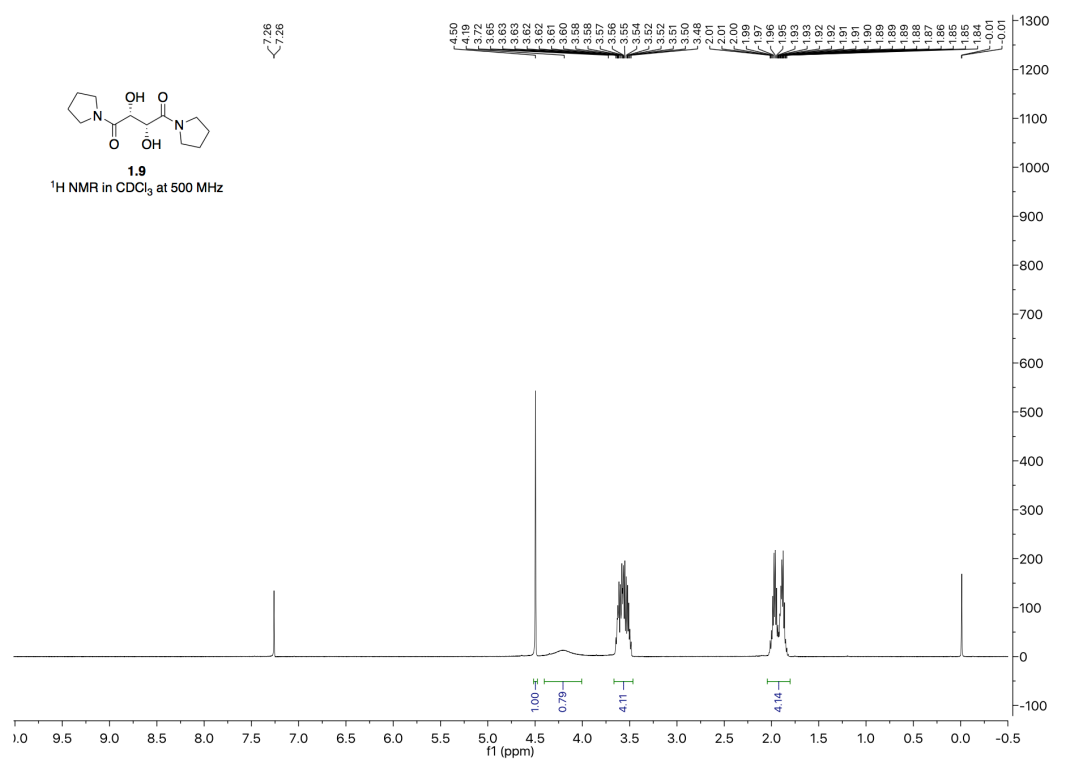
5.8 References:

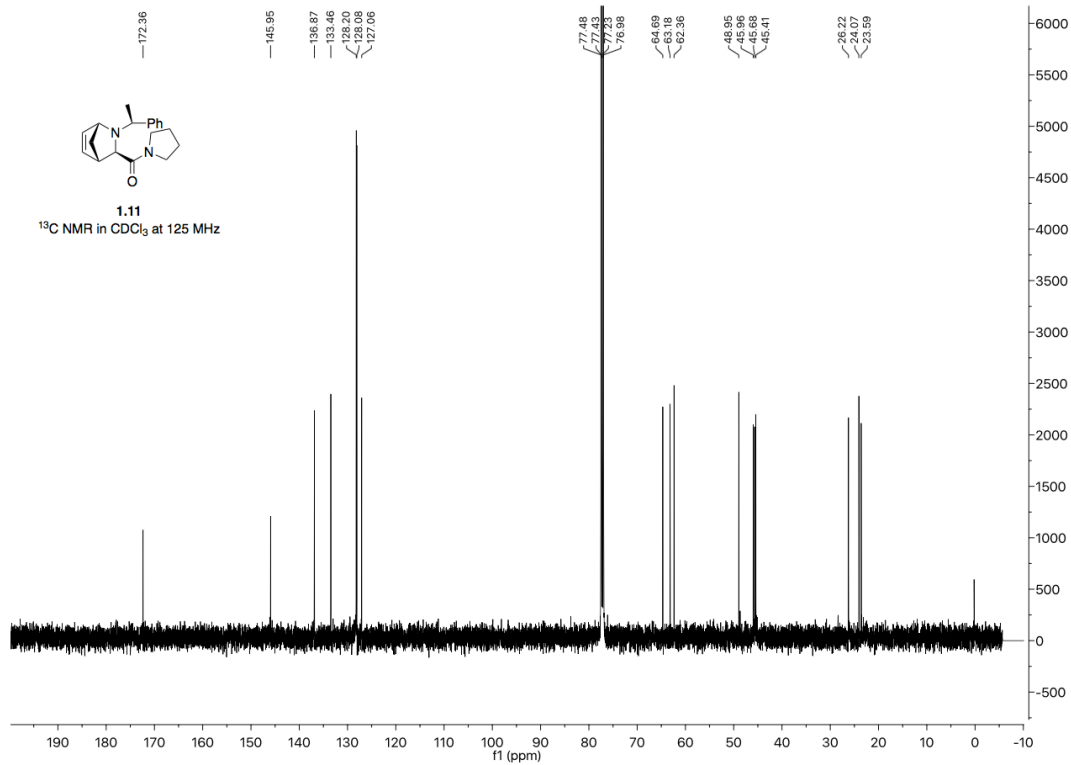
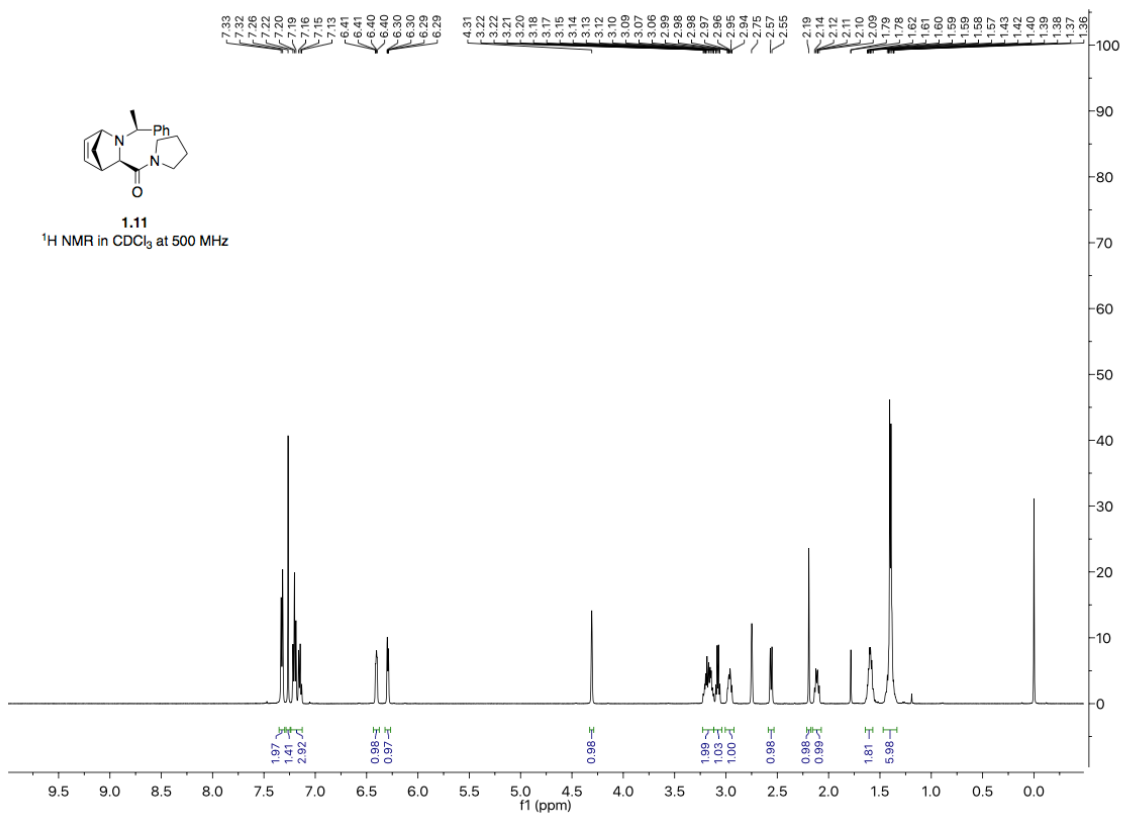
- (1) Samame, R. A.; Owens, C. M.; Rychnovsky, S. D. *Chem. Sci.* **2015**, 7 (1), 188–190.
- (2) Cheng, X.; Waters, S. P. *Org. Lett.* **2013**, 15 (16), 4226–4229.

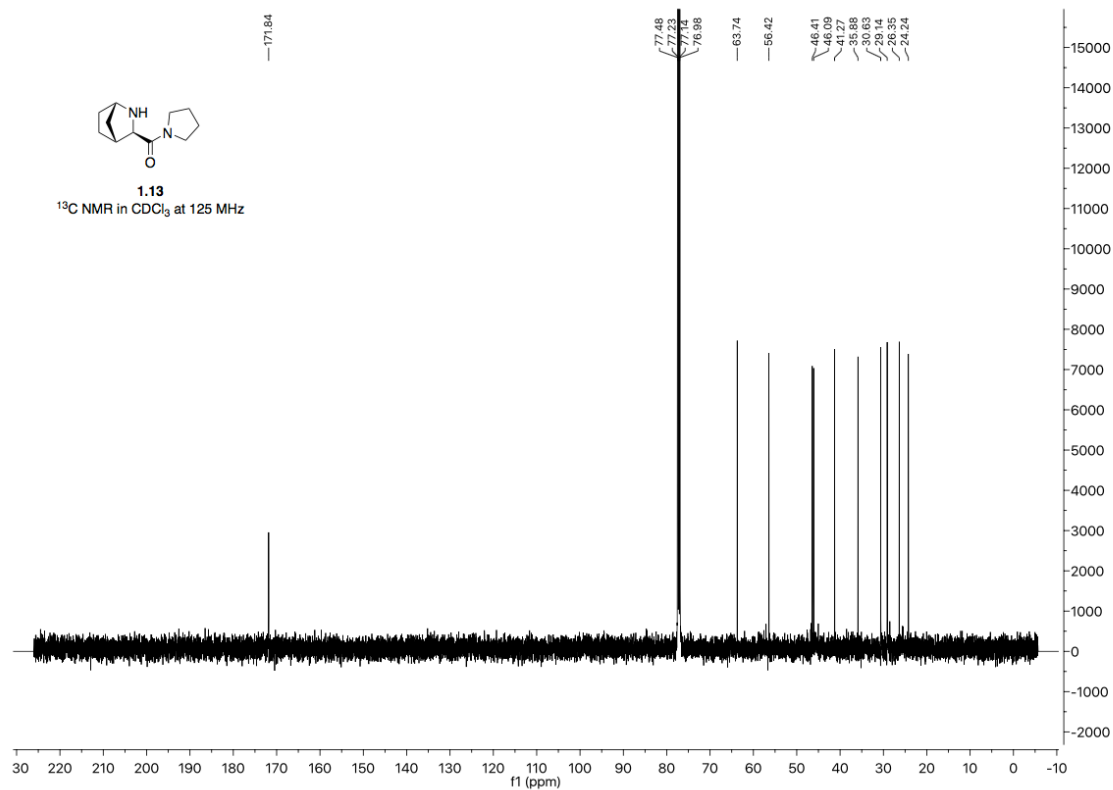
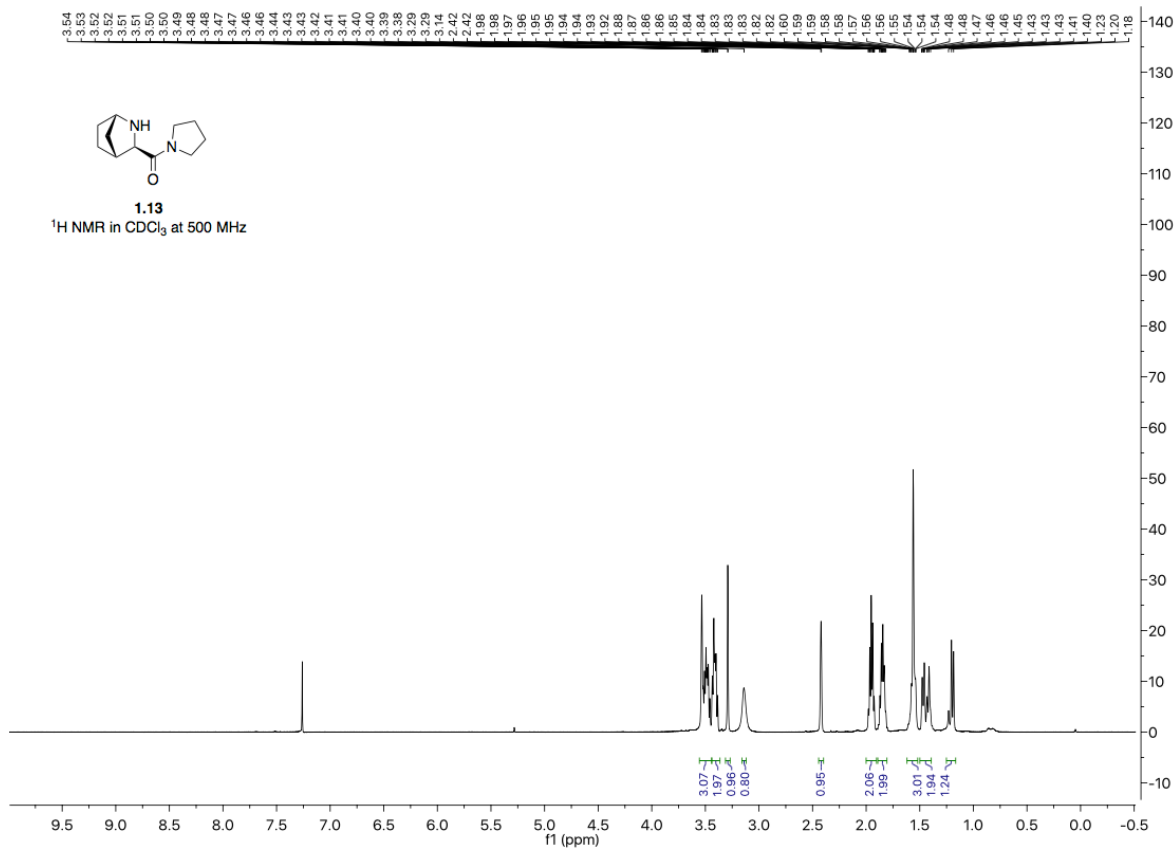
- (3) Nishimura, T.; Unni, A. K.; Yokoshima, S.; Fukuyama, T. *J. Am. Chem. Soc.* **2013**, *135* (8), 3243–3247.
- (4) Nishimura, T.; Unni, A. K.; Yokoshima, S.; Fukuyama, T. *J. Am. Chem. Soc.* **2011**, *133* (3), 418–419.
- (5) Yang, Y.; Haskins, C. W.; Zhang, W.; Low, P. L.; Dai, M. *Angew. Chem. Int. Ed.* **2014**, *53* (15), 3922–3925.
- (6) Chu, L.; Ohta, C.; Zuo, Z.; MacMillan, D. W. C. *J. Am. Chem. Soc.* **2014**, *136* (31), 10886–10889.
- (7) Miriyala, B.; Bhattacharyya, S.; Williamson, J. S. *Tetrahedron* **2004**, *60* (7), 1463–1471.
- (8) Menche, D.; Hassfeld, J.; Li, J.; Menche, G.; Ritter, A.; Rudolph, S. *Org. Lett.* **2006**, *8* (4), 741–744.
- (9) Einhorn, J.; Einhorn, C.; Luche, J.-L. *Synlett* **1991**, *1991* (1), 37–38.
- (10) Liu, K.-M.; Chau, C.-M.; Sha, C.-K. *Chem. Commun.* **2007**, No. 1, 91–93.
- (11) Burkhardt, E. R.; Matos, K. *Chem. Rev.* **2006**, *106* (7), 2617–2650.
- (12) Chea, H.; Sim, H.-S.; Yun, J. *Adv. Synth. Catal.* **2009**, *351* (6), 855–858.
- (13) Mun, S.; Lee, J.-E.; Yun, J. *Org. Lett.* **2006**, *8* (21), 4887–4889.
- (14) Molander, G. A.; Petrillo, D. E. *Org. Lett.* **2008**, *10* (9), 1795–1798.
- (15) Molander, G. A.; Ham, J.; Seapy, D. G. *Tetrahedron* **2007**, *63* (3), 768–775.
- (16) Klapars, A.; Buchwald, S. L. *J. Am. Chem. Soc.* **2002**, *124* (50), 14844–14845.
- (17) Izgu, E. C.; Hoye, T. R. *Chem. Sci.* **2013**, *4* (5), 2262–2266.
- (18) Kats-Kagan, R.; Herzon, S. B. *Org. Lett.* **2015**, *17* (8), 2030–2033.
- (19) Lin, H.; Yang, M.; Huang, P.; Cao, W. *Molecules* **2003**, *8* (8), 608–613.
- (20) Lee, A. S.; Liau, B. B.; Shair, M. D. *J. Am. Chem. Soc.* **2014**, *136* (38), 13442–13452.
- (21) Trost, B. M.; Probst, G. D.; Schoop, A. *J. Am. Chem. Soc.* **1998**, *120* (36), 9228–9236.
- (22) Yeom, C.-E.; Kim, Y. J.; Lee, S. Y.; Shin, Y. J.; Kim, B. M. *Tetrahedron* **2005**, *61* (52), 12227–12237.
- (23) Zhao, M.; Li, J.; Mano, E.; Song, Z.; Tschaen, D. M.; Grabowski, E. J. J.; Reider, P. J. *J. Org. Chem.* **1999**, *64* (7), 2564–2566.

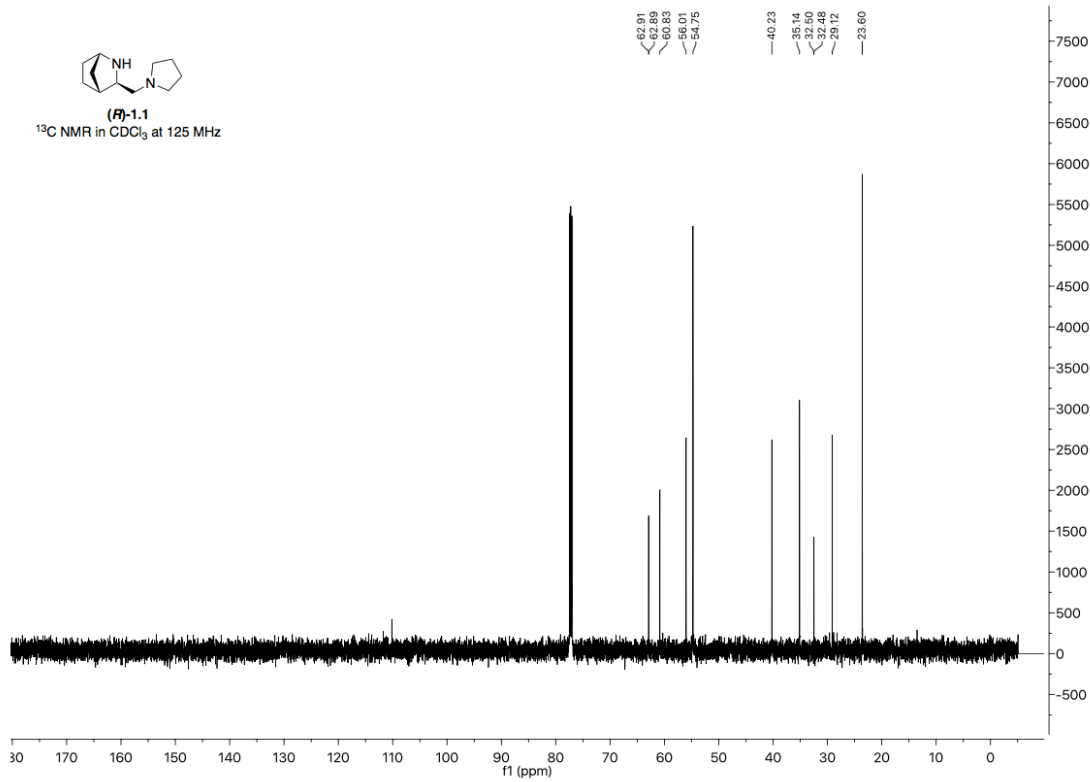
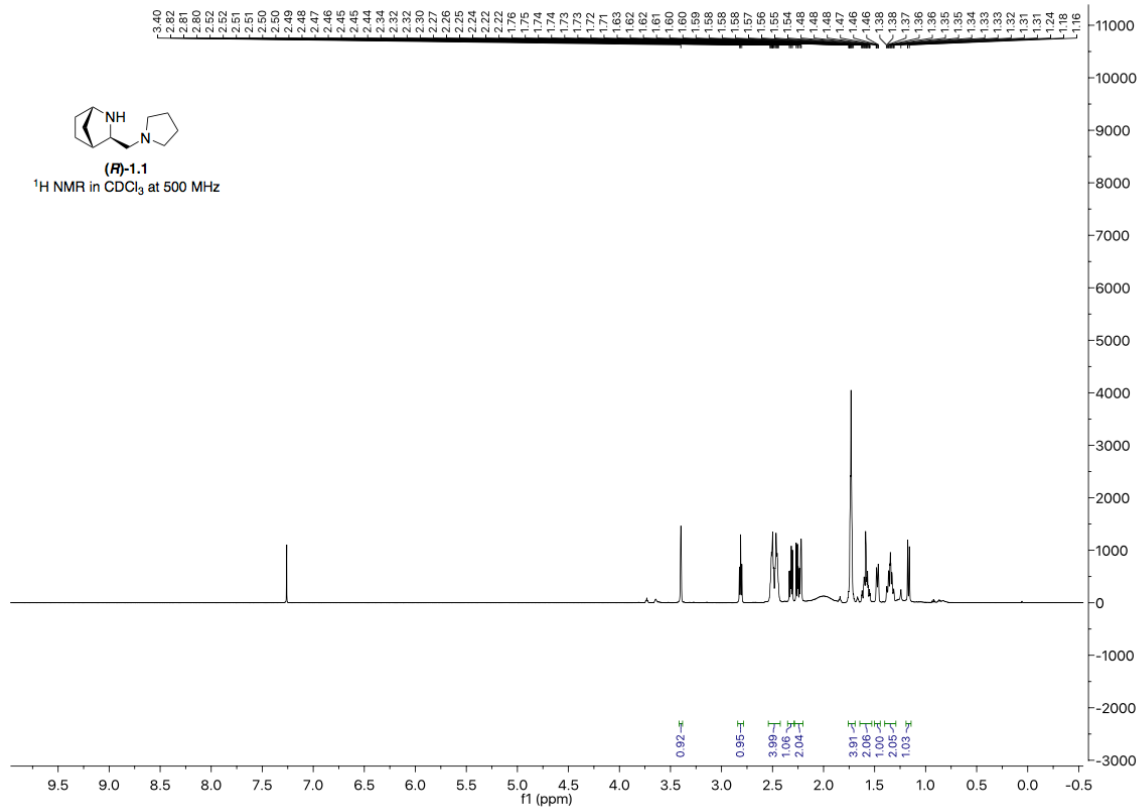
- (24) Pangborn, A. B.; Giardello, M. A.; Grubbs, R. H.; Rosen, R. K.; Timmers, F. J. *Organometallics* **1996**, *15* (5), 1518–1520.
- (25) Still, W. C.; Kahn, M.; Mitra, A. *J. Org. Chem.* **1978**, *43* (14), 2923–2925.
- (26) Li, K.; Alexakis, A. *Angew. Chem. Int. Ed.* **2006**, *45* (45), 7600–7603.
- (27) Tsui, G. C.; Menard, F.; Lautens, M. *Org. Lett.* **2010**, *12* (11), 2456–2459.
- (28) Nangia, A.; Prasuna, G. *Synth. Commun.* **1994**, *24* (14), 1989–1998.
- (29) Kozak, J. A.; Dake, G. R. *Angew. Chem. Int. Ed.* **2008**, *47* (22), 4221–4223.
- (30) Scheller, M. E.; Frei, B. *Helv. Chim. Acta* **1990**, *73* (4), 922–931.
- (31) Mukherjee, S.; Corey, E. J. *Org. Lett.* **2010**, *12* (3), 632–635.
- (32) Inman, M.; Moody, C. J. *J. Org. Chem.* **2010**, *75* (17), 6023–6026.
- (33) Gao, M.; Thorpe, S. B.; Santos, W. L. *Org. Lett.* **2009**, *11* (15), 3478–3481.
- (34) Zhao, D.; Fei, Z.; Ohlin, C. A.; Laurency, G.; Dyson, P. J. *Chem. Commun.* **2004**, No. 21, 2500–2501.
- (35) Choi, S.; Breugst, M.; Houk, K. N.; Poulter, C. D. *J. Org. Chem.* **2014**, *79* (8), 3572–3580.
- (36) Rossi, R.; Carpita, A.; Bellina, F.; Cossi, P. *J. Organomet. Chem.* **1993**, *451* (1), 33–43.
- (37) Berrée, F.; Gernigon, N.; Hercouet, A.; Lin, C. H.; Carboni, B. *Eur. J. Org. Chem.* **2009**, *2009* (3), 329–333.
- (38) Waser, J.; Nambu, H.; Carreira, E. M. *J. Am. Chem. Soc.* **2005**, *127* (23), 8294–8295.
- (39) Ridgway, B. H.; Woerpel, K. A. *J. Org. Chem.* **1998**, *63* (3), 458–460.

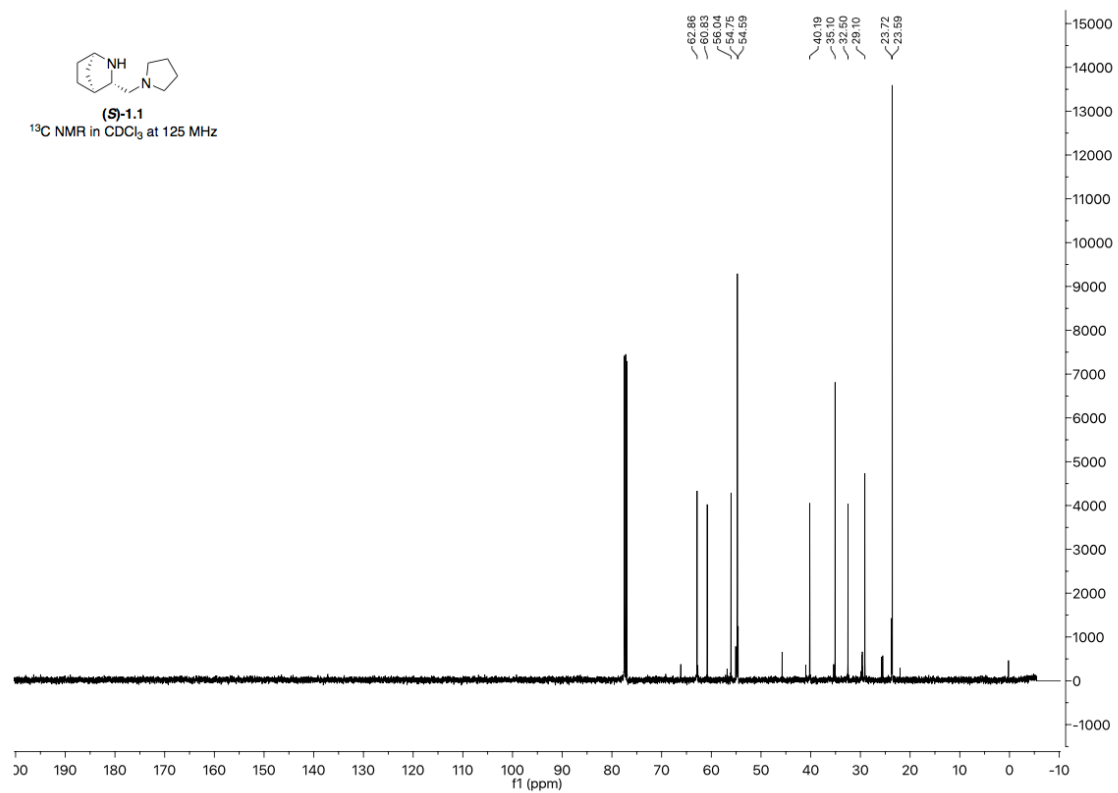
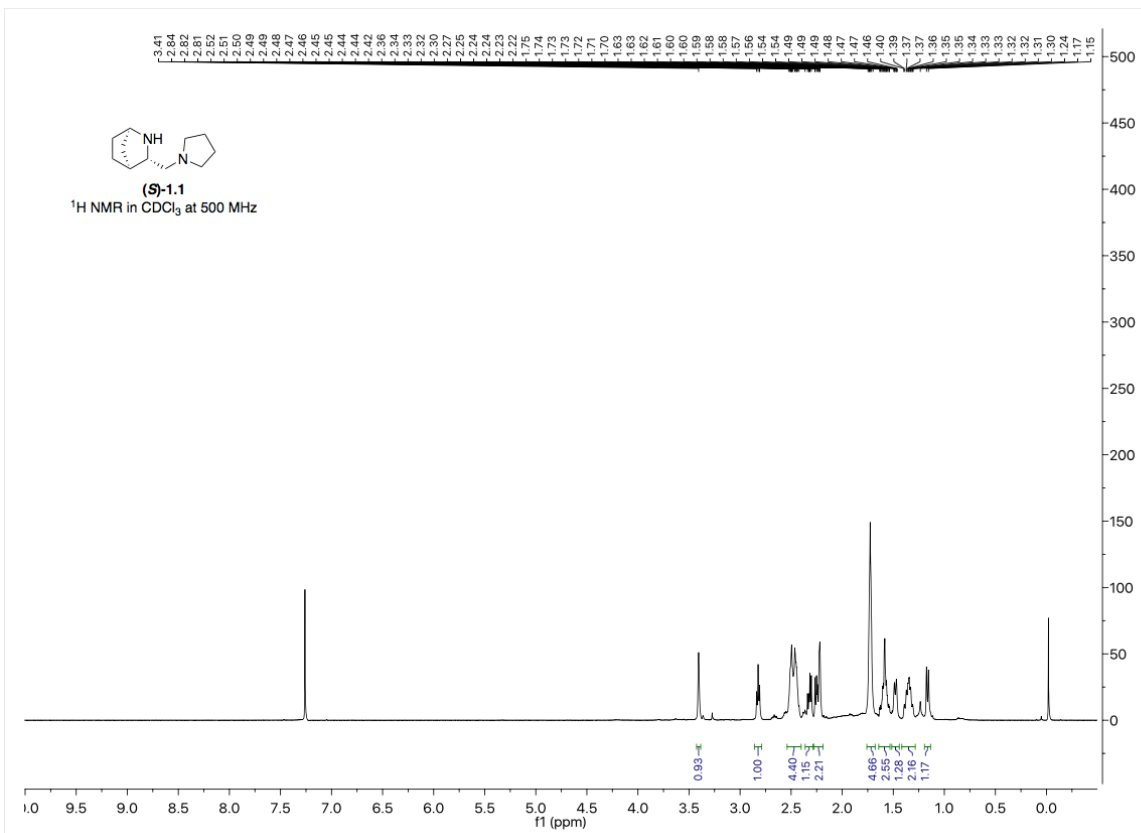
Appendix A. Chapter 1 Supporting Data

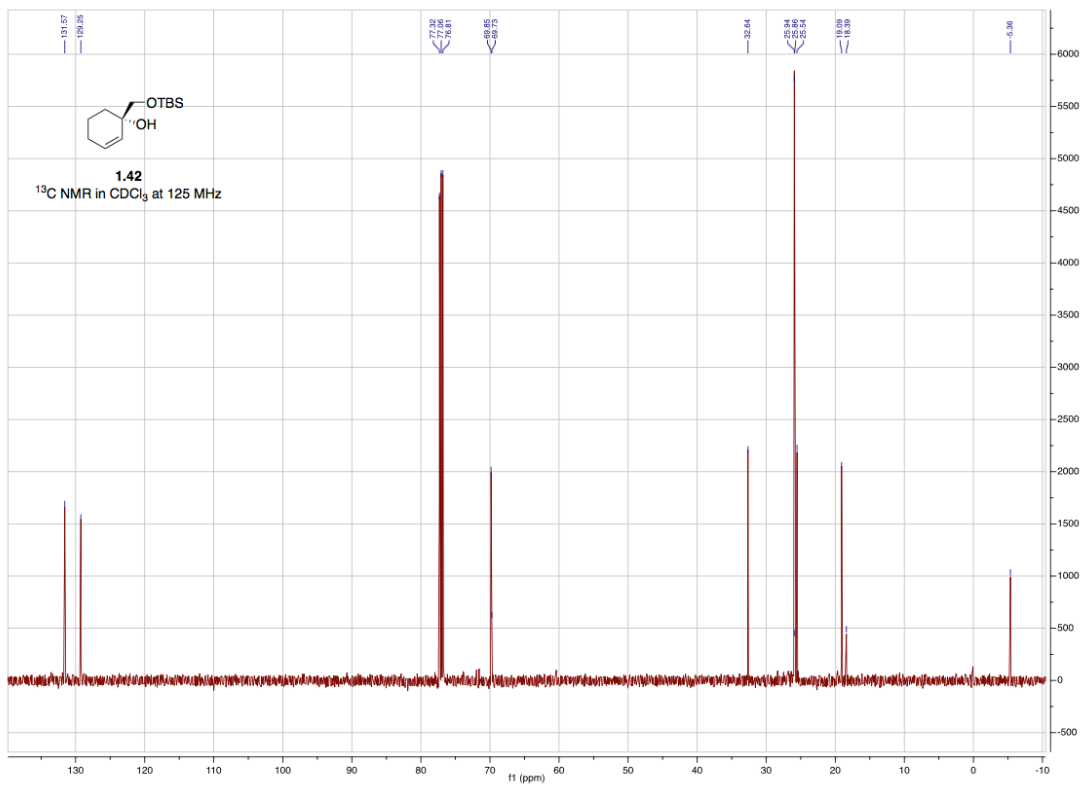
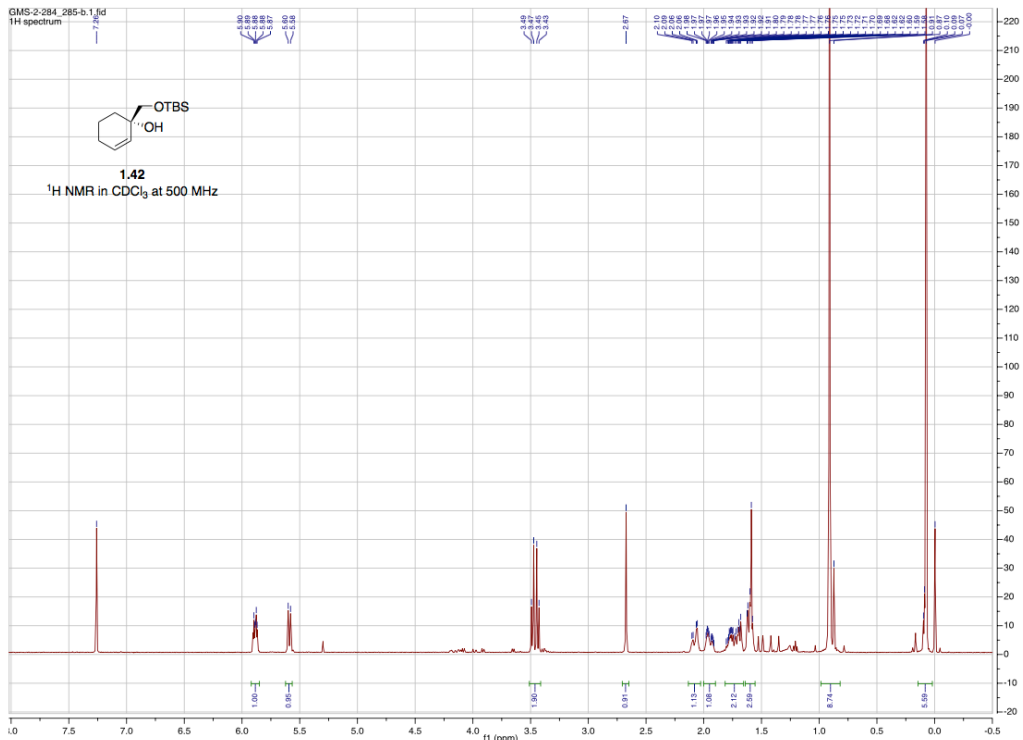


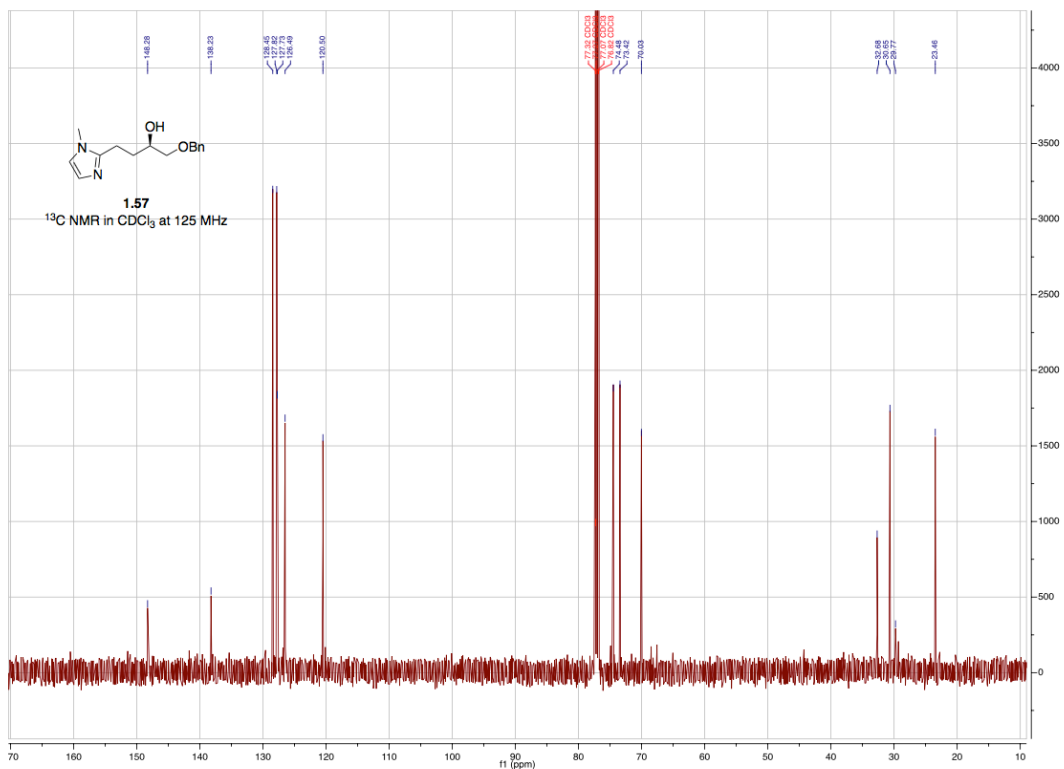
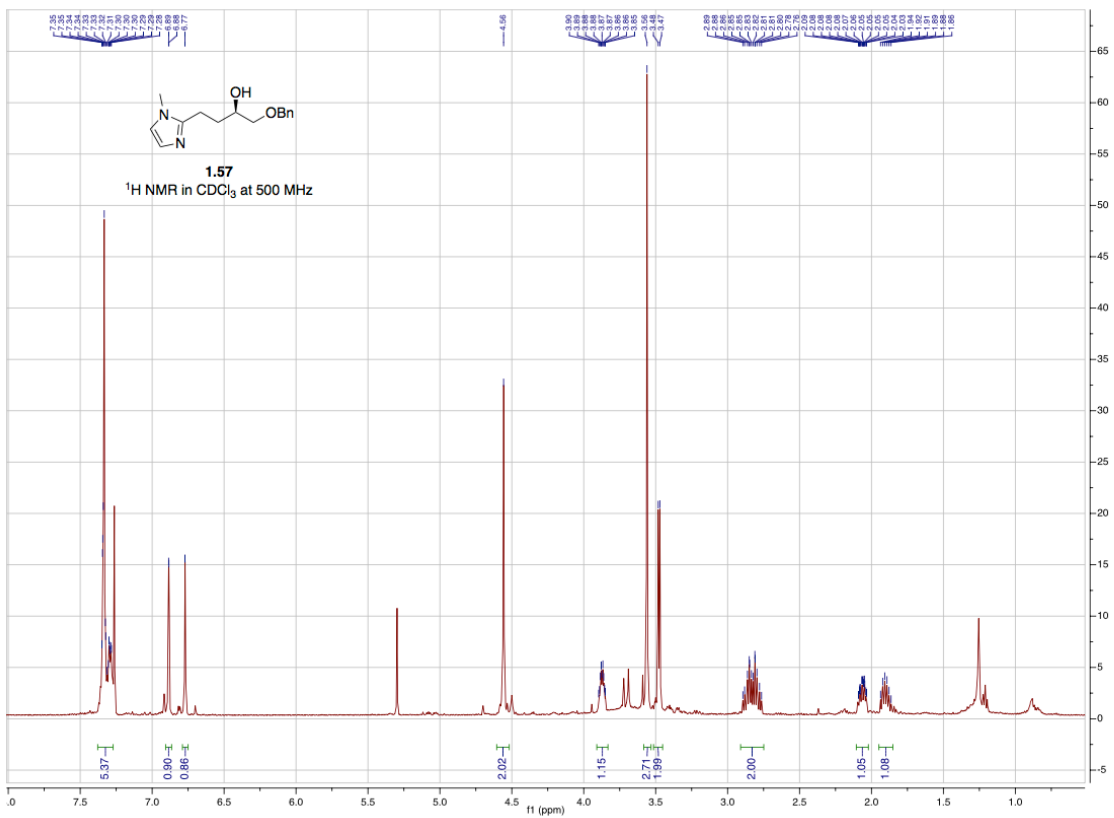




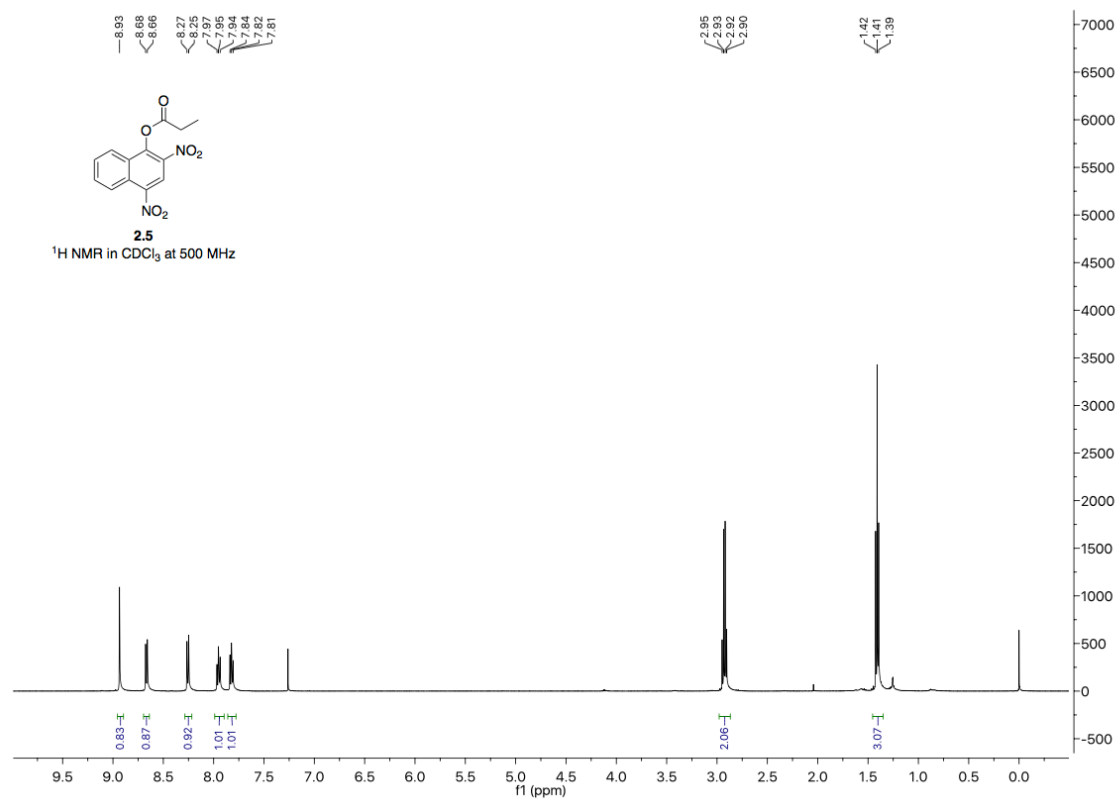
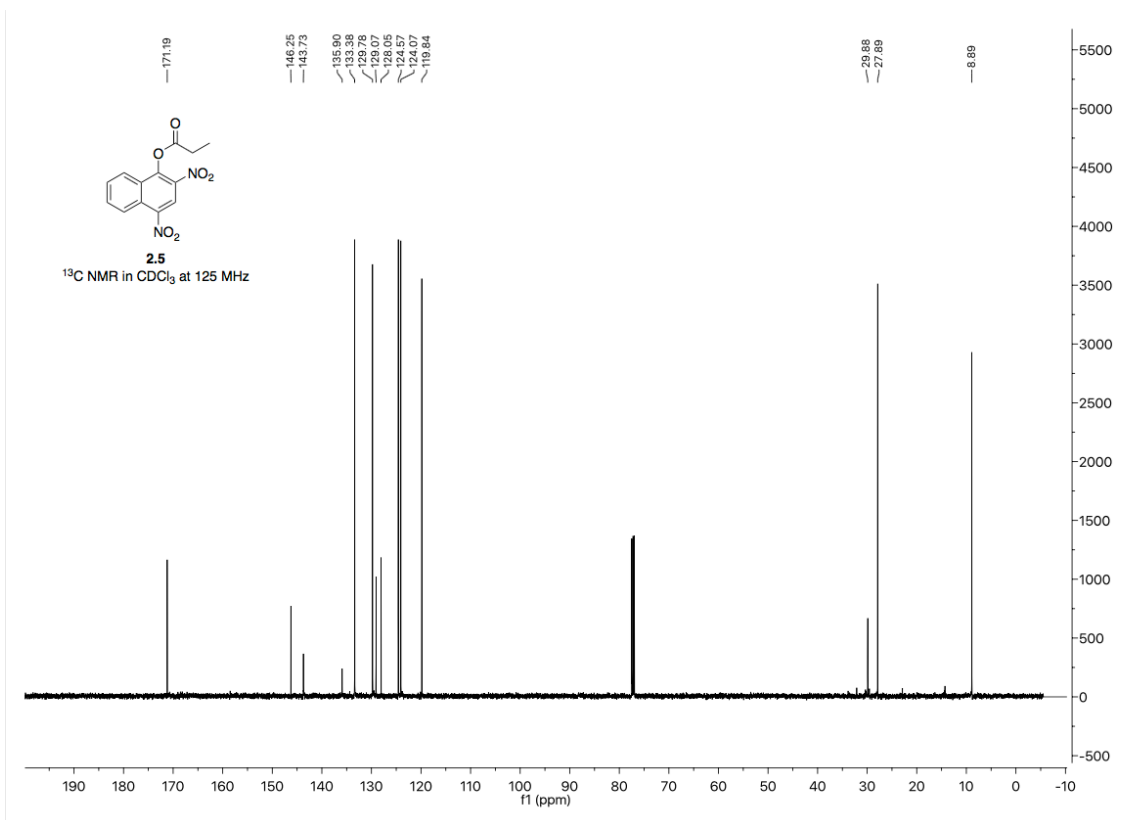


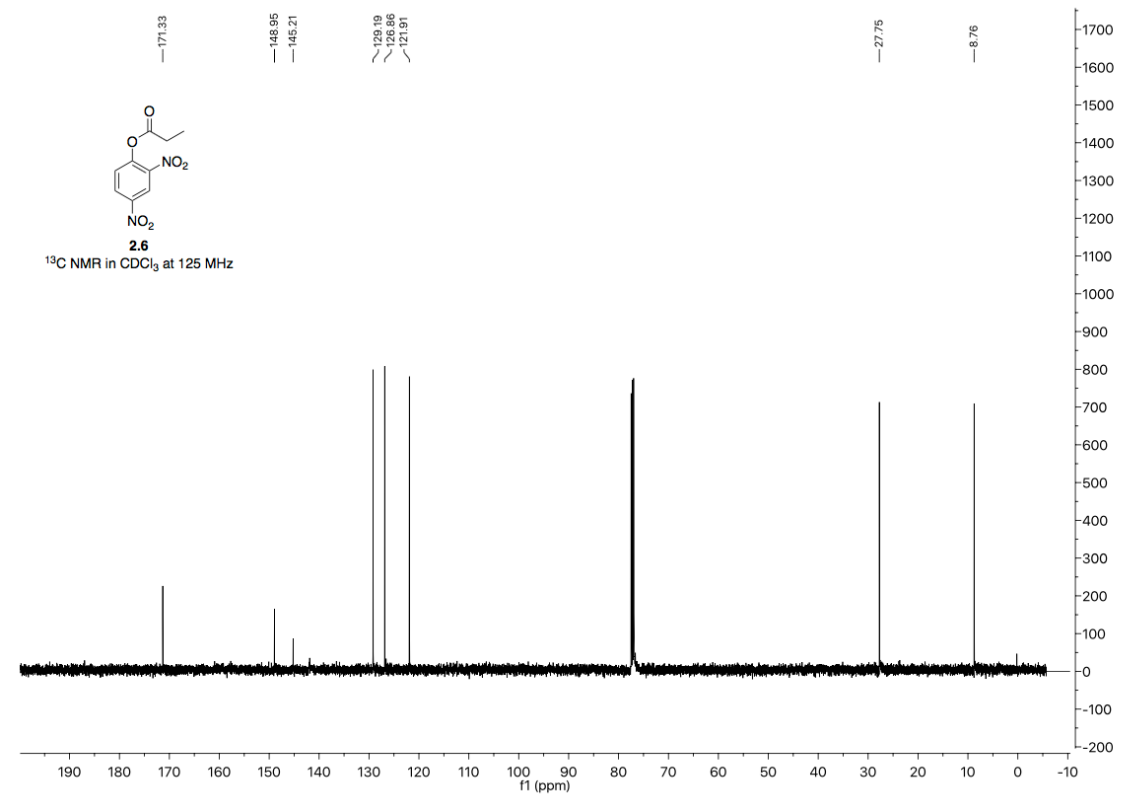
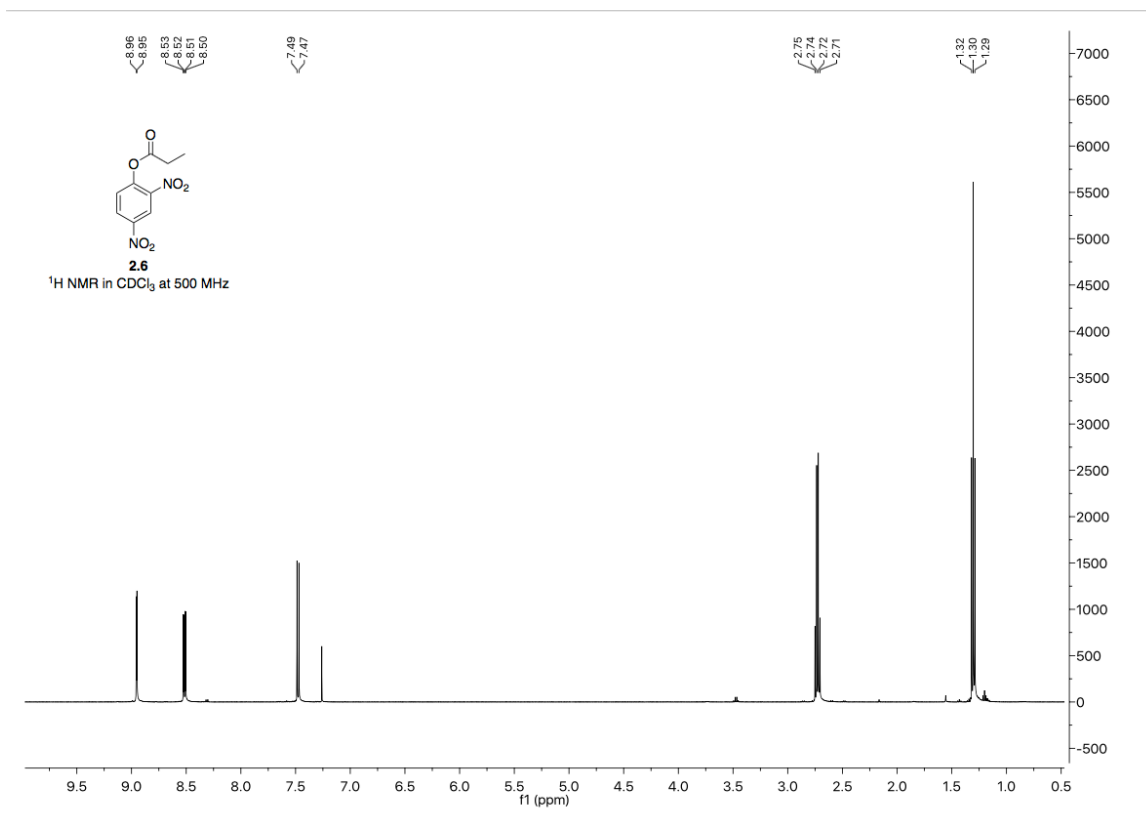


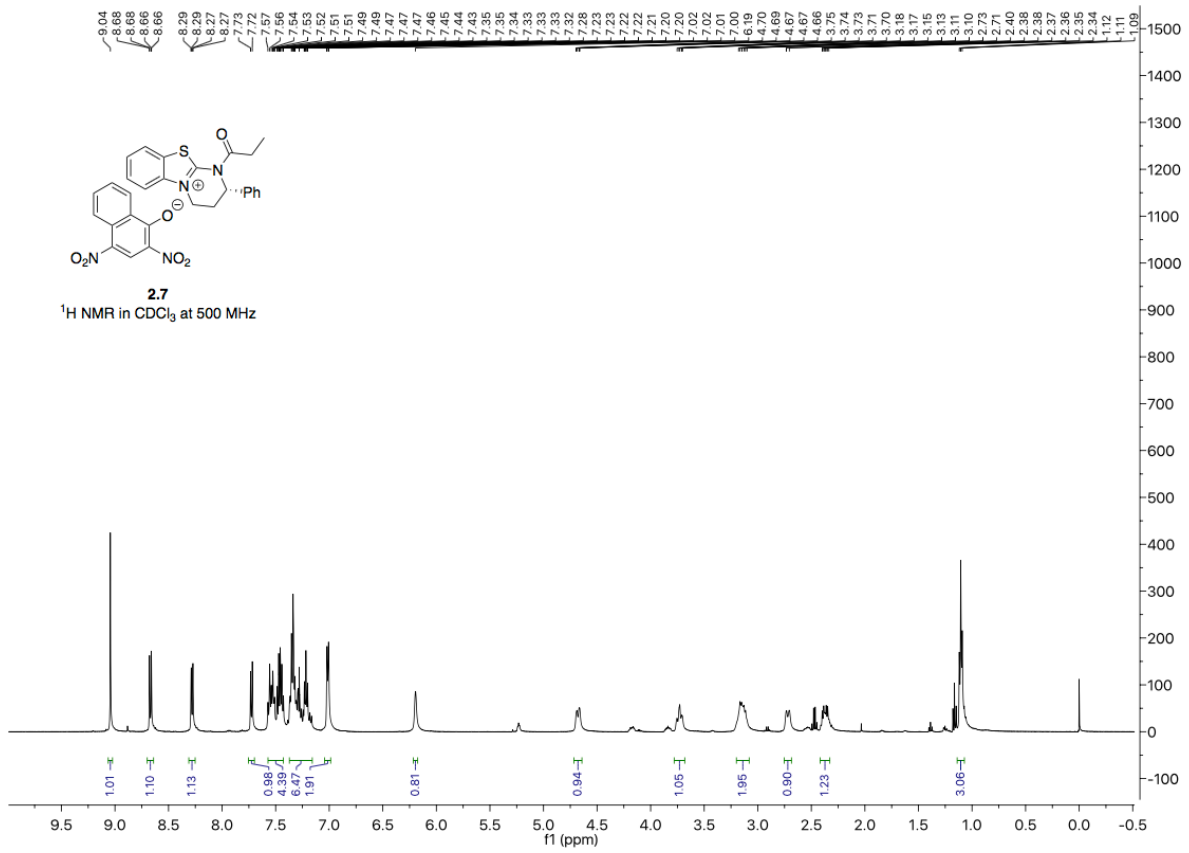


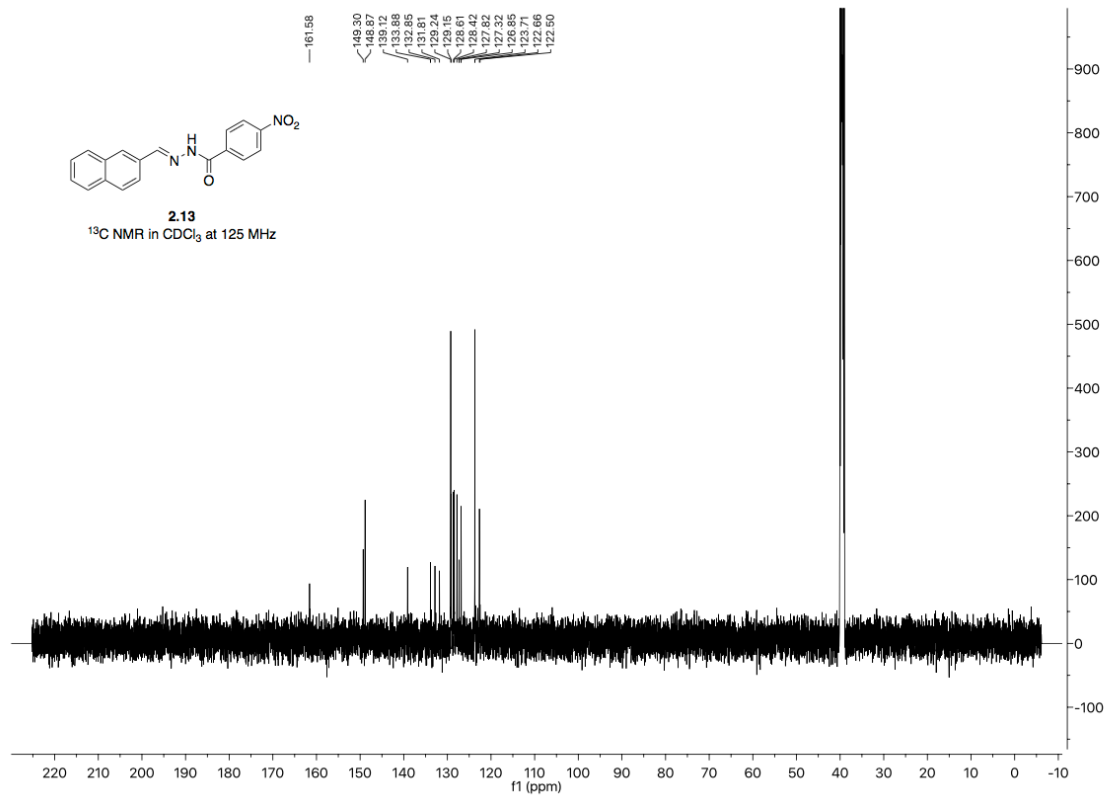
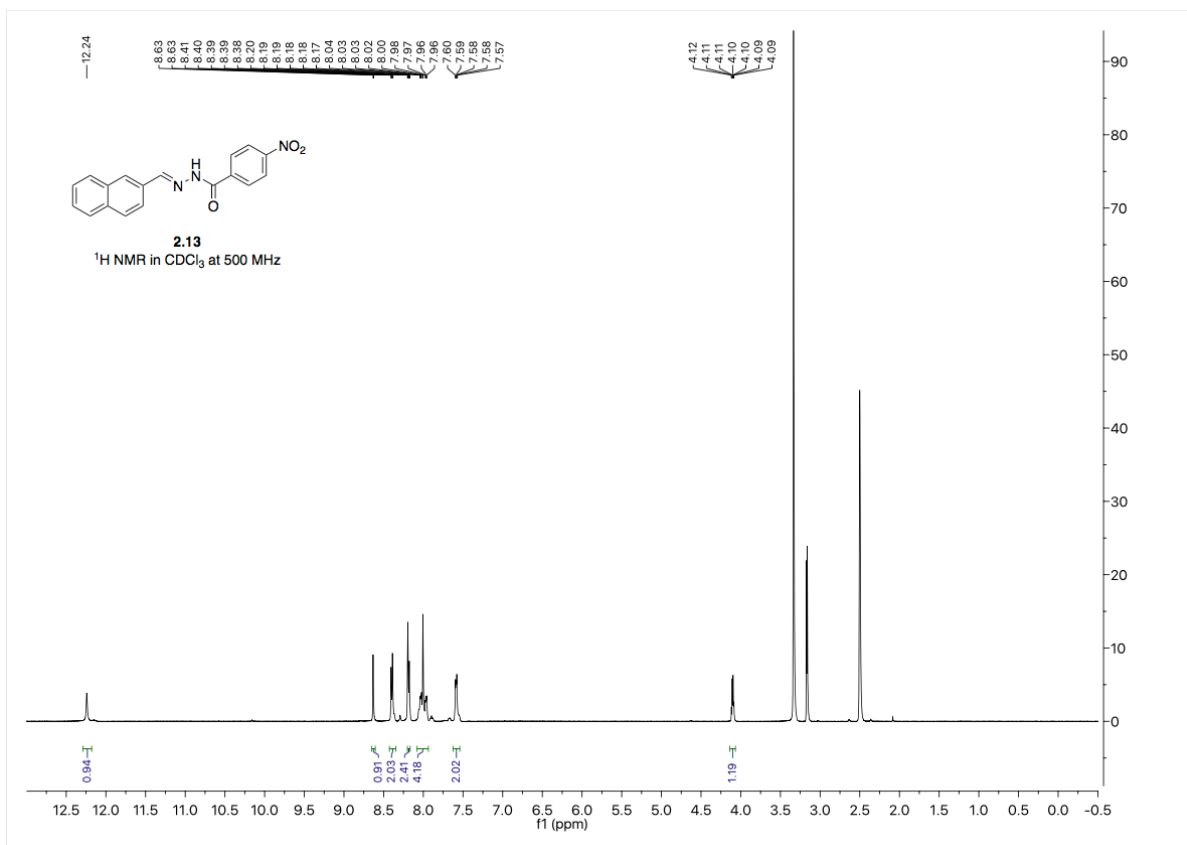


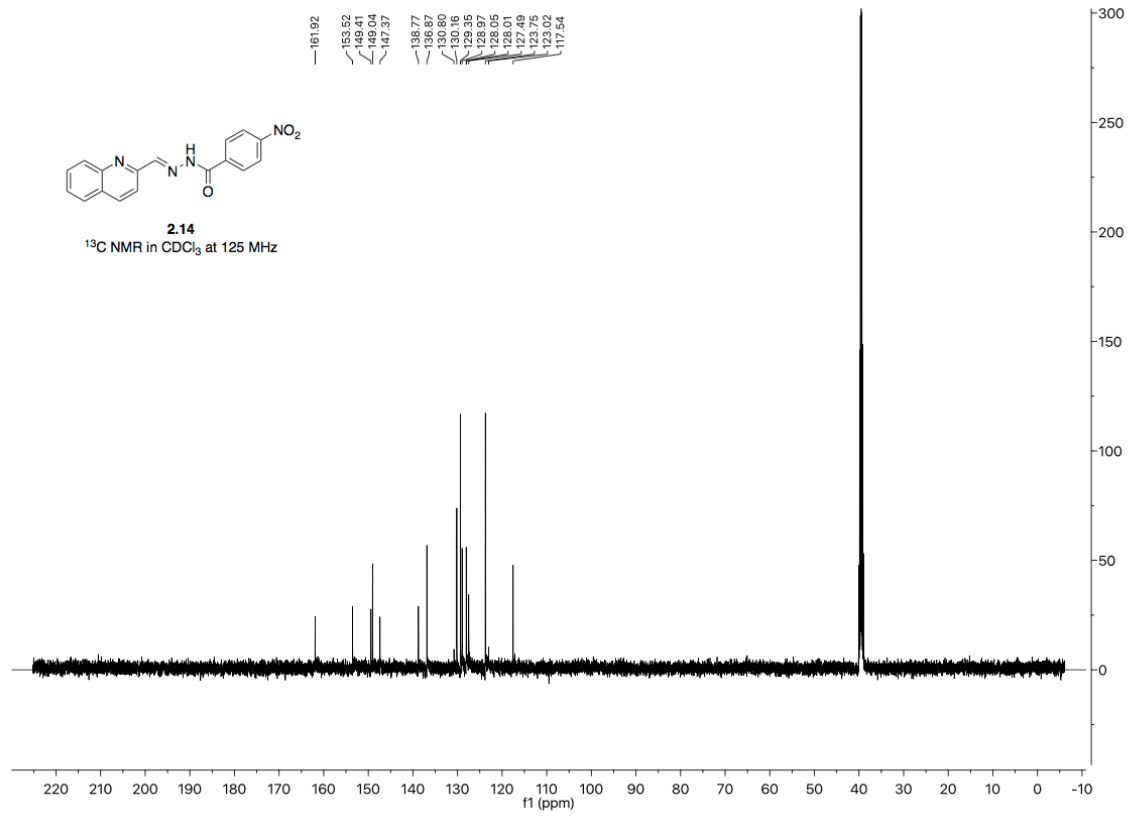
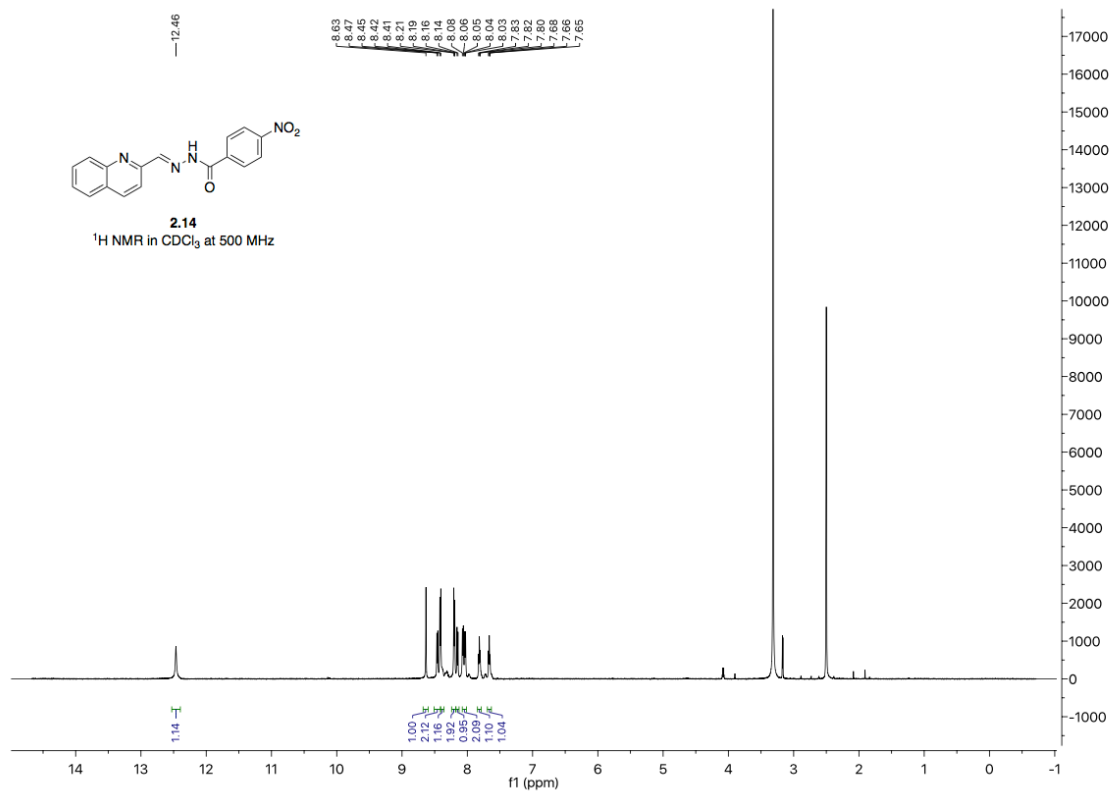
Appendix B. Chapter 2 Supporting Data

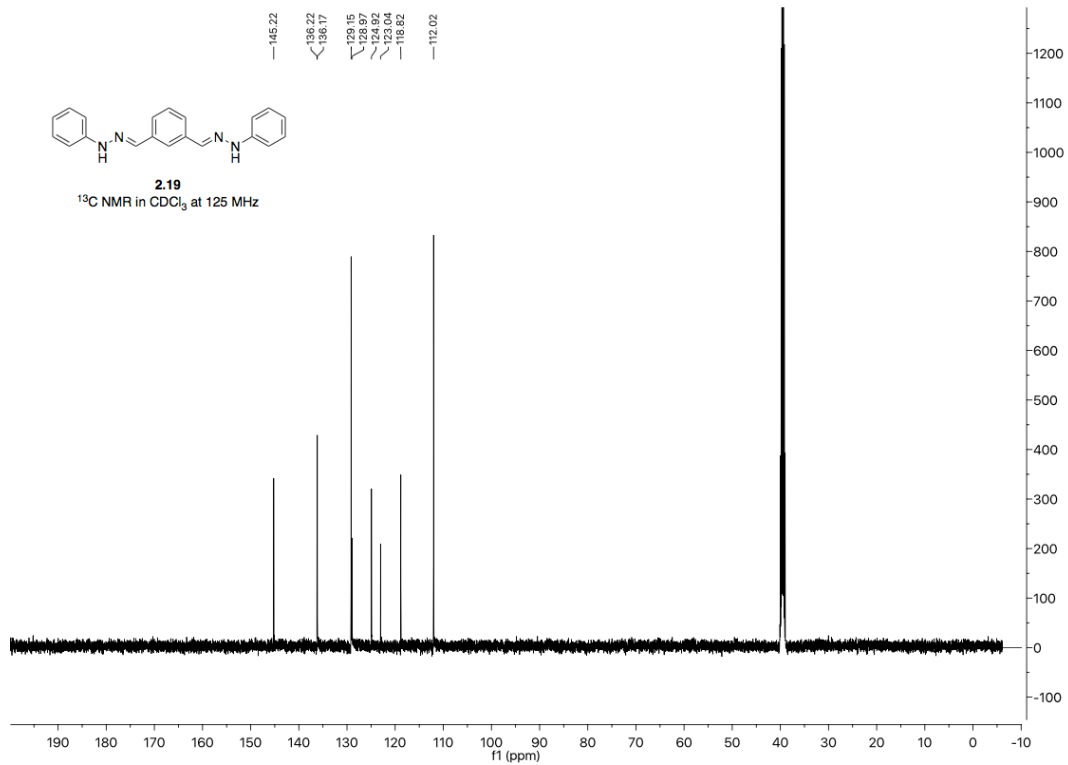
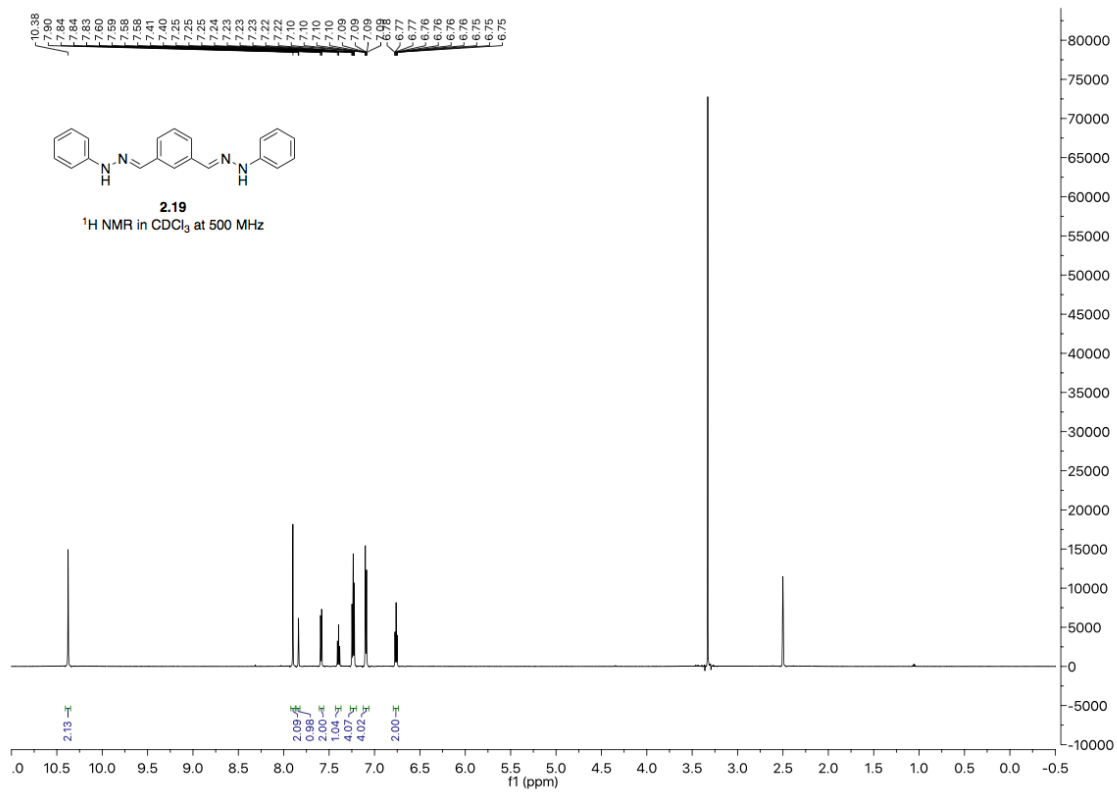


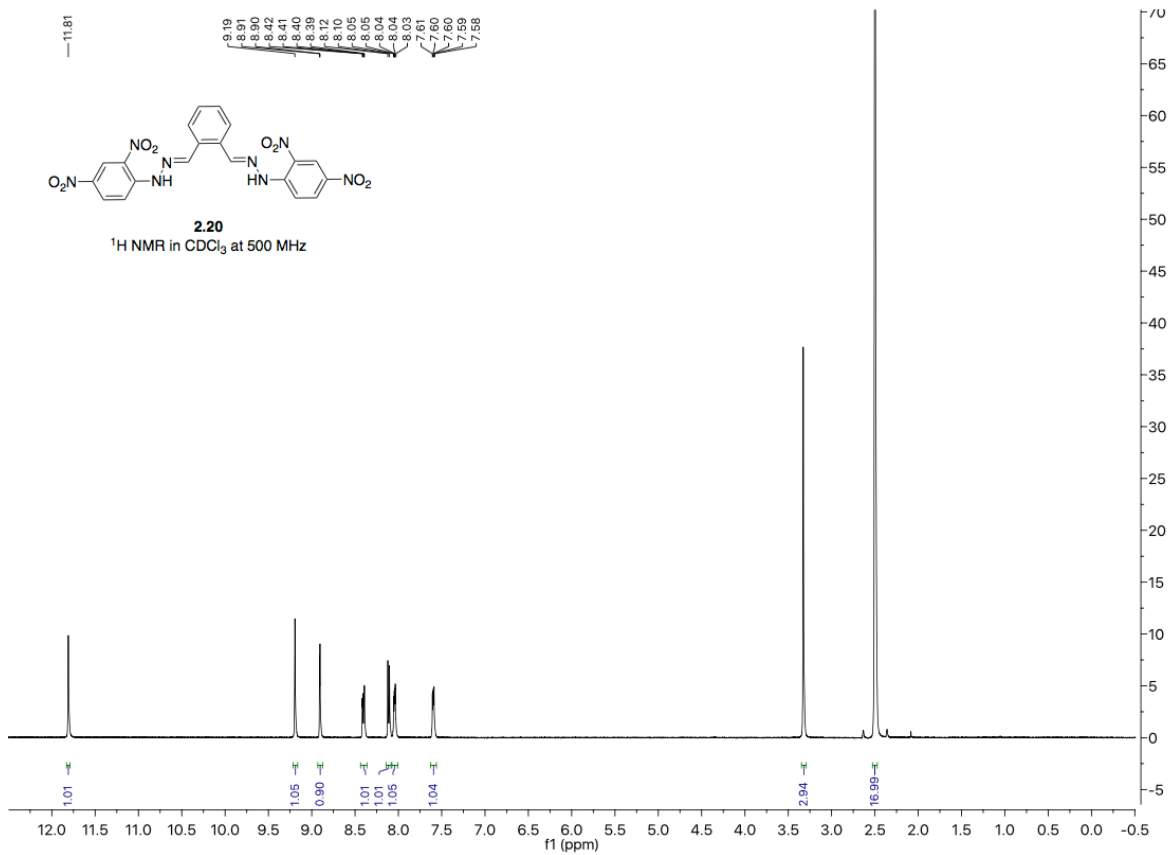












UV-VIS Spectra for Chapter 2

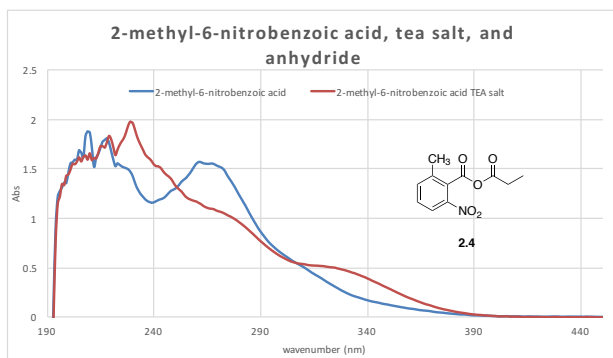
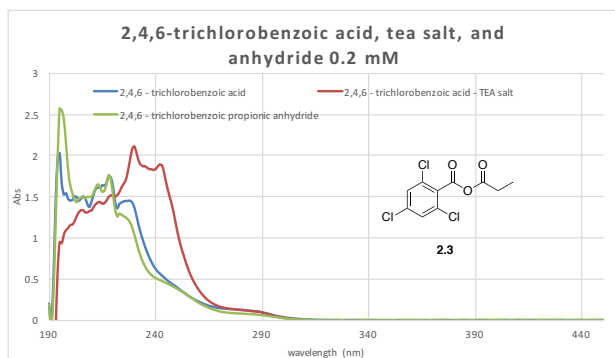


Figure B1. UV-VIS spectra of **2.3** and **2.4** as the phenol, Et₃N salt, and propionate ester.

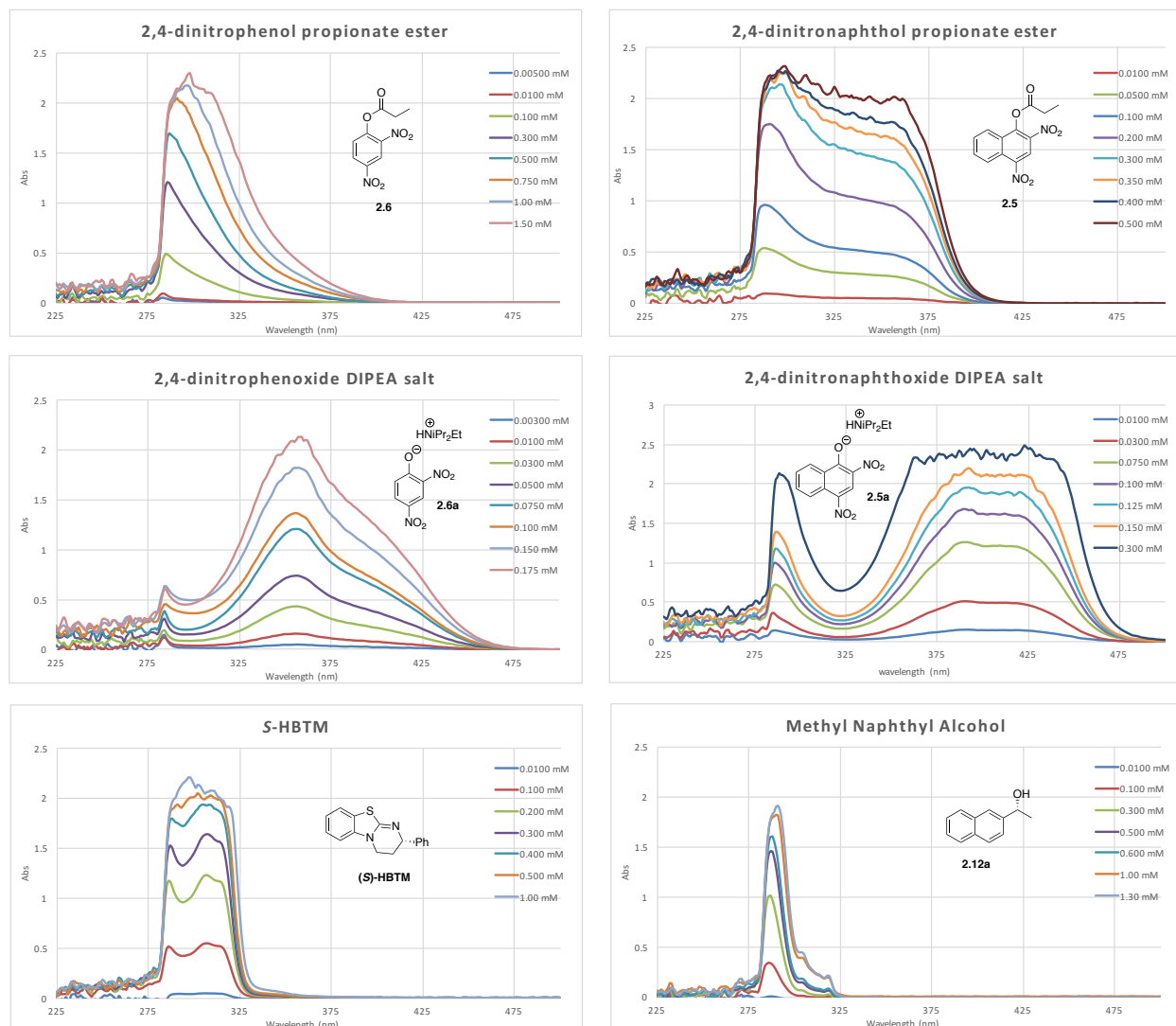


Figure B2. Concentration study of various possible species in the CEC reaction.

Figure B3. ¹H NMR studies of **2.5** with HBTM.

Figure B4. UV-VIS spectra of additional benzoic acids studied.

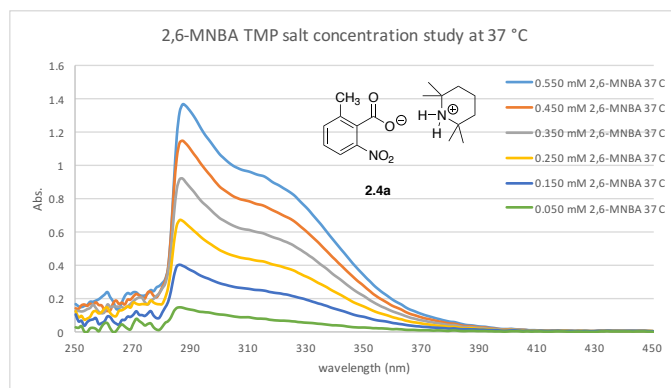
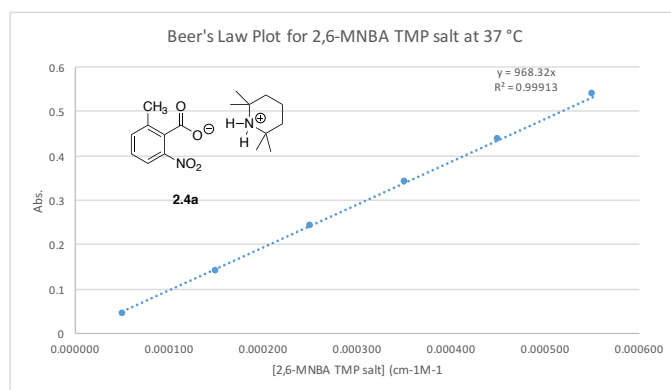


Figure B5. Concentration study of 2-methyl-6-nitro benzoate tetramethylpiperidine salt **2.4a**.

UV-VIS spectra run at 37 °.



[2.4a] mM	Abs. (340 nm)	ϵ	[2.4a] M	Abs. (340 nm)	ϵ
0.550	0.538	0.978	0.000550	0.538	978
0.450	0.435		0.000450	0.435	967
0.350	0.338		0.000350	0.338	966
0.250	0.239		0.000250	0.239	956
0.150	0.137		0.000150	0.137	913
0.0500	0.042		0.000050	0.042	840
				average	937

Figure B6. Beer's Law plot generated using the Abs vs [**2.4a**] (M), and the molar extinction coefficient (ϵ) determined.

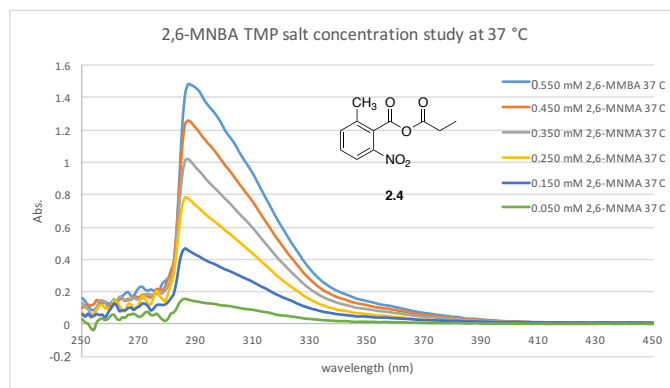
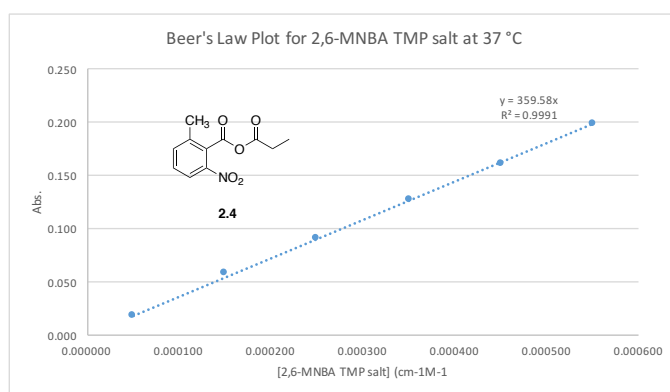


Figure B7. Concentration study of 2-methyl-6-nitro benzoate tetramethylpiperidine salt **2.4a**.

UV-VIS spectra run at 37 °C.



[2.4] mM	Abs. (340 nm)	ϵ	[2.4] M	Abs. (340 nm)	ϵ
0.550	0.198	0.360	0.000550	0.198	360
0.450	0.160	0.356	0.000450	0.160	356
0.350	0.126	0.360	0.000350	0.126	360
0.250	0.090	0.360	0.000250	0.090	360
0.150	0.058	0.387	0.000150	0.058	387
0.0500	0.018	0.360	0.000050	0.018	360
				average	364

Figure B8. Beer's Law plot generated using the Abs vs [**2.4**] (M), and the molar extinction coefficient (ϵ) determined.

$$A_{\text{obs}} = \sum A_n = L \sum c_n \epsilon_n = \cancel{L} \epsilon_{\text{salt}} [\text{salt}] + \cancel{L} \epsilon_{\text{MA}} [\text{MA}] \Rightarrow A_{\text{obs}} - \epsilon_{\text{MA}} [\text{MA}] = [\text{salt}] \epsilon_{\text{salt}}$$

$$[\text{salt}] = \frac{(A_{\text{obs}} - \epsilon_{\text{MA}} [\text{MA}])}{\epsilon_{\text{salt}}} \quad \text{if } [\text{MA}] = [\text{MA}]_0 - [\text{salt}]$$

$$[\text{salt}] = \frac{A_{\text{obs}} - \epsilon_{\text{MA}} ([\text{MA}]_0 - [\text{salt}])}{\epsilon_{\text{salt}}} = \frac{A_{\text{obs}} - 366 (0.00533 - [\text{salt}])}{\epsilon_{\text{salt}} 993}$$

$$[\text{salt}] = \frac{A_{\text{obs}} - 0.195 + 366 [\text{salt}]}{\epsilon_{\text{salt}} 993} = \frac{A_{\text{obs}}}{993} - 0.000196 + 0.392 [\text{salt}]$$

$$0.608 [\text{salt}] = \frac{A_{\text{obs}}}{993} - 0.000196 \Rightarrow [\text{salt}] = 0.000652 A_{\text{obs}} - 0.000322$$

$$[\text{salt}] = 0.000652 (0.244) - 0.000322 = -0.000163$$

$$A_{\text{obs}} = \overset{\epsilon_{\text{salt}}}{\downarrow} 993 [\text{salt}] + \overset{\epsilon_{\text{MA}}}{\downarrow} 366 ([\text{MA}]_0 - [\text{salt}]) \Rightarrow A_{\text{obs}} = 993 [\text{salt}] + 366 [\text{MA}]_0 - 366 [\text{salt}]$$

$$A_{\text{obs}} = 627 [\text{salt}] + 366 (0.00533)$$

$$A_{\text{obs}} = 627 [\text{salt}] + 0.195$$

$$A_{\text{obs}} - 0.195 = 627 [\text{salt}]$$

$$[\text{salt}] = \frac{A_{\text{obs}} - 0.195}{627}$$

$$\frac{1 - 2 + 3(4)}{2} = 5.5$$

$$\frac{1}{2} - \frac{2}{2} + \frac{12}{2} = 5\frac{1}{2} = 5.5$$

Figure B9. Calculations relating Abs_{obs} to [salt].

$$A_{\text{obs}} = A_{\text{MA}} + A_{\text{salt}} \quad \text{if } A_{\text{MA}} = [\text{MA}] \epsilon_{\text{MA}} \text{ and } A_{\text{salt}} = [\text{salt}] \epsilon_{\text{salt}} \text{ then}$$

$$A_{\text{obs}} = \epsilon_{\text{MA}} [\text{MA}] + \epsilon_{\text{salt}} [\text{salt}] \quad \text{if } [\text{MA}]_0 = [\text{MA}] + [\text{salt}] \text{ then } \llbracket$$

$$[\text{MA}] = [\text{MA}]_0 - [\text{salt}]$$

$$\text{so } A_{\text{obs}} = \epsilon_{\text{MA}} ([\text{MA}]_0 - [\text{salt}]) + \epsilon_{\text{salt}} [\text{salt}]$$

$$\Rightarrow A_{\text{obs}} = \epsilon_{\text{MA}} [\text{MA}]_0 - \epsilon_{\text{MA}} [\text{salt}] + \epsilon_{\text{salt}} [\text{salt}] \Rightarrow A_{\text{obs}} = \epsilon_{\text{MA}} [\text{MA}]_0 + [\text{salt}] (\epsilon_{\text{salt}} - \epsilon_{\text{MA}})$$

$$\Rightarrow A_{\text{obs}} - \epsilon_{\text{MA}} [\text{MA}]_0 = [\text{salt}] (\epsilon_{\text{salt}} - \epsilon_{\text{MA}}) \Rightarrow \frac{A_{\text{obs}} - \epsilon_{\text{MA}} [\text{MA}]_0}{\epsilon_{\text{salt}} - \epsilon_{\text{MA}}} = [\text{salt}]$$

$$\text{if } [\text{OH}] = [\text{OH}]_0 - [\text{salt}] \text{ then } [\text{OH}] = [\text{OH}]_0 - \left(\frac{A_{\text{obs}} - \epsilon_{\text{MA}} [\text{MA}]_0}{\epsilon_{\text{salt}} - \epsilon_{\text{MA}}} \right)$$

$$\text{if } A_{\text{obs}} = 0.195 \quad \epsilon_{\text{MA}} = 366 \frac{\text{L}}{\text{cm} \cdot \text{M}} \quad \epsilon_{\text{salt}} = 993 \frac{\text{L}}{\text{cm} \cdot \text{M}} \quad [\text{OH}]_0 = 0.000350 \text{ M} \quad , \quad [\text{MA}]_0 = 0.000533 \text{ M}$$

$$\text{then } [\text{OH}] = 0.000350 - \left(\frac{A_{\text{obs}} - 366(0.000533)}{993 - 366} \right)$$

$$\Rightarrow [\text{OH}] = 0.000350 - \left(\frac{A_{\text{obs}} - 0.195}{627} \right)$$

$$\text{@ } 37^\circ\text{C} \quad \epsilon_{\text{MA}} = 360 \frac{\text{L}}{\text{cm} \cdot \text{M}} \quad \epsilon_{\text{salt}} = 968 \frac{\text{L}}{\text{cm} \cdot \text{M}}$$

$$\text{so } [\text{OH}] = 0.000350 - \left(\frac{A_{\text{obs}} - 360(0.000533)}{968 - 360} \right)$$

$$[\text{OH}] = 0.000350 - \left(\frac{A_{\text{obs}} - 0.192}{608} \right)$$

Figure B10. Calculations relating A_{obs} to $[\text{OH}]$ (alcohol in reaction).

conversion(%)	[salt](mM)	microL 10.00 mM stock solution	[alc](mM)	microL alcohol (14.5 mM)	[ester](mM)	microL ester (15.9 mM)	microL HBTM (2.9 mM)	[anhydride](mM)	microL 10.00 mM stock solution	microL methanol	toluene	toluene	toluene (no alc)	conversion(%)
0	0	0	0.35	72.4	0	0	72.4	0.533	160.0	0.0647	2.695	2.695	2.7676	0
10	0.035	10.5	0.315	65.2	0.035	6.6	72.4	0.498	149.4	0.0604	2.696	2.696	2.7676	10
20	0.07	21.0	0.28	57.9	0.07	13.2	72.4	0.463	138.9	0.0562	2.697	2.697	2.7676	20
30	0.105	31.5	0.245	50.7	0.105	19.8	72.4	0.428	128.4	0.0519	2.697	2.697	2.7676	30
40	0.14	42.0	0.21	43.4	0.14	26.4	72.4	0.393	117.9	0.0477	2.698	2.698	2.7676	40
50	0.175	52.5	0.175	36.2	0.175	33.0	72.4	0.358	107.4	0.0434	2.698	2.698	2.7676	50
60	0.21	63.0	0.14	29.0	0.21	39.6	72.4	0.323	96.9	0.0392	2.699	2.699	2.7676	60
70	0.245	73.5	0.105	21.7	0.245	46.2	72.4	0.288	86.4	0.0350	2.700	2.700	2.7676	70
80	0.28	84.0	0.07	14.5	0.28	52.8	72.4	0.253	75.9	0.0307	2.700	2.700	2.7676	80
90	0.315	94.5	0.035	7.2	0.315	59.4	72.4	0.218	65.4	0.0265	2.701	2.701	2.7676	90
100	0.35	105.0	0	0.0	0.35	66.0	72.4	0.183	54.9	0.0222	2.702	2.702	2.7676	100

Figure B11. Calculations and amounts for simulating the conversion of mixed anhydride **2.4** to the benzoate salt **2.4a**.

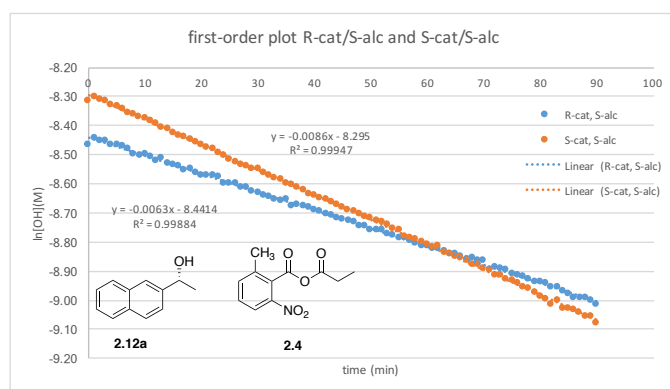


Figure B12. Conversion of Abs_{obs} to conversion for both enantiomers of HBTM catalyst with (*S*)-alcohol with anhydride **2.4** as the acyl source.

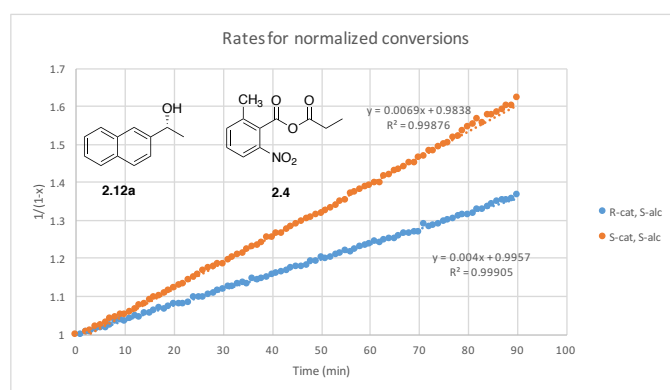


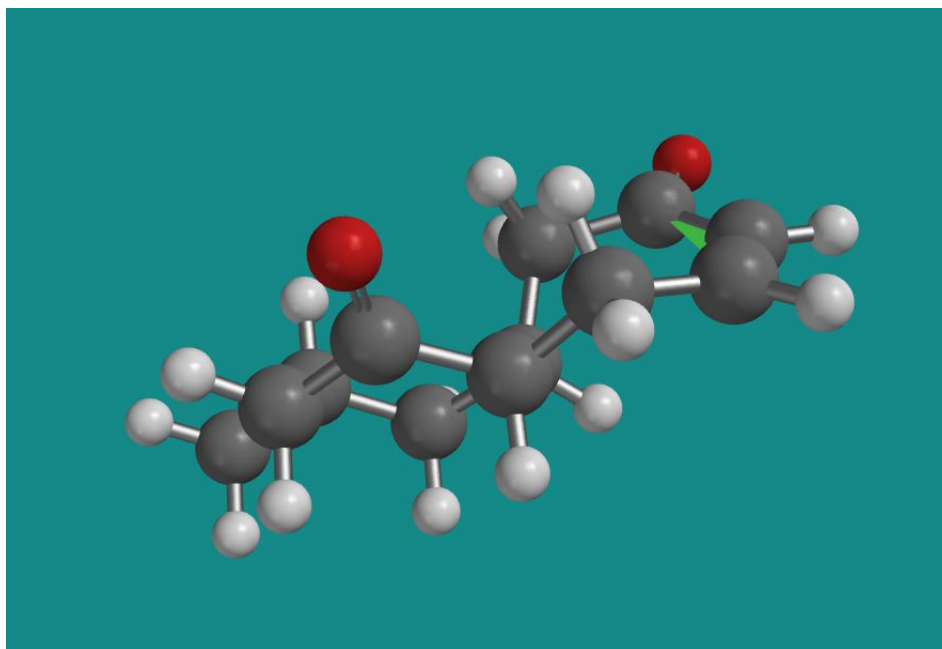
Figure B13. Rate plots of $1/(1-x)$ utilizing the normalized conversion x (initial conversion set to 0).

Appendix C. Chapter 4 Supporting Data

Figure C14. Conformations for ketones **4.11–4.14** DFT: B3LYP/6-31G(d)

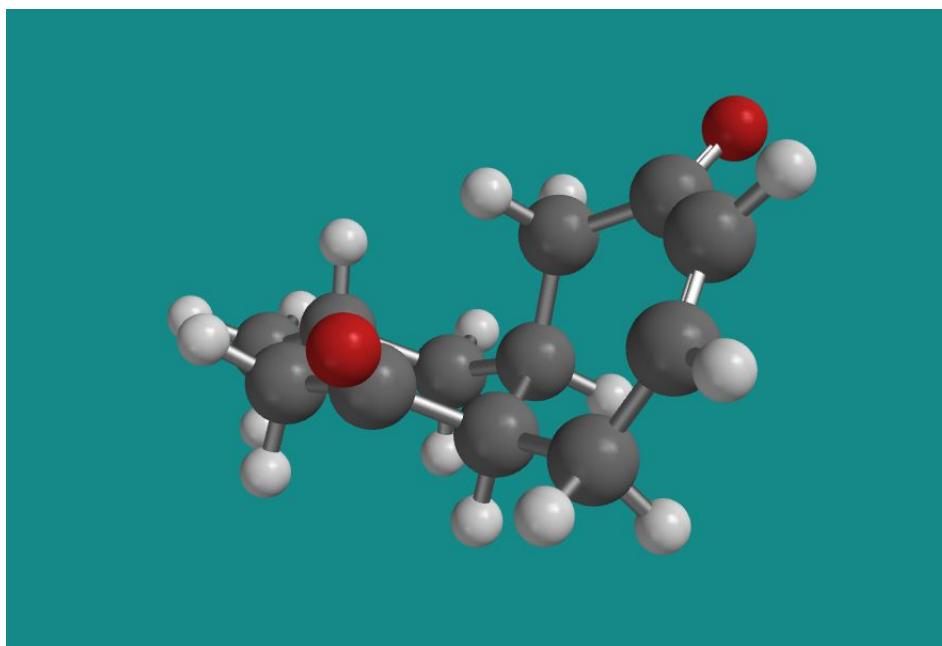
Label	rel. E (kcal/mol)	Boltzmann Dist	MMFF (kcal/mol)
M0001	0.00	0.847	0.00
M0003	1.24	0.105	2.04
M0006	2.06	0.026	4.44
M0002	2.33	0.017	1.31
M0004	3.37	0.003	3.56
M0007	3.82	0.001	3.78
M0005	4.53	0.000	4.79

Ketone **4.6** Conformation 1 (M0001)



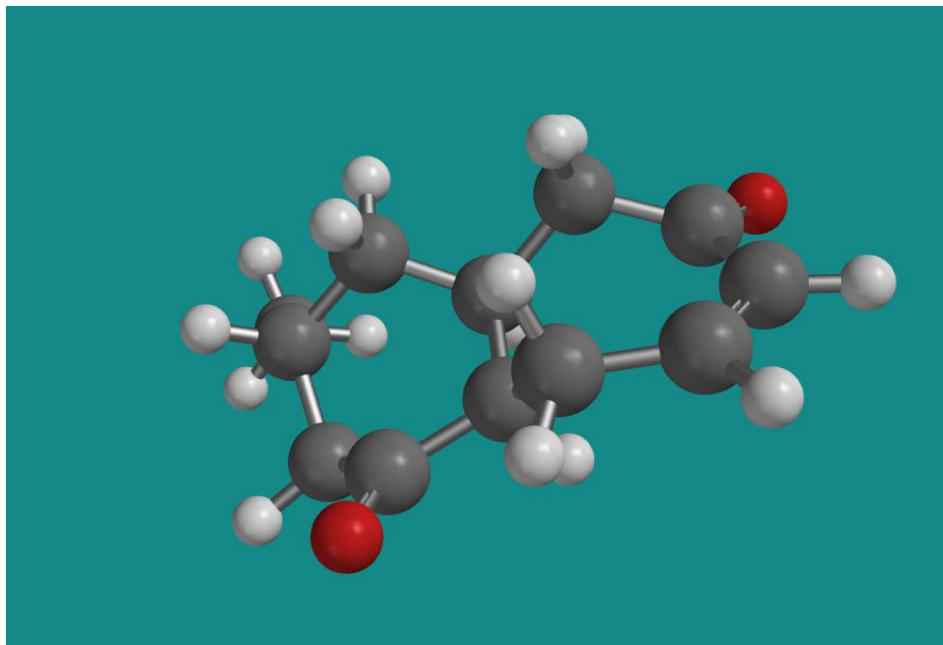
Description: Chair, equatorial methyl, flap down

Ketone **4.6** Conformation 2 (M0003)



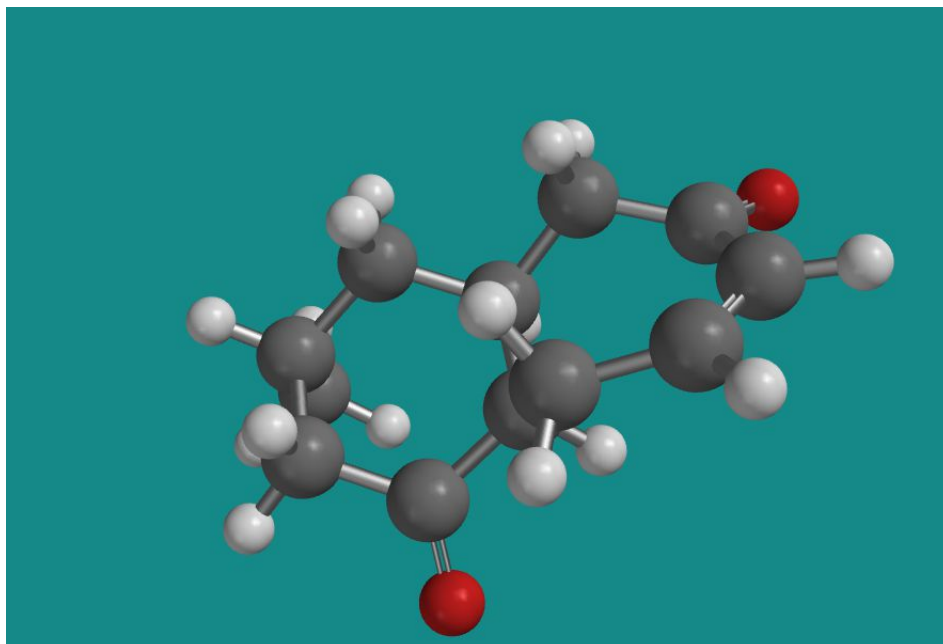
Chair, equatorial methyl, flap up

Ketone **4.6** Conformation 3 (M0006)



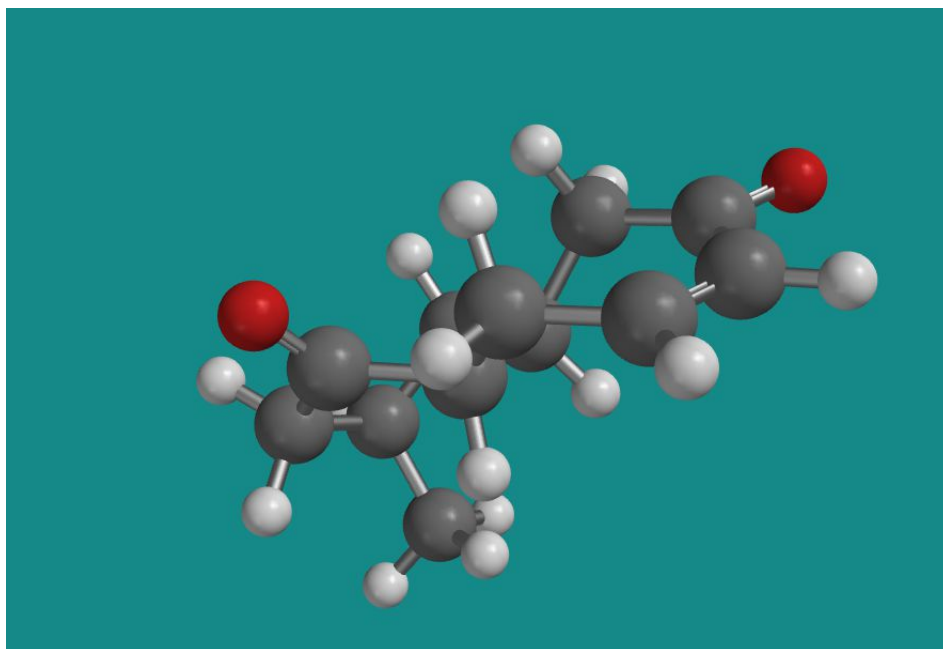
Twist-boat, equatorial methyl, flap down

Ketone **4.6** Conformation 4 (M0002)



Chair, axial methyl. Flap down

Ketone **4.6** Conformation 5 (M0004)



Twist-boat, axial methyl, flap down

Table 2: Conformations of different protected alcohols 4.11–4.14.

Conformer	Description	β -OTBS (4.12)	Number	α -OTBS (4.11)	number
C1	Chair, equat. Me, flap down	0.00	M0001	0.00	M0001
C2	Chair, equat Me, flap up	1.29	M0005	0.76	M0002
C3	Twist boat, equat Me, flap up	3.46	M0010		
C4	Chair, axial Me, flap down	0.44	M0002	2.36	M0006

Table 3: Conformations of protected beta-alcohol

Conformer	Description	β -OBz	Number	β - OTIPS (4.13)	number	β - OTBDPS (4.14)	number
C1	Chair, equat. Me, flap down	0.00	M0001	1.29	M0007	1.20	M0009

C2	Chair, equat Me, flap up	1.64	M0005				
C3	Twist boat, equat Me, flap up						
C4	Chair, axial Me, flap down	1.10	M0002	0.00	M0001	0.00	M0001

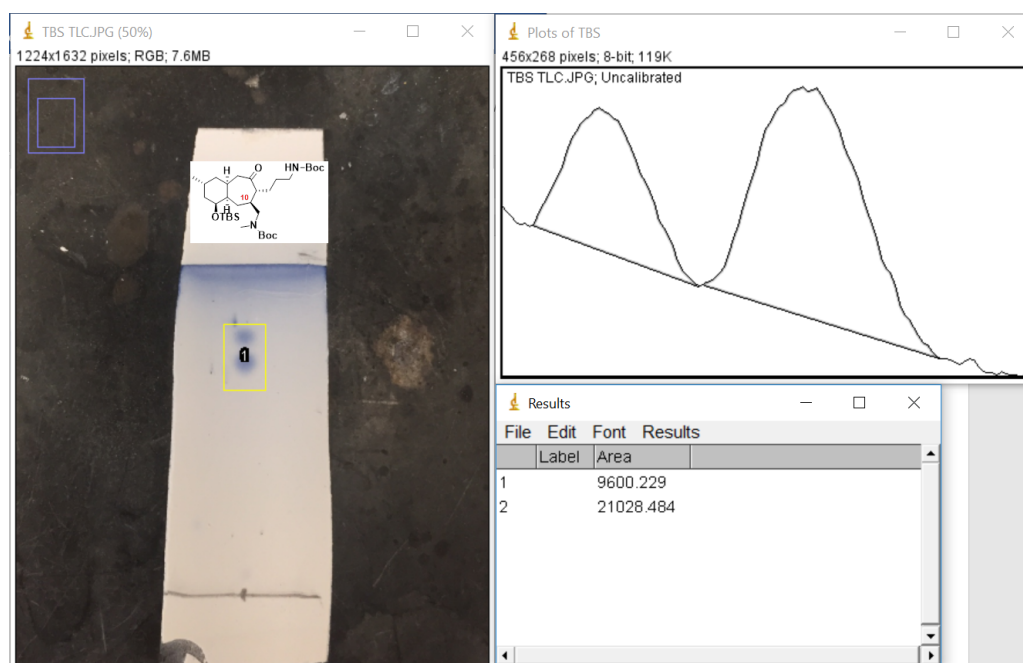


Figure C15. TLC data of the ratio for β -TBS alcohol **4.27** and β -TIPS alcohol **4.28** showing an ~1.0:2.2 ratio for the desired diastereomer.

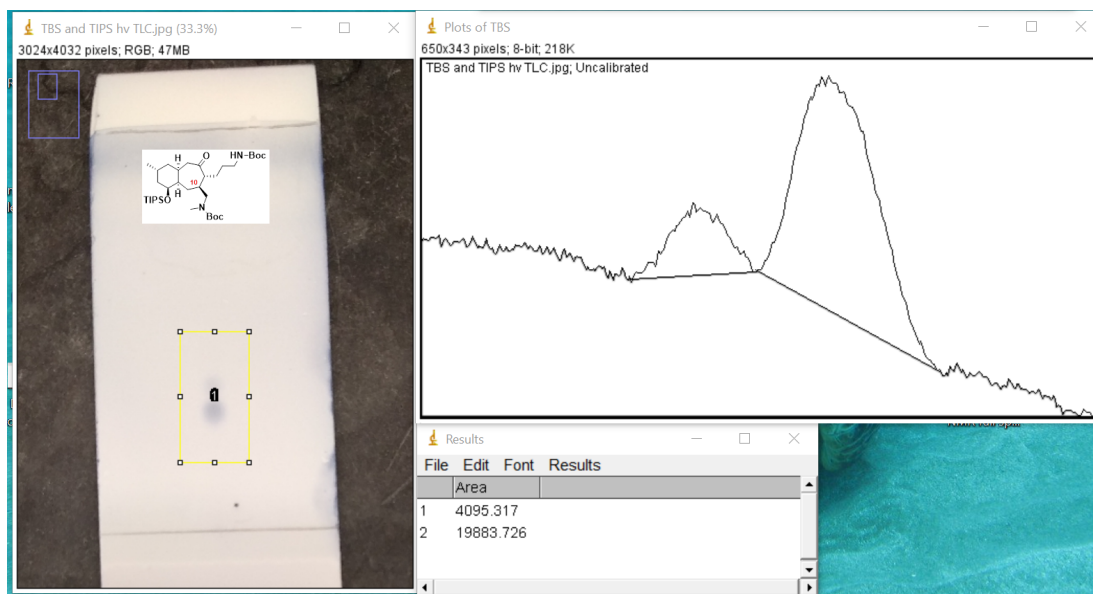


Figure C16. TLC data of the ratio for β -TIPS alcohol **4.28** showing an \sim 1:4.9 ratio for the desired diastereomer.

Appendix D. Chapter 5 Supporting Data

